Essays on differentiated and dynamic pricing in shared mobility systems

Von der Mercator School of Management, Fakultät für Betriebswirtschaftslehre, der

Universität Duisburg-Essen

zur Erlangung des akademischen Grades

eines Doktors der Wirtschaftswissenschaften (Dr. rer. oec.)

genehmigte Dissertation

von

Christian Müller

aus

Gelsenkirchen

Referent:	Prof. Dr. Jochen Gönsch
Koreferent:	Prof. Dr. Rouven Schur
Tag der mündlichen Prüfung:	15.01.2024

Acknowledgements

First of all, I would like to express my sincere gratitude to my PhD supervisor Prof. Dr. Jochen Gönsch for his ideas and continuous support of my research, motivation and enthusiasm. He always helped me to answer my numerous questions and encouraged me to look at further perspectives. I am also very grateful to Prof. Dr. Rouven Schur, who did not hesitate to be a second reviewer.

I would also like to thank Dr. Matthias Soppert for the collaboration on several papers. In particular, his ambition, critical thinking and effort have improved these papers.

Furthermore, I am grateful to my colleagues at the Chair of Service Operations for their helpful comments and various suggestions regarding my research.

Above all, however, I would like to thank my parents Annemarie and Dieter Müller, who have been by my side throughout my life, strengthening and motivating me with helpful and encouraging advices. Additionally, I would like to thank my two sisters Cathrin and Carolin, who supported me during the sometimes very difficult times. Special thanks go to my partner Binia Stieger, with whom I got through this time together and who helped me through the roller coaster ride of emotions during the PhD. I am also grateful to my friends who understood the sometimes stressful phases of the doctorate and nevertheless remained by my side. I dedicate this work to my parents, both passed away during my PhD, and to my daughter Anna, who was born during this time.

Contents

List of Figures

List of Tables

Chapter 1

Introduction

Currently, many cities and municipalities are striving for an integrated mobility concept. In addition to public transportation, this also includes shared mobility systems (SMSs), such as bike or car sharing. It is a component that can contribute to an useful and sustainable mobility concept. For example, in the best case, an integrated mobility concept replaces private vehicles and thus reduces the congestion and emissions caused by cars.

Car sharing has become increasingly popular among providers and customers in recent years. For example, in the EU, the share of sold cars used for new mobility (car sharing, ride hailing, ride sharing, and robocabs) is predicted to rise from 2 % in 2015 up to 15 % in 2025 (Destatis, 2018a). Bike sharing is also becoming increasingly popular. The number of bike sharing providers increased from 388 in 2010 to more than 1,250 in 2017 worldwide. In the same period, the number of bike sharing vehicles increased from 367k in 2010 to more than 10,000k in 2017 (Destatis, 2018b).

This thesis addresses the question of how to set optimal prices in SMSs. It is based on five papers (see Table 1.1), some of which have been published, accepted for publication, or are under review. The order of the papers corresponds to their appearance in this thesis.

Chapter 1 introduces the terminology used in SMSs and the two modeling techniques (linear programming and dynamic programming) applied in the papers.

Chapter 2 is based on the paper entitled "Differentiated Pricing of Shared Mobility Systems Considering Network Effects" by Matthias Soppert, Claudius Steinhardt, Christian Müller and Jochen Gönsch. We introduce an origin-based differentiated, profit-maximizing pricing problem for SMSs. The problem is to determine spatially and temporally differentiated minute prices, taking network effects on the supply side as well as several practice relevant aspects into account. Based on a deterministic network flow model, we formulate the problem as a mixed-integer linear program and prove that it is NP-hard. For its solution, we propose a temporal decomposition approach based on approximate dynamic programming. The approach integrates a value function approximation to incorporate future profits and to account for network effects.

Chapter 3 is based on the paper entitled "Practicable Solution Approaches for Differentiated Pricing of Shared Mobility Systems" by Christian Müller and considers an origin-based SMS, where prices originate from a predefined discrete price set. For this, we develop two different practicable solution approaches to determine spatially and temporally differentiated minute prices that take supply-side network effects into account. The first solution approach does not differentiate between rentals and demand and calculates continuous prices for every period and location. The second solution approach determines the vehicle distributions for each period and then calculates the optimal prices for each period backwards.

Chapter 4 is based on the paper entitled "Matching Functions for Free-Floating Shared Mobility System Optimization to Capture Maximum Walking Distances" by Matthias Soppert, Claudius Steinhardt, Christian Müller and Jochen Gönsch. In this paper, we address the issue of accurate optimization model formulation for free-floating SMSs. Thereby, we build on the state-of-the-art concept of considering a spatial discretization of the operating area into zones. We formally derive two novel analytical matching functions specifically suited for free-floating system optimization, incorporating additional parameters besides supply and demand, such as

Authors	**Journal**	**Status***	**Individual work of Müller, C.**
Paper 1: **Differentiated Pricing of Shared Mobility Systems Considering Network Effects**			
First Author: Soppert, M. Co-Authors: Steinhardt, C.; Müller C., Gönsch, J.	Transportation Science	published	abstract, computational study
Paper 2: **Practicable Solution Approaches for Differentiated Pricing of Shared Mobility Systems**			
Müller, C.	Transportation Research: Part B	under review: first round	exclusive authorship
Paper 3: **Matching Functions for Free-Floating Shared Mobility System Optimization to Capture Maximum Walking Distances**			
First Author Soppert, M. Co-Authors: Steinhardt, C.; Müller, C.; Gönsch, J.; Bhogale, P.M.	European Journal of Operational Research	published	abstract, computational study
Paper 4: **Customer-Centric Dynamic Pricing for Free-Floating Vehicle Sharing Systems**			
First Author Müller, C., Co-Authors: Gönsch, J.; Soppert, M.; Steinhardt, C.	Transportation Science	accepted	conception of the research project and the entire study, literature review, solution method, computational study, case study
Paper 5: **Dynamic Pricing for Shared Mobility Systems Based on Idle Time Data**			
First Author Müller, C., Co-Authors: Gönsch, J.; Soppert, M.; Steinhardt, C.	OR Spectrum	accepted	conception of the research project and the entire study, literature review, solution method, computational study

Table 1.1: Overview of written papers (*at time of writing the thesis)

customers' maximum walking distance and zone sizes. We investigate their properties, such as their linearizability and integrability into existing optimization models.

Chapter 5 is based on the paper entitled "Customer-Centric Dynamic Pricing for Free-Floating Vehicle Sharing Systems" by Christian Müller, Jochen Gönsch, Matthias Soppert and Claudius Steinhardt.[1] We develop a profit-maximizing dynamic pricing approach that is built on adopting the concept of customer-centricity. Customer-centric dynamic pricing here means that, whenever a customer opens the provider's mobile application to rent a vehicle, the price optimization incorporates the customer's location as well as disaggregated choice behavior to precisely capture the effect of price and walking distance to the available vehicles on the customer's probability for choosing a vehicle. Two other features characterize the approach. It is

[1]In this paper, we use the term "vehicle sharing system" synonymously with the term "SMS" due to the changes during the review process.

origin-based, i.e., prices are differentiated by location and time of rental start, which reflects the real-world situation where the rental destination is usually unknown. Further, the approach is anticipative, using a stochastic dynamic program to foresee the effect of current decisions on future vehicle locations, rentals, and profits. We propose an approximate dynamic programming-based solution approach with non-parametric value function approximation. It allows direct application in practice, because historical data can readily be used and main parameters can be pre-computed so that the online pricing problem becomes tractable.

Chapter 6 is based on the paper entitled "Dynamic Pricing for Shared Mobility Systems Based on Idle Time Data" by Christian Müller, Jochen Gönsch, Matthias Soppert and Claudius Steinhardt. We develop a novel dynamic pricing approach that determines prices by online optimization and thereby anticipates future profits through the integration of idle time data. With regard to application in practice, the approach is generic in the sense that different types of readily available historical idle time data with different spatio-temporal granularity can be seamlessly integrated.

Chapter 7 concludes this thesis.

1.1 Shared Mobility Systems

Shared Mobility Systems (SMSs)[2] are systems for spontaneous, short-term rentals of vehicles. There are two types of SMSs: free-floating (see Figure 1.1a) and station-based SMSs (see Figure 1.1b). In free-floating SMSs, customers can pick-up and drop-off vehicles at any location throughout the business area. In station-based SMSs, stations are distributed throughout the business area, where customers can pick-up or drop-off vehicles. A distinction is also made between two-way (see Figure 1.1c) and one-way station-based SMSs (see Figure 1.1d). In two-way SMSs, the customer must drop-off the vehicle at the station where she picked it up, whereas in one-way SMSs, the customer can pick-up a vehicle at one station and drop it off at another station.

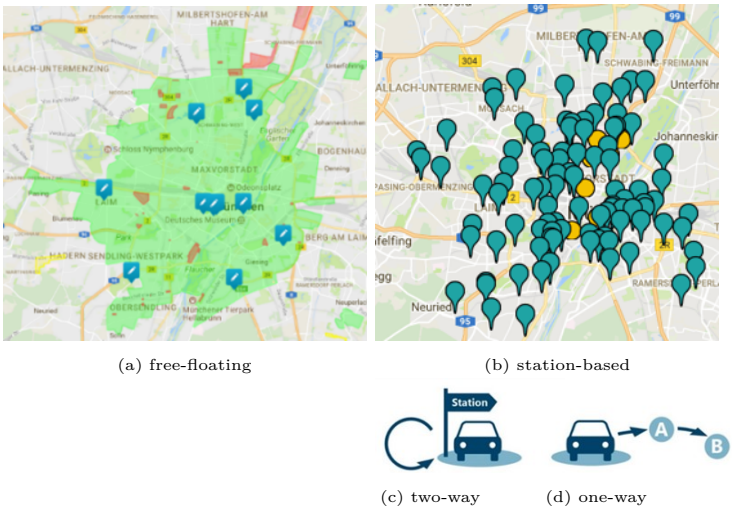

(a) free-floating (b) station-based

(c) two-way (d) one-way

Figure 1.1: Different forms of SMSs

From an operations research perspective decision problems in SMSs belong to different planning levels (see Figure 1.2). It can be distinguished between operative and strategical/tactical planning in SMSs. Whereas the decision problems of station location and dimensioning or fleet size belong to the strategical/tactical problems, the decision problem of station inventory is an operative planning problem. However, there are also dependencies between these different decision problems. The decision about station locations and their size influences the decision about fleet size. The fleet size, in turn, has an impact on the station inventory.

The station inventory decision problem is composed of two parts: *operator-based* and *user-based* relocation.

The *operator-based* relocation is handled by the provider and requires resources such as staff or further equipment (such as trucks). It can be performed statically or dynamically. Static, on the one hand, means that the relocation is performed when the system is closed, usually at night. Dynamic, on the other hand, means that the relocation is performed while the SMS is running.

In *user-based* relocation, incentives are set so that customers participate in the relocation process. It can also be divided into static and dynamic. Whereas in static user-based relocation,

[2]Please note that the term “vehicle sharing system" is used in this thesis as a synonym for SMS (Chapter 5).

incentives are set to remain constant over a longer period of time, e.g., several months, in dynamic user-based relocation, incentives are set based on the short-term status of the SMS.

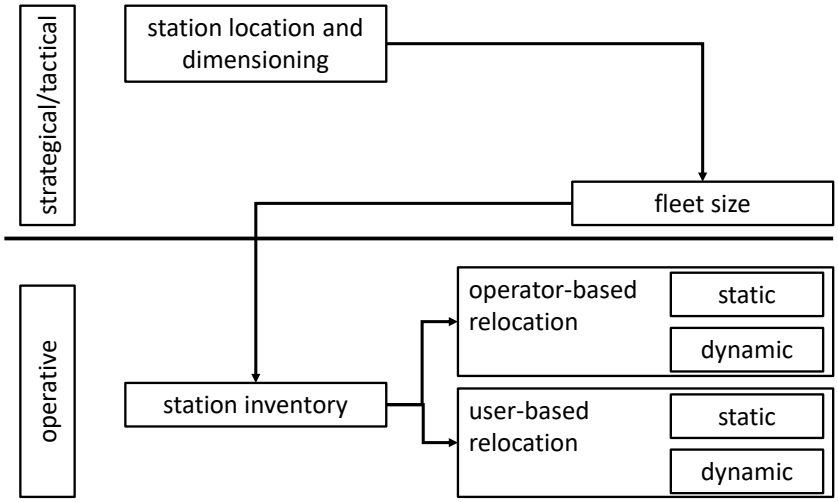

Figure 1.2: Illustration of different planning levels of decision problems in SMSs (Gönsch and Kruk, 2017)

All chapters deal with pricing, that has an impact on the station/zone inventory. Chapters 2 and 3 consider differentiated pricing that accounts for supply-side network effects for better vehicle distributions throughout the day. In Chapter 4 we additionally examine the difference of free-floating and station-based SMSs. Chapters 5 and 6 consider dynamic pricing that considers future states and thus (expected) supply-side network effects for better vehicle distributions throughout the day.

1.2 Applied Techniques

We formulate solution approaches for differentiated and dynamic pricing. For differentiated pricing we use mixed integer linear programming to model the problem. Based on the linear model, we develop different solution approaches. For the dynamic pricing, we formulate the problem as a dynamic program which depends on the current state. Since the dynamic program suffers from the curse of dimensionality, we develop different approximate dynamic programs.

The following sections include a simple example based on a consistent problem to support the explanation of the different methods used.

Example: A provider of a free-floating car sharing system aims to determine the profit-optimal, origin-based prices for all vehicles.

1.2.1 Linear Programming

Linear programming is one of the most studied and developed methods to deal with decision problems. Linear programming techniques are used for many problems such as human resources management, transport problems or scheduling flights. It is a powerful tool to get an optimal solution for limited resources. In the following, we explain the different components and aspects of linear programs (see Section 1.2.1.1) and the linearization of non-linear programs we use (see Section 1.2.1.2).

1.2.1.1 Components and Aspects of Linear Programs

Every linear program consists of three components: *decision variables*, *objective function* and *constraints*.

The *decision variables* are the components, that can be affected by the decision maker (Poler et al., 2014, Chapter 1). Thus, they "are the quantities whose values are to be determined" (Denardo, 2011, Chapter 1). They may take fractional values.

Example: The decision variables are the expectation values of rentals $r_{i,j,t}$ from zone i to zone j at period t.

The *objective function* defines the goal of the decision maker and represents the relation between the decision variables and the parameters. In a linear program, the objective function must be linear (Poler et al., 2014, Chapter 1).

Example: If the provider optimizes the number of rentals, the objective function is linear ($max \sum_{i,j \in \mathcal{Z}, t \in \mathcal{T}} r_{i,j,t}$) , but if the provider optimizes profit, it is non-linear ($max \sum_{i,j \in \mathcal{Z}, t \in \mathcal{T}} r_{i,j,t} \cdot (p_i - c)$) because the decision variables for rentals $r_{i,j,t}$ are multiplied by the decision variables for prices $p_{i,t}$.

The *constraints* indicate the limitation of the objective function due to the given environmental conditions, such as limited capacity, limited time, flow conditions, etc. (Poler et al., 2014, Chapter 1).

Example: Limiting the rentals $\sum_{j \in \mathcal{Z}} r_{i,j,t}$ in zone i and period t to the number of available vehicles $a_{i,t}$ in zone i and period t.

Integer linear programming is an extension of linear programming. The difference is that some or all of the decision variables can no longer take fractional values (Poler et al., 2014,

Chapter 2). An integer linear program becomes a linear program if we relax the constraint that the decision variables are integer (Denardo, 2011, Chapter 1).

Integer linear programming also considers binary variables, which can take two values (0 or 1) (Poler et al., 2014, Chapter 2).

Example: We consider a discrete price list of M possible prices. A binary decision variable for a price $y_{i,t}^m$ for station i and price point m at period t is 1 if the price p^m is chosen and 0 otherwise.

We distinguish between *feasible solutions* and *optimal solutions*. A *feasible solution* is a solution that satisfies each constraint and assigns an objective value to the linear program. Thus, a linear program is feasible, if it has at least one feasible solution, otherwise it is infeasible (Denardo, 2011, Chapter 1).

Example: For profit optimization one feasible solution is to set always the lowest price.

An *optimal solution* is the feasible solution with the largest (smallest) objective value of a maximization (minimization) problem (Denardo, 2011, Chapter 1). A linear program cannot be solved simply in most cases, but requires solution methods (for example simplex algorithm or branch-and-bound).

We also distinguish between *unbounded* and *bounded* linear programs. A linear program is *unbounded*, if it is feasible and there is no limit for the objective value and *bounded* otherwise (Denardo, 2011, Chapter 1).

Example: We consider a rental maximization problem $max \sum_{i,j \in \mathcal{Z}, t \in \mathcal{T}} r_{i,j,t}$ in a car sharing system without any constraints. This problem is unbounded. In contrast, the same problem with the capacity constraint $\sum_{j \in \mathcal{Z}} r_{i,j,t} \leq a_{i,t} \quad \forall i \in \mathcal{Z}, t \in \mathcal{T}$ (the rentals from a zone i in period t are less than or equal to the available vehicles in zone i in period t.) is bounded.

1.2.1.2 Linearizing Non-linear Programs

In operations research there are a lot of problems that are formulated as a non-linear program. A non-linear program has an objective and/or constraints that are described by non-linear functions (Denardo, 2011, Chapter 1). Most linear programming problems can be solved in much less computational time than the non-linear programming problems. Therefore, in most cases, it is useful to reformulate non-linear programs as linear programs. There are several techniques to linearize non-linear programs (Asghari et al., 2022):

1. Transforming the non-linear equations or functions into exact linear equivalents.
2. Linear approximation, which finds an equivalent for the non-linear functions with the smallest deviation.

1.2.1.2.1 Transformation into exact linear equivalents The non-linear problem results from multiplication of variables, maximum or minimum operators, absolute value functions, etc. However, in this subsection, we consider only the linearization of a *minimum operator*. For other transformations, we refer to Asghari et al. (2022).

The minimum operator is an explicit non-linear term. Assume there is a non-linear minimum operator $z_i = \min_{i \in I}(x_i, y_i)$, where $I = \{1, ..., n\}$. We convert this structure by adding a new

continuous variable z_i, a set of new binary variables a_i and introduce the following constraints (Asghari et al., 2022):

$$z_i \leq x_i \qquad \forall i \in I \tag{1.1}$$
$$z_i \leq y_i \qquad \forall i \in I \tag{1.2}$$
$$x_i - y_i \leq M \cdot a_i \qquad \forall i \in I \tag{1.3}$$
$$z_i \geq x_i - M \cdot a_i \qquad \forall i \in I \tag{1.4}$$
$$z_i \geq y_i - M \cdot (1 - a_i) \qquad \forall i \in I \tag{1.5}$$
$$a_i \in \{0, 1\} \qquad \forall i \in I \tag{1.6}$$

Constraints 1.1 and 1.2 ensure that z_i is lower or equal than x_i and y_i. Constraints 1.3 enforce the binary variables a_i to 1, if y_i is greater than x_i. The next two constraints ensure that either $z_i = x_i$ if $a_i = 0$ (Constraints 1.4) or $z_i = y_i$ if $a_i = 1$ (Constraints 1.5). Constraints 1.6 define the variable y_i as binary.

Example: Assume there is a minimum-operator $r_{i,t} = \min(a_{i,t}, \sum_{j \in \mathcal{Z}} d_{i,j,t})$ that defines that the decision variables $r_{i,t}$ (rentals) from zone i at period t are the minimum of reachable vehicles $a_{i,t}$ (decision variables) in zone i at period t and the sum of demand $\sum_{j \in \mathcal{Z}} d_{i,j,t}$ from zone i to zone j at period t. The following Constraints 1.7 -1.13 linearize this minimum-operator:

$$r_{i,t} \leq a_{i,t} \qquad \forall i \in \mathcal{Z}, t \in \mathcal{T} \tag{1.7}$$
$$r_{i,t} \leq \sum_{j \in \mathcal{Z}} d_{i,j,t} \qquad \forall i \in \mathcal{Z}, t \in \mathcal{T} \tag{1.8}$$
$$\sum_{j \in Z} d_{i,j,t} - a_{i,t} < M \cdot q_{i,t} \qquad \forall i \in \mathcal{Z}, t \in \mathcal{T} \tag{1.9}$$
$$a_{i,t} - \sum_{j \in \mathcal{Z}} d_{i,j,t} \leq M(1 - q_{i,t}) \qquad \forall i \in \mathcal{Z}, t \in \mathcal{T} \tag{1.10}$$
$$r_{i,t} \geq a_{i,t} + M \cdot q_{i,t} \qquad \forall i, j \in \mathcal{Z}, t \in \mathcal{T} \tag{1.11}$$
$$r_{i,t} \geq \sum_{j \in Z} d_{i,j,t} + M \cdot (1 - q_{i,t}) \qquad \forall i \in \mathcal{Z}, t \in \mathcal{T} \tag{1.12}$$
$$q_{i,t} \in \{0, 1\} \qquad \forall i \in \mathcal{Z}, t \in \mathcal{T} \tag{1.13}$$

Constraints 1.7 and 1.8 limit the rentals of zone i at period t to the available vehicles $a_{i,t}$ at zone i at period t or to the given demand $\sum_{j \in \mathcal{Z}} d_{i,j,t}$ for zone i at period t. Constraints 1.9 and 1.10 determine the value of the binary variables $q_{i,t}$. $q_{i,t}$ is 1, if $\sum_{j \in Z} d_{i,j,t}$ is greater than $a_{i,t}$ and 0 if $a_{i,t}$ is greater than $\sum_{j \in Z} d_{i,j,t}$. Constraints 1.11 and 1.12 define the upper bounds for the rentals $r_{i,t}$. If $q_{i,t} = 1$ (that means $\sum_{j \in Z} d_{i,j,t} > a_{i,t}$), then Constraints 1.11 define the upper bounds, otherwise Constraints 1.12 define the upper bounds for the rentals.

1.2.1.2.2 Linear Approximation Approximations of non-linear functions with simple linear functions are one of the most common techniques for linearization. One of these approximations is a linear approximation to a known curve by dividing the curve into several parts and use linear interpolation for these parts. For other approximation techniques, we refer to Asghari et al. (2022). To integrate a piece-wise linear approximation, we need additional variables

and constraints. Thus, a function is replaced by a sequence of linear divisions. By using this technique, the previous non-linear program becomes linear and can be solved by common linear program solution techniques.

Example: We consider a non-linear function $f(a_{i,t})$ (see red dashed line in Figure 1.3) that yields a certain profit as a function of the number of available vehicles $a_{i,t}$ in zone i in period t. This function can be approximated by piece-wise linear functions (see blue line in Figure 1.3). The function is decomposed into K buckets (in Figure 1.3 $K = 5$) and for each bucket k, a linear function is found that minimizes the deviation from the non-linear function. Thus, the available vehicles are divided into K buckets with the bucket size of $\Delta\hat{a}_i^k$ (number of vehicles in bucket k, see Table 1.2). Each vehicle in a bucket k contributes with the common marginal value per vehicle ($\bar{v}_i^k$, see Table 1.2). In order to obtain the profit for five vehicles, the following calculation must be done: $2 \cdot 15 + 2 \cdot 10 + 1 \cdot 6 = 56$

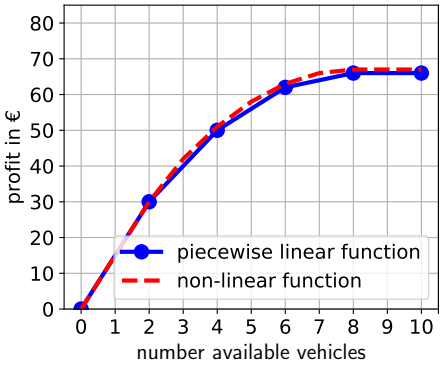

Figure 1.3: Non-linear and piece-wise linear function of profit in dependency of the number of available vehicles

k	$\Delta\hat{a}_i^k$	$\bar{v}_i^k$
1	2	15
2	2	10
3	2	6
4	2	2
5	2	0

Table 1.2: Values of different parts of the piece-wise function in Figure 1.3

1.2.2 Dynamic Programming

Dynamic programming is useful for sequential decision problems. A sequential decision problem is defined as "a problem in which a sequence of decisions must be made with each decision affecting future decisions" (Howard, 1966).

In these problems, making a decision alternates with gathering information. This means that decisions are made over time. In contrast to linear programming, the required information is not deterministic, but stochastic. Thus, the state of the system is also stochastic. This means, however, that with linear programming, all decisions are made at the beginning, whereas with dynamic programming, the decisions are made successively depending on the state of the system.

Example: Differentiated pricing determines all prices for every period of the day before the day begins. Dynamic pricing using (approximate) dynamic programming determines prices based on the current system state (Powell, 2011, Chapter 5).

1.2.2.1 Parts of Dynamic Programming

A dynamic program consists of five parts:

1. State variable: variables, we need to know.
2. Decision variables: variables, we control.
3. Exogenous information process: arriving information, representing randomness.
4. Transition function: describes how the state evolves.
5. Objective function: optimal profit or costs after a sequence of decisions.

We divide the entire problem into stages. In every stage t, we observe a state S_t and take an action a_t. Our transition function $S_{t+1} = S^M(S_t, a_t, W_t)$ describes in which state we evolve, depending on the current state S_t, the action a_t and the exogenous information W_t. Thus, we need a function $V_{t+1}(S_{t+1})$ that shows the value of the next stage until the end of the considered period. With this function, we evaluate every possible action a_t and choose the action a_t with the maximal expected contribution $C_t(S_t, a_t, W_t)$ at this stage t plus the expected contribution until the end of the considered period $V_{t+1}(S_{t+1})$. Thus, we search the action that solves the following function (Powell, 2011, Chapter 3):

$$a^*(S_t) = \arg\max_{a_t \in \mathcal{A}} \mathbb{E}(C_t(S_t, a_t, W_t) + V_{t+1}(S_{t+1})) \tag{1.14}$$

We explain each part of the dynamic program in a separate subsection.

1.2.2.1.1 State variable The goal of the state variable S_t is to "completely specify the instantaneous situation [...] "(Howard, 1966) for every stage t. Thus, it includes all information we need to know (Powell, 2011, Chapter 5), and it contains (fully or partially) information about the decisions made in the previous stages (Lew and Mauch, 2007, Chapter 1.1). The state includes every information that is either in the decision function, the transition function or the contribution function. However, if an information is in the state but in none of these three functions, this information can be dropped (Powell, 2011, Chapter 5). Powell (2011, Chapter 5) called this "minimally dimensioned function", which means that "our state variable is as compact as possible". The state space $\mathcal{S}_t$ contains all feasible states in stage t. It can be finite or infinite (Powell, 2011, Chapter 5.4).

Example: The state of a free-floating car sharing system at the beginning of period t consists of six vectors $S_t = (\vec{x}_t^v, \vec{y}_t^v, \vec{\tau}_t^v, \vec{x}_t^c, \vec{y}_t^c, \vec{\tau}_t^c)$. Each vector has the dimension $C \times 1$, where the i_t-th element in each vector describes a property of the i_t-th vehicle of the fleet. The first three vectors contain all information about the vehicles. The vectors $\vec{x}_t^v$ and $\vec{y}_t^v$ contain the x- and y-coordinates of each vehicle. If the vehicle is idle, it contains the current coordinates and otherwise it contains the coordinates where the vehicle is picked-up. The vector $\vec{\tau}_t^v$ contains the starting time of every vehicle. The entry of an idle vehicle is 0. The next three vectors contain information about the customers, where also the i_t-th element in each vector describes a property of the i_t-th vehicle of the fleet. The vectors $\vec{x}_t^c$ and $\vec{y}_t^c$ contain the x- and y-coordinates

of the customers opening the mobile application, if they picked-up a vehicle. If a vehicle is idle, the entry is 0. The vectors $\vec{\tau}_t^c$ describe the time point when the customers have requested the rentals. This means for a driving vehicle, when the customer initially opened the mobile application.

1.2.2.1.2 Action variable In every stage t, the decision maker has to choose an action $a_t \in \mathcal{A}$. This decision is the challenge of the dynamic programming. Thus, we need a decision function $a_t = A^\pi(S_t)$ that returns an action a_t at the given state S_t (Powell, 2011, Chapter 5.5). The action space $\mathcal{A}$ is the set of all possible actions a_t at the stage t and depends on the state S_t (Lew and Mauch, 2007, Chapter 1.1).

Example: The car sharing system provider decides about the prices for the vehicles. Thus, the action variable is the optimal price vector including prices for each vehicle.

1.2.2.1.3 Exogenous Information The exogenous information W_t changes the state of the system. The main challenge is to make decisions before all the information is available. The exogenous information W_t becomes available during interval t. It can be a single variable or a collection of variables (Powell, 2011, Chapter 5.6).

Example: One exogenous information after the prices are set is, if and which vehicle is picked-up: $W_t(S_t, i_t, t)$.

1.2.2.1.4 Transition Function The transition function defines how the system evolves after the decision is made and the exogenous information arrived (Powell, 2011, Chapter 5.7). This defines the state in the next stage (Lew and Mauch, 2007, Chapter 1.1): $S_{t+1} = S^M(S_t, a_t, W_t)$. Thus, the state of the system at stage $t+1$ depends on the state S_t at stage t, the action a_t, that is made at stage t and the exogenous information W_t arriving after the action a_t was made at stage t (Powell, 2011, Chapter 5.7).

Example: The transition function contains the state of stage (in this example micro period) t, the customer's location (x_t^O, y_t^O), the chosen vehicle i_t (0 indicates that the customer decides against renting a vehicle), and the returned vehicle j_t together with its drop-off location (x_t^D, y_t^D), i.e.,

$$S_{t+1} = S_{t+1}\big(S_t, (x_t^O, y_t^O), i_t, (x_t^D, y_t^D), j_t\big). \tag{1.15}$$

Please note that this transition function is not comparable to the usual transition functions, because the specific choices i_t depend on the price vector $\vec{p}_t$. More precisely, the action of the provider does not directly affect the choice of the customer. That means, the state S_{t+1} is *probabilistically dependent* (Powell, 2011, Chapter 3) on the pricing decision $\vec{p}_t$.

1.2.2.1.5 Objective Function The objective function evaluates the profit or costs after a sequence of decisions (Lew and Mauch, 2007, Chapter 1.1). It is an indicator how well the optimization is conducted. However, we can maximize a contribution (or profit) $C_t(S_t, a_t, W_t)$ which depends on the action a_t, the state S_t and the exogenous information W_t at stage t. This means the contribution (profit) is random and the decision maker has to wait until he receives information about the realization. Thus, he decides about an action a_t with no access to the

exogenous information W_t. Therefore, action a_t considers the **expected** contribution (profit): $C_t(S_t, a_t) = \mathbb{E}[\hat{C}_{t+1}(S_t, a_t, W_t)|S_t]$ (Powell, 2011, Chapter 5.8).

Example: We optimize the expected profit of a car sharing system provider: $C_t = \mathbb{E}[C_{t+1}(S_t, i_t, W_t)]$. The profit depends on the state S_t, the chosen vehicle i_t and the exogenous information W_t.

1.2.2.1.6 Recursive Bellman Equation We can formulate the recursive Bellman Equation as follows:

$$V_t(S_t) = \max_{a_t} \mathbb{E}[C_t(S_t, a_t, W_t) + V_{t+1}(S_{t+1}|S_t, a_t)] \tag{1.16}$$

s.t.

$$S_{t+1} = S_t^M(S_t, a_t, W_t) \tag{1.17}$$

$$a_t \in A_t(S_t) \tag{1.18}$$

with the boundary condition: $V_T(S_T) = 0$. The standard approach to solve the Bellman Equation is backwards recursion.

Example: For a detailed example please see Chapter 5.

1.2.2.2 Approximate Dynamic Programming

The main drawback of the dynamic programming is the "curse of dimensionality". This describes the fact, that the state S_t can be very large, which makes a backwards recursion computationally complex (Talluri and Van Ryzin, 2004). Powell (2011, Chapter 1.2) defines three curses of dimensionality:

1. State space.
2. Exogenous information space.
3. Action space.

The dynamic pricing problems in Chapters 5 and 6 suffer from the curse of dimensionality. More precisely, the state space of the dynamic programs described in in these chapters depends, among other things, on where customers arrive and the current distribution of vehicles within the business area. Since we consider a free-floating SMS and the business area is not divided into zones, the business area is continuous. Thus, the customer can arrive and the vehicle can be dropped-off at any location. Therefore, the state is continuous and cannot be discretized.

The space of exogenous information of the dynamic pricing programs described in Chapters 5 and 6 contains at maximum two information. First, if and which vehicle was picked-up by a customer and second, if and which vehicle is dropped-off by another customer.

The action space of these dynamic pricing programs depends on the number of possible discrete prices $|\mathcal{M}|$ and vehicles $|\mathcal{C}|$. Therefore, the size of the action space for this problem is $|\mathcal{M}|^{|\mathcal{C}|}$, implying that the calculation time in one single stage of the dynamic program increases exponentially with the number of vehicles $|\mathcal{C}|$ and polynomially with the number of price points $|\mathcal{M}|$.

In order to circumvent the curse of dimensionality, approximate dynamic programming is often used. One of the most commonly used approximation techniques is the *value function approximation*.

Powell (2011, Chapter 6.4) describes the value function approximation as the "most powerful and visible method for solving dynamic programs [which] involves replacing the value function $V_t(S_t)$ with an approximation of some form." Three different broad classes of approximation strategies exist that we could use. They are outlined in the following:

- Lookup Tables: Lookup tables contain a stored value for every discrete state s. Thus, they are only useful for discrete states. It is possible to update these values by the following function: $\bar{V}^n(S^n) = (1-\alpha) \cdot \bar{V}(S^n) + \alpha \cdot \hat{V}(S^n)$. The benefit is that if we have a discrete state space, we can approximate $V(S)$ very well. The disadvantage is that the value for one state s does not provide information about another state s'.

- Parametric Models: Specific kinds of regression models can be used for approximation. For this, we have to identify the important features, so that we can specify a value function approximation using the following function: $\bar{V}(S) = \sum_{f \in \mathcal{F}} \Theta_f \cdot \phi_f(S)$, where Θ_f is a vector of regression parameters and $\phi_f \forall f \in \mathcal{F}$ is a function, that draws information from S. The benefit is that parametric models are powerful. The parameters of a vector Θ_f can be estimated by a relative small number of observations. The disadvantage is that it is necessary to choose the right functions ϕ_f for a good approximation.

- Non-parametric Models: Non-parametric models are hybrids between lookup tables and parametric models. There are many non-parametric models, but all use simple models to present small regions of a function. The benefit is that we do not need to specify the structure of a parametric model. They also provide accurate approximations if we have enough observations. Some examples for non-parametric models are *k-nearest neighbor*, *kernel regression* or *local polynomial regression*.

In Chapters 5 and 6, we use non-parametric models (kernel regression) to approximate the value function.

Bibliography

Asghari M, Fathollahi-Fard AM, Mirzapour Al-E-Hashem SMJ, Dulebenets MA (2022) Transformation and linearization techniques in optimization: A state-of-the-art survey. *Mathematics* 10(2): 283

Destatis (2018a) Global Automotive Supplier Study 2018. Accessed July 2, 2023, https://de.statista.com/statistik/daten/studie/796395/umfrage/prognose-des-fahrzeugabsatzes-fuer-new-mobility-service-nach-regionen/.

Destatis (2018b) Bike-sharing boomt. Accessed July 2, 2023, https://de.statista.com/infografik/15138/verbreitung-von-bike-sharing-weltweit/.

Denardo EV (2011) Linear programming and generalizations: A problem-based introduction with spreadsheets, 1st ed. (Springer, New York, NY)

Gönsch J, Kruk N (2017) Shared Mobility Systeme (Shared Mobility Systems). *Wirtschaftswiss. Stud.* 46(6): 9–14.

Howard RA (1966) Dynamic programming. *Manag. Sci.* 12(5): 317–348.

Lew A, Mauch H (2007) Dynamic programming: A computational tool, 1st ed. (Springer, New York, NY).

Poler R, Mula J, Díaz-Madroñer, M (2014) Operations research problems statements and solutions, 1st ed. (Springer, London, GB).

Powell, WB (2011) Approximate dynamic programming: Solving the curses of dimensionality, 2nd ed. (John Wiley & Sons, Hoboken, NJ).

Talluri KT, Van Ryzin GJ (2004) The theory and practice of revenue management, 1st ed. (Springer, Boston, MA).

Chapter 2

Differentiated Pricing of Shared Mobility Systems Considering Network Effects

2.1 Introduction

Shared mobility systems (SMSs) such as car sharing or bike sharing offer flexible short-term rentals in many major cities of the world. Globally, the number of car sharing vehicles has increased from 11,500 in 2006 to 112,000 in 2015, with 427,000 cars forecast for 2025 (ACEA and Frost & Sullivan, 2016). In terms of annual growth, projections for the global car sharing market were recently at 30%. Also, bike sharing systems have experienced a strong market growth of 20% per year (Roland Berger Strategy Consultants, 2014). Their increasing importance, as well as the challenge to operate such systems profitably, have led to an ongoing academic interest, as survey papers by Jorge and Correia (2013) and Laporte, Meunier, and Wolfler Calvo (2018), among others, demonstrate.

As the fleet is the most important cost driver, high utilization is key to profitably operating an SMS. This, however, is difficult to achieve due to existing *imbalances* between supply and demand. First, customers' demand varies across time and space. Second, a rental not only instantly decreases available capacity at its origin, but also influences future supply across the whole system. These *supply-side network effects* result from the fact that modern systems mostly allow one-way trips, that is, the customer does not need to return the vehicle to the same location as where the trip originated. A practical consequence is that in most real-world systems, because of asymmetric demand, rental vehicles tend to accumulate at certain locations, usually in the city's outskirts.

The described imbalances are widely addressed by supply-oriented operational control mechanisms such as vehicle relocation. However, as relocations are quite costly, pricing has been identified as a promising demand-oriented means in practice as well as in research. Most recently, Huang et al. (2020) have compare relocation and pricing optimization (also see Di Febbraro, Sacco, and Saeednia (2012); Jorge, Molnar, and Correia (2015); Lippoldt, Niels, and Bogenberger (2018, 2019)). While the existing research tends to focus on pricing problems with a high degree of details and high pricing flexibility, current practical implementations strive for simple, more restrictive pricing mechanisms that are more easily applied and communicated to customers. Interestingly, the restriction to simple pricing mechanisms while network effects prevail, turns out to create its own challenges.

Three dimensions characterize pricing mechanisms for SMSs, all of which impact the mentioned trade-off between flexibility and practicability, as explicated below.

- *Pricing basis:* The first pricing dimension concerns the basis on which rental fees are calculated. The rental duration is usually central. *Usage-based pricing*, for example with prices in cents per minute, is most commonly used, therefore we focus on this in our work. The final rental fee is then determined by the rental duration and the price that is valid at the start of the journey. In addition, some SMS providers offer *package pricing* for long rentals of multiple hours, fixed rental fees, or monthly membership fees that are not linked to usage.

- *Spatio-temporal pricing features:* The second pricing dimension refers to whether the SMS provider sets prices depending on a rental's time and the location of start (origin), end (destination) or a combination of these (trip). Note that in this terminology, origin and

destination consider both spatial and temporal aspects, i.e., two rentals that begin at the same location, but at different times of the day, have different origins. *Trip-based* pricing mechanisms use prices which depend on origin as well as destination, allowing a very detailed level of pricing. By contrast, *origin-based* and *destination-based* mechanisms only depend on the origin or destination, respectively. Although trip-based pricing may seem most powerful, there are several practical disadvantages. First, the customer's destination is usually unknown in advance (Lippoldt, Niels, and Bogenberger, 2018, 2019). Second, pricing mechanisms that include the destination become much more complicated (Lippoldt, Niels, and Bogenberger, 2018). Third, prices need to be transparently communicated to the customer before a rental. Attempts to prepare all origin-destination combinations in a price table are impractical. The SMS provider then would have to ask a user to (truthfully) disclose the intended destination, which would considerably change the user experience of most real SMSs and thus would be unacceptable in most practical settings. Due to these drawbacks, trip-based pricing seems not to be realizable in practice, and we are not aware of a single SMS provider who has actually implemented such trip-based pricing (see Appendix 2.I). This paper, therefore, focuses on origin-based pricing as a mechanism most commonly used in current practice, because the SMS provider then requires less information than otherwise. It also entails a more efficient user-provider interaction process and fairly simple implementation.

- *State dependency:* The third pricing dimension distinguishes between dynamic and differentiated pricing. *Dynamic pricing* mechanisms determine prices in real-time and have the theoretical advantage of recurrently adjusting prices to the current state of the system, in particular the current spatial vehicle distribution. *Differentiated pricing* mechanisms also allow for temporal and spatial price variations, but prices are determined off-line and do not depend on the current state of the system (Agatz et al., 2013). Note that some authors use the term static pricing for this pricing mechanism (Waserhole and Jost, 2012). For SMSs, these differentiated pricing mechanisms, on which we focus in this paper, are preferred in practice. This is mainly because differentiated mechanisms are easier to implement and again, quite importantly, easy to communicate transparently to customers, for example via price tables.

The problem we consider in this paper can therefore be summarized as follows: A one-way SMS provider applies *origin-based differentiated pricing* by varying minute prices across different locations and depending on the time of day in order to scale demand. Consistent with the common situation in practice, there are no parallel operational steering means beyond pricing (*pure pricing assumption*). In particular, there is no availability control, i.e., whenever vehicle and customer match, a rental results. However, if at a certain location and point in time, demand exceeds supply, demand for all destinations is served proportionally (*proportional demand fulfilment assumption*) and excess demand is lost. This can be interpreted as customers with different destinations arriving in random order. Resulting rentals evoke network effects in the aforementioned sense of influencing supply at their destinations later in the day. To ensure simple and transparent customer communication, prices must originate from a predefined discrete price set. Given this setting, the optimization task is now to set prices optimally for all location-

time combinations, with the SMS provider's overall objective being profit maximization. We refer to this optimization problem as the *origin-based differentiated pricing problem* (OBDPP) in SMSs.

Given its broad relevance to practice and across all SMS types, it is remarkable that the problem has not yet been addressed in the academic literature. Our contributions, more precisely, are the following:

- To the best of our knowledge, we are the first to focus on origin-based differentiated pricing, which is highly relevant for various SMS types in practice because the corresponding pricing mechanism is transparent to the customer and relatively easy for the provider to implement. In addition, we include other novel problem characteristics such as a realistic modeling of the SMS provider's control ability. The problem's practical relevance is ensured by, among other things, close cooperation we have established with Share Now, Europe's largest car sharing provider operating in eight countries and 16 cities (Share Now, 2021).

- Second, we prove that the problem is NP-hard and therefore computationally intractable for real-life instances. While some authors (e.g. Waserhole and Jost (2012); Ren et al. (2019)) discuss the computational effort SMS pricing problems require, to the best of our knowledge, we are the first to derive a formal proof of computational complexity for such a problem, to validly justify the development of solution heuristics.

- Third, we develop a problem-specific, temporal decomposition heuristic based on approximate dynamic programming (ADP). The approach is scalable and applicable to real-world problems. Its integrated value function approximation (VFA) anticipates the network effects of the entire problem endogenously in the optimization, although only parts of the original problem are explicitly optimized during the decomposition. This is enabled by specifying piece-wise linear VFAs that reflect the available vehicles' decreasing marginal value while maintaining linearity for efficiently integrating it in the decomposed optimization problems.

- Fourth, we generate a number of relevant managerial insights based on extensive computational experiments with different problem sizes, considering many relevant parameter settings and demand patterns, and on a real-world case study of Share Now. In particular, we demonstrate that origin-based pricing is capable of substantially increasing profit compared to the de facto industry standard of constant uniform pricing. Further, we show that our approach can adequately capture both short-term and long-term network effects due to its VFA.

The remainder of the paper is organized as follows. In Section 2.2, we review the relevant literature, focusing on pricing problems. In Section 2.3, we formalize the origin-based differentiated pricing problem, derive its model formulation, and discuss its complexity. We present the proposed solution approach in Section 2.4. Section 2.5 contains the computational experiments, and Section 2.6 presents the Share Now case study. Based on the obtained results, Section 2.7 discusses the managerial insights we derived. Section 2.8 concludes the paper and gives an outlook on future research. The appendix contains the complexity proof, as well as additional data and results for the computational experiments and case study.

2.2 Literature Review

General overviews on SMS problems have been given in survey papers on bike sharing (e.g. DeMaio (2009), Fishman, Washington, and Haworth (2013), Ricci (2015)), car sharing (e.g. Jorge and Correia (2013), Ferrero et al. (2015a), Ferrero et al. (2015b), Illgen and Höck (2019)), and shared mobility in general (e.g. Laporte, Meunier, and Wolfler Calvo (2015, 2018)). We begin by reviewing the literature on differentiated pricing problems in Section 2.2.1 and dynamic pricing problems in Section 2.2.2. Then, we give a detailed delineation of our work from the papers most closely related in Section 2.2.3. Please note that since most pricing mechanisms are not limited to a single SMS type like bike sharing or car sharing, we refrain from mentioning whether the authors considered a specific SMS type. Also, we do not state explicitly whether the authors considered other optimization problems besides pricing, such as fleet sizing or relocation.

2.2.1 Differentiated Pricing

The literature on optimizing differentiated pricing for SMSs focuses on trip-based pricing.

Waserhole and Jost (2012) propose a fluid approximation for the revenue-maximizing trip-based pricing problem, which is the limit of the stochastic model when demand and supply are scaled to infinity. In another paper from the same research group, Waserhole, Jost, and Brauner (2012) present a model optimizing revenue in a single scenario, that is, they focus on solving the discrete problem with perfect hindsight information. This can be used to derive an upper bound for the stochastic problem. They also consider pick-up and drop-off fees. To our knowledge, this paper is the only one in the related literature that has investigated computational complexity.

The following papers apply a certainty equivalent approach that replaces stochastic quantities (i.e. rentals) with a deterministic value (Bertsektas, 2019, chapter 2.3.2). Jorge, Molnar, and Correia (2015) use a continuous (expected) demand function and round rentals to the next integer value in the model. They formulate a profit-maximizing trip-based pricing problem as mixed-integer nonlinear program and propose an iterated local search meta-heuristic solution approach. Building on this work, Ren et al. (2019) integrate the vehicle-grid interaction of electric vehicles into the model, and use a nonlinear solver for the resulting problem. The next two papers simply require rentals to be integral values not exceeding a continuous demand function. Xu, Meng, and Liu (2018) formulate a mixed-integer nonlinear and non-convex program. On this basis, they develop a computationally tractable convex model which has the same objective in the optimum, and solve the latter arbitrarily close to optimality. Huang et al. (2020) use a deterministic, continuous demand function. They discuss two pricing approaches that they compare to relocation. While the first is a classic trip-based pricing approach, the second involves simultaneously optimizing pick-up and drop-off fees. They formulate mixed-integer nonlinear programs and solve them with a combined rolling horizon and iterated local search heuristic, which the authors point out can also be applied in a dynamic context.

Lu et al. (2021) use yet another formulation, i.e., a bi-level nonlinear program based on a fluid approximation in which the provider determines profit-maximizing prices on the upper level. The lower level's objective minimizes customers' total cost by a binary choice between two modes of transportation, namely shared vehicles and private cars. In an odd interpretation of a

discrete choice model, rentals are additionally bounded from above by a logit model. The authors transform the bi-level problem to a single-level one using Karush-Kuhn-Tucker conditions, and heuristically solve it with a genetic algorithm.

Finally, there are two other more distant lines of work, parallel to the aforementioned. One analytically investigated the steady state of highly stylized, stationary settings with time-invariant demand using techniques from closed-queuing networks. Waserhole and Jost (2016) maximize the number of trips taken, assuming null travel time. They approximate the problem and show a bound for the solution quality. In a working paper, Banerjee, Freund, and Lykouris (2016) basically extended this result using a different proof and approximation techniques. A second parallel line of work considered pricing in SMSs but without optimization. For example, Brendel et al. (2017) developed a framework for a decision support system that could help to define contingent areas with low or high demand. The provider can then manually choose pick-up and drop-off discounts and fees for these areas.

2.2.2 Dynamic Pricing

Dynamic pricing problems make up the majority of pricing problems considered in the literature on SMSs. We structure the discussion along the spatio-temporal pricing features (second dimension introduced in Section 2.1). We begin with the dynamic mechanisms that exclusively use either origin-based or destination-based pricing. Next we refer to a class of approaches that simultaneously considers dynamic origin- and destination-based pricing, after which we discuss those using classic trip-based pricing.

Giorgione, Ciari, and Viti (2019) are the only scholars to have considered pure origin-based dynamic pricing. They analyze a dynamic pricing policy which links the price to the availability of vehicles at a rental's origin and demonstrate the advantage of dynamic pricing over a constant uniform price.

Destination-based dynamic pricing was first investigated by Di Febbraro, Sacco, and Saeednia (2012). In a first step, they determine a service maximizing fleet distribution, while the second step determines optimal drop-off discounts that incentivize customers to return their vehicle to a specific destination. Following up on this work, Di Febbraro, Sacco, and Saeednia (2019) changed the second step's objective to profit maximization. Brendel, Brauer, and Hildebrandt (2016) proposed a dynamic drop-off incentive for users who accept the option of returning their vehicle to a different location than that initially intended. Pfrommer et al. (2014) suggest a model predictive control approach. The objective is a weighted sum of the deviation from an optimal vehicle distribution and the cost of incentive payments. Wagner et al. (2015) propose a system that dynamically suggests alternative rental destinations, and incentivizes customers with free minutes. Chemla et al. (2013) consider a service maximizing fleet utilization, measured by successful and unsuccessful intended customer interactions like finding an available vehicle. They suggest dynamic drop-off fees to influence customer behavior. Marecek, Shorten, and Yu (2016) propose a dynamic pricing scheme that derives drop-off fees to incentivize drivers to distribute cars more evenly.

Some authors simultaneously consider dynamic origin- and destination-based pricing. Singla et al. (2015) investigate the problem of minimizing customers' dissatisfaction about not finding

an available vehicle or parking slot under a given budget restriction. They propose dynamic pick-up and drop-off fees to incentivize users to choose an alternative origin or destination. Kamatani, Nakata, and Arai (2019) take a reinforcement learning approach to derive dynamic pick-up and drop-off fees with the objective of maximizing fleet utilization. Wang and Ma (2019) consider the objective of keeping inventories in a certain range, and they determine dynamic pick-up and drop-off rewards and charges by a quadratic programming formulation.

Finally, there are papers that use a dynamic trip-based pricing mechanism. Barth, Todd, and Xue (2004) consider maximizing fleet utilization by incentivizing customers with the same journey to share a ride or to split up and use multiple vehicles. Prices are reduced according to a simple rule-based mechanism without any optimization. For example, if two users are asked to take two cars, each pays half-price. Angelopoulos et al. (2016) consider the problem of dynamically setting budget-constrained trip-based incentives in an SMS to balance the vehicle inventory. The approach uses graph-theoretic modeling and proposes a heuristic method to solve the resulting weighted packing problem. Haider et al. (2018) dynamically set trip-based prices to minimize the number of unbalanced stations, that is, SMS stations with a surplus or lack of vehicles, to ease the subsequent need to reposition using trucks. In their bi-level programming approach, the upper level sets prices and minimizes the imbalance, while the lower level represents customers' cost minimization route choices. They convert the problem to a single-level problem, and propose a heuristic which iteratively adjusts prices and customer decisions.

2.2.3 Delineation from Closest Related Work

In this section, we discuss that the closest related works cannot be simply adapted to meet the given characteristics of the origin-based differentiated pricing problem this paper considers.

Among the papers discussed here, which all focus on trip-based pricing, we identify two groups that differ regarding the modeling of demand and rentals. For both groups, we have to conclude that central structural differences impede an inclusion of the OBDPP's characteristics.

The first group of papers does not distinguish between demand and rentals. It encompasses Jorge, Molnar, and Correia (2015); Ren et al. (2019); Waserhole and Jost (2012), as well as Haider et al. (2018) who study differentiated and dynamic trip-based pricing. The former three consider unrestricted, continuous prices that scale demand. Thus, it is always optimal to set prices such that capacity is not scarce and, so that demand will equal rentals. The key issue is that with the restricted and especially discrete price points prevalent in practice, this equivalence of demand and rentals no longer holds and is usually even infeasible. Allowing for discrete prices requires a differentiation between demand and rentals, as well as explicitly incorporating the *pure pricing* and *proportional demand fulfillment assumptions*. Thus it would require major modeling changes.

By contrast, Haider et al. (2018) do not scale demand by continuous prices; they only influence customers' route choices in a bi-level problem with an infinite fleet size. Moreover, their model is optimistic, that is, if customers are indifferent, the provider chooses the itinerary for them. While including discrete prices with demand scaling, profit maximization, and origin-based pricing in their model seems possible, this alone would yield an entirely new model.

However, there are two key issues. First, incorporating a limited fleet size would also necessitate accounting for the *pure pricing assumption*. Second, the problem that we consider with its *proportional demand fulfillment assumption* is neither optimistic nor pessimistic. As optimistic approaches are usually the most tractable ones, including these two assumptions appears to be complex.

The second group of papers encompasses Xu, Meng, and Liu (2018), Lu et al. (2021), and Huang et al. (2020), who distinguish between demand and rentals in their models, but do not satisfy the *pure pricing* and *proportional demand fulfillment assumptions*. Xu, Meng, and Liu (2018) and Huang et al. (2020) include demand scaling with continuous prices. Their models bound rentals only from above by supply and demand. Thus, the provider can freely choose the number of rentals going to the different destinations up to these bounds, as it is beneficial in the long term. This violates the *pure pricing* and *proportional demand fulfilment assumptions*. An extension of their models that includes the assumptions in respective constraints seems possible, but the changes would be so extensive that basically any network flow model could be used.

Slightly similar to Haider et al. (2018), Lu et al. (2021) do not scale total demand by continuous prices, but only influence customers' mode choices on the lower level of their bi-level problem, where they work with the assumption of customers collectively minimizing cost. As in Haider et al. (2018), the key issue is that the model is optimistic. If customers' costs are the same for carsharing and private cars on a trip, the provider can choose the number of customers up to the logit model's bound. Even more importantly, if this holds for several trips, the provider can freely choose the number of customers for each trip. Again, there is no clear path to include the two assumptions.

Note that the work of Giorgione, Ciari, and Viti (2019) is not closely related. Although they do analyze a pure origin-based pricing problem, they do so without pricing optimization, without considering network effects, and in a dynamic context which fundamentally differs from the differentiated pricing problem that we analyze.

2.3 The Origin-Based Differentiated Pricing Problem in Shared Mobility Systems

In this section, we define and analyze the origin-based differentiated pricing problem in SMSs (OBDPP). Section 2.3.1 formally states the problem and introduces the notation. In Section 2.3.2, we present a mixed-integer linear programming formulation for the OBDPP based on a fluid network flow model. Section 2.3.3 investigates the computational complexity of the problem.

2.3.1 Problem Statement and Notation

We take the perspective of a one-way SMS provider whose task is to apply differentiated pricing to determine minute prices over a given time interval, for example, one day. The SMS consists of locations $\mathcal{Z} = \{1, 2, \ldots, Z\}$. The considered time interval is discretized into periods $\mathcal{T} = \{0, 1, \ldots, T-1\}$. For all rentals which originate at a specific combination of location $i \in \mathcal{Z}$ and period $t \in \mathcal{T}$ the same minute price p_{it} is charged, regardless of a trip's destination (origin-based pricing). The minute prices have to be selected from M given price points $p^m \in \mathbb{R}_0^+$ with $m \in \mathcal{M} = \{1, 2 \ldots, M\}$. Now, the provider's objective is to set the prices such that they maximize the profit generated from the resulting rentals over the given time interval. The corresponding solution to the problem – i.e., the optimized prices – can be presented in the form of a price table, as shown in Table 2.1.

On a more detailed level, additional key aspects of the problem definition are the assumptions regarding demand, rental realization, and system dynamics, which we now discuss in more detail.

- *Demand:* We considered the demand and its dependence on the price points on an aggregate level as described, for example, in Talluri and van Ryzin (2004, chapter 7.3). More specifically, the base demand for every location-location-time combination – from location i to location j at period t – is given by $d_{ijt} \in \mathbb{R}_0^+$ and builds the base demand matrix $\mathbf{d} = [d_{ijt}]_{Z \times Z \times T}$. Each entry is scaled by an i-j-t specific sensitivity factor f_{ijt}^m, depending on the price p^m, to obtain the actual demand $d_{ijt}^m = d_{ijt} \cdot f_{ijt}^m$. The price where $f_{ijt}^m = 1$ and thereby $d_{ijt}^m = d_{ijt}$ is denoted as base price.

- *Rental realization:* The rentals r_{it}^m that realize for a specific origin, meaning a location-time (i-t) combination, and price p_{it}, are determined by the minimum of the available vehicle count a_{it} and the prevailing actual demand, meaning $r_{it}^m = \min(a_{it}, \sum_{j \in \mathcal{Z}} d_{ijt}^m)$. Note that this implicit realization of rentals based on the prevailing supply and demand implies that the SMS provider can only influence rentals via prices (*pure pricing assumption*). We assume that rentals at period t in location i, that is, r_{it}^m, split up proportionally to demand regarding their destination into the i-j-t specific rentals r_{ijt}^m. This means that we model r_{ijt}^m as a fraction of r_{it}^m proportional to $d_{ijt}^m / \sum_{j \in \mathcal{Z}} d_{ijt}^m$ (*proportional demand fulfillment assumption*). We assume rentals have a variable cost per minute $c \in \mathbb{R}_0^+$.

- *Dynamics:* We think of the SMS dynamics as a sequential process with successive periods, as it is done in practice and commonly found in the literature, for example in Xu, Meng,

		$\mathcal{T}$				
		0	1	2	...	$T-1$
$\mathcal{Z}$	1	p_{10}	p_{11}	p_{12}	...	$p_{1(T-1)}$
	2	p_{20}	p_{21}	p_{22}	...	$p_{2(T-1)}$
	...	...	...	...	...	...
	Z	p_{Z0}	p_{Z1}	p_{Z2}	...	$p_{Z(T-1)}$

Figure 2.1: Structure of the origin-based, differentiated price table

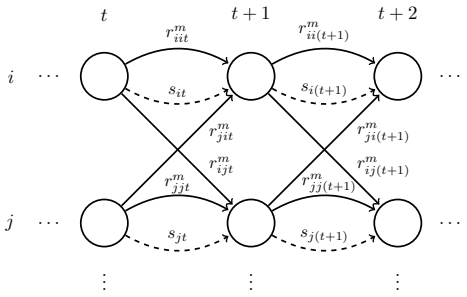

Figure 2.2: Structure of the spatio-temporal network (columns: time periods, rows: locations)

and Liu (2018). More precisely, we assume that rentals start at the beginning of a period and the vehicles, at latest, always become available again at the beginning of the respective next period. The average rental duration $l_{ij} \in \mathbb{R}_0^+$ (in minutes) is shorter than the period length, but can vary according to the spatial distance between different locations i-j.

Finally, note that the initial vehicle distribution at the beginning of the considered time interval (beginning of the day) $\hat{a}_{i0}$ for every location i is given as a consequence of regular relocation activity (usually performed during the night). Thus, fixed costs related to these regular relocations are out of the problem's scope.

2.3.2 Mathematical Model

We formulate the OBDPP based on a deterministic network flow problem in which vehicles move through a spatio-temporal network (Figure 2.2). The resulting fluid model considers expected values of the vehicle movements and available vehicles in the SMS. Deterministic models for pricing decisions are standard in pricing and revenue management (Talluri and van Ryzin, 2004, chapter 3.3.1), and are also applied in SMS optimization (see e.g., Illgen and Höck (2019); Waserhole and Jost (2012)).

The model contains multiple continuous variables: As depicted in Figure 2.2, rentals from location i to location j in period t that are charged with minute price p^m are represented by the continuous variable r^m_{ijt}; these build the elements of the vector $\mathbf{r} = [r^m_{ijt}]_{Z\times Z\times T\times M}$. Vehicles that are not rented in location i at period t and therefore remain in that location are represented by the continuous variable s_{it} and are the elements of $\mathbf{s} = [s_{it}]_{Z\times T}$. The number of vehicles at the beginning of a period t in a certain location i is represented by the continuous variable a_{it} with the corresponding vector $\mathbf{a} = [a_{it}]_{Z\times(T+1)}$.

Additionally, the model contains the following binary decision variables. The pricing decisions build the elements of $\mathbf{y} = [y^m_{it}]_{Z\times T\times M}$. A specific decision variable y^m_{it} takes the value 1, if and only if price p^m is set in location i at period t. To formulate all necessary constraints – in particular that vehicle movements and availabilities are the result of existing demand and selected prices (see *pure pricing* and *proportional demand fulfillment assumptions* in Sections 2.1 and 2.3.1) – additional auxiliary binary variables are required, represented by $\mathbf{q} = [q_{it}]_{Z\times T}$.

Based on the decision variables and the parameters defined so far, the model can be stated

as a mixed-integer linear program as follows:

$$\max_{\mathbf{y},\mathbf{q},\mathbf{r},\mathbf{a},\mathbf{s}} \quad \sum_{t\in\mathcal{T}}\sum_{i\in\mathcal{Z}}\sum_{j\in\mathcal{Z}}\sum_{m\in\mathcal{M}} r_{ijt}^m \cdot l_{ij} \cdot (p^m - c) \tag{2.1}$$

$$\text{s.t.} \quad a_{it} = \sum_{j\in\mathcal{Z}}\sum_{m\in\mathcal{M}} r_{ijt}^m + s_{it} \qquad \forall i \in \mathcal{Z}, t \in \mathcal{T} \tag{2.2}$$

$$\sum_{i\in\mathcal{Z}}\sum_{m\in\mathcal{M}} r_{ijt}^m + s_{jt} = a_{j(t+1)} \qquad \forall j \in \mathcal{Z}, t \in \mathcal{T} \tag{2.3}$$

$$a_{i0} = \hat{a}_{i0} \qquad \forall i \in \mathcal{Z} \tag{2.4}$$

$$\sum_{m\in\mathcal{M}} y_{it}^m = 1 \qquad \forall i \in \mathcal{Z}, t \in \mathcal{T} \tag{2.5}$$

$$r_{ijt}^m \leq d_{ijt}^m \cdot y_{it}^m \qquad \forall i, j \in \mathcal{Z}, t \in \mathcal{T}, m \in \mathcal{M} \tag{2.6}$$

$$r_{ijt}^m \leq d_{ijt}^m / \sum_{k\in\mathcal{Z}} d_{ikt}^m \cdot a_{it} \qquad \forall i, j \in \mathcal{Z}, t \in \mathcal{T}, m \in \mathcal{M} \tag{2.7}$$

$$\sum_{j\in\mathcal{Z}}\sum_{m\in\mathcal{M}} d_{ijt}^m \cdot y_{it}^m - a_{it} \leq \bar{M} \cdot q_{it} \qquad \forall i \in \mathcal{Z}, t \in \mathcal{T} \tag{2.8}$$

$$\sum_{j\in\mathcal{Z}}\sum_{m\in\mathcal{M}} -d_{ijt}^m \cdot y_{it}^m + a_{it} \leq \bar{M} \cdot (1 - q_{it}) \qquad \forall i \in \mathcal{Z}, t \in \mathcal{T} \tag{2.9}$$

$$\sum_{m\in\mathcal{M}} d_{ijt}^m \cdot y_{it}^m \leq \sum_{m\in\mathcal{M}} r_{ijt}^m + \bar{M} \cdot q_{it} \qquad \forall i, j \in \mathcal{Z}, t \in \mathcal{T} \tag{2.10}$$

$$s_{it} \leq \bar{M} \cdot (1 - q_{it}) \qquad \forall i \in \mathcal{Z}, t \in \mathcal{T} \tag{2.11}$$

$$y_{it}^m \in \{0, 1\} \qquad \forall i \in \mathcal{Z}, t \in \mathcal{T}, m \in \mathcal{M} \tag{2.12}$$

$$q_{it} \in \{0, 1\} \qquad \forall i \in \mathcal{Z}, t \in \mathcal{T} \tag{2.13}$$

$$r_{ijt}^m \in \mathbb{R}_0^+ \qquad \forall i, j \in \mathcal{Z}, t \in \mathcal{T}, m \in \mathcal{M} \tag{2.14}$$

$$s_{it} \in \mathbb{R}_0^+ \qquad \forall i \in \mathcal{Z}, t \in \mathcal{T} \tag{2.15}$$

$$a_{it} \in \mathbb{R}_0^+ \qquad \forall i \in \mathcal{Z}, t \in \{0, 1, \ldots, T\} \tag{2.16}$$

The objective function (2.1) maximizes the contribution margin across all periods and results from the rentals at different prices minus the variable costs. Note that since decisions related to fixed costs cannot be made at this point and are therefore out of scope, maximizing the contribution margin is equivalent to optimizing profit here. Constraints (2.2) and (2.3) form the flow conservation that ensure a constant fleet size at all periods. More precisely, (2.2) connect the available vehicles a_{it} in location i at the beginning of period t to the rentals at all possible prices r_{ijt}^m that originate at this specific spatio-temporal node, plus the vehicles not rented s_{it}. Constraints (2.3) determine the available vehicles at the beginning of the next period $a_{j(t+1)}$ by summing up the arriving rentals and the vehicles not moved. Clearly, (2.2) and (2.3) could be formulated in one set of constraints; however, the description of the solution approach in Section 2.4 becomes more comprehensible with an explicit decision variable a_{it}. The initial vehicle distribution is set by constraints (2.4). Constraints (2.5) ensure that at every location-time combination only one price p^m is set.

Constraints (2.6) and (2.7) define upper bounds on the rentals, depending on whether de-

mand or supply limits the rentals. For every i-j-t combination, constraints (2.6) limit the rentals observed at a certain price to the actual demand at this price. Additionally, these constraints ensure that only those variables r_{ijt}^m whose corresponding price p^m was selected can be positive. Constraints (2.7) limit the rentals to the number of available vehicles for every location-time combination. More specifically, the rentals from location i to location j at period t and price p^m must not exceed the fraction $d_{ijt}^m / \sum_{k \in \mathcal{Z}} d_{ikt}^m \cdot a_{it}$ of available vehicles. The factor $d_{ijt}^m / \sum_{k \in \mathcal{Z}} d_{ikt}^m$ splits the available vehicles proportionally into vehicle flows according to the demand relation.

The next constraints (2.8) to (2.11) are necessary to enforce lower bounds on the rentals, which thereby ensure that if $p_{it} = p^m$, rentals realize according to $r_{it} = \min(a_{it}, \sum_{j \in \mathcal{Z}} d_{ijt}^m)$ (see *pure pricing* and *proportional demand fulfillment assumptions* in Sections 2.1 and 2.3.1). They incorporate a sufficiently large number $\bar{M}$. Constraints (2.8) and (2.9) force q_{it} to 1, if the demand exceeds the available vehicles, and to zero otherwise. Now, if demand exceeds the supply, such that $q_{it} = 1$, constraints (2.11) ensure that all available vehicles are rented. In the other case where $q_{it} = 0$, constraints (2.10) set the demand as a lower bound for the rentals. As described in the review of the closest related literature in Section 2.2.3, to the best of our knowledge, none of the existing works on SMS pricing optimization enforces such lower bounds on the rentals. Consequently, these models have a degree of freedom which allows them to reject certain rentals. They therefore do not adequately reflect the real decision problem.

Note that from a technical viewpoint, the OBDPP falls into the class of deterministic sequential decision problems, which are characterized by the fact that they can be divided into stages (see e.g. Winston and Goldberg (2004, chapter 18.2)). In the OBDPP, these stages correspond to the multiple time periods. The corresponding model given in (2.1) to (2.16) has the same structure as the general deterministic sequential decision problem stated, e.g., in Powell (2011, chapter 4.8.4).

2.3.3 Computational Complexity

Theorem. *The origin-based differentiated pricing optimization problem in SMSs (OBDPP)* (2.1)-(2.16) *is NP-hard.*

Proof. See Appendix 2.A.

The proof is performed by polynomial-time reduction of the *three-satisfiability problem* (3-SAT), which is well-known to be NP-hard (Garey and Johnson, 1990), to the OBDPP. In 3-SAT, multiple *clauses* of 3 *literals* each build a Boolean *formula*, where the clauses are connected by conjunctions and the literals in each clause by disjunctions, meaning that the formula is in conjunctive normal form (CNF). 3-SAT now asks whether a given 3-CNF formula is *satisfiable*, thus asking whether there exists a consistent *truth assignment* of `TRUE`/`FALSE` to the literals, such that the formula is `TRUE`. The idea of the proof is to construct an OBDPP instance where location-time combinations correspond to a 3-SAT instance's clauses. For each location-time combination, the price selection corresponds to the selection of a literal that is guaranteed to be `TRUE`. For the constructed OBDPP instance, determining the optimal solution implies deciding satisfiability of the corresponding 3-SAT instance.

2.4 Approximate Dynamic Programming Decomposition Approach

Given that the OBDPP is NP-hard, in this section, we develop a problem-specific heuristic approach for its solution. More precisely, we propose a decomposition approach based on approximate dynamic programming (ADP). We start by explaining the theoretical foundation of the approach in Section 2.4.1, followed by its formal description in Section 2.4.2. In Section 2.4.3, we describe the specific design of the VFA which is a central element of the approach. We explain the estimation process of the VFA parameters in Section 2.4.4.

2.4.1 Theoretical Foundation

The solution approach builds on the general idea of using ADP as a decomposition technique. As Powell (2011) noted, while ADP is known as a solution framework for solving stochastic dynamic decision problems, it can also be applied as a decomposition technique for deterministic sequential decision problems (Powell, 2011, chapter 4.8.4), like the OBDPP. Through this technique, multiple smaller problems are solved instead of the original large problem, with each smaller problem containing a VFA that attempts to compensate for the neglected parts of the original problem (see also Powell (2009, 2016)). These VFAs are functions of the decision variables, such that the profits-to-come they approximate are endogenously incorporated within the optimization of the smaller problems. Powell points out that ADP decomposition approaches in principle allow to solve extremely large mathematical programs, which even modern commercial solvers find difficult, but the challenge is to design effective, problem-specific VFAs that yield adequate solution quality.

The ADP decomposition approach we developed for the OBDPP in this study implies a time-based decomposition of the original problem. That is, while in the original problem (2.1)-(2.16), all periods $t \in \mathcal{T}$ are optimized simultaneously, our approach is based on the iterative solution of multiple smaller and adapted versions of the original problem (termed substitute problem). More precisely, the approach loops chronologically across all periods $\tau \in \mathcal{T}$, and for each τ, a substitute problem with fewer explicitly considered periods (termed horizon) but with a period-specific VFA at the end of the horizon is optimized.

It is important to note that the ADP decomposition approach goes beyond the basic rolling horizon solution approach for deterministic sequential decision problems, as it is described, e.g., by Grossmann (2012). In fact, the key idea is to integrate sophisticated VFAs which allow us to implicitly consider all remaining parts of the original problem which are not considered explicitly in the optimized substitute problem. In our case, these VFAs are functions of the vehicle distribution (decision variables in the substitute problems) such that for *any* resulting vehicle distribution at the end of the horizon, the approximated profit-to-come is endogenously incorporated in the optimization. Thereby, the ADP decomposition approach has an obvious advantage over the basic rolling-horizon approach and comes along with the theoretical potential, in case of perfect VFAs, to indeed find the optimal solution of the overall problem. We describe the details of the approach next.

2.4.2 Formal Description

We begin the more formal description of the ADP decomposition approach by formalizing the substitute problem at a specific period τ. To reduce the problem size, the number of explicitly modeled periods in the substitute problem at period τ is limited to the horizon length H that has to be prespecified. For a certain H, the explicitly considered periods in the substitute problem at τ are the elements of the horizon $\mathcal{H}_\tau = \{\tau, \tau+1, \ldots, \min(\tau+H-1, T-1)\}$. In other words, this means that periods $t < \tau$ and $t > \min(\tau+H-1, T-1)$ are not considered explicitly and that the number of periods in the substitute problem can also be fewer than H in case it would otherwise exceed $T-1$. To compensate for the reduction of explicitly considered periods, the VFA is additionally integrated in the objective function.

To obtain a formulation of the substitute problem on the basis of the original OBDPP (2.1)-(2.16), it must be adapted to the considered periods in $\mathcal{H}_\tau$ and the VFA should be integrated. For that purpose, the decision variable vectors $\mathbf{y}, \mathbf{q}, \mathbf{r}, \mathbf{a}, \mathbf{s}$ are replaced by τ-specific vectors with appropriate time-dimension, that is $\mathbf{y}_{\mathcal{H}_\tau} = [y^m_{it}]_{Z \times H_\tau \times M}$, $\mathbf{q}_{\mathcal{H}_\tau} = [q_{it}]_{Z \times H_\tau \times M}$, $\mathbf{r}_{\mathcal{H}_\tau} = [r^m_{ijt}]_{Z \times Z \times H_\tau \times M}$, $\mathbf{s}_{\mathcal{H}_\tau} = [s_{it}]_{Z \times H_\tau}$, where $H_\tau = \min(H, T-\tau-1)$, and $\mathbf{a}_{\mathcal{H}_\tau} = [a_{it}]_{Z \times (H_\tau+1) \times M}$, respectively. For each horizon $\mathcal{H}_\tau$ with $\tau \in \mathcal{T}$, a corresponding substitute problem with initial vehicle distribution $\hat{\mathbf{a}}_\tau$ is then given by the following MILP:

$$\max_{\substack{\mathbf{y}_{\mathcal{H}_\tau}, \mathbf{q}_{\mathcal{H}_\tau}, \\ \mathbf{r}_{\mathcal{H}_\tau}, \mathbf{a}_{\mathcal{H}_\tau}, \mathbf{s}_{\mathcal{H}_\tau}}} \quad \sum_{t \in \mathcal{H}_\tau} \sum_{i \in \mathcal{Z}} \sum_{j \in \mathcal{Z}} \sum_{m \in \mathcal{M}} r^m_{ijt} \cdot l_{ij} \cdot (p^m - c) + \mathbb{1}_{\{\tau+H<T-1\}} \cdot \bar{V}_{\tau+H}(\mathbf{a}_{\tau+\mathbf{H}}) \tag{2.17}$$

$$\text{s.t.} \quad \text{Constraints (2.2)-(2.3), (2.5)-(2.15) with } \mathcal{T} \text{ replaced by } \mathcal{H}_\tau, \tag{2.18}$$

$$\text{and (2.16) with } \{0, 1, \ldots, T\} \text{ replaced by } \{\tau, \tau+1, \ldots, \min(\tau+H, T)\}$$

$$\text{Constraints (2.4) with vehicle distribution } \hat{\mathbf{a}}_\tau \tag{2.19}$$

$$\text{Constraints depending on choice of } \bar{V}_{\tau+H}(\mathbf{a}_{\tau+\mathbf{H}}). \tag{2.20}$$

Compared to the original OBDPP (2.1)-(2.16), the objective function in the substitute problem (2.17) contains the additional VFA $\bar{V}_{\tau+H}(\mathbf{a}_{\tau+\mathbf{H}})$. For each substitute problem, the *function* $\bar{V}_{\tau+H}(\mathbf{a}_{\tau+\mathbf{H}})$ *approximates* the *value* at the end of the horizon (that is, from period $t = \tau + H$ until the end of the day), referring to the optimal profit-to-come in the original problem for the remaining periods $\mathcal{R}_{\tau+H} = \{\tau+H, \tau+H+1, \ldots, T-1\}$. Since the VFA depends on the vehicle distribution $\mathbf{a}_{\tau+\mathbf{H}} = [a_{i(\tau+H)}]_{Z \times 1}$, the approximated profit-to-come is endogenously incorporated in the optimization of the substitute problem. More formally, the link between the approximation $\bar{V}_{\tau+H}(\mathbf{a}_{\tau+\mathbf{H}})$ and the original problem for a certain period $t = \tau + H$ under the respective constraints is

$$\bar{V}_{\tau+H}(\mathbf{a}_{\tau+\mathbf{H}}) \approx \max_{\substack{\mathbf{y}_{\mathcal{R}_{\tau+H}}, \mathbf{q}_{\mathcal{R}_{\tau+H}}, \mathbf{r}_{\mathcal{R}_{\tau+H}}, \\ \mathbf{a}_{\mathcal{R}_{\tau+H}}, \mathbf{s}_{\mathcal{R}_{\tau+H}}}} \sum_{t \in \mathcal{R}_{\tau+H}} \sum_{i \in \mathcal{Z}} \sum_{j \in \mathcal{Z}} \sum_{m \in \mathcal{M}} r^m_{ijt} \cdot l_{ij} \cdot (p^m - c), \tag{2.21}$$

again with adapted vectors of decision variables that now contain the respective variables for all remaining periods $t \in \mathcal{R}_{\tau+H}$. Note that the indicator function $\mathbb{1}_{\{\tau+H<T-1\}}$ in (2.17) ensures that the VFA is not used beyond the last period of the original problem. We present the details of the VFA design, as well as of determining the function parameters in Section 2.4.3

and Section 2.4.4, respectively.

Further, while constraints (2.18) in the substitute problem in principle correspond to the original constraints (2.2)-(2.3) and (2.5)-(2.16), they now account for the new time periods considered explicitly, meaning that $\mathcal{T}$ is replaced by $\mathcal{H}_\tau$ and $\{0, 1, \ldots, T\}$ is replaced by $\{\tau, \tau + 1, \ldots, \min(\tau + H, T)\}$. Likewise, constraints (2.19) concerning the substitute problem's initial vehicle distribution remain largely unchanged from (2.4), but the initial vehicle distribution $\hat{\mathbf{a}}_\tau = [\hat{a}_{i\tau}]_{Z\times 1}$ at τ now is the distribution at the beginning of the substitute problem's horizon. Depending on the specific choice of the VFA $\bar{V}_{\tau+H}(\mathbf{a}_{\tau+\mathbf{H}})$, additional constraints might be necessary (constraints (20)). We discuss these regarding our specific VFA design in Section 2.4.3.

Given the formulation of the substitute problem, we can now solve the original problem using the decomposition approach by chronologically looping over $\mathcal{T}$, from $\tau = 0$ to $\tau = T-1$. In each iteration, we solve a substitute problem (2.17)-(2.20) at period τ with horizon $\mathcal{H}_\tau$. For $\tau = 0$, the vehicle distribution is initialized with the vehicle distribution of the original problem $\hat{\mathbf{a}}_\mathbf{0}$. For all other substitute problems at $\tau > 0$, the respective initial vehicle distribution $\hat{\mathbf{a}}_\tau$ is determined by the vehicle distribution $\mathbf{a}_\tau$ that realized after one period in the previous substitute problem with horizon $\mathcal{H}_{\tau-1}$. The prices $\mathbf{p}_\tau = [p_{i\tau}]_{Z\times 1}$ that result from the optimization for the first period of each substitute problem at τ are the final prices to be recorded in column τ of the price table (see Table 2.1), while all other calculated prices are discarded. Similarly, vehicle distributions are computed for the entire horizon, but only the vehicle distribution $\mathbf{a}_{\tau+\mathbf{1}}$ of the next period $\tau+1$ is used as initial vehicle distribution $\hat{\mathbf{a}}_{\tau+\mathbf{1}}$ for the next substitute problem. Note that, from a technical perspective, already calculated future prices and spatial vehicle distributions can be used as part of a warm start solution in the following substitute problem to speed up the overall solution process.

The general ADP decomposition approach is depicted as pseudo-code in Algorithm 1. The substitute problem including VFA given by (2.17)-(2.20) can be solved using a standard MIP solver. Remember that it is not fully specified yet. We still need to choose a specific VFA to be integrated in objective (2.17) and add its corresponding constraints as indicated by (2.20). We describe our choice of this VFA and the corresponding elements to add in the next subsection. The computation times for the entire process of pricing solution determination are discussed in Appendix 2.D.

Algorithm 1 Approximate dynamic programming decomposition approach

- start with initial vehicle distribution $\hat{\mathbf{a}}_\mathbf{0}$ according to original problem
for $\tau = 0$ **to** $\tau = T - 1$ **do**
  - solve substitute problem including VFA (2.17)-(2.20) with respective horizon $\mathcal{H}_\tau$
  - store prices $\mathbf{p}_\tau$ in price table
  - update initial vehicle distribution: $\hat{\mathbf{a}}_{\tau+\mathbf{1}} \leftarrow \mathbf{a}_{\tau+\mathbf{1}}$
end for

2.4.3 Design of the Value Function Approximation

Here we propose and discuss a problem-specific VFA to be used for $\bar{V}_{\tau+H}$ in (2.17) and state the additional constraints it requires (cf. (2.20)). The main focus in our VFA design is to effectively

approximate the network effects of the OBDPP. Please remember that the idea is to use the VFA to be able to evaluate *any* vehicle distribution that might arise in the substitute problem.

Basically, the VFA $\bar{V}_{\tau+H}$ can be any function that maps the decision variables at the end of the horizon to the desired value. In general, three alternative VFA types can be used in ADP, namely lookup tables, non-parametric value functions, and parametric value functions (Powell, 2011, chapter 6). We decided to follow the latter type, i.e., a parametric approach, because, different to the others, it can be incorporated in our MILP framework without excessively using auxiliary variables.

The choice of a specific VFA depends on two aspects. First, and most importantly, the VFA should be a good approximation of the true value function and capture all properties relevant for decision making. The second is tractability. As we integrate the VFA into a MILP, we aim as much as possible to reduce the additional complexity that inevitably results from the VFA integration with its additional decision variables and potential constraints. The first step of the VFA design is known as feature selection in the ADP realm. It determines the variables (a subset of the state) of which the VFA is a function. The vehicle distribution $\mathbf{a}_{\tau+\mathbf{H}}$ is the natural choice, as it is central to the SMS's state, and determines the potential for future rentals. The second step that defines the actual function is a bit more complicated. The key property here is that each additional vehicle in a specific location at time $\tau + H$ has a positive additional value, but as the number of vehicles increases, the marginal value of each additional available vehicle decreases. This is because the finite demand causes saturation and limits the profit that can be realized with additional vehicles, also taking future demand at other locations through network effects into account. Thus, a concave function seems appropriate. Regarding tractability, linearity in the vehicle distribution $\mathbf{a}_{\tau+\mathbf{H}}$ is desirable.

Combining these arguments and computational tests, we propose a piece-wise linear function of the number of vehicles in each location at time $\tau+H$. Additional constraints ensure concavity. Thus, the VFA captures the decreasing marginal value of available vehicles and retains linearity. In particular, the VFA (incorporated in the substitute problem (2.17)-(2.20)) is the following Z-dimensional piece-wise linear function with K pieces in each dimension.

$$\bar{V}_{\tau+H}(\mathbf{a}_{\tau+\mathbf{H}}) := \sum_{i\in\mathcal{Z}}\sum_{k\in\mathcal{K}} \bar{v}^{k}_{i(\tau+H)} \cdot \Delta a^{k}_{i(\tau+H)} + \bar{v}^{const}_{\tau+H} \tag{2.22}$$

Technically speaking, the VFA (2.22) for a specific period $\tau+H$ is a function of the respective spatial vehicle distribution $\mathbf{a}_{\tau+\mathbf{H}}$ and additive over the Z locations. For a specific location i, the present vehicles $a_{i(\tau+H)}$ are divided into K buckets that each represent a common marginal value per vehicle and correspond to the pieces of the piece-wise linear function. The number of vehicles in these buckets is modeled by additional decision variables $\Delta a^{k}_{i(\tau+H)}$ (=pieces) with $a_{i(\tau+H)} = \sum_{k\in\mathcal{K}} \Delta a^{k}_{i(\tau+H)}\ \forall i \in \mathcal{Z}$, where $\mathcal{K} = \{1, \ldots, K\}$. Thus, a specific share $\Delta a^{k}_{i(\tau+H)}$ of the vehicles at location i, period $(\tau + H)$ now corresponds to piece k and contributes with the respective marginal value $\bar{v}^{k}_{i(\tau+H)}$ to the overall value of the VFA. Additionally, the VFA contains the time specific constant $\bar{v}^{const}_{\tau+H}$.

The VFA parameters, meaning $\bar{v}^{k}_{i(\tau+H)}$ for $i \in \mathcal{Z}, \tau + H \in \mathcal{T}, k \in \mathcal{K}$ as well as $\bar{v}^{const}_{\tau+H}$ for $(\tau + H) \in \mathcal{T}$, are derived in an estimation process that we describe in Section 2.4.4. Due to the

decreasing marginal value of vehicles discussed above, during estimation, we enforce concavity of the function in each dimension i by requiring $\bar{v}^k_{i(\tau+H)} \geq \bar{v}^{k+1}_{i(\tau+H)}$ $\forall i \in \mathcal{Z}$ and $\forall k \in \{1, \ldots, K-1\}$. Further, we require $\bar{v}^k_{i(\tau+H)} \geq 0$ $\forall i \in \mathcal{Z}, k \in \mathcal{K}$ and $\bar{v}^{const}_{\tau+H} \geq 0$ for obvious reasons.

As a side note, for an efficient VFA of our problem, considering i-t-specific parameters $\bar{v}^k_{i(\tau+H)}$ is indeed decisive. The intuition behind this is that a vehicle's value depends on both location and time. In particular, parameters that were only time-specific would result in a valuation of the fleet at the end of the horizon which is identical for all possible fleet distributions.

Now, to plug the VFA (2.22) into the substitute problem (2.17)-(2.20) for period τ with horizon $\mathcal{H}_\tau$, we obviously substitute (2.22) into the objective function (2.17). Moreover, additional continuous and non-negative decision variables $\Delta a^k_{i(\tau+H)}$ $\forall i \in \mathcal{Z}, k \in \mathcal{K}$ are introduced. To ensure a correct evaluation of the vehicle distribution $\mathbf{a_{t+H}}$ with (2.22), the following additional constraints need to be integrated in the substitute problem for (2.20):

$$a_{i(\tau+H)} = \sum_{k \in \mathcal{K}} \Delta a^k_{i(\tau+H)} \qquad \forall i \in \mathcal{Z} \tag{20a}$$

$$\Delta a^k_{i(\tau+H)} \leq \Delta \tilde{a} \qquad \forall i \in \mathcal{Z}, \forall k \in \{1, 2, \ldots, K-1\} \tag{20b}$$

Constraints (20a) ensure that the $\Delta a^k_{i(\tau+H)}$ indeed sum up to the vehicle count. By constraints (20b), the number of vehicles in each bucket, except for the last bucket ($\Delta a^K_{i(\tau+H)}$), is limited to the respective predefined bucket size $\Delta \tilde{a}$. Note that because of the concavity of the VFA, the buckets are "automatically" filled in the correct order, beginning with $k = 1$.

To solve the substitute problem (2.17)-(2.20) incorporating this VFA, we still need values for its parameters. We describe their estimation in the next subsection.

2.4.4 Parameter Estimation

The estimation process we propose for the VFA parameters is performed before we loop over the time periods and iteratively solve the substitute problems as described in Sections 2.4.1 and 2.4.2. We followed the traditional idea of parameter estimation based on observed data, which, in our case, is artificial sample data generated from simulations, as common in ADP-based approaches. For the purpose of sample generation, we exploit that for a given spatial vehicle distribution at a certain period and with a given price table for the remaining periods, the resulting rentals of the remaining periods and thus the corresponding profit-to-come are easily calculated algorithmically. This profit-to-come evaluation is computationally efficient, even for real-life instances. The overall process can roughly be outlined as follows: First, we generate samples of vehicle distributions. Second, for each sample, we calculate the resulting profit-to-come. Finally, this data is used to estimate the VFA parameters by an adapted least squares estimation procedure.

More formally, for each period $(\tau + H) \in \{1, 2, \ldots, T-1\}$, multiple samples $n \in \mathcal{N} = \{1, 2, \ldots, N\}$ of vehicle distributions $\hat{\mathbf{a}}^{\mathbf{n}}_{\tau+\mathbf{H}} = [\hat{a}^n_{i(\tau+H)}]_{Z \times 1}$ are drawn by randomly splitting up the fleet among the Z locations. For each of these vehicle distribution samples $\hat{\mathbf{a}}^{\mathbf{n}}_{\tau+\mathbf{H}}$, a corresponding profit-to-come $\hat{V}^n_{\tau+H}(\hat{\mathbf{a}}^{\mathbf{n}}_{\tau+\mathbf{H}})$ is determined by evaluating a known (suboptimal) price table, for example one that only consists of a constant uniform price, over the remaining

periods. This could be done by applying a solver to evaluate the original problem (2.1)-(2.16) with fixed prices for the remaining periods in $\mathcal{R}_{\tau+H}$, but an equivalent algorithmic solution is straightforward and much faster. Moreover, for each vehicle distribution the number of vehicles in each bucket $\mathbf{\Delta\hat{a}^n_{\tau+H}} = [\Delta\hat{a}^{k,n}_{i(\tau+H)}]_{Z\times 1\times K\times N}$ is calculated. In particular, for each location, we simply assign as many vehicles as possible up to the bucket size $\Delta\hat{a}^{k,n}_{i(\tau+H)}$ to a bucket and then continue with the next with increased k.

Given the resulting sample data, the respective parameters $\bar{\mathbf{v}}_{\tau+\mathbf{H}} = [\bar{v}^k_{i(\tau+H)}]_{Z\times 1\times K}$ and $\bar{v}^{const}_{\tau+H}$ from the VFA (2.22) are simultaneously determined by constrained least squares estimation, that is, a variant of ordinary least squares estimation with additional equality and inequality constraints. More precisely, we minimize the mean squared error over the N generated data points by the following quadratic optimization problem:

$$\min_{\bar{\mathbf{v}}_{\tau+\mathbf{H}},\bar{v}^{const}_{\tau+H}} \quad \frac{1}{N}\sum_{n\in\mathcal{N}}(\hat{V}^n_{\tau+H}(\mathbf{\hat{a}^n_{\tau+H}}) - \bar{V}^n_{\tau+H}(\mathbf{\Delta\hat{a}^n_{i(\tau+H)}}))^2 \tag{2.23}$$

$$\text{s.t.} \quad \bar{V}^n_{\tau+H}(\mathbf{\Delta\hat{a}^n_{i(\tau+H)}}) = \sum_{i\in\mathcal{Z}}\sum_{k\in\mathcal{K}} \bar{v}^k_{i(\tau+H)}\cdot\Delta\hat{a}^{k,n}_{i(\tau+H)} + \bar{v}^{const}_{\tau+H} \qquad \forall n\in\mathcal{N} \tag{2.24}$$

$$\bar{v}^k_{i(\tau+H)} \geq 0 \qquad \forall i\in\mathcal{Z}, k\in\mathcal{K} \tag{2.25}$$

$$\bar{v}^{const}_{\tau+H} \geq 0 \tag{2.26}$$

$$\bar{v}^k_{i(\tau+H)} \geq \bar{v}^{k+1}_{i(\tau+H)} \qquad \forall i\in\mathcal{Z}, k\in\{1,2,\ldots,K-1\}. \tag{2.27}$$

The error minimized in (2.23) is the mean of the squared difference between the observed (evaluated) profits-to-come $\hat{V}^n_{\tau+H}$ and the profits-to-come $\bar{V}^n_{\tau+H}$ predicted with (2.22) (identical to (2.24)), for the respective observed (randomly drawn) spatial vehicle distribution, over all samples N. Constraints (2.25)-(2.26) ensure the non-negativity of the parameters and constraints (2.27) ensure the VFA's concavity. Remember that $\bar{\mathbf{v}}_{\tau+\mathbf{H}}$ and $\bar{v}^{const}_{\tau+H}$ are parameters in their eventual use as parts of the VFA in the substitute problem (2.17)-(2.20), but here in (2.23)-(2.27), they are the decision variables to be determined.

Note that the parameter estimation is performed individually for each period $(\tau+H)\in\mathcal{T}$, but simultaneously over all Z locations each $(\tau+H)$ such that spatio-temporal interdependencies are captured by the VFA parameters. The process is depicted as pseudo-code in Algorithm 2. We solve (2.23)-(2.27) using a standard MIP solver. Computation times for the parameter estimation process are discussed in Appendix 2.D.

Algorithm 2 Parameter estimation algorithm

for $(\tau + H) = 1$ **to** $T - 1$ **do**
  for $n = 1$ **to** N **do**
    - randomly divide fleet into spatial vehicle distribution $\hat{\mathbf{a}}^{\mathbf{n}}_{\tau+\mathbf{H}}$
    - determine profit-to-come $\hat{V}^n_{\tau+H}$ by algorithmic evaluation of original problem (2.1)-(2.16) for remaining periods $\mathcal{R}_{\tau+H}$ with known (suboptimal) price solution
    - for each location, calculate number of vehicles in each bucket ($\boldsymbol{\Delta}\hat{\mathbf{a}}^{\mathbf{n}}_{\tau+\mathbf{H}}$)
  end for
  - determine VFA parameters $\bar{\mathbf{v}}_{\tau+\mathbf{H}}$ and $\bar{v}^{const}_{\tau+H}$ by (2.23)-(2.27)
end for

2.5 Computational Experiments

We investigate the performance of the ADP decomposition approach presented in Section 4 in comprehensive computational experiments. We vary the most relevant influencing factors systematically to triangulate the approach's performance. Section 2.5.1 introduces the scenarios and parameter values. In Section 2.5.2, we state all solution approaches that we investigate – including benchmarks – as well as the metrics we use for their evaluation. In Section 2.5.3, we present and discuss the computational results.

2.5.1 Scenarios and Parameters

We consider three *settings* of a free-floating SMS that primarily differ in the number of zones (=locations) – $Z = 9$, $Z = 16$ and $Z = 25$ – but also regarding the demand pattern. The process used to generate the base demand matrix $\mathbf{d}$ with values for all zone-zone-period combinations allows to incorporate typical demand characteristics that we observed in practice, namely a typical demand pattern over the course of the day and differentiation between zone types, like city center zones or peripheral zones (see, for example Reiss and Bogenberger (2016)). The exact procedure is explained in Appendix 2.B. The remaining parameters are constant over all three settings: we discretize the time interval of one day into $T = 48$ periods of 30 minutes each, in line with practice and literature (see, e.g., Kaspi et al. (2016) and Ferrero et al. (2015b)). The parameters $\hat{a}_{i0} = 2 \forall i \in \mathcal{Z}$ represent a realistic number of vehicles per zone. We select the $M = 3$ price points p^m according to typical prices in practice and literature (see, e.g. Lippoldt, Niels, and Bogenberger (2018)): we choose a base price of $p^{(2)} = 30$ ct/min and price differences of 20% to the low and high price, such that $p^{(1)} = 24$ ct/min and $p^{(3)} = 36$ ct/min. The corresponding sensitivity factors $f_{ijt}^{(1)} = 1.25, f_{ijt}^{(2)} = 1, f_{ijt}^{(3)} = 0.75 \ \forall i, j \in \mathcal{Z}, t \in \mathcal{T}$ are chosen according to observations from practice. Variable costs of $c = 7.5$ ct/min made up 25% of the base price. The average rental time was set to $l_{ij} = 15$ min $\forall i, j \in \mathcal{Z}$, again in line with literature (see e.g. Xu, Meng, and Liu (2018)) and after discussions with our practice partner.

To generate different *scenarios* within a *setting*, the overall demand level can be adjusted by the *demand-supply-ratio* δ, which determines the ratio of the maximum period demand during the day $\bar{d}$ and the fleet size $\sum_{i \in \mathcal{Z}} \hat{a}_{i0}$. While the fleet size remains constant for all *scenarios* within a *setting*, the overall demand varies according to δ, i.e., $\bar{d} = \sum_{i \in \mathcal{Z}} \hat{a}_{i0} \cdot \delta$. The required (base) demand of a scenario for every location-location-period combination d_{ijt} is then simply determined by scaling $\bar{d}$ according to the given demand pattern which is defined by *ratios* of the d_{ijt} amongst one another. As a result, $\bar{d} = \max_t(\sum_{i,j \in \mathcal{Z}} d_{ijt})$ holds. We use demand patterns that replicate typical spatio-temporal differences, e.g., that show the two characteristic demand peaks over the course of a day, as observed in practice by our practice partner (also see Figure 2.10b in the case study). This is typical for SMSs and has been similarly reported in many other studies, such as Reiss and Bogenberger (2016). Note that although the maximum period demand only reflects the demand of a single period, it is a representative, yet simple, metric for the overall demand, because all SMSs in practice show a comparable course of demand across the day. The demand-supply-ratios we use are $\delta \in \{2/6, 4/6, 6/6, 8/6\}$. Further, as already mentioned, each combination of a certain *setting* with a specific δ forms a *scenario*.

	description	configurations
ADP-H	ADP decomposition approach with horizon length H	ADP-1, ADP-4, ADP-8
CUP	benchmark: constant uniform pricing	-
OPT	benchmark: optimal pricing	-
UB	benchmark: best upper bound after a computation time limit	-
ROL-H	benchmark: rolling-horizon approach with horizon length H	ROL-1, ROL-4, ROL-8

Table 2.1: Overview of solution approaches investigated

2.5.2 Investigated Solution Approaches and Evaluation Metrics

Here, we describe the *solution approaches* that we investigate. Besides our ADP decomposition approach with three different configurations, we investigate four benchmark approaches, of which one again has three *configurations* (the approaches are summarized in Table 2.1):

- ADP-H is the ADP decomposition solution approach we presented in Section 2.4, and is configured with different horizon lengths H (ADP-1, ADP-4, ADP-8).
- CUP denotes a lower benchmark using constant uniform pricing. Due to its wide adoption over all SMS types, this pricing can be considered as the de facto standard applied in practice. Here we used the base price $p_{it} = p^{(2)}$ for all $i \in \mathcal{Z}$ and $t \in \mathcal{T}$.
- OPT denotes the optimal solution of the OBDPP in which all 48 periods are optimized simultaneously. It provides an upper bound. This benchmark can be calculated for some of the scenarios.
- UB denotes the best known upper bound that the solver returned after a computation time limit.
- ROL-H is a basic rolling-horizon approach. In the context of our work, it is best described as a variant of the ADP decomposition approach without the VFA at the end of the horizon, that is, $\bar{V}_{\tau+H} = 0 \; \forall(\tau + H) \in \mathcal{T}$. We considered this benchmark in order to analyze the impact of the VFA in our approach. Like ADP-H, it can be configured for different horizon lengths H (ROL-1, ROL-4, ROL-8). Note that this benchmark with $H = 1$ represents the myopic solution that only considers one period in each substitute problem without anticipating any network effects.

Each combination of scenario and solution approach configuration forms a *test instance* in our experiments. Table 2.6 in Appendix 2.C summarizes the test instances that we evaluate.

Regarding the VFA, we define the parameters that specify the structure of the function and the estimation process as follows. The number of buckets (pieces) is $K = 10$ and the bucket size is $\Delta\tilde{a} = 2$. For each scenario, we perform the parameter estimation as described in Section 2.4.4 on $N = 10,000$ samples. In each period $(\tau + H) \in \mathcal{T}$, we randomly generate the initial vehicle distribution $\hat{\mathbf{a}}^{\mathbf{n}}_{\tau+\mathbf{H}}$ following the Dirichlet distribution and use the CUP solution for evaluating the original problem (2.1)-(2.16) for the remaining periods in $\mathcal{R}_{\tau+h}$ to obtain $\hat{V}^n(\hat{\mathbf{a}}^{\mathbf{n}}_{\tau+\mathbf{H}})$.

We use various *metrics* to evaluate the solution approaches and to discuss further insights. We describe these metrics in the following exposition. We summarize them in Table 2.2, as

	description	variant
PR^{rel}	relative profit increase w.r.t. CUP	time-specific: PR^{rel}_t
RV^{rel}	relative revenue increase w.r.t. CUP	time-specific: RV^{rel}_t
RT^{rel}	relative rentals increase w.r.t. CUP	time-specific: RT^{rel}_t
$P^{prop}_{p^m}$	proportion of price p^m in pricing solution	time-specific: $P^{prop}_{p^m t}$
$RT^{prop}_{p^m}$	proportion of rentals at price p^m in pricing solution	time-specific: $RT^{prop}_{p^m t}$

Table 2.2: Evaluation metrics

well as formally define them in Table 2.7 in Appendix 2.C. Profit ($PR^{rel}_{(\cdot)}$), revenue ($RV^{rel}_{(\cdot)}$) and rentals ($RT^{rel}_{(\cdot)}$) are stated as relative improvements to the respective value from the uniform pricing solution. Depending on the analysis, we consider the overall improvements across all periods $t \in \mathcal{T}$ (for example PR^{rel}) or one particular period t (for example PR^{rel}_t). Further, we consider the proportion of location-time combinations in which a particular price p^m is selected ($P^{prop}_{(\cdot)}$) and the proportion of rentals that occur at price p^m ($RT^{prop}_{(\cdot)}$) for all periods $t \in \mathcal{T}$ ($P^{prop}_{p^m}, RT^{prop}_{p^m}$) as well as for a specific period t ($P^{prop}_{p^m t}, RT^{prop}_{p^m t}$).

We implement the algorithms in Python 3.7 and solve all MILPs with Gurobi 9.0.2. In all scenarios with 9 zones, we set the target optimality gap to zero in Gurobi and no time limit in any of the approaches is imposed. In all scenarios with 16 and 25 zones, the time limit is set at one hour for the substitute problems of the ADP-H and ROL-H approaches and at 48 hours for UB. Additionally, we use the CUP solution as a warm start solution in all instances. We execute our computations on a workstation with two Intel Xeon E7-8890 v3 2.5 Gigahertz processors with a total of 36 cores, and 512 Gigabyte RAM.

2.5.3 Results

In the following subsections, we present and discuss our computational results. First, we determine how much improvement is possible beyond myopic pricing (ROL-1) (Section 2.5.3.1). Next, we investigate how much of this potential can be realized with the ADP-H and ROL-H approaches (Section 2.5.3.2) and in this context we show the importance of the VFA by comparing ADP-H to ROL-H. Then, we discuss the impact of accounting for network effects on the pricing (Section 2.5.3.3) and intuitively illustrate how the VFA captures network effects, as well as the future value of available vehicles (Section 2.5.3.4). Finally, we analyze the robustness of the results by considering a stochastic environment (Section 2.5.3.5).

We discuss the results for all demand-supply-ratios δ here, but depict only those of the profit for δ =2/6, illustratively. All other results are depicted in Appendices 2.E (9-zone setting) and 2.F (16- and 25-zones settings). Computation times are discussed in Appendix 2.D.

2.5.3.1 Improvement Potential over Myopic Pricing

We begin by identifying the improvement potential over myopic pricing, that is, the relative difference in profit PR^{rel} between the myopic (ROL-1) and upper benchmarks. For the 9-zones setting, we use the optimal (OPT) solution as upper benchmark. For the 16- and 25-zones setting, the optimal solution can not be determined in reasonable time, therefore we use the

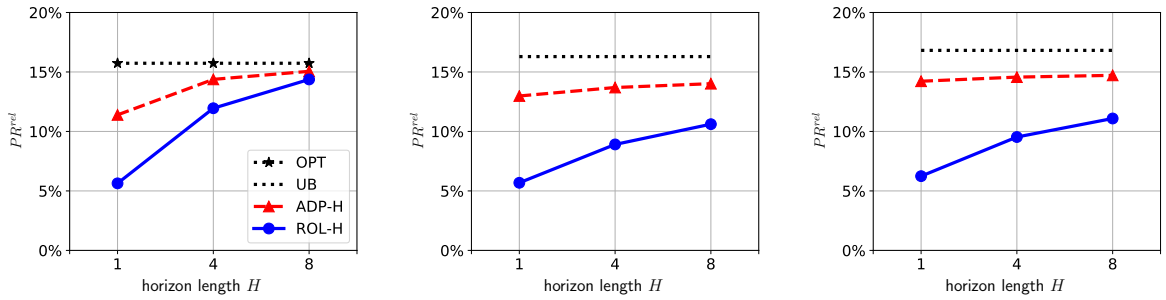

(a) $Z = 9$ (b) $Z = 16$ (c) $Z = 25$

Figure 2.3: Relative profit increase in settings with 9, 16, and 25 zones. Demand-supply-ratio $\delta = 2/6$.

best known upper bound (UB) as benchmark. The idea is that the range between the lower and upper benchmarks is an upper bound on the potential of PR^{rel} that can be achieved by the ADP decomposition approach. We consider the latter approach in Section 2.5.3.2.

This potential is graphically given in Figure 2.3. It depicts the profit obtained with the different solution approaches (for the later considered ADP-H and ROL-H in dependence of the horizon lengths H on the horizontal axis) relative to the profit with CUP, which the 0%-line marks. The profits obtained by OPT and UB are horizontal lines as they do not depend on H. We observe that OPT and UB yield a profit increase of about 15% over CUP. The myopic solution ROL-1 provides about 5% more profit than CUP. Thus, the potential improvement over myopic pricing is about 10 percentage points. Note that we return to Figure 2.3 in the following subsection to discuss the other results included.

Figure 2.15 in Appendix 2.E depicts the results for all scenarios with δ from 2/6 to 8/6 (rows) in the 9-zones setting. The potential for improvement between ROL-1 and OPT decreases from 10.1 percentage points for δ =2/6 to 2.3 percentage points for δ =8/6. Note that especially the scenarios with δ <6/6 are relevant for practice (Section 2.6.1). The above results are also valid for the 16- and 25-zones settings (see Figure 2.16 in Appendix 2.F).

What makes the difference between the scenarios, is obviously the relevance of network effect anticipation, because ROL-1 considers only one period in each substitute problem and includes no VFA, and therefore no network effects. The intuition is that in high-demand scenarios (large δ) there is almost always demand for an available vehicle, because the demand is never the limiting factor. In low-demand scenarios, however, vehicles remain unused more often. This conclusion is supported by the comparison of rentals (RT^{rel}) in the third column of Figure 2.15 which shows a substantial difference of 3.8 percentage points between ROL-1 and OPT for δ =2/6, and almost no difference for δ =8/6.

2.5.3.2 Performance of the ADP Decomposition Approach

After identifying the potential of up to 10 percentage points for improvement over the myopic solution ROL-1, we now analyze the performance of the proposed ADP decomposition approach (ADP-H). To do so, we revisit Figure 2.3a and consider the profit PR^{rel} of ADP-1, ADP-4, and ADP-8. In the 9-zones setting, we observe that as the horizon length H increases, PR^{rel} increases from 11.4% (ADP-1) to 15.1% (ADP-8). Additionally, the improvement potential identified in Section 2.5.3.1, is almost entirely exploited. The results for the 16- and 25-zones

settings are similar. An additional profit increase does not necessarily go hand in hand with a revenue RV^{rel} and rentals RT^{rel} increase, as depicted for the 9-zones setting in the second and third columns of Figure 2.15 in Appendix 2.E. Sometimes profit increases because of a quantity effect when the differentiated pricing enables more rentals while the average price remains more or less constant. The underlying reason is a better positioning of vehicles due to the network effect consideration. At other times profit increases because of a price effect at rather constant rentals with increase average price or even at fewer rentals when the average price decreases under-proportionally.

Again referring to Figure 2.3a, we see that the integrated VFA in ADP-1 and ADP-4 has a substantial benefit of 5.8 and 2.4 percentage points over their ROL-H counterparts. For ROL-8/ADP-8, the benefit is smaller. For smaller horizon lengths, the potential for improvement by the VFA is obviously higher than for larger horizon lengths because both the explicit consideration of additional periods in a longer horizon and the VFA aim to consider the spatio-temporal network effects. As settings become larger, the benefit of ADP-H over ROL-H increases, and with 16- and 25-zones even ADP-1 performs considerably better than the ROL-8 benchmark procedure (Figures 2.3b and 2.3c)

The results for all scenarios in the 9-zones setting (Figure 2.15, Appendix 2.E) and all scenarios in the 16- and 25-zones settings (Figure 2.16, Appendix 2.F) confirm the findings discussed above. Most importantly, the profits obtained with ADP-H are at least as high as the respective variant of ROL-H, but especially for the practice-relevant scenarios with low δ there is substantial improvement. This demonstrates that integrating the VFAs can partly compensate for not considering all spatio-temporal network effects explicitly. The fewer network effects are captured within the horizon, the stronger the effect.

Another benefit of the ADP decomposition approach concerns its scalability to large problem instances. As preliminary studies have shown, problem complexity (NP-hardness of the OBDPP) takes its toll, and finding good solutions in reasonable time cannot be guaranteed. By contrast, ADP-H benefits from the decomposition and can therefore cope with the larger problem size while simultaneously considering network effects.

2.5.3.3 Investigation of Pricing

The differences in considering network effects of the myopic (ROL-1) and the optimal solution (OPT) identified in Section 2.5.3.1 are also reflected in the pricing decisions, depicted as price tables in Figures 2.4a and 2.4b for the 9-zones setting with δ =2/6. On an aggregate level, these differences become obvious in comparing the proportions of the ROL-1 and OPT prices PR^{prop} in the fourth column of Figure 2.15 in Appendix 2.E. For δ =2/6, for example, the ROL-1 solution consists of 1.6% low, 76.9% base, and 21.5% high prices. The OPT solution consists of 34.5% low, 28.7% base, and 36.8% high prices.

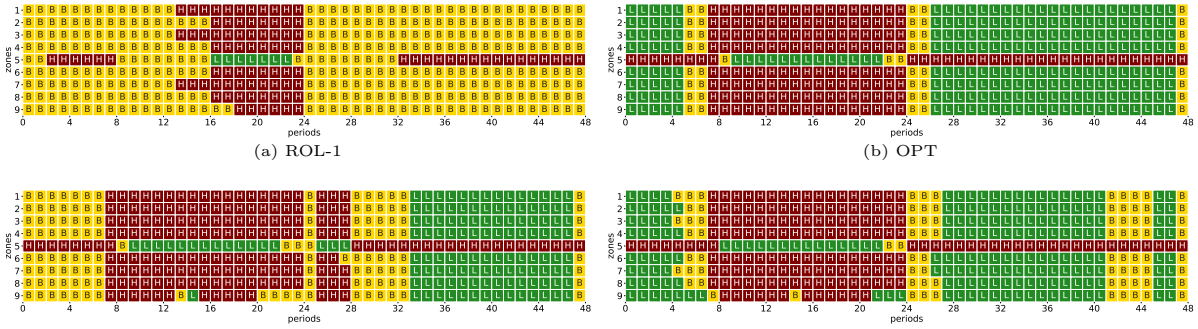

(a) ROL-1 (b) OPT

(c) ADP-1 (d) ADP-8

Figure 2.4: Pricing with different solution approaches in 9-zones setting. Demand-supply-ratio δ =2/6. Green: L=low price, yellow: B=base price, red: H=high price

The better network effects are captured, the more the resulting pricing decisions resemble the optimal pricing, as the price tables for ADP-1 and ADP-8 depicted in Figures 2.4c and 2.4d demonstrate. Especially the difference between ROL-1 and ADP-1 is insightful. Again, the aggregate price proportions $P_{p^m}^{prop}$ which are depicted in Figure 2.15 (Appendix 2.E) and Figure 2.16 (Appendix 2.F) underline how the network effect integration, especially with ADP-H, affects the pricing.

2.5.3.4 Investigation of the Value Function Approximation

Integrating the VFA that captures the spatio-temporal network effects beyond the explicitly considered horizon's end is an integral component of the ADP decomposition approach. In this section, we illustrate how the VFA works and illustratively interpret the estimated values we obtained. In particular, the following analyses demonstrate how the VFA's parameters reflect the demand pattern, and thus capture short-term as well as long-term vehicle values. For ease of readability, we first repeat the VFA given in Section 2.4.3:

$$\bar{V}_{\tau+H}(\mathbf{a}_{\tau+\mathbf{H}}) = \sum_{i\in\mathcal{Z}} \sum_{k\in\mathcal{K}} \bar{v}^k_{i(\tau+H)} \cdot \Delta a^k_{i(\tau+H)} + \bar{v}^{const}_{\tau+H} \tag{2.28}$$

For the sake of clearer analyses, we define its zone specific parts as

$$\bar{V}^{part}_{i(\tau+H)}(a_{i(\tau+H)}) = \sum_{k\in\mathcal{K}} \bar{v}^k_{i(\tau+H)} \cdot \Delta a^k_{i(\tau+H)} \tag{2.29}$$

such that

$$\bar{V}_{\tau+H}(\mathbf{a}_{\tau+\mathbf{H}}) = \sum_{i\in\mathcal{Z}} \bar{V}^{part}_{i(\tau+H)}(\mathbf{a}_{\mathbf{i}(\tau+\mathbf{H})}) + \bar{v}^{const}_{\tau+H}. \tag{2.30}$$

Table 2.3 contains an extract of the slope parameters $\bar{v}^k_{i(\tau+H)}$ and the constants $\bar{v}^{const}_{\tau+H}$ for two periods ($(\tau+H) = 16$ at morning peak time and $(\tau+H) = 32$ at evening peak time) and two zones (center zone $i = 5$ and peripheral zone $i = 1$). The values result from the estimation process of the scenario with $Z = 9$ zones and demand-supply-ratio δ =2/6. The biggest absolute difference between the respective parameters concerns the constants with $\bar{v}^{const}_{16} = 140.63$ and $\bar{v}^{const}_{32} = 1.36$. As the value function $\bar{V}_{\tau+H}$ approximates the profit-to-come from a certain period $(\tau+H)$ onwards, the difference in the constants reflects the higher demand-to-come at an earlier

		$\bar{v}^k_{i(\tau+H)}$										$\bar{v}^{const}_{\tau+H}$
		$k=1$	$k=2$	$k=3.$	$k=4$	$k=5$	$k=6$	$k=7$	$k=8$	$k=9$	$k=10$	
$(\tau+H)$ $=16$	$i=1$	9.79	2.30	1.54	1.54	1.42	1.27	0.00	0.00	0.00	0.00	140.63
	$i=5$	6.45	5.82	5.82	5.66	5.44	5.44	5.22	3.49	0.00	0.00	
$(\tau+H)$ $=32$	$i=1$	3.31	3.25	3.25	3.25	3.25	3.25	3.25	0.00	0.00	0.00	1.36
	$i=5$	7.33	7.28	7.17	7.06	6.96	6.85	6.85	0.00	0.00	0.00	

Table 2.3: Parameter estimates of VFA for two exemplary periods and zones

time. This time dependence of $\bar{v}^{const}_{\tau+H}$ is also visible in Figure 2.5. The close connection to the demand-to-come is obvious from comparing its course over the day, as depicted in Figure 2.6.

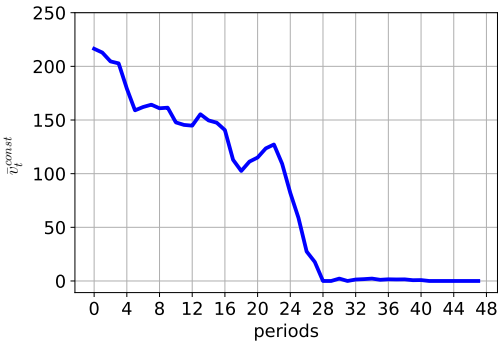

Figure 2.5: Value of the constant $\bar{v}^{const}_t$ in the VFA

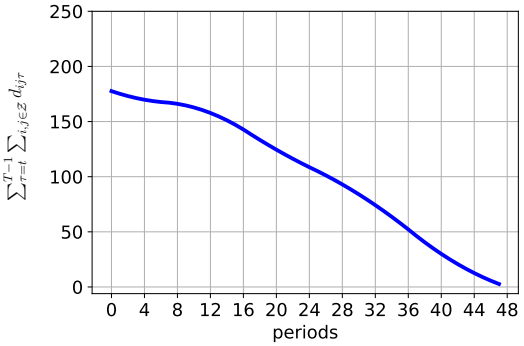

Figure 2.6: Base demand-to-come $\sum_{\tau=t}^{T-1}\sum_{i,j\in\mathcal{Z}} d_{ij\tau}$

The slope parameters $\bar{v}^k_{i(\tau+H)}$ during the evening peak period $(\tau+H)=32$ take larger values for the center zone $i=5$ than for the peripheral zone $i=1$, reflecting that vehicles in the center have a higher value. This is because demand in the center zone is higher during the evening peak. This is reflected in the VFA by the parts $\bar{V}_{1,32}(a_{1,32})$ and $\bar{V}_{5,32}(a_{5,32})$ for zones 1 and 5, which are depicted in Figure 2.7b. Both curves, the solid one representing the value in zone $i=1$ and the dashed one for zone $i=5$, are concave with a positive slope in the origin and a saturation with zero slope from a certain vehicle count a_{it} onwards. Concavity and saturation represent the diminishing marginal value of additional vehicles and the assumptions imposed in the estimation process.

During the morning peak period at $(\tau+H)=16$, the zone specific VFAs $\bar{V}_{i16}(a_{i16})$ for the same two zones $i=1$ and $i=5$ are depicted in Figure 2.7a. There is also concavity and saturation, but the functions intersect. As the slope parameters in Table 2.3 show, the first slope parameter for zone 1 takes higher values than the corresponding values of zone 5, meaning $\bar{v}^k_{1,16} > \bar{v}^k_{5,16}$ for $k=1$. For $k>1$ however, the order of slope values switches, such that $\bar{v}^k_{1,16} \leq \bar{v}^k_{5,16}$. These parameters and the resulting curves can be explained by analyzing the demand. Figure 2.7c shows that at $(\tau+H)=16$, the demand of zone 1 is slightly higher than that of zone 5. The demand-to-come from $(\tau+H)=16$ on in zone 5, however, is much higher, as Figure 2.7d displays. Because the demand after the morning peak in zone 1 is low, putting more than two vehicles in that zone will not deliver high value, and for more than 12 vehicles zero additional value will accrue. In contrast, the higher demand-to-come in zone 5 will lead

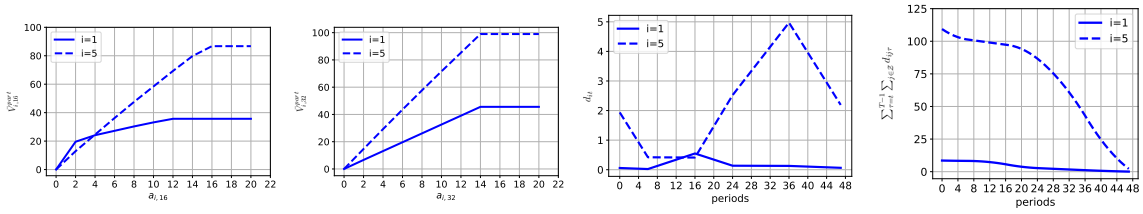

(a) $\bar{V}^{part}_{i16}$ (b) $\bar{V}^{part}_{i32}$ (c) d_{it} (d) $\sum_{\tau=t}^{T-1} \sum_{j \in Z} d_{ij\tau}$

Figure 2.7: Parts of the VFA for two selected zones at periods 16 (a) and 32 (b), base demand (c), and cumulated base demand (d) over the course of the day

to a positive value for additional vehicles, which explains the later saturation of $\bar{V}_{5,16}(a_{5,16})$ at higher vehicle count $a_{5,16}$. This shows how the VFA reflects short-term and long-term network effects due to temporal demand variations. Note that the magnitudes of the $\bar{v}^k_{i(\tau+H)}$ values and $\bar{v}^{const}_{\tau+H}$ values (with an average of two vehicles per zone) in Table 2.3 indicate that they both represent decisive VFA features.

2.5.3.5 Stochastic Demand

To analyze the robustness of the results, we additionally evaluate the pricing resulting from different solution approaches in a stochastic environment. For this purpose, we apply a *multiplicative stochastic demand function*, which is one of the standard approaches of modeling demand as described, e.g., in Talluri and van Ryzin (2004, Chapter 7.3.4). More precisely, base demand is now a random variable D_{ijt} with

$$D_{ijt} = \xi \cdot d_{ijt} \tag{2.31}$$

where ξ is a stochastic error term which is assumed to follow a normal distribution $\mathcal{N}(1, \sigma^2)$.

Based on this demand model, we evaluate all scenarios from Section 2.5.1, i.e., the 9-, 16- and 25-zones settings with all demand-supply-ratios δ. For each scenario, we consider different degrees of stochasticity, expressed by different standard deviations $\sigma \in \{0, 0.1, 0.2, 0.3, 0.4\}$ of the factor ξ. These values are in the range of demand uncertainties we observed in practice. For each of the resulting combinations of scenario and degree of stochasticity, we draw $S = 1000$ demand matrices $\mathbf{d}^s$ with $s \in \{1, \ldots, S\}$ as realizations of $[D_{ijt}]_{Z \times Z \times T}$ and use them to evaluate the ADP-H and ROL-H solution approaches, i.e., to evaluate the price table which was optimized for the corresponding base demand matrix $\mathbf{d}$. Appendix 2.G contains all results with confidence intervals.

Figure 2.8 illustratively depicts the results for $\delta = 2/6$ and the three different zone numbers. On the vertical axis, the mean value of the relative profit increase with respect to the CUP benchmark (0%-line) is depicted for ROL-1, ROL-8, ADP-1, and ADP-8. On the horizontal axis, the standard deviation σ is varied.

Overall, the proposed pricing approaches and our results are robust to the stochasticity of demand. However, all profit increases tend to decrease slightly with increasing stochasticity. The more sophisticated procedures are obviously more sensitive to stochasticity than CUP. However, these reductions in profit increase amount to at most two percentage points compared to zero stochasticity ($\sigma = 0$) and the order of the different approaches regarding their performance does

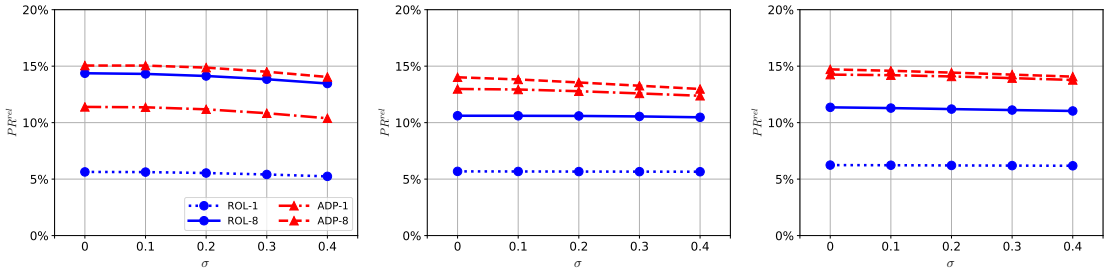

(a) $Z = 9$ (b) $Z = 16$ (c) $Z = 25$

Figure 2.8: Stochastic evaluation of solution approaches in 9-, 16- and 25-zones setting with demand-supply-ratio $\delta = 2/6$.

not change with increasing stochasticity. All proposed approaches still perform substantially better than the benchmark CUP, and as in Section 2.5.3.2, the anticipatory approach ADP-8 we propose is always the best.

As a technical remark, note that in the stochastic demand model, demand realization $D_{ijt} < 0$ could potentially result, in particular for high values of σ (see the corresponding discussion in Talluri and van Ryzin (2004, Chapter 7.3.4)). We correct for this by setting negative draws to 0. Note that the small positive bias resulting from this truncation is not relevant to our study, as for each degree of stochasticity, we use the same 1000 scenarios for all approaches we compare.

2.5.3.6 Assessment of Pricing Approaches covered in the Literature

As stated in Section 2.1, the OBDPP – despite its relevance for practice, which we trace to the pricing approach's advantages compared to others – is a novel problem which has not been discussed in the literature yet. Thus, a *direct* comparison with pricing approaches covered in the literature is not feasible. Still, in this section, we assess pricing solutions *derived* from pricing approaches suggested in the literature to determine whether they could be applied to the problem at hand.

We explained in Section 2.2.3 that all of the closest related studies differ from the OBDPP on two decisive points: The existing studies consider *Trip-based* pricing instead of *origin-based* pricing, and they do not make the two central assumptions of *pure pricing* and *proportional demand fulfillment* (see Section 2.1). Therefore, we formulate two variants of the original OBDPP model (2.1)-(2.16):

- *TBDPP-RLX* mimics *trip-based* pricing (*TBDPP*) as the closest related work suggests (see Section 2.2.3). Similar to all of these studies, the model omits – or technically speaking, *relaxes* (*RLX*) – the *pure pricing* and *proportional demand fulfillment* assumptions that are operative in the original OBDPP model. The TBDPP-RLX is formulated by (2.34)-(2.44) in Appendix 2.H.1.

- *OBDPP-RLX* considers *origin-based* pricing as in the OBDPP but also *relaxes* the *pure pricing* and *proportional demand fulfillment* assumptions. By relaxing the OBDPP's two central assumptions, this model allows us to asses the two assumptions' realistic modeling in the OBDPP in isolation. The OBDPP-RLX is formulated by (2.45)-(2.55) in Appendix 2.H.2.

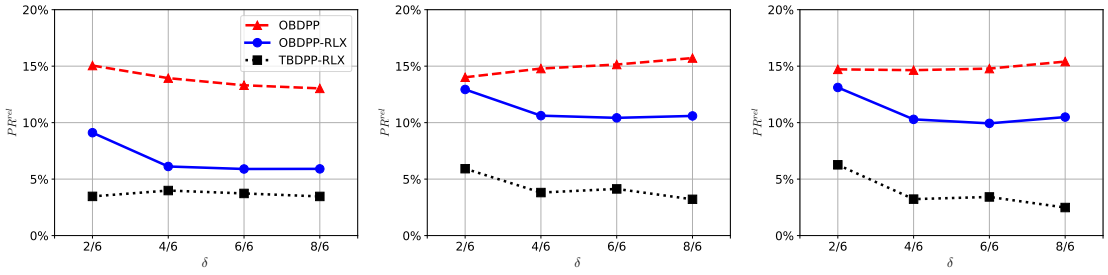

(a) $Z = 9$ (b) $Z = 16$ (c) $Z = 25$

Figure 2.9: Comparison of profit obtained by pricing solutions with OBDPP, OBDPP-RLX, and TBDPP-RLX in settings of 9, 16 and 25 zones with different demand-supply-ratios δ.

To assess the pricing solutions derived from the TBDPP-RLX and the OBDPP-RLX, we evaluate the resulting pricing solutions in the OBDPP and compare the resulting profits with the result we achieved by solving the OBDPP with our ADP decomposition approach (ADP-8). For the TBDPP-RLX, we determine origin-based prices from the trip-based pricing solution as follows: In a first step, for every location-period combination, all corresponding trip-based prices are averaged. In the second step, the nearest price point from the given price set is determined. Regarding the solution methods for the OBDPP-RLX and the TBDPP-RLX, all periods of the respective problems are solved simultaneously (as for OPT and UB) with a computation time limit of 48 hours. Due to the reduced complexity of these two problems compared to the OBDPP, they can be solved close to optimally for all settings and scenarios: All solutions have a gap of less than 0.5% to the respective best known upper bound.

Figure 2.9 states the results for the three settings with 9, 16, and 25 zones, where each has four scenarios with different demand-supply ratios. Independent of the setting and scenario, the pricing determined by TBDPP-RLX performs worst of all pricing approaches. Also, the pricing determined by OBDPP-RLX is consistently worse than the one that OBDPP determined. In terms profit PR^{rel} (percentage points w.r.t. CUP), pricing solutions delivered by OBDPP-RLX perform 0.1 to 7.2 percentage points worse than those of ADP-8, and the ones delivered by TBDPP-RLX perform 7.8 to 12.8 percentage points worse than those of ADP-8. This is because the OBDPP-RLX, and especially the TBDPP-RLX, suppose too high an influence on the resulting rentals than is possible in reality. Without the *pure pricing* and *proportional demand fulfillment* assumptions, the models can perform a kind of *availability control* (see Section 2.1). This means that rentals do not – as in reality – realize solely from dependence on the prevailing supply and demand, but that the model can decide to reject certain rentals and to favor others that have specific destinations. For the TBDPP-RLX, this effect is even stronger, because the model can influence demand more flexibly with trip-based prices (location-location-period level), while in reality prices are limited to being origin-based (location-period level).

Overall, these results clearly justify two findings: First, pricing approaches such as those suggested in the literature (TBDPP-RLX), cannot be applied to determine prices for the OBDPP. Second, the exact modeling of the two central assumptions as they are prevalent in the reality of the OBDPP is indeed decisive in determining the best possible pricing solutions.

Note that these results do not allow any statements regarding the effectiveness of origin-based pricing in comparison to *actual* trip-based pricing of an SMS. Clearly, if an SMS provider

were able to put trip-based pricing into practice, this cannot perform worse than origin-based pricing, simply due to the additional flexibility. However, as explained in Section 2.1, practice – for very good reasons – exclusively applies origin-based pricing.

2.6 Case Study

In this section, we consider a real-world scenario that reflects the origin-based differentiated pricing optimization of Share Now for a weekday in Florence, Italy. On the one hand, this case study allows us to conclude results and managerial insights in an instance of real-world size. On the other hand, compared to the rather stylized scenarios given in Section 2.5, all parameters in this case study are based on real historic data which was collected over several months at Share Now. We introduce the scenario in Section 2.6.1 and discuss the results in Section 2.6.2.

2.6.1 Scenario and Parameters

Share Now's area of operation in Florence is divided into 59 zones, as shown in Figure 2.10a. To respect the non-disclosure agreement, we only share values for demand and rentals that are normalized to the maximum period demand $\max(d_t)$, where $d_t = \sum_{i,j \in \mathcal{Z}} d_{ijt}$. Figure 2.10b depicts the normalized base demand $(d_t / \max(d_t)\ \forall t \in \mathcal{T})$, as well as the resulting normalized rentals with the uniform pricing solution $(\sum_{i,j \in \mathcal{Z}} r^{(2)}_{ijt} / \max(d_t)\ \forall t \in \mathcal{T})$ during the course of the day. The day is discretized into 48 periods of 30 minutes each. The demand curve shows the typical pattern with two peaks at the rush hour times, in the morning at $t = 17$ (08:30) and in the evening at $t = 39$ (21:30), with the lowest level during the night at $t = 8$ (04:00). The rental curve follows the general course of the demand curve, with less pronounced peaks. During the night, the difference between demand and rentals is smaller than during the day. This can be explained by the higher availability of vehicles during the night, implying that potential customers almost always find an available vehicle. During the day, in particular during peak times, the probability that demand results in a rental is lower due to the relatively high number of vehicles in use. Note that the demand-supply-ratio in this scenario is approximately $\delta = 0.7$, which is in the range of scenarios with $\delta < 1$ on which we focused in the computational experiments we described in Section 2.5.

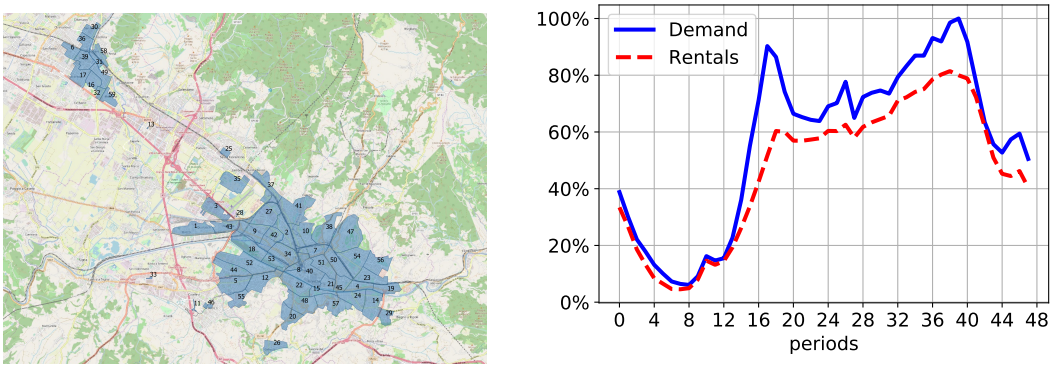

(a) Operating area with 59 zones

(b) Normalized demand and rentals over the course of the day

Figure 2.10: Share Now scenario in Florence, Italy

Demand parameters are obtained from data Share Now recorded in April and May 2018. More precisely, the base demand matrix $\mathbf{d}$ with entries d_{ijt} results from unconstraining the constrained demand, i.e., the observed rentals. Unconstraining is a standard issue in revenue management (see, e.g., Talluri and van Ryzin (2004, chapter 9.4)). We chose all other parameters

real-life scenario	solution approach	change w.r.t. CUP			$P^{prop}_{p^m}$			$RT^{prop}_{p^m}$		
		PR^{rel}	RV^{rel}	RT^{rel}	low	base	high	low	base	high
Florence, 59 zones	ROL-1	3.9%	0.9%	-8.2%	11.1%	45.7%	43.2%	8.5%	33.5%	58.1%
	ADP-1	7.0%	4.1%	-4.4%	8.8%	54.0%	37.1%	6.0%	43.2%	50.8%
	ROL-4	6.8%	4.0%	-4.3%	8.4%	56.1%	35.5%	5.4%	45.5%	49.1%
	ADP-4	9.2%	6.2%	-2.8%	13.7%	45.3%	41.0%	6.4%	41.1%	52.5%

Table 2.4: Results from real-life scenario in Florence, Italy

as in the computational experiments (Section 2.5.1). The only difference concerns the VFA design and its parameter estimation process. We increased the number of pieces to $K = 20$ to adapt to the larger fleet size. Finally, we compared our ADP decomposition approach's results in the ADP-4 configuration to the myopic benchmark ROL-1.

2.6.2 Results

Section 2.6.2.1 discusses the profit increase from ADP-4. Section 2.6.2.2 analyzes the resulting pricing decisions, rentals, and revenue.

2.6.2.1 Profit

Table 2.4 summarizes the PR^{rel} results for the Florence scenario. With our ADP decomposition approach (ADP-4), the profit improvement PR^{rel} is 9.2%. Thus, the explicit and implicit consideration of network effects in ADP-4 realized an additional improvement of 5.3 percentage points compared to the myopic solution ROL-1, and an improvement of 2.4 percentage points over the ROL-4 benchmark. These results demonstrate the scalability of our solution approach to real-life scenarios and show a substantial improvement potential compared to the de facto standard of CUP through network effect consideration.

2.6.2.2 Pricing Decisions, Rentals, Revenue

We now analyze the effect of optimization on the pricing decisions, the rentals, as well as the revenue. Figure 2.11a depicts the $PR^{prop}_{p^m t}$ results of ADP-4 during the course of the day and shows that the prices vary considerably. The largest proportion of highly priced rentals is set at demand peak times $t = 17$ and $t = 40$. At non-peak times, the base price accounts for the largest proportion of rentals, with an exception in the very first period only. Table 2.4 shows the price proportions $P^{prop}_{p^m}$ over the whole day. We observe that, on average, ADP-4 leads to higher prices compared to the CUP benchmark, lower average prices compared to the myopic solution and comparable prices with ROL-4.

To gain more insight, we now illustratively consider four zones in more detail. Figure 2.12 depicts absolute demand, absolute available vehicles, and the prices of the ADP decomposition solution ADP-4 over all periods for the four zones with indexes 2, 7, 49, and 59. Zones 2 and 59 are characterized by relatively low demand, zone 49 has the highest demand of the four, and zone 7's demand lies approximately halfway between the two extremes. During the first half of the day, especially during the morning peak time, zone 2 has relatively many vehicles available – more than the demand requires. This results in low prices at the beginning of the day and

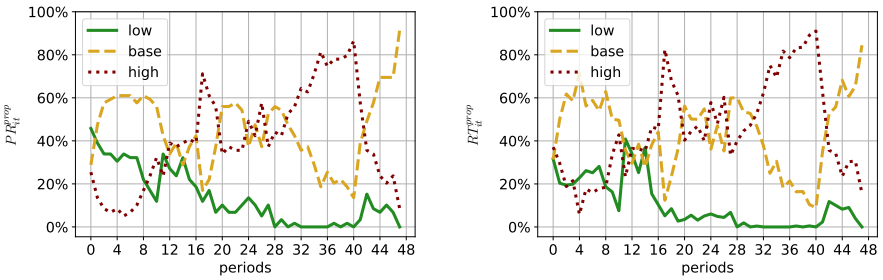

(a) (b)

Figure 2.11: Prices (a) and rentals (b) over the course of the day (ADP-4)

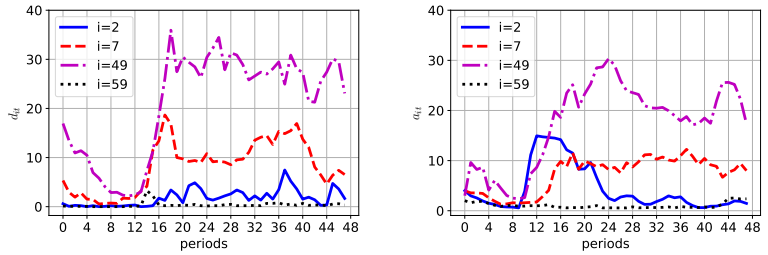

(a) Base demand d_{it} (b) Available vehicles a_{it}

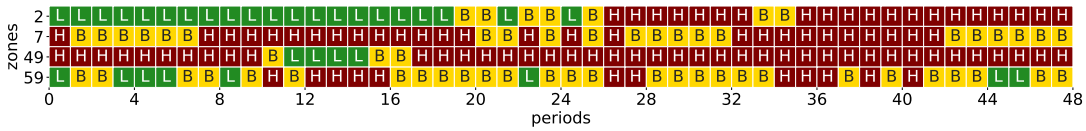

(c) Prices p_{it}

Figure 2.12: Base demand (a), available vehicles (b) and prices (c) in four selected zones (ADP-4)
Green: L=low price, yellow: B=base price, red: H=high price

a declining vehicle count towards midday. During the evening peak, the levels of supply and demand are largely balanced and high prices are set. Zone 7 shows the typical demand pattern, with two peaks that exceed the available vehicle count at these times. The resulting prices also show this shortage of vehicles at peak times, as high prices are set during these periods. Zone 49 has a higher demand than vehicle supply during most periods of the day, and therefore often has high prices. The only exception is during the morning peak, when many vehicles arrive in that zone and lower prices are set to compensate for the oversupply. Zone 59 is characterized by relatively low demand and only a few available vehicles throughout the day, with high prices at peak times and low prices in the first periods. These observations show that the resulting pricing decisions differ considerably in their patterns. To some extent they can be explained by current supply and demand, but regarding the above-mentioned differences between the $P^{prop}_{p^m}$ of the myopic benchmark and the ADP decomposition approach, they are also the result of network effect considerations.

Table 2.4 shows that RT^{rel} decreases by 8.2% with the myopic solution and by 2.8% with the ADP decomposition approach solution, while RV^{rel} increases by 0.9% and 6.2%, respectively. Considering these figures in combination with the $P^{prop}_{p^m}$ discussed above, the additional PR^{rel} increase through network effect consideration of ADP-4 with respect to ROL-1 is a result of overall lower prices with more rentals and revenue. Figure 2.11b displays the $RT^{prop}_{p^m t}$ of ADP-4.

Their courses over the day resemble the courses of the respective $PR^{prop}_{p^m t}$. More precisely, during peak times most of the rentals take place at a high price and in almost all other times most rentals are at the base price.

To summarize the results of the case study of Share Now in Florence, our solution approach generates considerably higher profits compared to the de facto standard of constant uniform prices and, more importantly, to the myopic benchmark. In fact, our solution even gets quite close to a theoretical upper bound. This increase is realized by a considerable price differentiation that allows for generating more revenue with fewer rentals in comparison to CUP at base price. High prices exploit the higher demand at peak times, and the larger proportion of low and base prices under network effect consideration allows for creating a more favorable fleet distribution and more rentals compared to the myopic solution.

2.7 Managerial Insights

The systematic computational experiments (abbreviated below as *experiments*) of OBDPP scenarios given in Section 2.5 in combination with the analyses of the Share Now case study (abbreviated below as *case*) given in Section 2.6 reveal important managerial insights for shared mobility providers, which we summarize in this section.

Benefit of origin-based differentiated minute pricing: The results demonstrate that origin-based differentiated minute pricing is more advantageous than constant uniform pricing which is still the de facto industry standard. With our approximate dynamic programming decomposition solution approach, profits consistently increased throughout the considered instances, i.e., in both experiments (10% to 15%) and in the case (9%). For SMS providers, this is an insightful outcome, because origin-based differentiated minute prices are the first natural extension going beyond constant uniform prices. This is mainly because compared to other pricing mechanisms, origin-based differentiated pricing is relatively simple to implement, does not require upfront information about a trip's destination, and, very importantly, is easy to communicate to customers.

Scalability requires sophisticated solution approaches: The problem is computationally complex. More precisely, determining profit-maximizing pricing solutions is NP-hard. This is reflected by the fact that a straightforward solution using out-of-the-box commercial solvers is not possible. The supposedly obvious idea of directly solving the pricing problem in an integrated way, i.e., simultaneously for all locations and in a reasonable time frame (e.g. a day), already fails for the smallest SMS that consists of only a few dozens locations. The standard next step is temporal decomposition, i.e., considering multiple smaller problems with fewer periods instead of the entire day. This has a reasonable run time, but in general lacks in solution quality. We show that more sophisticated approaches are necessary and possible, thereby striking a balance between the ideas of integrated and decomposed problem solving. In particular, our approximate dynamic programming decomposition approach provides a computationally tractable means for SMS providers applicable in instances of real-life size.

Importance of network effect consideration: The consideration of network effects is decisive for high-quality solutions. Our results demonstrate that SMSs are characterized by a complex interaction between supply and demand. Consequently, vehicle values differ considerably across locations and time. Further, additional available vehicles at the same location and time have a decreasing marginal value because of limited demand. In contrast to straightforward pricing approaches like a myopic optimization, our approximate dynamic programming decomposition approach yields very good solutions that are close to an upper bound for the optimal solution. Key is its design for and ability to capture these network effects. This led to a profit increase over myopic pricing of up to 9.4 percentage points in the experiments, and up to 5.3 percentage points in the case. Please note that these profit improvements depend on the instance. Especially for ratios of supply and demand prevalent in practice, there is a considerable improvement. Marginal vehicle values vary considerably in the range of 0 to 9.8 monetary units, which is equivalent to 2-3 rentals at base price where profit is 3.4 monetary units. For SMS providers, the different marginal vehicle values provide a means of quantifying short- and long-term network effects, and they are also informative for other planning tasks, such as relocation.

Profit increase due to price and quantity effect: Profit maximization is not always equivalent to an increase in rentals. In the experiments, we indeed observed an increase of both profit and rentals for the best solutions we found. In the case, however, the profit increase was realized with less rentals and higher prices. For SMS providers this is an important observation, as it also affects other service-oriented metrics like the availability of vehicles.

High degree of price differentiation: Finally, we observe that the best pricing solutions have a high degree of differentiation across time and space. In the case, for example, over all location-time combinations, we have an average of 15% low, 45% base, and 40% high prices. These proportions do not remain constant throughout the day. A deeper analysis of the price table revealed that some zones have high prices during the morning and evening rush hours, while others have lower prices at these times. We showed that these different pricing patterns result from the supply and demand level in these zones over time, but are also a consequence of network effects. All these aspects indicate that the optimal price tables are complex. From a customer perspective, switching from constant uniform pricing to origin-based differentiated minute pricing means that prices now vary frequently. Therefore, it is important for SMS providers to accompany the introduction of origin-based minute price differentiation with a communications campaign that thoroughly explains the reasons for and benefits of the new approach, i.e., to ensure customer satisfaction and loyalty.

2.8 Conclusion and Outlook

Motivated by our collaboration with Share Now, in this paper we defined and analyzed the problem of origin-based differentiated pricing for SMSs. The paper has addressed the problem of determining spatially and temporally differentiated origin-based minute prices to maximize profit. Despite such price differentiation increasingly being adopted in practice, the research literature has not yet focused on these origin-based pricing mechanisms.

To model the SMS, we proposed a mixed-integer linear program based on a fluid formulation in which vehicle movements are described as flows through a spatio-temporal network. It naturally incorporates network effects, that is, the complex interactions between the moving vehicle supply and varying demand in an SMS. The problem turns out to be NP-hard, thus, heuristic solution approaches are warranted. We therefore proposed an approach that simultaneously scales to real-life scenarios and approximately incorporates the network effects. We designed the approach in such a way that it combines the benefits of decomposition on the one hand and VFA from the realm of approximate dynamic programming on the other. The decomposition allows providers to quickly solve multiple smaller problems with limited time horizons instead of the original problem that simultaneously considers all periods. At the end of the considered horizon, a VFA allows for endogenously incorporating the profit-to-come in dependence of any resulting vehicle distribution.

Extensive computational experiments with a varying number of zones, demand patterns, and overall demand levels demonstrated the benefit of our approach. It considerably improves profit (up to 15%) compared to the de facto standard of constant uniform prices, as well as compared to a myopic benchmark without consideration of network effects (up to 10 percentage points). In settings where the optimal solution can be determined, our approach finds a solution close to optimality. The resulting price tables show high similarity to the optimal price tables, in contrast to the price tables from the myopic pricing approach. We further demonstrated that the proposed VFA structure can reflect the decreasing marginal value of vehicles, which allows taking into account both short-term and long-term network effects.

In a real-life case study based on Share Now data, we demonstrated the scalability and performance of our solution approach. Profits increase 9% with respect to the de facto industry standard, although rentals decrease by 3%, leading to higher vehicle availability and 6% more revenue – two additional important operative indicators for SMS providers. Therefore, this illustrates that profit increases can result from price and quantity effect, to the extent that profit increases can also realize with reduced rentals. A detailed analysis of prices showed considerable differentiation across the location-time combinations and that there are various price patterns in the different zones. SMS providers should bear this in mind when introducing origin-based differentiated minute pricing, as frequent price changes could affect the customer experience. Also, the consideration of network effects in our approach causes an overall price reduction compared to the myopic solution, resulting in more rentals and revenue. Considering both profit and pricing, we conclude that simple pricing rules cannot exploit the total potential for increased profit. We refer the reader to Section 2.7 for a generalized discussion of managerial insights that follow from jointly considering our computational experiments and the case.

To summarize, this work demonstrates the potential of origin-based differentiated minute

pricing in SMSs and the importance of considering network effects. Our ADP decomposition approach provides a scalable means for integrating these effects successfully.

Based on the presented results and methodology, we believe there are several promising directions for future work. First, the fleet of car sharing providers typically consists of different vehicle types that could be represented in a formulation based on multi-commodity network flow problems. Second, although our approach has already proved to be robust in a stochastic setting, developing approaches explicitly based on stochastic optimization models could be another useful way of extending our work and potentially further improving the promising results. Third, we believe that integrating VFAs in the vast field of other tactical and operational decision-making problems in SMSs is promising. This applies in particular to dynamic problems that require decision making in real-time, and reveals the problem of provider-based relocation, potentially in combination with pricing, as a relevant topic for future work.

2.A Proof of NP-hardness

We prove the NP-hardness of the OBDPP (2.1)-(2.16) by polynomial-time reduction of the *three-satisfiability problem* (3-SAT) to the OBDPP.

We begin with the definition of 3-SAT. Let $\mathcal{X} = \{x_1, \ldots, x_n\}$ be a set of n Boolean variables. A *literal* is a Boolean variable x_n or its negation $\bar{x}_n$. A k-CNF (conjunctive normal form) *formula* is a logic expression, consisting of a conjunction (AND,$\wedge$) of C *clauses*, where each clause is a disjunction (OR,$\vee$) of k literals. Such a k-CNF formula $F(x_1, \ldots, x_n)$ is *satisfiable* if a *truth assignment* $\alpha : \mathcal{X} \to \{\texttt{TRUE}, \texttt{FALSE}\}^n$ exists for which $F(\alpha) = \texttt{TRUE}$. For example, $F = (x_1 \vee \bar{x}_2 \vee x_3) \wedge (x_1 \vee x_2 \vee \bar{x}_4) \wedge (\bar{x}_1 \vee \bar{x}_3 \vee x_4)$, is a 3-CNF formula with four variables and three clauses. The 3-SAT problem is the following: *Given a 3-CNF formula F, is F satisfiable?*

The core idea of the proof is to construct an OBDPP instance where prices correspond to literals of the 3-SAT problem. The OBDPP instance is constructed such that optimal profit equals a known upper bound if and only if the corresponding 3-SAT is satisfiable.

To understand this underlying idea, think of 3-SAT as the problem of selecting one literal per clause that is guaranteed to be TRUE. The other two literals in each clause can be given by the selected ones, if they share a variable (i.e. x_n and $\bar{x}_n$). Otherwise, they are arbitrary. Of course, the selection must be consistent (i.e. selecting a literal with $x_1 = \texttt{TRUE}$ and another with $\bar{x}_1 = \texttt{TRUE}$ would be contradictory). Each clause now corresponds to a location-period combination i-t that must be priced in the OBDPP instance. Also, the selection of the literal m as guaranteed to be TRUE corresponds to the selection of price point p^m in the location-period combination (i.e. $y^m_{it} = 1$). Overall, the OBDPP instance is constructed to ensure optimal profit reaches a known upper bound if and only if the selected literals are not contradictory. Thus, satisfiability of the 3-SAT instance is equivalent to the existence of a pricing that reaches the upper bound in the OBDPP instance.

More precisely, consider the following reduction from 3-SAT to the OBDPP. Let $x_1, \ldots, x_n$ be n Boolean variables and F be a formula in 3-CNF consisting of C clauses and literals $\lambda_{c'm}$:

$$F = \bigwedge_{c'=1}^{C} (\lambda_{c'1} \vee \lambda_{c'2} \vee \lambda_{c'3}). \tag{2.32}$$

Inspired by Roch, Savard, and Marcotte (2005), who consider a toll pricing problem, we construct an OBDPP subnetwork for each clause, as shown in Figure 2.13. The subnetwork consists of three time steps $t, t+1, t+2$ and at least five locations. Figure 2.13 illustratively depicts eight locations $k', l', \ldots, r'$. Only the arcs on which the flow of vehicles can be positive are represented. Each of the three solid arcs outgoing from the l'-t node represents one literal $\lambda_{c'm}$ which corresponds to price $y^m_{l't} = 1$. The dashed arcs represent the s_{it} arcs for vehicles not moved (compare Figure 2.2) and, thus, remaining at their location i. The thin solid, thick solid and dot-dashed arcs represent the r^m_{ijt} arcs for rented vehicles.

The demand on the thin solid arcs is denoted by $\bar{d}_{c'}$, and $\bar{\bar{d}}$ on the thick solid arcs. While $\bar{d}_{c'}$ can vary over different subnetworks, $\bar{\bar{d}}$ is constant. The specific choice of these demand parameters depends on the instance, as we explain below. We always set $d^m_{ijt} = 1$ for each dot-dashed arc.

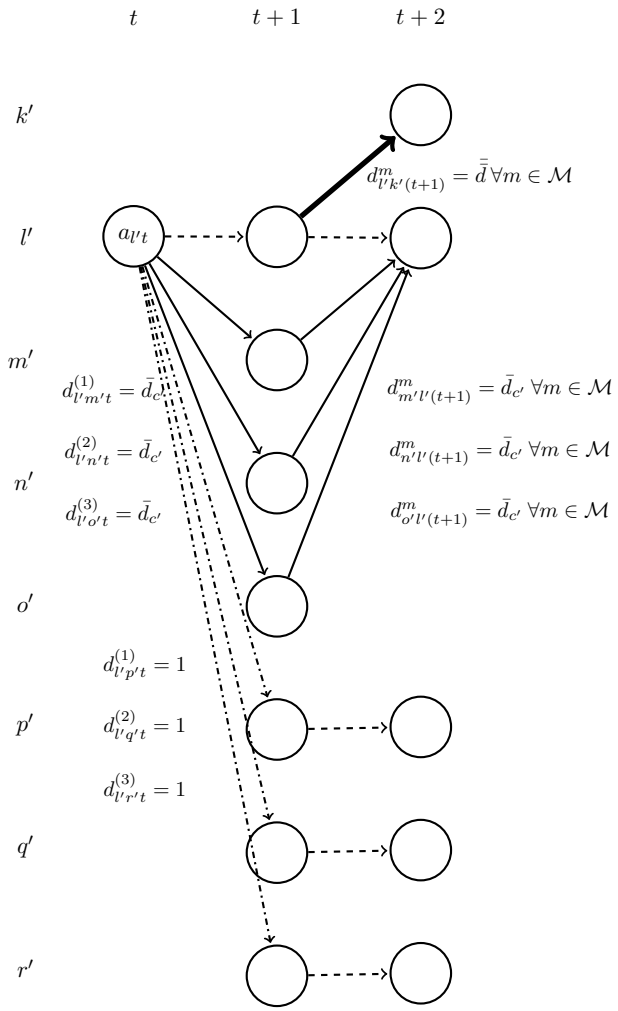

Figure 2.13: Subnetwork corresponding to clause $(\lambda_{c'1} \vee \lambda_{c'2} \vee \lambda_{c'3})$

Only the thick solid arcs represent the rentals that have a positive contribution to the objective, i.e., the rental duration (compare OBDPP objective function (2.1)) is set to zero for all location-location combinations, except for $l_{l'k'} = 1$. All three minute prices are $p^{(1)} = p^{(2)} = p^{(3)} = 1$ and the variable minute cost is $c = 0$. With these parameters, every rental that realizes between the locations l' and k' has a profit of 1, and for all other location-location combinations it is 0.

Note that because exactly one price is set at the l'-t node, exactly one of the thin solid paths has a positive flow in the subnetwork. Remember that if price p^m is selected at the l'-t node, the corresponding literal $\lambda_{c'm}$ is `TRUE`. It is important to keep in mind that this is an implication, not equivalence: If the price at the l'-t node is not p^m, the literal $\lambda_{c'm}$ is irrelevant regarding satisfiability (we already have another `TRUE` one in that clause) and could be `TRUE` or `FALSE`. Note that if $\lambda_{c'm} = \bar{x}_n$, then $x_n =$ `FALSE`. Each of the thin solid paths in a subnetwork can have up to $3(C - c')$ corresponding dot-dashed paths (3 for every subnetwork with larger c'), that is, they have the same price index. Figure 2.13 illustrates one corresponding dot-dashed arc per solid arc.

The 3-SAT reduction is performed by connecting multiple subnetworks in series, as shown in Figure 2.14. When connecting the subnetworks, we introduce an additional set of rental arcs represented by dotted arcs and with $d^m_{ijt} = 1\ \forall m \in \mathcal{M}$ and $l_{ij} = 0$. Each dash-dotted arc that originates in a subnetwork requires a corresponding dotted arc that closes the path between two clauses. We denote these paths as *interclause paths*. They connect every pair of literals corresponding to a variable and its negation, where a contradiction might arise. The idea is that if the first literal (at the origin of the interclause path) is guaranteed to be `TRUE`, vehicles flow over the path. If the second literal (at the destination of the path) is guaranteed to be `TRUE`, vehicles will flow over the corresponding thin solid arc. If both are `TRUE`, and we therefore have a contradiction, we have excess vehicles at the node where the aforementioned thin solid arc and the dotted arc end and will lose profit, which makes attaining the bound impossible. In Figure 2.14 four interclause paths originate in node $i = 2$, $t = 0$ and one originates in node $i = 2$ and $t = 2$.

We already stated the parameters p^m, c, l_{ij}, and d^m_{ijt} for the dotted arcs above. Regarding the other parameters, we set $\bar{d}_{c'} = 1$ for the last and second to last clauses C and $C-1$, meaning $\bar{d}_C = \bar{d}_{C-1} = 1$. We now iterate backwards over the clauses from $c' = C - 2$ to $c' = 1$. For each of these clauses with $c' < C - 1$, we set $\bar{d}_{c'} = \bar{d}_{c'+1} + \max_{m\in\mathcal{M}}\{z_{(c'+1)m}\}$. The fleet size is set to $\hat{a}_{2,0} = \bar{d}_1 + \max_{m\in\mathcal{M}}\{z_{1m}\}$. Note that with this choice of demand parameters and fleet size, the available vehicles $a_{2,2(c'-1)}$ for each subnetwork c' are sufficient for the possible rentals in all periods $t \geq c'$, independent of the set prices. Note further, that an inconsistent selection of guaranteed literals thus leads to more vehicles than demand in the destination node of an interclause path. For all thick solid arcs, the demand is set to the fleet size, meaning $\bar{\bar{d}} = \hat{a}_{2,0}$. Finally, the demand for the first and last arc of all interclause paths is set to 1 for all prices, meaning $d^m_{ijt} = 1\ \forall m \in \mathcal{M}$.

In our example, this implies $\bar{d}_3 = \bar{d}_2 = 1$. As clause 2 has only one assignment restriction, with clause 3 for price $y^{(3)}_{2,2}$, we set $\bar{d}_1 = 1 + 1$. In the first clause, we set $\max_{m\in\mathcal{M}}\{z_{1m}\} = 2$, because price $y^{(3)}_{2,0}$ has two assignment restrictions with clauses 2 and 3. The fleet size is $\hat{a}_{2,0} =$

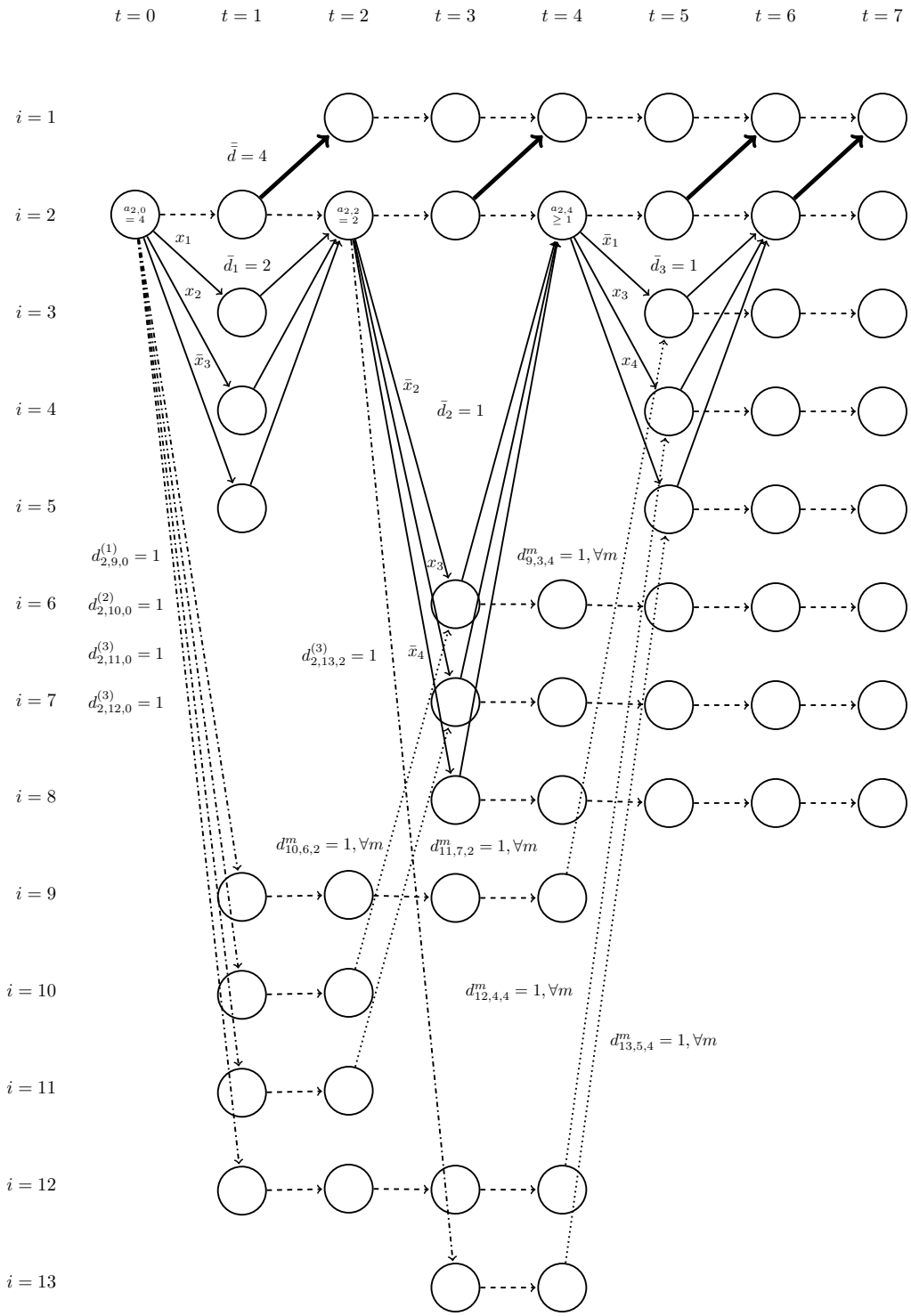

Figure 2.14: An instance of the OBDPP for the formula $(x_1 \vee x_2 \vee \bar{x}_3) \wedge (\bar{x}_2 \vee x_3 \vee \bar{x}_4) \wedge (\bar{x}_1 \vee x_3 \vee x_4)$. An optimal solution with prices $y^{(2)}_{2,0} = y^{(2)}_{2,2} = y^{(2)}_{2,4} = 1$ attains the upper profit bound. The corresponding assignment $x_2 = x_3 = \texttt{TRUE}$ with arbitrary x_1 and x_4 is satisfiable.

$2+2$. Now consider the following inconsistent selection of guaranteed literals: $y^{(1)}_{2,0} = y^{(1)}_{2,4} = 1$ (inconsistent because $x_1 = \bar{x}_1 = \texttt{TRUE}$). Then, we have $a_{3,5} = 2$ and since $\bar{d}_3 = 1$, one vehicle would remain unused, meaning $s_{3,t} = 1$ for $t = 5, 6$.

Since our choice of parameters causes a profit of 1 for every rental between locations $i = 2$ and $i = 1$ (see above), and our setup of the network allows every vehicle of the fleet to realize at most 1 rental from $i = 2$ to $i = 1$, a profit that equals the fleet size is an upper bound. We claim that F is satisfiable if and only if the optimal profit is equal to that bound. Formally, we show that the following equivalence holds:

$$F \text{ is satisfiable} \iff \exists \mathbf{y} \text{ such that } \sum_{t\in\mathcal{T}} \sum_{i\in\mathcal{Z}} \sum_{j\in\mathcal{Z}} \sum_{m\in\mathcal{M}} r^m_{ijt} \cdot l_{ij} \cdot (p^m - c) = \hat{a}_{2,0}. \tag{2.33}$$

$\Leftarrow$: Assume that the optimal profit is equal to the fleet size. As each vehicle can only flow once over a thick solid arc where it earns a profit of 1, this is the upper bound. Obviously, no vehicle must end up in a node where it remains unused, and thus will not be rented at a profit, otherwise the upper bound cannot be reached. Now assume we were inconsistent and the pricing corresponded to guaranteeing literals with a variable and its negation. Then, the number of vehicles at the destination node of the corresponding interclause path would exceed demand, and some vehicles would remain unused until the end of the horizon. They would not flow over a thick solid arc and earn no profit. This yields a contradiction. Therefore a pricing with a profit attaining the bound must correspond to a consistent assignment, and F is satisfiable.

$\Rightarrow$: Conversely, if F is satisfiable, a satisfying assingment exists. There, at least one literal per clause is `TRUE`. For each clause, we pick a price that corresponds to a `TRUE` literal (if there are several, we take an arbitrary one). Because the assignment is consistent, we will never pick contradicting literals and there are never more vehicles in a node than the outgoing demand. Thus, all vehicles of the fleet are being rented at some period from location $i = 2$ to $i = 1$ with a profit of 1, and the upper bound is reached.

We now analyze the OBDPP construction's computational complexity. First, we consider the size of the network. It consists of $T = 2C+2$ periods; in our example in Figure 2.14 there are two periods each for the $C = 3$ clauses with $t = 0, \ldots, 5$ and two additional periods $t = 6, 7$. The number of locations is, at most, $Z = 2+3(C-1)+(3C)^2$ and depends on the number of clauses and interclause paths. The first two locations are required for the rentals with a positive profit, in our example $i = 1, 2$. Independent of the interclause arcs, the first and last clauses require three locations, one for each price and $i = 3, 4, 5$ in our example. For every additional clause, three additional locations are required, here $i = 6, 7, 8$. For each interclause path, an additional location is required, and the number of interclause paths is bounded by $(3C)^2$. In our example, there are five interclause paths with locations $i = 9, \ldots, 13$. The entire network thereby consists of $Z \cdot T = \mathcal{O}(C^3)$ spatio-temporal nodes. Note that while considering the interclause paths in the network construction, we count and store the number of outgoing paths for every clause c' and price m in $z_{c'm}$.

Overall, because all of the above operations are polynomial in C, the construction of the OBDPP instance is polynomially bounded in C. This completes the proof. □

2.B Base Demand Matrix Generation

In this section, we describe the generation process of the base demand matrices that we used in the computational experiments in Section 2.5. The base demand matrix for a specific scenario is defined by $\mathbf{d} = [d_{ijt}]_{Z \times Z \times T}$, where each element d_{ijt} represents the base demand from zone i to zone j in period t (Section 2.3.1). The process of base demand matrix generation has two general steps. First, the period demand d_t in the course of the day, meaning $\forall t \in \mathcal{T}$, is determined. Second, the specific d_{ijt} values are calculated. The two steps are elaborated in the following.

- We determine $d_t \; \forall t \in \mathcal{T}$ by specifying d_t for some of the periods $\mathcal{U} \subseteq \mathcal{T}$ in relation to the maximum period demand $\max(d_t)$ and subsequently use linear interpolation to calculate d_t for all other periods $\mathcal{T} \setminus \mathcal{U}$.

  More precisely, we first decide on the period τ with maximum period demand and determine this $d_\tau = \max(d_t)$ based on the fleet size $\hat{a}_0$ and the respective scenario-specific demand-supply-ratio δ (Section 2.5.1), i.e., $d_\tau = \hat{a}_0/\delta$. In our scenarios, in order to replicate the demand patterns observed in practice, we chose the maximum period demand to occur at the evening peak $\tau = 36$ (18:00h).

  Second, we define a set of periods $\mathcal{U} \subseteq \mathcal{T}$ with $|\mathcal{U}| = U$, for which the period demand $d_t \; \forall t \in \mathcal{U}$ is defined in relation to the maximum period demand d_τ, i.e., $d_t = u_t \cdot d_\tau$. In our settings, to replicate the typical course of demand, we define $U = 4$ period demands: the evening peak $t = 36$ with $u_{36} = 100\%$, the night low $t = 8$ (04:00) with $u_8 = 10\%$, the morning peak $t = 16$ (08:00) with $u_{16} = 80\%$, and midday $t = 24$ (12:00h) with $u_{24} = 60\%$.

  Third, the remaining $d_t \; \forall t \in \mathcal{T} \setminus \mathcal{U}$ are calculated by linear interpolation, where for some $t \in \mathcal{T} \setminus \mathcal{U}$ the d_t values of the respective next smaller and larger $t \in \mathcal{U}$ are used as supporting points. At this point, the absolute period demand $d_t \; \forall t \in \mathcal{T}$ is defined.

- We calculate the specific base demand matrix entries d_{ijt} based on d_t in a hierarchical process where the demand streams are first determined on an aggregate *zone-type* level. Subsequently, we specify the demand streams for the original zones, which allows us to replicate typical demand patterns observed in practice.

  More precisely, in order to replicate typical demand streams observed in practice, we first define $\mathcal{Q} = \{1, 2, \ldots, Q\}$ different zone types. Each of the original Z zones is assigned to one of the zone types with an injective mapping, resulting in Q sets of zones $\mathcal{Z}_q \subseteq \mathcal{Z} \forall q \in \mathcal{Q}$, with $\bigcap_{q=1}^{Q} \mathcal{Z}_q = \emptyset$ and $\bigcup_{q=1}^{Q} \mathcal{Z}_q = \mathcal{Z}$. In our scenarios, we define $Q = 4$ zone types, which we denote *center, inner, outer, peripheral*.

  Second, for each of the U periods defined above, a typical demand pattern can now be defined on the zone type level by specifying proportions of the respective d_t for every zone-type-zone-type combination. Table 2.5 depicts an example from one of our scenarios, in which we chose the parameters to reflect that most of the demand at the morning peak $t = 16$ is directed from the non-center zones to the center zones. Note that the proportions sum up to 100%, such that at this point, the absolute demand values d_{xyt} for all $Q \cdot Q \cdot U$ zone-type $x \in \mathcal{Q}$ to zone-type $y \in \mathcal{Q}$ combinations are defined for all periods $t \in \mathcal{U}$.

Third, considering the number of zones in a specific zone-type, meaning $|\mathcal{Q}_q|$, the absolute demand values d_{ijt} for all $Z \cdot Z \cdot U$ original zones for all periods $t \in \mathcal{U}$ are calculated. For example, a specific d_{xyt} with $x, y \in \mathcal{Q}$ has to be divided into multiple d_{ijt} with $i \in \mathcal{Z}_x$ and $j \in \mathcal{Z}_y$ according to $d_{ijt} = d_{xyt}/(|\mathcal{Z}_x| \cdot |\mathcal{Z}_y|)$.

Fourth, the remaining $d_{ijt} \forall i, j \in \mathcal{Z}, t \in \mathcal{T} \setminus \mathcal{U}$ are calculated by linear interpolation between the supporting points $d_{ijt}\ \forall i, j \in \mathcal{Z}, t \in \mathcal{U}$. More precisely, for a specific i-j-t combination with $t \in \mathcal{T} \setminus \mathcal{U}$, the surrounding d_{ijt} with the respective next smaller and next larger $t \in \mathcal{U}$ are used as supporting points. The interpolation is linear in the number of periods that separate the d_{ijt} to be calculated from the respective two supporting points.

		destination zone type			
		center	inner	outer	peripheral
origin zone type	center	0.05	0.1	0.025	0.025
	inner	0.1	0.05	0.025	0.025
	outer	0.15	0.1	0.025	0.025
	peripheral	0.15	0.1	0.025	0.025

Table 2.5: Example of demand proportions for zone types at morning peak $t = 16$

2.C Test Instances and Evaluation Metrics

		scenarios with number of zones and demand-supply-ratio														
solution approach	time limit	9					16					25				
		2/6	4/6	6/6	8/6	12/6	2/6	4/6	6/6	8/6	12/6	2/6	4/6	6/6	8/6	12/6
ADP-1, ROL-1	none	x	x	x	x	x										
ADP-4, ROL-4	none	x	x	x	x	x										
ADP-8, ROL-8	none	x	x	x	x	x										
OPT	none	x	x	x	x	x										
UB	48h						x					x				
ADP-1, ROL-1	48×1h						x	x	x	x	x	x	x	x	x	x
ADP-4, ROL-4	48×1h						x	x	x	x	x	x	x	x	x	x
ADP-8, ROL-8	48×1h						x	x	x	x	x	x	x	x	x	x
CUP	none	x	x	x	x	x	x	x	x	x	x	x	x	x	x	x

Table 2.6: Considered test instances

metric	all periods $t \in \mathcal{T}$, (* price p^m)	period t, (* price p^m)
$PR^{rel}_{(\cdot)}$	$\frac{\sum_{t\in\mathcal{T}}\sum_{i,j\in\mathcal{Z}}\sum_{m\in\mathcal{M}} r^m_{ijt}\cdot l\cdot(p^m-c)}{\sum_{t\in\mathcal{T}}\sum_{i,j\in\mathcal{Z}} r^{(2)}_{ijt}\cdot l\cdot(p^{(2)}-c)} - 1$	$\frac{\sum_{i,j\in\mathcal{Z}}\sum_{m\in\mathcal{M}} r^m_{ijt}\cdot l\cdot(p^m-c)}{\sum_{i,j\in\mathcal{Z}} r^{(2)}_{ijt}\cdot l\cdot(p^{(2)}-c)} - 1$
$RV^{rel}_{(\cdot)}$	$\frac{\sum_{t\in\mathcal{T}}\sum_{i,j\in\mathcal{Z}}\sum_{m\in\mathcal{M}} r^m_{ijt}\cdot l\cdot p^m}{\sum_{t\in\mathcal{T}}\sum_{i,j\in\mathcal{Z}} r^{(2)}_{ijt}\cdot l\cdot p^{(2)}} - 1$	$\frac{\sum_{i,j\in\mathcal{Z}}\sum_{m\in\mathcal{M}} r^m_{ijt}\cdot l\cdot p^m}{\sum_{i,j\in\mathcal{Z}} r^{(2)}_{ijt}\cdot l\cdot p^{(2)}} - 1$
$RT^{rel}_{(\cdot)}$	$\frac{\sum_{t\in\mathcal{T}}\sum_{i,j\in\mathcal{Z}}\sum_{m\in\mathcal{M}} r^m_{ijt}}{\sum_{t\in\mathcal{T}}\sum_{i,j\in\mathcal{Z}} r^{(2)}_{ijt}} - 1$	$\frac{\sum_{i,j\in\mathcal{Z}}\sum_{m\in\mathcal{M}} r^m_{ijt}}{\sum_{i,j\in\mathcal{Z}} r^{(2)}_{ijt}} - 1$
$P^{prop*}_{(\cdot)}$	$\frac{\sum_{t\in\mathcal{T}}\sum_{i\in\mathcal{Z}} y^m_{it}}{\sum_{t\in\mathcal{T}}\sum_{i\in\mathcal{Z}}\sum_{q\in\mathcal{M}} y^q_{it}}$	$\frac{\sum_{i\in\mathcal{Z}} y^m_{it}}{\sum_{i\in\mathcal{Z}}\sum_{q\in\mathcal{M}} y^q_{it}}$
$RT^{prop*}_{(\cdot)}$	$\frac{\sum_{t\in\mathcal{T}}\sum_{i,j\in\mathcal{Z}} r^m_{ijt}}{\sum_{t\in\mathcal{T}}\sum_{i,j\in\mathcal{Z}}\sum_{q\in\mathcal{M}} r^q_{ijt}}$	$\frac{\sum_{i,j\in\mathcal{Z}} r^m_{ijt}}{\sum_{i,j\in\mathcal{Z}}\sum_{q\in\mathcal{M}} r^q_{ijt}}$

Table 2.7: Evaluation metrics used

2.D Computation Times for VFA Parameter Estimation

As explained in Section 2.4.2, the entire process of determining pricing solutions requires a parameter estimation (Algorithm 2, Section 2.4.4) and subsequently the ADP decomposition approach (Algorithm 2). Here, we consider the computation times for the parameter estimation. Algorithm 2 shows that for every period this parameter estimation has two general components. The first is to generate samples of vehicles' distribution and to calculate a corresponding profit-to-come for every sample; the second is to determine the VFA parameters by solving the adapted least squares problem (2.23)-(2.27). To provide more insight on the respective computation times, we state the average computation times for these two components, i.e., *data generation* and *solve* (2.23)-(2.27) separately in the rows of Table 2.8. The idea is to generate all required data (for all periods) first, and then, in a second step, to solve (2.23)-(2.27) for all periods.

		setting			
		9Z	16Z	25Z	59Z
data generation	per data sample [sec.]	1.1	2.9	6.6	67.6
	1000 samples [h.]	0.3	0.8	1.8	18.7
solve (2.23)-(2.27)	total process [sec.]	27.8	46.9	67.9	195.8

Table 2.8: Computational times for data generation and parameter estimation

The data generation for all periods' computation time with each 1000 samples that we used lies between less than one hour for the 9-zones setting and roughly 19 hours for the Florence case study which has 59 zones. Solving (2.23)-(2.27) for all periods requires, at its maximum, several minutes, because (2.23)-(2.27) is a quadratic programming problem which can be solved efficiently by standard solvers.

As explained in Section 2.1, the OBDPP is an *off-line* pricing problem, where – as for every off-line problem – the overall computation time for determining a solution is not crucial, while the solution quality is indeed decisive. Of course, even for off-line problems, the computation time needs to be reasonable, so that application in practice is possible. For the considered problem and the proposed approach, the following is given: Considering the computation times in Table

2.8 and the maximum duration of determining a pricing solution with our ADP decomposition approach, which was 48 hours (see Section 2.5.1), prices are obtained in less than three days. In practice, the applied pricing solutions are kept stable for several months to ensure that an adapted demand pattern can be observed with statistical significance. Only then can a recalculation of prices be reasonable. Thus, the overall computation time does not pose any limitations for practice. Moreover, the presented computation times for generating the data can be considered as an upper bound for this process step, since all samples were generated sequentially, while a complete parallelization was possible. This means that the data generation is limited by the potential for parallelization and not by the generation of a sample data point, which in the Florence example, on average, requires only 67.6 seconds.

2.E Small Setting - 9 Zones - Additional Results

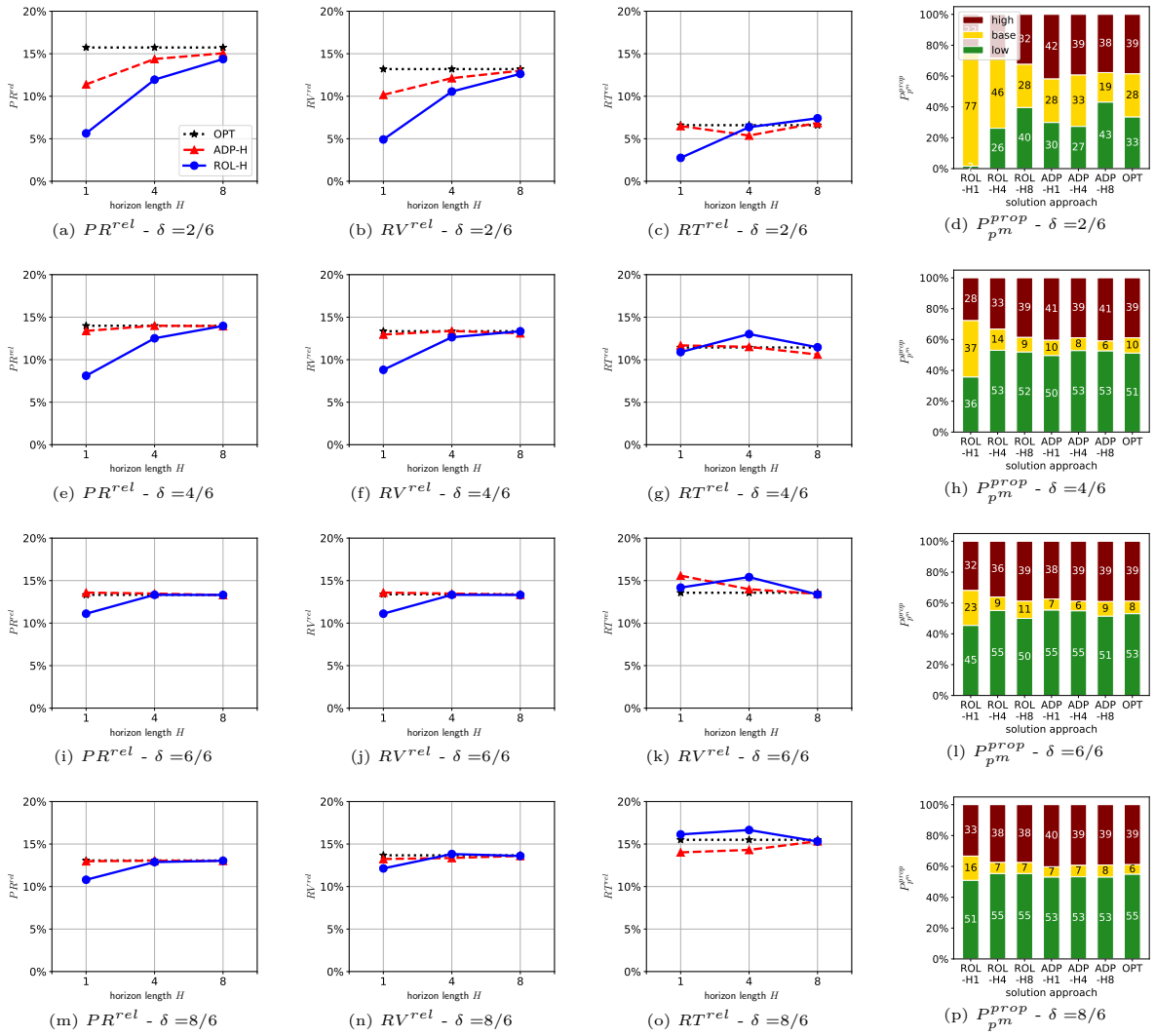

(a) PR^{rel} - δ =2/6 (b) RV^{rel} - δ =2/6 (c) RT^{rel} - δ =2/6 (d) $P^{prop}_{p^m}$ - δ =2/6

(e) PR^{rel} - δ =4/6 (f) RV^{rel} - δ =4/6 (g) RT^{rel} - δ =4/6 (h) $P^{prop}_{p^m}$ - δ =4/6

(i) PR^{rel} - δ =6/6 (j) RV^{rel} - δ =6/6 (k) RV^{rel} - δ =6/6 (l) $P^{prop}_{p^m}$ - δ =6/6

(m) PR^{rel} - δ =8/6 (n) RV^{rel} - δ =8/6 (o) RT^{rel} - δ =8/6 (p) $P^{prop}_{p^m}$ - δ =8/6

Figure 2.15: Relative increase of profit (PR^{rel}), revenue (RV^{rel}), rentals (RT^{rel}) and price proportions ($P^{prop}_{p^m}$) in 9-zones setting.
Columns: PR^{rel}, RV^{rel}, RT^{rel}, $P^{prop}_{p^m}$; Rows: Ascending demand-supply-ratio δ

2.F Enlarged Settings - 16, 25 Zones

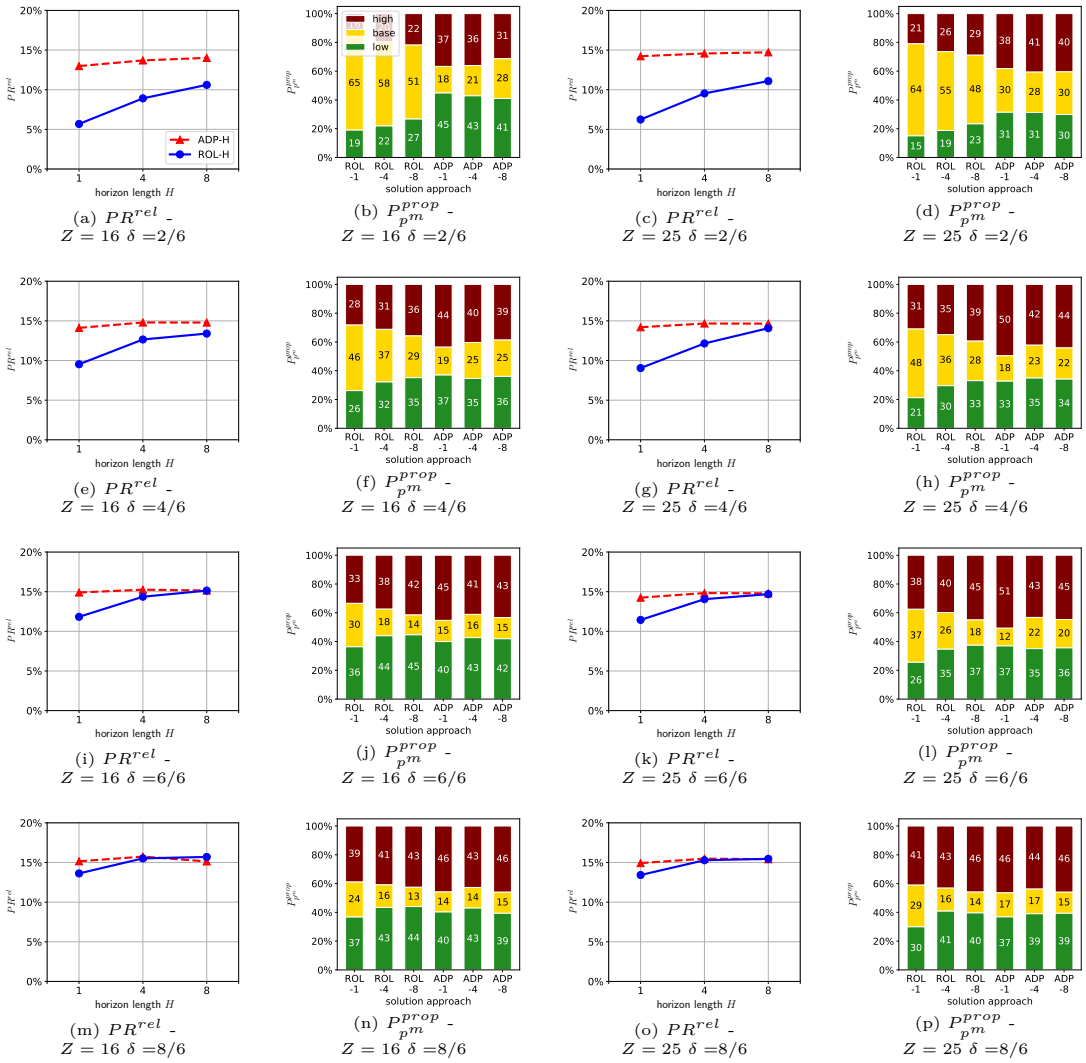

(a) PR^{rel} - $Z = 16$ δ =2/6
(b) $P^{prop}_{p^m}$ - $Z = 16$ δ =2/6
(c) PR^{rel} - $Z = 25$ δ =2/6
(d) $P^{prop}_{p^m}$ - $Z = 25$ δ =2/6
(e) PR^{rel} - $Z = 16$ δ =4/6
(f) $P^{prop}_{p^m}$ - $Z = 16$ δ =4/6
(g) PR^{rel} - $Z = 25$ δ =4/6
(h) $P^{prop}_{p^m}$ - $Z = 25$ δ =4/6
(i) PR^{rel} - $Z = 16$ δ =6/6
(j) $P^{prop}_{p^m}$ - $Z = 16$ δ =6/6
(k) PR^{rel} - $Z = 25$ δ =6/6
(l) $P^{prop}_{p^m}$ - $Z = 25$ δ =6/6
(m) PR^{rel} - $Z = 16$ δ =8/6
(n) $P^{prop}_{p^m}$ - $Z = 16$ δ =8/6
(o) PR^{rel} - $Z = 25$ δ =8/6
(p) $P^{prop}_{p^m}$ - $Z = 25$ δ =8/6

Figure 2.16: Relative profit increase (PR^{rel}) and price proportions ($P^{prop}_{p^m}$) in 16- and 25-zones settings. Columns: $Z = 16$ PR^{rel}, $P^{prop}_{p^m}$ – $Z = 25$ PR^{rel}, $P^{prop}_{p^m}$; Rows: Ascending demand-supply-ratio δ

2.G Stochastic Evaluation

	Mean profit increase with respect to CUP in %														
	$Z = 9$					$Z = 16$					$Z = 25$				
	$\sigma = 0$	$\sigma = 0.1$	$\sigma = 0.2$	$\sigma = 0.3$	$\sigma = 0.4$	$\sigma = 0$	$\sigma = 0.1$	$\sigma = 0.2$	$\sigma = 0.3$	$\sigma = 0.4$	$\sigma = 0$	$\sigma = 0.1$	$\sigma = 0.2$	$\sigma = 0.3$	$\sigma = 0.4$
CUP	0.0	0.0	0.0	0.0	0.0	0.0	0.0	0.0	0.0	0.0	0.0	0.0	0.0	0.0	0.0
ROL-1	5.6	5.6	5.5	5.4	5.2	5.7	5.7	5.7	5.7	5.7	6.2	6.2	6.2	6.2	6.2
ROL-4	12.0	11.8	11.7	11.4	11.0	8.9	8.9	8.9	8.9	8.8	9.5	9.4	9.4	9.3	9.2
ROL-8	14.4	14.3	14.1	13.8	13.5	10.6	10.6	10.6	10.5	10.5	11.4	11.3	11.2	11.1	11.0
ADP-1	11.4	11.4	11.2	10.8	10.4	13.0	12.9	12.8	12.6	12.4	14.3	14.2	14.1	13.9	13.8
ADP-4	14.4	14.3	13.9	13.9	13.5	13.7	13.5	13.3	13.0	12.8	14.6	14.5	14.3	14.1	13.9
ADP-8	15.1	15.1	14.9	14.5	14.0	14.0	13.8	13.6	13.3	13.0	14.7	14.6	14.4	14.3	14.1

(a) $\delta = 2/6$

	Mean profit increase with respect to CUP in %														
	$Z = 9$					$Z = 16$					$Z = 25$				
	$\sigma = 0$	$\sigma = 0.1$	$\sigma = 0.2$	$\sigma = 0.3$	$\sigma = 0.4$	$\sigma = 0$	$\sigma = 0.1$	$\sigma = 0.2$	$\sigma = 0.3$	$\sigma = 0.4$	$\sigma = 0$	$\sigma = 0.1$	$\sigma = 0.2$	$\sigma = 0.3$	$\sigma = 0.4$
CUP	0.0	0.0	0.0	0.0	0.0	0.0	0.0	0.0	0.0	0.0	0.0	0.0	0.0	0.0	0.0
ROL-1	8.1	8.1	8.0	7.9	7.8	9.5	9.5	9.4	9.3	9.2	9.0	9.0	9.0	9.0	9.0
ROL-4	12.5	12.5	12.4	12.3	12.2	12.7	12.5	12.4	12.2	12.1	12.2	12.1	12.0	11.9	11.9
ROL-8	14.0	14.0	13.9	13.8	13.7	13.4	13.3	13.2	13.0	12.8	14.1	14.0	13.9	13.8	13.7
ADP-1	13.4	13.4	13.3	13.2	13.1	14.1	14.0	13.9	13.7	13.5	14.2	14.2	14.1	14.0	13.9
ADP-4	14.0	13.9	13.8	13.6	13.4	14.8	14.6	14.4	14.1	13.9	14.7	14.6	14.4	14.3	14.1
ADP-8	13.9	14.0	13.9	13.8	13.7	14.8	14.7	14.5	14.2	14.0	14.6	14.6	14.5	14.3	14.2

(b) $\delta = 4/6$

	Mean profit increase with respect to CUP in %														
	$Z = 9$					$Z = 16$					$Z = 25$				
	$\sigma = 0$	$\sigma = 0.1$	$\sigma = 0.2$	$\sigma = 0.3$	$\sigma = 0.4$	$\sigma = 0$	$\sigma = 0.1$	$\sigma = 0.2$	$\sigma = 0.3$	$\sigma = 0.4$	$\sigma = 0$	$\sigma = 0.1$	$\sigma = 0.2$	$\sigma = 0.3$	$\sigma = 0.4$
CUP	0.0	0.0	0.0	0.0	0.0	0.0	0.0	0.0	0.0	0.0	0.0	0.0	0.0	0.0	0.0
ROL-1	10.1	10.1	10.0	9.9	9.7	11.8	11.7	11.5	11.3	11.2	11.4	11.4	11.3	11.2	11.1
ROL-4	12.6	12.6	12.5	12.4	12.2	14.4	14.2	14.0	13.8	13.5	14.1	14.0	13.8	13.6	13.5
ROL-8	13.3	13.3	13.3	13.2	13.0	15.1	15.0	14.8	14.6	14.4	14.7	14.6	14.5	14.4	14.3
ADP-1	12.9	12.9	12.8	12.6	12.4	14.9	14.8	14.7	14.5	14.4	14.2	14.2	14.1	14.0	13.9
ADP-4	13.3	13.3	13.2	13.1	13.0	15.3	15.1	14.9	14.7	14.5	14.8	14.9	14.6	14.5	14.3
ADP-8	13.3	13.3	13.3	13.2	13.0	15.1	15.0	14.8	14.6	14.4	14.8	14.7	14.6	14.5	14.3

(c) $\delta = 6/6$

	Mean profit increase with respect to CUP in %														
	$Z = 9$					$Z = 16$					$Z = 25$				
	$\sigma = 0$	$\sigma = 0.1$	$\sigma = 0.2$	$\sigma = 0.3$	$\sigma = 0.4$	$\sigma = 0$	$\sigma = 0.1$	$\sigma = 0.2$	$\sigma = 0.3$	$\sigma = 0.4$	$\sigma = 0$	$\sigma = 0.1$	$\sigma = 0.2$	$\sigma = 0.3$	$\sigma = 0.4$
CUP	0.0	0.0	0.0	0.0	0.0	0.0	0.0	0.0	0.0	0.0	0.0	0.0	0.0	0.0	0.0
ROL-1	10.8	10.8	10.6	10.5	10.3	13.6	13.5	13.4	13.2	13.0	13.4	13.4	13.3	13.3	13.2
ROL-4	12.9	12.8	12.6	12.4	12.3	15.5	15.4	15.2	14.8	14.3	15.3	15.2	15.0	14.8	14.6
ROL-8	13.0	13.0	13.0	12.9	12.7	15.7	15.6	15.3	14.9	14.4	15.5	15.4	15.3	15.1	14.9
ADP-1	13.0	13.0	13.0	13.0	12.9	15.2	15.1	15.1	14.8	14.5	14.9	14.9	14.9	14.8	14.6
ADP-4	13.0	13.1	13.1	13.0	12.9	15.7	15.7	15.5	15.1	14.6	15.5	15.4	15.3	15.1	14.9
ADP-8	13.0	13.0	12.9	12.9	12.7	15.7	15.7	15.4	15.1	14.6	15.4	15.4	15.3	15.1	14.9

(d) $\delta = 8/6$

Table 2.9: Mean profit increase for different demand-supply-ratios δ. For all analyzes, the half-width of the 95% confidence interval was at most ± 0.2 percentage points.

2.H Model variants

As described in Section 2.5.3.6, we develop two model variants for the OBDPP (2.1)-(2.16) in the following two subsections.

2.H.1 Trip-based pricing with relaxation of pure pricing and proportional demand fulfillment

The TBDPP-RLX mimics a *trip-based differentiated pricing problem* (TBDPP) which omits the two central assumptions made for the OBDPP, i.e., technically speaking, compared to the OBDPP, it *relaxes* (RLX) the *pure pricing* and the *proportional demand fulfillment* assumptions (see Section 1) in the model. The TBDPP-RLX is given by (2.34)-(2.44).

Compared to the OBDPP model (2.1)-(2.16), the TBDPP-RLX model (2.34)-(2.44) delineates as follows: The constraints (2.8)-(2.11) as well as the auxiliary binary decision variables $\mathbf{q} = [q_{it}]_{Z\times T}$ become obsolete. Constraints (2.8) in the OBDPP change to (2.40) in the TBDPP-RLX. Since pricing is *trip-based*, the binary *origin-based* pricing decision variables $\mathbf{y} = [y^m_{it}]_{Z\times T\times M}$ in the OBDPP are replaced by binary *trip-based* variables $\mathbf{y} = [y^m_{ijt}]_{Z\times Z\times T\times M}$ in the TBDPP.

$$\max_{\mathbf{y},\mathbf{q},\mathbf{r},\mathbf{a},\mathbf{s}} \quad \sum_{t\in\mathcal{T}}\sum_{i\in\mathcal{Z}}\sum_{j\in\mathcal{Z}}\sum_{m\in\mathcal{M}} r^m_{ijt}\cdot l_{ij}\cdot(p^m - c) \tag{2.34}$$

s.t.

$$a_{it} = \sum_{j\in\mathcal{Z}}\sum_{m\in\mathcal{M}} r^m_{ijt} + s_{it} \qquad \forall i\in\mathcal{Z}, t\in\mathcal{T} \tag{2.35}$$

$$\sum_{i\in\mathcal{Z}}\sum_{m\in\mathcal{M}} r^m_{ijt} + s_{jt} = a_{j(t+1)} \qquad \forall j\in\mathcal{Z}, t\in\mathcal{T} \tag{2.36}$$

$$a_{i0} = \hat{a}_{i0} \qquad \forall i\in\mathcal{Z} \tag{2.37}$$

$$\sum_{m\in\mathcal{M}} y^m_{ijt} = 1 \qquad \forall i,j\in\mathcal{Z}, t\in\mathcal{T} \tag{2.38}$$

$$r^m_{ijt} \le d^m_{ijt}\cdot y^m_{ijt} \qquad \forall i,j\in\mathcal{Z}, t\in\mathcal{T}, m\in\mathcal{M} \tag{2.39}$$

$$\sum_{j\in\mathcal{Z}}\sum_{m\in\mathcal{M}} r^m_{ijt} \le a_{it} \qquad \forall i,j\in\mathcal{Z}, t\in\mathcal{T} \tag{2.40}$$

$$y^m_{ijt}\in\{0,1\} \qquad \forall i,j\in\mathcal{Z}, t\in\mathcal{T}, m\in\mathcal{M} \tag{2.41}$$

$$r^m_{ijt}\in\mathbb{R}^+_0 \qquad \forall i,j\in\mathcal{Z}, t\in\mathcal{T}, m\in\mathcal{M} \tag{2.42}$$

$$s_{it}\in\mathbb{R}^+_0 \qquad \forall i\in\mathcal{Z}, t\in\mathcal{T} \tag{2.43}$$

$$a_{it}\in\mathbb{R}^+_0 \qquad \forall i\in\mathcal{Z}, t\in\{0,1,\ldots,T\} \tag{2.44}$$

2.H.2 Origin-based pricing with relaxation of pure pricing and proportional demand fulfillment

The OBDPP-RLX also omits/*relaxes* (RLX) the two central OBDPP assumptions, but apart from this, is identical to the model for the original origin-based differentiated pricing problem (OBDPP). The OBDPP-RLX is given by (2.45)-(2.55).

Compared to the OBDPP model (2.1)-(2.16), the OBDPP-RLX model (2.45)-(2.55) delineates as follows: The constraints (2.8)-(2.11) as well as the auxiliary binary decision variables

$\mathbf{q} = [q_{it}]_{Z \times T}$ become obsolete. Constraints (2.8) in the OBDPP change to (2.51) in the OBDPP-RLX.

$$\max_{\mathbf{y},\mathbf{q},\mathbf{r},\mathbf{a},\mathbf{s}} \quad \sum_{t\in\mathcal{T}}\sum_{i\in\mathcal{Z}}\sum_{j\in\mathcal{Z}}\sum_{m\in\mathcal{M}} r_{ijt}^m \cdot l_{ij} \cdot (p^m - c) \tag{2.45}$$

s.t.

$$a_{it} = \sum_{j\in\mathcal{Z}}\sum_{m\in\mathcal{M}} r_{ijt}^m + s_{it} \qquad \forall i \in \mathcal{Z}, t \in \mathcal{T} \tag{2.46}$$

$$\sum_{i\in\mathcal{Z}}\sum_{m\in\mathcal{M}} r_{ijt}^m + s_{jt} = a_{j(t+1)} \qquad \forall j \in \mathcal{Z}, t \in \mathcal{T} \tag{2.47}$$

$$a_{i0} = \hat{a}_{i0} \qquad \forall i \in \mathcal{Z} \tag{2.48}$$

$$\sum_{m\in\mathcal{M}} y_{it}^m = 1 \qquad \forall i \in \mathcal{Z}, t \in \mathcal{T} \tag{2.49}$$

$$r_{ijt}^m \leq d_{ijt}^m \cdot y_{it}^m \qquad \forall i, j \in \mathcal{Z}, t \in \mathcal{T}, m \in \mathcal{M} \tag{2.50}$$

$$\sum_{j\in\mathcal{Z}}\sum_{m\in\mathcal{M}} r_{ijt}^m \leq a_{it} \qquad \forall i, j \in \mathcal{Z}, t \in \mathcal{T} \tag{2.51}$$

$$y_{it}^m \in \{0,1\} \qquad \forall i \in \mathcal{Z}, t \in \mathcal{T}, m \in \mathcal{M} \tag{2.52}$$

$$r_{ijt}^m \in \mathbb{R}_0^+ \qquad \forall i, j \in \mathcal{Z}, t \in \mathcal{T}, m \in \mathcal{M} \tag{2.53}$$

$$s_{it} \in \mathbb{R}_0^+ \qquad \forall i \in \mathcal{Z}, t \in \mathcal{T} \tag{2.54}$$

$$a_{it} \in \mathbb{R}_0^+ \qquad \forall i \in \mathcal{Z}, t \in \{0,1,\ldots,T\} \tag{2.55}$$

2.I Pricing of Shared Mobility Systems in Practice

In Section 2.1 where we introduce the *origin-based differentiated pricing problem* (OBDPP), we explain that there are three dimensions to classify pricing mechanisms. Regarding the second dimension, i.e., the *spatio-temporal pricing features*, we consider *origin-based* pricing in our work, whereas the closest related studies (Section 2.2.3) all focus on *trip-based* pricing.

To underline the relevance of this *origin-based* pricing, the following exposition shows which pricing mechanisms are actually applied in practice. In particular, in Table 2.10 we state how the ten largest car sharing providers worldwide do their pricing.

Provider	Location	Fleet size	Pricing mechanism	
			Spatio-temporal pricing feature	Subject of price differentiation
EvCard	China	30,000	Not found	
Delimobil	Russia	16,000+	Origin	Time
Yandex.Drive	Russia	16,000	Origin	Not found
Zipcar	United States	12,000	No price differentiation	
Share Now	**Germany**	**11,240**	**Origin**	**Location and time**
Flinkster	Germany	6,500+	Origin	Time
GoGet	Australia	3,300+	Origin	Time
Car Next Door	Australia	3,000+	Origin	Time
Cambio	Germany	2,700	Origin	Time
Enjoy	Italy	2,670	Origin	Time

Table 2.10: Pricing in the largest car sharing systems in practice (based on internet research)

The status quo of SMS pricing in practice can be summarized as follows:

- *Practice exclusively applies origin-based pricing*: Of the ten largest car sharing providers worldwide, seven apply origin-based pricing, two do not apply price differentiation at all, and for the remaining one we could find no information on their basis for pricing. In other words, none of these providers applies trip-based pricing, despite the fact that this is the dominant pricing mechanism discussed in literature.
- *Share Now is pioneering in the field by differentiating prices with regard to both location and time*: Of the seven providers who do apply origin-based pricing, only Share Now – Europe's largest car sharing provider that operates in 16 cities in 8 countries (Share Now, 2021) – differentiates prices with regard to location *and* time. The remaining six providers differentiate prices only with regard to time. Hence, we regard Share Now as a pioneer in determining prices for SMSs. The OBDPP that we consider in this paper reflects Share Now's problem one-to-one and the resulting pricing solutions have been applied in practice since the end of 2019.

Additional investigations reiterate these two findings. Besides car sharing, there are several other SMSs, such as bike sharing or scooter sharing, for which we searched the internet thoroughly to find information on their applied pricing mechanisms. To the best of our knowledge, not a single provider actually applies trip-based pricing. As for the car sharing discussed above, providers either do not differentiate prices at all, or they use origin-based pricing in which the company differentiates only with regard to time.

Bibliography

ACEA, Frost & Sullivan (2016) Number of vehicles in global car sharing market from 2006 until 2025. *Statista*. Accessed September 1, 2020, https://de.statista.com/statistik/daten/studie/388012/umfrage/anzahl-der-fahrzeuge-auf-dem-weltweiten-carsharing-markt/.

Agatz N, Campbell AM, Fleischmann M, Van Nunen J, Savelsbergh M (2013) Revenue management opportunities for internet retailers. *J. Revenue Pricing Manag.* 12(2):128–138.

Angelopoulos A, Gavalas D, Konstantopoulos C, Kypriadis D, Pantziou G (2016) Incentivization schemes for vehicle allocation in one-way vehicle sharing systems. *2016 IEEE Internat. Smart Cities Conf. (ISC2)*, 1–7.

Banerjee S, Freund D, Lykouris T (2016) Pricing and optimization in shared vehicle systems: An approximation framework. Working paper, Cornell University, Ithaca, NY.

Barth M, Todd M, Xue L (2004) User-based vehicle relocation techniques for multiple-station shared-use vehicle systems. Working paper, *Transp. Res. Board 80th Annual Meeting*.

Bertsektas DP (2019) Reinforcement learning and optimal control. (Athena Scientific, Belmont, MA).

Brendel AB, Brauer B, Hildebrandt B (2016) Toward user-based relocation information systems in station-based one-way car sharing. *AMCIS Proc.*, 1–10.

Brendel AB, Brennecke JT, Zapadka P, Kolbe LM (2017) A decision support system for computation of carsharing pricing areas and its influence on vehicle distribution. *Proc. Internat. Conf. Inf. Syst. (ICIS)*, 1–21.

Chemla D, Meunier F, Pradeau T, Wolfler Calvo R, Yahiaoui H (2013) Self-service bike sharing systems: Simulation, repositioning, pricing. Working paper, CERMICS, École des Ponts ParisTech, Champs-sur-Marne, France.

DeMaio P (2009) Bike-sharing: History, impacts, models of provision, and future. *J. Public Transp.* 12(4):41–56.

Di Febbraro A, Sacco N, Saeednia M (2012) One-way carsharing. *Transp. Res. Record* 2319(1):113–120.

Di Febbraro A, Sacco N, Saeednia M (2019) One-way car-sharing profit maximization by means of user-based vehicle relocation. *IEEE Trans. Intell. Transp. Syst.* 20(2):628–641.

Ferrero F, Perboli G, Vesco A, Caiati V, Gobbato L (2015a) Car-sharing services – Part A taxonomy and annotated review. Working paper, Istituto Superiore Mario Boella, Turin, Italy.

Ferrero F, Perboli G, Vesco A, Musso S, Pacifici A (2015b) Car-sharing services – Part B business and service models. Working paper, Istituto Superiore Mario Boella, Turin, Italy.

Fishman E, Washington S, Haworth N (2013) Bike share: A synthesis of the literature. *Transp. Rev.* 33(2):148–165.

Garey MR, Johnson DS (1990) *Computers and intractability; A guide to the theory of NP-completeness* (W. H. Freeman & Co., New York, NY).

Giorgione G, Ciari F, Viti F (2019) Availability-based dynamic pricing on a round-trip carsharing service: an explorative analysis using agent-based simulation. *Proc. Comp. Sci.* 151(2018):248–255.

Grossmann IE (2012) Advances in mathematical programming models for enterprise-wide optimization. *Comput. Chem. Eng.* 47:2–18.

Haider Z, Nikolaev A, Kang JE, Kwon C (2018) Inventory rebalancing through pricing in public bike sharing systems. *Eur. J. Oper. Res.* 270(1):103–117.

Huang K, Kun A, Rich J, Ma W (2020) Vehicle relocation in one-way station-based electric carsharing systems: A comparative study of operator-based and user-based methods. *Transp. Res. Part E: Logist. Transp. Rev.* 142.

Illgen S, Höck M (2019) Literature review of the vehicle relocation problem in one-way car sharing networks. *Transp. Res. Part B: Methodological* 120:193–204.

Jorge D, Correia GHDA (2013) Carsharing systems demand estimation and defined operations: A literature review. *Eur. J. Transp. Infrastructure Res.* 13(3):201–220.

Jorge D, Molnar G, Correia GHDA (2015) Trip pricing of one-way station-based carsharing networks with zone and time of day price variations. *Transp. Res. Part B: Methodological* 81:461–482.

Kamatani T, Nakata Y, Arai S (2019) Dynamic pricing method to maximize utilization of one-way car sharing service. *IEEE Internat. Conf. Agents (ICA)*, 65–68.

Kaspi M, Raviv T, Tzur M, Galili H (2016) Regulating vehicle sharing systems through parking reservation policies: Analysis and performance bounds. *Eur. J. Oper. Res.* 251(3):969–987.

Laporte G, Meunier F, Wolfler Calvo R (2015) Shared mobility systems. *4OR* 13(4):341–360.

Laporte G, Meunier F, Wolfler Calvo R (2018) Shared mobility sytems: An updated survey. *Ann. Oper. Res.* 271(1):105–126.

Lippoldt K, Niels T, Bogenberger K (2018) Effectiveness of different incentive models in free-floating carsharing systems: A case study in Milan. *IEEE Intell. Transp. Syst. Conf. (ITSC)*, 1179–1185.

Lippoldt K, Niels T, Bogenberger K (2019) Analyzing the potential of user-based relocations on a free-floating carsharing system in Cologne. *Transp. Res. Proc.* 37:147–154.

Lu R, Correia GHDA, Zhao X, Liang X, Lv Y (2021) Performance of one-way carsharing systems under combined strategy of pricing and relocations. *Transp. B: Transp. Dyn.* 9(1):134–152.

Marecek J, Shorten R, Yu JY (2016) Pricing vehicle sharing with proximity information. *2016 3rd MEC Internat. Conf. Big Data and Smart City (ICBDSC)*, 1–7.

Pfrommer J, Warrington J, Schildbach G, Morari M (2014) Dynamic vehicle redistribution and online price incentives in shared mobility systems. *IEEE Trans. Intell. Transp. Syst.* 15(4):1567–1578.

Powell WB (2009) What you should know about approximate dynamic programming. *Naval Res. Logist.* 56(3):239–249.

Powell WB (2011) Approximate dynamic programming. *Wiley Series in Probability and Statistics* (Wiley, Hoboken, NJ).

Powell WB (2016) Perspectives of approximate dynamic programming. *Ann. Oper. Res.* 241(1-2):319–356.

Reiss S, Bogenberger K (2016) Optimal bike fleet management by smart relocation methods: Combining an operator-based with an user-based relocation strategy. *IEEE Intell. Transp. Syst. Conf. (ITSC)*, 2613–2618.

Ren S, Luo F, Lin L, Hsu SC, LI XI (2019) A novel dynamic pricing scheme for a large-scale electric vehicle sharing network considering vehicle relocation and vehicle-grid-integration. *Internat. J. Prod. Econ.* 218:339–351.

Ricci M (2015) Bike sharing: A review of evidence on impacts and processes of implementation and operation. *Res. Transp. Bus. Manag.* 15:28–38.

Roch S, Savard G, Marcotte P (2005) An approximation algorithm for Stackelberg network pricing. *Networks* 46(1):57–67.

Roland Berger Strategy Consultants (2014) Shared mobility. *Think Act*, 1–18.

Share Now (2021) Overview countries and cities. *Share Now*. Accessed February 25, 2021, https://www.share-now.com/de/en/country-list/.

Singla A, Santoni M, Bartok G, Mukerji P, Meenen M, Krause A (2015) Incentivizing users for balancing bike sharing systems. *Proc. Twenty-Ninth AAAI Conf. Artificial Intelligence Pattern*, 723–729.

Talluri KT, van Ryzin GJ (2004) The theory and practice of revenue management (Springer, Boston, MA).

Wagner S, Willing C, Brandt T, Neumann D (2015) Data analytics for location-based services: Enabling user-based relocation of carsharing vehicles. *Proc. Internat. Conf. Inf. Syst. (ICIS)* 3:279–287.

Wang L, Ma W (2019) Pricing approach to balance demands for one-way car-sharing systems. *2019 IEEE Intell. Transp. Syst. Conf. (ITSC)*, 1697–1702.

Waserhole A, Jost V (2012) Vehicle sharing system pricing regulation: A fluid approximation. Working paper, ENSTA ParisTech, Palaiseau, France.

Waserhole A, Jost V (2016) Pricing in vehicle sharing systems: Optimization in queuing networks with product forms. *EURO J. Transp. Logist.* 5(3):293–320.

Waserhole A, Jost V, Brauner N (2012) Vehicle sharing system optimization: Scenario-based approach. Working paper, ENSTA ParisTech, Palaiseau, France.

Winston WL, Goldberg JB (2004) Operations research: Applications and algorithms, Vol. 4 (Thomson/Brooks/Cole, Belmont, CA).

Xu M, Meng Q, Liu Z (2018) Electric vehicle fleet size and trip pricing for one-way carsharing services considering vehicle relocation and personnel assignment. *Transp. Res. Part B: Methodological* 111:60–82.

Chapter 3

Practicable Solution Approaches for Differentiated Pricing of Shared Mobility Systems

3.1 Introduction

The ongoing debate about climate crisis leads to different concepts on how this issue can be addressed. One component that can contribute to an useful and sustainable mobility concept are shared mobility systems (SMSs). For example, ideally, car or bike sharing systems with widely available vehicles do not only partially replace private vehicles, but also reduce the emissions caused by mobility. This is one of the reasons why the concept of car sharing has become increasingly popular among providers and customers in recent years. For example, in the EU, the proportion of shared mobility is predicted to rise from 2 % in 2015 up to 15 % in 2025 (Destatis, 2017).

However, SMS providers face mainly two challenges:

1. The distribution of vehicles is uneven across locations, because origin and destination locations are influenced by the customer's preferences. These preferences and thus the demand vary during the day (uneven nature of the travel pattern). This is the so-called "tide phenomenon", which represents the oscillation of demand intensity throughout the day (spatio-temporal demand asymmetries) (Côme, 2014; Jorge and Correia, 2013). Besides, the current number of available vehicles in a location affects the number of future rentals in that location (supply-side network effects). Therefore, it must be taken into account that a rental not only decreases the current amount of vehicles in a origin location and increases the amount of vehicles in the destination location, but also has an impact on future rentals in these two locations. Neglecting supply-side network effects in relocation leads to an accumulation or absence of vehicles at popular locations. As a result, the system is no longer able to serve demand and may lose customers (Di Febbraro, Sacco, and Saeednia, 2012).

2. Maximization of profit is a central objective. SMS can be operated by different institutions, such a public municipalities or private companies. Especially private SMS providers are interested in maximizing profit (minimizing costs) (Pantuso, 2022).

With regards to the first challenge of imbalance, a possible solution is relocation, which decreases imbalance. More precisely, relocation can be distinguished into operator-based and user-based relocations. Operator-based relocation involves repositioning of vehicles by employees, while user-based relocation is performed by customers and is incentivized by the provider. The operator-based relocation increases the operational costs, as providers need additional staff and extra equipment, e.g. operator-based relocation of bikes is handled with trucks (Dötterl et al., 2017). Although operator-based relocation is one of the main cost drivers (Jorge and Correia, 2013) and (time) inefficient (vehicle cannot be used while it is relocated by staff) (Schiffer et al., 2021), almost all SMS providers use it to obtain reduced imbalance.

A more cost-effective method is user-based relocation (Brendel, Brauer, and Hildebrandt, 2016). Ideally, the provider sets prices to encourage customers to drive from a low-demand location to a high-demand location (Angelopoulos et al., 2016). Furthermore, no additional vehicles or additional trips are needed. In short, user-based relocation is more preferable from an environmental and economic perspective (Clemente et al., 2017), as it is a more sustainable and cost-effective alternative to operator-based relocation (Stokkink and Geroliminis, 2021).

With regard to the second challenge of profit maximization, a pricing approach that calculates the optimal price for a given period is useful.

Thus, both challenges can be solved with an appropriate and anticipative pricing approach that takes into account a longer time horizon (e.g. a day, a week), which incorporates supply-side network effects.
In addition, providers should consider customers' needs. Customers have two interests regarding the pricing approaches of SMSs:

1. Customers prefer an easy and comfortable booking process in SMSs, i.e. booking a vehicle without much effort. They cannot and/or do not want to disclose their destination or the duration of the intended rental. Therefore, SMS providers do not know the destination in advance. If SMS providers ask customers to (truthfully) disclose their intended destination, this would considerably change the customers experience of SMSs and thus would be unacceptable in most practical settings.

2. Customers prefer clear and transparent prices. This means that customers would like to know (minute) prices before the rental starts.

Against this background, this paper focuses on origin-based pricing, where the SMS provider sets prices depending on a rental's time and origin. Since origin-based pricing is most commonly used in current practice, the providers of such SMSs do not have to change their booking process by asking customers for the destination or rental duration. This means a more efficient interaction between user and provider and an easier implementation. To be precise, in this work, we consider the problem of differentiated (=static) pricing of free-floating SMS providers with a focus on its *practicability*, by using different heuristic solution approaches.

The contributions of our work are the following:

- First, we develop two *practicable*, problem-specific, easy to implement and new solution approaches. The first one is a simplified model, so that the problem can be solved quickly, even for large instances. The second solution approach is a backwards algorithm for determining the best prices for all location-period-combinations. Thus, the major advantage of both solution approaches is that they do not require any pre-processing, but still provide similar results compared to existing, more complex benchmarks. These new solution approaches are beneficial for practitioners to get a *practicable* and straightforward solution and for researchers to benchmark other upcoming solution approaches.

- Second, we generate a number of relevant managerial insights based on an extensive computational study and a sensitivity analysis with different problem sizes, considering various relevant parameter settings and demand patterns.

The remainder of the paper is organized as follows. In Section 3.2, we review the relevant literature, focusing on differentiated pricing problems using optimization. In Section 3.3, we describe the problem and present two proposed solution approaches. Section 3.4 contains the computational study. After the computational study, we perform a sensitivity analysis in Section 3.5. Section 3.6 concludes the paper and gives an outlook on future research. The appendix contains additional data and results for the computational experiments.

3.2 Literature

The literature on SMS optimization is quite extensive, so for general overviews we refer to the following papers:

- bike sharing: DeMaio (2009), Fishman, Washington, and Haworth (2013), Ricci (2015)
- car sharing: Jorge and Correia (2013), Ferrero et al. (2015a), Ferrero et al. (2015b), Illgen and Höck (2019)
- SMS in general: Laporte, Meunier, and Wolfler Calvo (2015, 2018)

In our literature review, we focus on differentiated pricing in SMSs in the sense that the pricing does not depend on the system's current state (e.g. current vehicle distribution). Furthermore, we only consider papers that apply collective, not individual pricing (targeted to all customers, see Pantuso (2022)) using optimization. We exclude papers that apply business rules (e.g. Ruch, Warrington, and Morari (2014); Brendel, Brauer, and Hildebrandt (2016); Wagner et al. (2015); Barth, Todd, and Xue (2004)).

In the following, we introduce dimensions for differentiated pricing approaches (Section 3.2.1). Using these dimensions, Section 3.2.2 considers differentiated pricing and Section 3.2.3 presents further literature that developed single-period solution approaches in a rolling-horizon fashion for dynamic pricing.

3.2.1 Dimensions of Differentiated Pricing

We propose two dimensions of the customer perspective and four dimensions of the provider perspective to structure the different solution approaches (see also Table 3.1). The following dimensions describe the customer perspective:

1. Spatio-temporal pricing: Origin-based prices depend only on time and location of a rental's start. Other variants are destination-based prices (prices depend on location of destination) or trip-based prices (prices depend on both origin and destination).
2. Number of possible prices: Some pricing approaches set only one price for all locations and periods, whereas others set different prices selected from a discrete set of prices (price list). Still others either have a defined upper and lower bound for prices, or the restriction that prices must be positive, or no restrictions regarding the prices at all.

The following four dimensions characterize the provider's perspective:

1. Control of rentals: There are providers that can influence the number of rentals only by the price (price control). However, there are also providers that can additionally reject requests (trip selection).
2. Objective: Different pricing approaches aim either at improving the distribution (balance) of vehicles in the SMS or at increasing profit (reducing costs).

	spatio-temporal pricing			number of possible prices					control of rentals		objective		foresight		additional parameters	
	origin	destination	trip	one	price list	upper and lower bound	positive	no restriction	price control	price control, trip selection	profit	balance	myopic	anticipative	no requirement	requires estimation
Differentiated Pricing																
Waserhole and Jost (2012)			x					x	x		x			x	x	
Guo and Kang (2022)			x					x	x		x		x		x	
Xu, Meng, and Liu (2018)			x				x			x	x			x	x	
Jiao et al. (2020)			x				x			x	x			x	x	
Huang et al. (2020)			x				x			x	x			x	x	
Lu et al. (2021)			x			x				x	x			x	x	
Zhang and Kan (2020)			x			x			x		x			x	x	
Jorge, Molnar, and Correia (2015)			x				x		x		x			x	x	
Ren et al. (2019)			x				x		x		x			x	x	
Huang et al. (2020)			x				x		x		x			x	x	
Zhang and Kan (2020)			x			x			x		x			x	x	
Soppert et al. (2022)	x				x				x		x			x		x
Müller (2022)	x				x				x		x			x	x	
Further related literature																
Pfrommer et al. (2014)		x				x			x			x	x		x	
Chemla et al. (2013)		x				x			x			x	x		x	
Haider et al. (2018)			x			x			x			x	x		x	
Wang and Ma (2019)			x					x	x			x	x		x	
Pantuso (2022)			x		x				x		x		x		x	

Table 3.1: Literature overview on differentiated pricing and further related literature in shared mobility systems.

3. Foresight: Some pricing approaches determine prices based on the current period without considering the supply-side network effects for the next period(s) (myopic). In contrast, other pricing approaches additionally consider how pricing decisions in the current period affect future vehicle supply, and thus future rentals at each location in subsequent periods, by considering supply-side network effects (anticipative).

4. Additional parameters: Some pricing approaches require some pre-processing, for instance, additional estimation of parameters in advance to perform the price determination.

3.2.2 Literature on Differentiated Pricing

Most of the published papers considering differentiated pricing in SMS deal with trip-based prices. There are solution approaches that use a fluid approximation to determine prices. In fluid approximations, the model sets the prices so that the rentals of a station match the demand, i.e. there is no distinction between demand and rentals. This means that the price is not constrained (even negative prices are possible). Waserhole and Jost (2012) propose a fluid approximation for the revenue-maximizing trip-based pricing problem, which is the upper bound of the stochastic model if demand and supply are scaled to infinity. Guo and Kang (2022) also propose a fluid model to maximize profit, which considers the pricing and re-balancing problem of electric vehicles.

However, other papers distinguish between demand and rentals. More precisely, rentals depend on supply, demand and prices. Only positive prices are determined here. We distinguish

between papers where the provider cannot reject users and controls rentals only by price (i.e. price control) and papers where the provider can reject users (i.e. trip selection).

First, we consider papers where the provider can (indirectly) reject users. Xu, Meng, and Liu (2018) formulate a mixed-integer non-linear and non-convex program. On this basis, they develop a computationally tractable mixed-integer convex program which has the same objective in the optimum, and solve the latter arbitrarily close to optimality. Jiao et al. (2020) integrate trip selection and price incentives with user-based relocation in one model. Therefore this model distinguishes between three different types of demands: 1. potential travel demand, 2. adopted demand (demand after customers see the price), and 3. final served demand (after trip selection). They consider a mixed-integer non-linear program to maximize the profit and propose an iterative algorithm between the two decomposition programming sub-problems (a linear master sub-problem and a non-linear sub-problem). Huang et al. (2020) compare operator-based and user-based relocation. They formulate two mixed-integer non-linear programs for the user-based relocation. The first one sets trip-based prices, whereas the second optimizes pick-up and drop-off fees. They solve both programs with a combined rolling-horizon and iterated local search heuristic. Lu et al. (2021) use another model formulation, i.e. a bi-level non-linear program in which the provider determines profit-maximizing prices on the upper level. In this case, these prices are within the previously defined bounds. The lower level's objective minimizes customers' total cost by a binary choice between two modes of transportation (shared vehicles vs. private cars). In an interpretation of a discrete choice model, rentals are additionally bounded from above by a logit model. The authors transform the bi-level program to a single-level one using Karush-Kuhn-Tucker conditions, and heuristically solve it with a genetic algorithm.

Second, we consider papers where the providers only control rentals by price. Jorge, Molnar, and Correia (2015) formulate a profit-maximizing trip-based pricing problem as mixed-integer non-linear, non-concave program, which is not tractable for real-world-instances. They propose an iterated local search meta-heuristic to solve the program. Ren et al. (2019) extend the previous program to include a vehicle-grid interaction of electric vehicles. They use non-linear solvers. Huang et al. (2020) combine tactical and operational decisions for a one-way station-based car sharing system on a mixed-integer non-linear program. This program optimizes profit by considering fleet size, pricing (both tactical) and relocation. They linearize this program, decompose it into two interdependent stages, and develop a gradient search method to solve the two stages. Zhang and Kan (2020) formulate a non-linear, non-concave program that maximizes the profit for an entire planning horizon of a station-based, one-way car sharing system by setting trip-based prices. Particle swarm optimization is used to solve the program.

In contrast to the presented literature above, Soppert et al. (2022) consider origin-based, differentiated pricing. They formulate a profit-maximizing, mixed-integer linear program that distinguishes between rentals and demand. This program determines origin-based prices from a discrete price set. The rentals of a location are calculated as a minimum of demand and supply (number of idle vehicles). The demand can be influenced only by the price (price control). Since the model cannot be solved due to its complexity, Soppert et al. (2022) propose a solution method using value function approximation. To apply this method, the provider has to estimate

some parameters in pre-processing.

We also consider a provider, who determines origin-based prices from a discrete price set (i.e. price control). We suggest two solution approaches to solve this mixed-integer linear program without the need to estimate any parameters in pre-processing.

3.2.3 Further Literature

In addition, there are other models that are developed in such a way that they have to be solved for each single period with the currently available data (without considering supply-side network effects). Although they apply dynamic pricing, they have similarities with our problem.

The following papers do not distinguish between demand and rentals. They assume that prices do not affect the demand, but affect the customers' destinations. Pfrommer et al. (2014) propose a model predictive control approach. The objective of the quadratic program is a weighted sum of the deviation from an optimal vehicle distribution and the cost of incentive payments. Chemla et al. (2013) use a linear program to determine the number of customers who change their travel plans due to the price incentive in order to reach the given target inventory of vehicles for each station. Haider et al. (2018) formulate a bi-level program, where the upper level determines prices and minimizes vehicle imbalance, while the lower level represents the cost-minimizing route choice of customers. The problem is transformed into a single-level program. Wang and Ma (2019) consider the objective of keeping the vehicle inventory within a certain range for a period. For this purpose, they define lower and upper thresholds for each station. The number of rentals from or to a station can be affected by pick-up and drop-off fees. To this end, they formulate a simple quadratic program to calculate such optimal dynamic fees.

Other papers distinguish between demand and rentals. Pantuso (2020, 2022) formulates an extensive mixed-integer two-stage stochastic program, which maximizes the profit by setting trip-based prices and decides about operator-based relocation. Pantuso (2020) also proposes a compact integer programming reformulation and compares the two formulations in terms of ease of solution. Pantuso (2022) proposes an exact solution algorithm for the mixed-integer two-stage stochastic program.

3.3 Solution Approaches for Differentiated Pricing

In this section, we describe two solution approaches for differentiated pricing.

3.3.1 Problem Statement and Notation

There is a one-way SMS provider with Z locations ($\mathcal{Z} = 1, ..., Z$), which sets origin-based prices. This means for all rentals, which have the same origin, the same minute price $p_{i,t}$ is charged. The considered time horizon is subdivided into T periods ($\mathcal{T} = 0, ..., T-1$). The provider maximizes its profit by setting minute prices $p_{i,t}$ for every location $i \in \mathcal{Z}$ and period $t \in \mathcal{T}$, regardless of the destination. The minute prices are chosen from a given price set $\mathcal{P}^{\mathcal{M}} = p^1, ..., p^M$ with M price points.

We also have the following assumptions concerning *demand*, *rental realization* and *dynamics*. *Demand* depends on the price points. A base demand (demand at the median price) $d_{i,j,t}$ for each rental combination $i-j$ of possible origins and destinations at period t is given. We assume that if the price is lower (than the median price), demand increases and if the price is higher (than the median price) demand decreases. Thus, we scale the base demand with sensitivity factors f^m, which depend on the chosen price $p_{i,t}$ from a given price set $\mathcal{P}^{\mathcal{M}} = p^1, ..., p^M$ with M price points. For the *rental realization*, we assume that the provider cannot reject any user at a location, if there are vehicles available (no trip selection, but price control). Therefore, the number of trips is the minimum of the supply (number of idle vehicles at the location) and the demand at each location i. Furthermore, we assume that the rentals split proportionally to the demand regarding their destinations. Thus, the provider can only affect the system and thereby the rentals by price. For the *dynamics*, we assume that rentals start at the beginning of a period t and the vehicles, at latest, always become available again at the beginning of the respective next period $t+1$. The average rental duration $l_{i,j} \in \mathbb{R}_0^+$ (in minutes) is shorter than the period length, but can vary according to the spatial distance between different locations $i-j$. Also, the initial inventory $\hat{a}_{i,0}$ of each location is given at the beginning of the period $t = 0$.

3.3.2 Simplified Model for Differentiated Pricing

This section describes the first solution approach, which is a simplified model.

The idea of this solution approach is that we only consider demand in a fluid approximation. The approach controls demand with the scaled continuous sensitivity factor $q_{i,t}$ (and therefore indirectly with the price). The simplified model does not distinguish between demand and rentals, thus demand equals rentals. This has several advantages. First, we do not need the decision variables for rentals in the model. Therefore, we do not need to define constraints regarding rentals, e.g. ensuring that rentals do not exceed demand or that rentals are the minimum of demand and supply (available vehicles). Second, prices are not discrete and therefore the choice of discrete prices does not need to be represented by binary variables. This makes the model faster compared to other origin-based pricing models, e.g. origin-based pricing from Soppert et al. (2022), which considers discrete prices and distinguishes between demand and rentals, which is NP-hard. However, one drawback is that the continuous prices in the simplified model must be converted to discrete prices.

The model only contains the continuous variables for sensitivity factors $q_{i,t}$ and available vehicles $a_{i,t}$. The sensitivity factor $q_{i,t}$ is defined between 0 and 1, so we have to scale the demand $d_{i,j,t}$ to the demand at the lowest price $d^{scaled}_{i,j,t}$. We obtain this demand by multiplying the demand $d_{i,j,t}$ at the median price with the sensitivity factor for the lowest price f^1. The price $p^{con}_{i,t}$ itself is continuous and a function of the sensitivity factor ($p^{con}_{i,t} = f(q_{i,t})$) (line 2).

We formulate the simplified model based on a deterministic network flow problem in which vehicles move through a spatio-temporal network. The resulting fluid model considers expected values of the demand and available vehicles in the shared mobility system.

The model is embedded in an algorithm (see Algorithm 3, line 3) that converts the continuous prices of the simplified model into prices of the discrete price set $\mathcal{P}^{\mathcal{M}}$ (line 4).

Algorithm 3 Applying Simplified Model

1: Results: Best prices for the whole day
2: Step 1: Find a linear price function $f(q_{it})$ that describes the price as a function of price sensitivity
3: Step 2: Solve the following MINLP:

$$\max_{\mathbf{q},\mathbf{a},\mathbf{p}} \quad \sum_{t\in\mathcal{T}}\sum_{i\in\mathcal{Z}}\sum_{j\in\mathcal{Z}}(f(q_{i,t}) - c^{var}) \cdot l_{ij} \cdot d^{scaled}_{i,j,t} \cdot q_{i,t} \tag{3.1}$$

$$\text{s.t.} \quad a_{i,t+1} = a_{i,t} - \sum_{j\in\mathcal{Z}} d^{scaled}_{i,j,t} \cdot q_{i,t} + \sum_{k\in\mathcal{Z}} d^{scaled}_{k,i,t} \cdot q_{k,t} \quad \forall i \in \mathcal{Z}, t \in \mathcal{T} \tag{3.2}$$

$$a_{i,0} = \hat{a}_{i,0} \quad \forall i \in \mathcal{Z} \tag{3.3}$$

$$a_{i,t} \geq \sum_{j\in\mathcal{Z}} d^{scaled}_{i,j,t} \cdot q_{i,t} \quad \forall i \in \mathcal{Z}, t \in \mathcal{T} \tag{3.4}$$

$$q_{i,t} \geq 0 \quad \forall i \in \mathcal{Z}, t \in \mathcal{T} \tag{3.5}$$

$$q_{i,t} \leq 1 \quad \forall i \in \mathcal{Z}, t \in \mathcal{T} \tag{3.6}$$

$$q_{i,t} \in \mathbb{R}^+_0 \quad \forall i \in \mathcal{Z}, t \in \mathcal{T} \tag{3.7}$$

$$a_{i,t} \in \mathbb{R}^+_0 \quad \forall i \in \mathcal{Z}, t \in \{1, 2, \ldots, T+1\} \tag{3.8}$$

4: Step 3: Round to the nearest discrete price of price set $\mathcal{P}^{\mathcal{M}}$

The contribution margin (3.1) is the product of the rentals ($d_{i,j,t} \cdot q_{i,t}$), the rental time ($l_{i,j}$), and the price minus the variable costs ($f(q_{i,t}) - c^{var}$). Note that maximizing contribution margin here is equivalent to optimizing profit, since decisions about fixed costs cannot be made at this point and are therefore out of scope. Constraints (3.2) provide flow conservation. They ensure a constant fleet size at all times. The initial vehicle distributions are defined through Constraints (3.3). Constraints (3.4) set upper bounds on the number of rentals, so that the rentals are limited by the number of vehicles available in a zone. The next constraints (3.5 and 3.6) define the upper and lower bounds of the sensitivity factors $q_{i,t}$. The range is between 0 and 1. The last constraints (3.7 and 3.8) define that all variables are real positive numbers.

The prices we get from solving the model are continuous. They must be converted to the discrete prices (line 4). To do this, we first compute the absolute differences of all resulting

continuous prices $p_{i,t}^{con}$ for all $i-t$ combinations at all discrete price points p^m. Then, we convert the continuous prices to discrete prices with the smallest absolute difference.

3.3.3 Backwards Algorithm for Differentiated Pricing

This section describes the second solution approach, called a backwards algorithm (see Algorithm 4 and Figure 3.1). The idea of this solution is to decompose the problem into smaller problems. These smaller problems can be solved more quickly. To do this, we first compute the vehicle distribution at the beginning of each period (Step 1), taking advantage of the fact that demand is deterministic. Then, starting backwards from period T, we compute prices for each period based on the calculated initial vehicle distributions of this period, taking into account the next periods (Step 2). The advantage of this method lies in its solvability and computational speed, and it takes supply-side network effects into account, at least to a some extent. The disadvantage of this solution approach is that the pricing approach can only determine the prices of the considered period.

The solution approach is divided into two steps (see Figure 3.1). In the first step, a simple solution approach is used to calculate the network flows and vehicle distributions at the beginning of each period for the entire day. The results of the first step are the available vehicles $a_{i,t}^{pre}$ for each zone i at the beginning of each period t. This is the basis for the next step.

In Step 2, we use pre-calculated vehicle distributions for every period t from Step 1 as input. Starting from the last period T, we calculate the prices period by period, taking into account the next periods. However, when calculating prices $p_{i,t}$ for every zone i of the current period t, the prices $p_{i,k}^{fix}$ for every zone i of the next periods $k \in \{t+1, ..., T\}$ are fixed and determined by the previous calculation. Thus, only the prices $p_{i,t}$ of the considered period t are the decision variables. However, with the prices of the considered period $p_{i,t}$, the provider also decides on the network flows of the considered period t and thus on the vehicle distributions of the next periods $k \in \{t+1, ..., T\}$, since the vehicle distributions of the next periods depend on the vehicle distribution at the end of the considered period t.

Algorithm 4 Backwards Algorithm

1: Results: Best prices for the whole day
2: Step 0: Define fixed prices: $p_{i,t}^{fix} = \emptyset \quad \forall i \in I, t \in \mathcal{T}$ and pre-calculated vehicle-distribution $a_{i,t}^{pre} = \emptyset \quad \forall i \in I, t \in \mathcal{T}$
3: Step 1: Solve the problem using a simple and fast solution approach to get a vehicle distribution $a_{i,t}^{pre} \quad \forall i \in \mathcal{I}, t \in \mathcal{T}$
4: Step 2: Solve the following:
5: **for** $t \in \mathcal{T}$ **do**
6: $t^{backwards} = T - 1 + 1$
7: Set the initial distribution $a_{i,t^{backwards}} = a_{i,t^{backwards}}^{pre} \quad \forall i \in I$
8: Solve the problem for the period $t^{backwards}$ taking into account the fixed prices $p_{i,t}^{fix} \quad \forall i \in I, t \in t^{backwards}...T$
9: Save the resulting prices $p_{i,t^{backwards}}^{fix} = p_{i,t^{backwards}} \quad \forall i \in I, t \in T-t...T-t+1$
10: **end for**

To calculate the prices backwards, the Algorithm 4 first defines the following two parameters

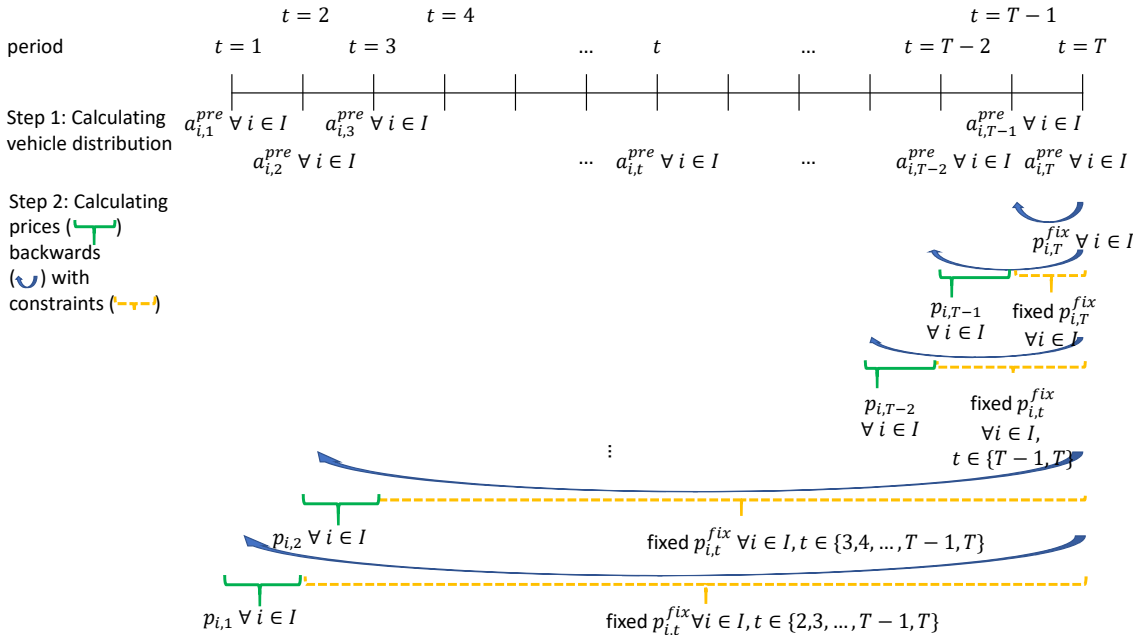

Figure 3.1: Illustration backwards algorithm.

as empty sets (line 2): fixed prices $p_{i,t}^{fix}$ and pre-calculated available vehicles $a_{i,t}^{pre}$ for each zone i at the beginning of each period t. Since there was no calculation of available vehicles and prices yet, the algorithm cannot assign a value to these parameters. Thus, in a first step (line 3), the algorithm solves the problem with a simple and fast solution approach, obtaining the values for the available vehicles $a_{i,t}^{pre}$ for each zone i and period t. In a second step, the backwards calculation determines the prices in different substeps. First, based on the pre-calcuated available vehicles $a_{i,T}^{pre}$ for each zone i and the last period T (line 7), the algorithm computes the prices $p_{i,T}$ for each zone i for the last period T (line 8). In this substep, the pricing approach does not need to consider the next periods. After this, the calculated prices $p_{i,T}$ are fixed for the next substep ($p_{i,T}^{fix} = p_{i,T}$, line 9), which is to calculate the prices $p_{i,T-1}$ for each zone i for period $T-1$ based on the pre-calculated available vehicles $a_{i,T-1}^{pre}$ for each zone i for period $T-1$ (line 7). In this substep, the algorithm considers both periods (T and $T-1$), but the prices of period T are fixed. After getting the computed prices $p_{i,T-1}$ for each zone i for period $T-1$, we fix these prices ($p_{i,T-1}^{fix}$, line 9) as well. This continues until the first period is reached. Here, the algorithm calculates prices based on the pre-calculated available vehicles $a_{i,1}^{pre}$ for each zone i for the first period. For this, the algorithm considers all periods, but only the prices $p_{i,1}$ for each zone i for the first period are decision variables, and the prices of the next periods $t \in \{2,\dots,T\}$ are fixed. After this last calculation, the provider has prices for all zones and periods.

3.4 Computational Study

In extensive computational studies, we investigate the performance of two solution approaches presented in Section 3.3. We systematically vary the most important influencing factors to triangulate how the solution approaches in comparison to benchmarks perform. Section 3.4.1 introduces the scenarios and parameter values. In Section 3.4.2, we present the solution approaches and the benchmarks we investigate. Section 3.4.3 presents the computational results.

3.4.1 Scenarios and Parameters

We consider three settings (SMALL, MEDIUM, LARGE) of a free-floating SMS that primarily differ in the size of the operating area and the number of locations Z (SMALL: $Z = 9$, MEDIUM: $Z = 16$ and LARGE: $Z = 25$). Each of the three settings is examined for three different overall demand levels, which differ in the demand-supply-ratio (DSR). The DSR is the maximum period demand divided by the fleet size and we consider the values $\in \{\frac{1}{3}, \frac{2}{3}, \frac{3}{3}\}$ by scaling demand appropriately. The remaining parameters are constant over all three settings: we discretize the time interval of one day into $T = 48$ periods of 30 minutes each, in line with practice and literature (see e.g. Kaspi et al. (2016) and Ferrero et al. (2015b)). We select the $M = 3$ price points p^m according to typical prices in practice and literature (see e.g. Lippoldt, Niels, and Bogenberger (2018)). We chose a base price per minute of $p^2 = 0.30$ €/min and price differences of 0.06 €/min to the so-called low and high prices, so that $p^1 = 0.24$ €/min and $p^3 = 0.36$ €/min. Variable costs are $c = 0.075$ €/min. The rental time is set to $l = 15$ min, in line with, for example, Xu, Meng, and Liu (2018), Soppert et al. (2022) and the discussions with our industry partner. The corresponding sensitivity factors $f^{(1)}_{i,j,t} = 0.75, f^{(2)}_{i,j,t} = 1, f^{(3)}_{i,j,t} = 1.25 \quad \forall i, j \in Z, t \in \mathcal{T}$ are chosen according to observations from practice.

3.4.2 Investigated Solution Approaches and Evaluation Metrics

Here, we describe the solution approaches that we investigate.

- MODSIM denotes the solution of a simplified model neglecting the assumption of rental realization (see Section 3.3.2).
- BAW denotes the backwards algorithm that computes the vehicle distribution in a first step using either the rolling-horizon with horizon $H = 1$ (BAW-ROL-1) or MODSIM (BAW-MODSIM) and calculating the optimal prices backwards in a second step.

Besides the solution approaches, we investigate four benchmarks:

- BASE denotes a benchmark using constant uniform pricing. Here we use the base price $p_{i,t} = p^{(2)} \quad \forall i \in Z, t \in \mathcal{T}$.
- MOD48h denotes the solution of the model with a given time limit for the solver of 48h in which all 48 periods are optimized simultaneously.
- ROL-H is a basic rolling-horizon approach and is configured with different horizon lengths H (ROL-1, ROL-4, ROL-8). Note that this benchmark with $H = 1$ represents the myopic solution that only considers one period in each substitute problem.

- ADP-H is the ADP decomposition solution approach presented in Soppert et al. (2022), and is configured with different horizon lengths H (ADP-1, ADP-4, ADP-8). It uses a value function approximation to approximate the future after the horizon H that is being considered.

Each combination of settings and *DSR*s forms a instance in our experiments. We implement the algorithms in Python 3.8 and solve all solution approaches and benchmarks with Gurobi 9.1.2. In all scenarios, we set the optimality gap to zero and the time limit is set to one hour for ADP-H, ROL-H, BAW-ROL-1, BAW-MODSIM and to 48 hours for MOD48h and MODSIM. We execute the computations on a workstation with an AMD Ryzen 9 3900 X 12-Core processor with 12 cores, and 64 Gigabyte RAM. Please note that we use the MILP of Soppert et al. (2022) to evaluate the computed prices of the solution approaches and the benchmarks.

3.4.3 Results

In this section we present the results regarding the analyses of profit (see Section 3.4.3.1), pricing (see Section 3.4.3.2), rentals (see Section 3.4.3.3) and computational time (see Section 3.4.3.4).

3.4.3.1 Profit

We begin with a comparison of the different solution methods and the benchmarks by identifying the improvement over BASE. The potential is graphically shown in Figure 3.2. It depicts the profit obtained with the different solution approaches and benchmarks (for the later considered ADP-H and ROL-H in dependence of the horizon lengths H on the horizontal axis) relative to the profit with BASE, which the 0%-line marks. The profits obtained by MODSIM, BAW-ROL-1, BAW-MODSIM and MOD48h are horizontal lines as they do not depend on horizon H.

We observe that MOD48h yield a profit increase of at least 13.5% over BASE. For SMALL with $DSR = 1/3$ MOD48h yields the optimal solution. For LARGE and a higher DSR than 1/3, MOD48h does not find any feasible solution within 48 h. The myopic solution ROL-1 provides at least 5% more profit than BASE.

The difference between ROL-1 and MOD48h (in the instance SMALL, $DSR = 1/3$) shows the whole effect of considering supply-side network effects. The exact supply-side network effect for larger instances cannot be determined because it is not possible to determine the optimal solution within 48 h. In the instance where an optimal solution can still be determined within 48 h (SMALL, $DSR = 1/3$), the profits of MODSIM, and BAW-ROL-1, BAW-MODSIM and ADP-8 are very similar to the profit of the optimal solution (MOD48h). This leads to the conclusion that these solution approaches and the benchmark consider the supply-side network effects best. This conclusion is further supported by analyzing the profits for the other instances. In contrast, the profit of ROL-8 is sometimes very similar (e.g. Figure 3.2a) to the profit of MOD48h, sometimes clearly lower (e.g. Figure 3.2b and Figure 3.2c).

Figure 3.13 in Appendix 3.B depicts the results for SMALL, MEDIUM and LARGE with all *DSR*s. In both figures it is obvious that BAW-ROL-1 and BAW-MODSIM make at least the same profit as ADP-8 in SMALL, MEDIUM and LARGE for every DSR. Also the solution

approach MODSIM provides results that are similar to BAW-ROL-1 and BAW-MODSIM for all instances, although it is always below the profit of BAW-ROL-1 and BAW-MODSIM.

Thus, we can draw the following conclusions:

1. Although the proposed solution approaches (MODSIM, BAW-ROL-1, BAW-MODSIM) are rather straightforward, they achieve equivalent results to more complex benchmarks (MOD48h, ADP-8).

2. The comparison of profit of both new solution approaches (MODSIM, BAW) shows that they consider supply-side network effects, as do the benchmarks MOD48h and ADP-8.

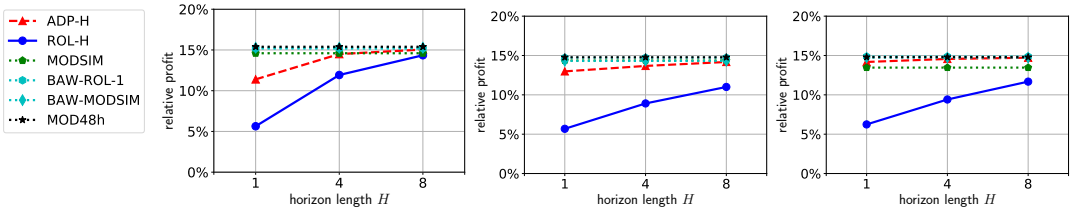

(a) $Z = 9$ (b) $Z = 16$ (c) $Z = 25$

Figure 3.2: Relative profit increase in a 9 zones- (SMALL), 16 zones- (MEDIUM), and 25 zones-setting (LARGE) , $DSR = 1/3$.

3.4.3.2 Pricing Decisions

The anticipative solution approaches MODSIM, BAW-ROL1 and BAW-MODSIM consider supply-side network effects as the benchmarks ADP-8 and MOD48h in contrast to ROL-1 (see Section 3.4.3.1). These supply-side network effects are also reflected in the pricing decisions.

The pricing decisions are depicted as price tables in Figure 3.4 for SMALL with $DSR = 1/3$. For the sake of simplicity, we only analyze the pricing decision of the benchmarks ROL-1 (as myopic pricing), ROL-8, MOD-48h, ADP-1 and ADP-8.

Since MOD48h (which is the optimal solution in this instance) considers the supply-side network effects throughout the day, we compare the price table of the other solution approaches and benchmarks with that of MOD48h. It is obvious that the price table of ROL-1 is very different from the price table of MOD48h, which shows the strong impact of supply-side network effects. The price tables of ROL-8, ADP-8, MODSIM, BAW-ROL-1, BAW-MODSIM and MOD48 h are very similar to the price pattern of MOD48h. That indicates that these solution approaches and benchmarks consider supply-side network effects.

On an aggregate level, these differences become also visible in comparing the proportion of different prices of the solution approaches and benchmarks. In SMALL with $DSR = 1/3$, for example, ROL-1 results in 2% low, 77% base, and 22% high prices (see Figure 3.3). Pricing decisions of MOD48h consists of 34% low, 29% base, and 37% high prices. The proportions of different prices of ADP-8 (43% low, 19% base, 38% high prices), MODSIM (45% low, 16% base, 39% high prices), BAW-ROL-1 (36% low, 28% base, 36% high prices) and BAW-MODSIM (35% low, 25% base, 37% high prices) are also similar to the proportion of different prices of MOD48h, especially for the high prices. This shows that the better supply-side network effects are captured, the more the resulting pricing decisions resemble the optimal pricing.

Thus, we can draw the following conclusions:

1. Supply-side network effects are visible in the price tables and price proportions of MOD48h.

2. MODSIM, BAW-ROL-1 and BAW-MODSIM create price tables which are very similar to those of MOD48h and ADP-8, which indicates that they consider supply-side network effects effectively.

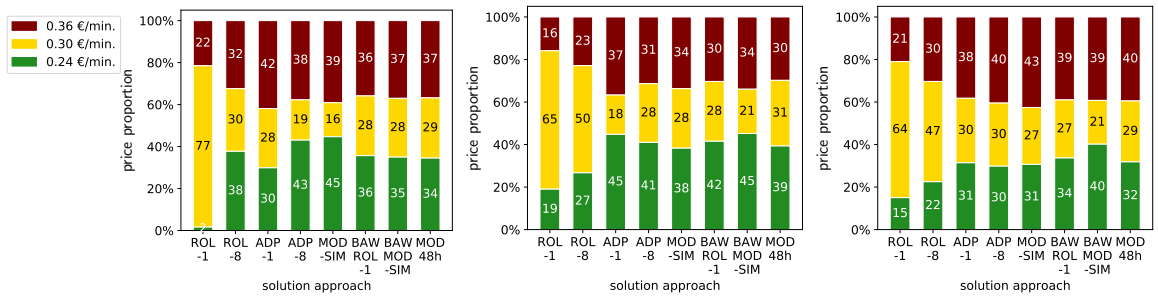

(a) $Z = 9, DSR = 1/3$ (b) $Z = 16, DSR = 1/3$ (c) $Z = 25, DSR = 1/3$

Figure 3.3: Price proportions.
Green: low price, yellow: base price, red: high price.

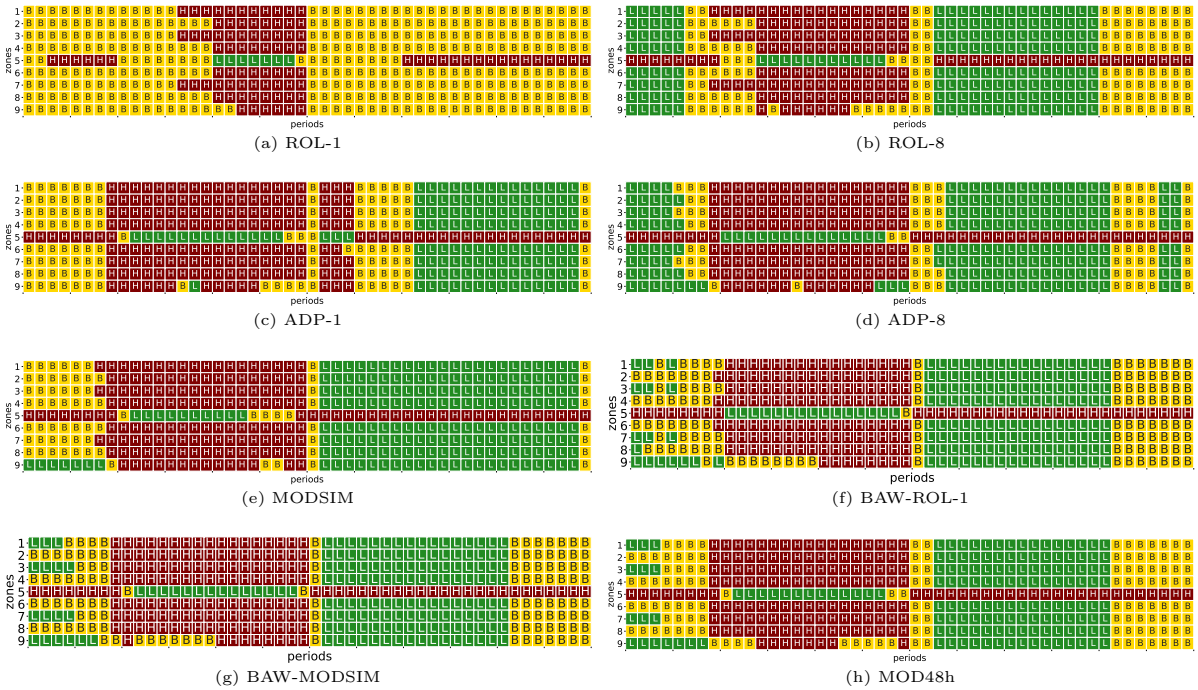

(a) ROL-1 (b) ROL-8

(c) ADP-1 (d) ADP-8

(e) MODSIM (f) BAW-ROL-1

(g) BAW-MODSIM (h) MOD48h

Figure 3.4: Pricing with different solution approaches and benchmarks in a 9 zones-setting (SMALL), $DSR = 1/3$.
Green: L=low price, yellow: B=base price, red: H=high price

3.4.3.3 Rentals

The consideration of supply-side network effects is evident in profit and pricing. We also consider the course of rentals for SMALL with a $DSR = 1/3$ (see Figure 3.5). Since prices affect demand and demand affects rentals, we study the extent to which supply-side network effects are evident for rentals. For the sake of simplicity, we only analyze the pricing decision of the benchmarks ROL-1 (as myopic pricing), ROL-8, MOD-48h and ADP-8.

The first thing to notice is that during the periods with low demand, BASE results in fewer rentals than MOD48h and during the peaks it generates more rentals than MOD48h. Furthermore, it is apparent that the rental-curve of ROL-1 fluctuates similar to the rental-curve of BASE, whereas the rental-curve of MOD48h fluctuates less than both. Another remarkable feature is that the rental curves of MOD48h, ADP-8, BAW-ROL-1 and BAW-MODSIM lie almost on top of each other. The rental curve of MODSIM deviates only slightly from these three rental curves.

From this we conclude that all anticipative solution approachesm and benchmarks (ROL-8, ADP-8, MODSIM, BAW-ROL-1, BAW-MODSIM) consider the supply-side network effects similarly and that apart from the similar prices, the rental curves of MOD48h, ADP-8 BAW-ROL-1, BAW-MODSIM and MODSIM are also very similar.

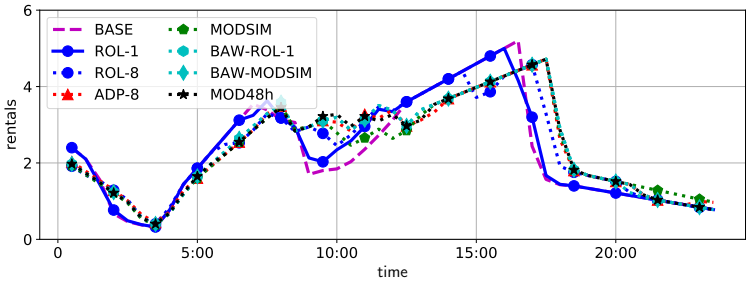

Figure 3.5: Rentals over the day in a 9 zones-setting (SMALL), $DSR = 1/3$.

3.4.3.4 Computational Time

An important aspect for the practicability of solution approaches is, among others, the computational time. For this purpose, we compare the computational time for SMALL, MEDIUM and LARGE for the $DSR = 1/3$ (see Figure 3.6).

First, we consider the different benchmarks. MOD48h (2.5 h up to over 48 h) always takes the longest time for SMALL. For MEDIUM and LARGE, MOD48h takes the full given time of 48 h. The computational times of the rolling-horizon and decomposition solution approaches depend on their horizon. ROL-1 (6 s up to under 1 min) takes the second lowest computational time. ROL-4 (18 s up to 8 min) requires a similar computational time. In contrast, ROL-8 (20 min up to over 12h) requires a clearly longer computational time than ROL-1 and ROL-4. The order of computational times for the different horizons is similar for the decomposition solution approaches. More precisely, ADP-1 (4 min up to over 12 min) and ADP-4 (4 min up to over 1.5 h) still require relatively short computational times, whereas the computational time for ADP-8 (23 min up to over 17.5 h) is clearly longer. Thus, when comparing each different horizon length of the rolling-horizon approaches with the decomposition solution approaches it is obvious that the decomposition solution approaches need longer computational times. This is due to the consideration of future states in the decomposition solution approaches. However, it should also be noted that the benchmarks ADP-1, ADP-4 and ADP-8 require parameter estimation in advance. The additional computational time of parameter estimation for all periods, which lies between less than 1 hour for SMALL and roughly 2 hours for LARGE, thus, must be considered (see also Soppert et al., 2022).

Second, we consider the proposed solution approaches. MODSIM (1 s up to 6 s) takes the least computational time for SMALL, MEDIUM and LARGE. BAW-ROL-1 (1.5 min up to 35 min) and BAW-MODSIM (1 min up to over 3.h) need relatively short computational times.

Comparing benchmarks with solution approaches, ADP-8 and MOD48h, which consider the supply-side network effects effectively, require more computational time than MODSIM, BAW-ROL-1 and BAW-MODSIM. In the most cases, even ADP-4 and ROL-8 require longer computational times than the proposed solution approaches. ROL-4 takes less time than BAW-MODSIM and BAW-ROL-1, but more time than MODSIM.

Figure 3.14 in Appendix 3.C depicts the results for SMALL, MEDIUM and LARGE with all DSRs.

From the obtained computational times we can conclude the following.

1. ROL-1 and ROL-4 require short computational times but do not consider the supply-side network effects effectively (see Section 3.4.3.1).

2. ADP-8 and MOD48h require long computational times.

3. MODSIM requires a short computational time and and is a preferred option due to the comparable results in Section 3.4.3.1 with the best benchmarks (MOD48h, ADP-8).

4. BAW-ROL-1 and BAW-MODSIM need about the same and clearly less computational time than the benchmarks that give similar results (ADP-8, MOD48h). Thus, they are also preferred options.

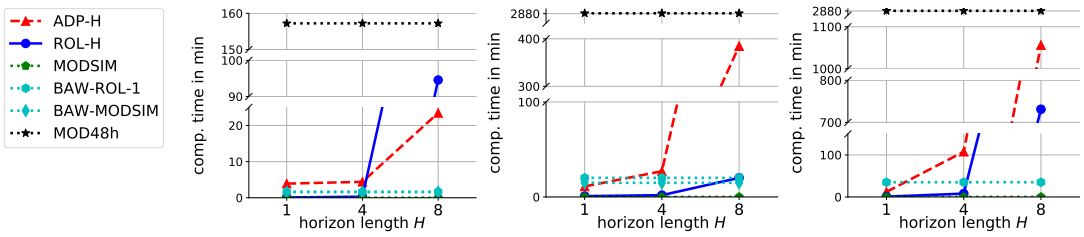

(a) $Z = 9$ (b) $Z = 16$ (c) $Z = 25$

Figure 3.6: Computational time in a 9 zones- (SMALL), 16 zones- (MEDIUM), and 25 zones-setting (LARGE) , $DSR = 1/3$.

3.5 Sensitivity Analysis

In this section, we perform a sensitivity analysis to show how stable the solutions of the different approaches are. First, we study the solution stability in a stochastic environment (see Section 3.5.1). Second, we analyze the effect of different intervals between prices in price sets and different numbers of prices in price sets by modifying the discrete price set (see Section 3.5.2). Third, we apply the different solution approaches and benchmarks for one week (see Section 3.5.3). Fourth, we study the impact of a start solution on results and computational time (see Section 3.5.4).

3.5.1 Stochastic Demand

We analyze the robustness of the prices generated by the different solution approaches and benchmarks in a stochastic environment. For this purpose, we use the multiplicative stochastic function, which generates a stochastic demand $D_{i,j,t}$ (Talluri and van Ryzin, 2004): $D_{i,j,t} = d_{i,j,t} \cdot \xi$ where ξ is a stochastic error term which is assumed to follow a normal distribution $N(1, \sigma)$. We evaluate all scenarios, i.e., SMALL, MEDIUM and LARGE with all DSRs. For each scenario, we consider different degrees of stochasticity, expressed by different standard deviations $\sigma \in 0, 0.1, 0.2, 0.3, 0.4$ of the factor ξ. These values are in the range of demand uncertainties we observed in practice. For each of the resulting combinations of scenario and degree of stochasticity, we draw $S = 1,000$ demand matrices.

Figure 3.7 illustrates the results for SMALL, MEDIUM and LARGE with $DSR = 1/3$. On the vertical axis, the mean value of the relative profit increases with respect to BASE. On the horizontal axis, the standard deviation σ is varied. Overall, the solution approaches MODSIM, BAW-ROL-1 and BAW-MODSIM are robust to the stochasticity of demand. Similar to the profits of the benchmarks ROL-1, ROL-8, ADP-1 and ADP-8, the relative profits of MODSIM, BAW-ROL-1 and BAW-MODSIM decrease slightly with increasing stochasticity. The order of the different solution approaches and benchmarks with respect to their performance does not change in most instances. MODSIM, BAW-MODSIM and BAW-ROL-1 deliver profits that are *not* worse than the benchmark ADP-8 for all scenarios and all stochasticities (see Appendix 3.D).

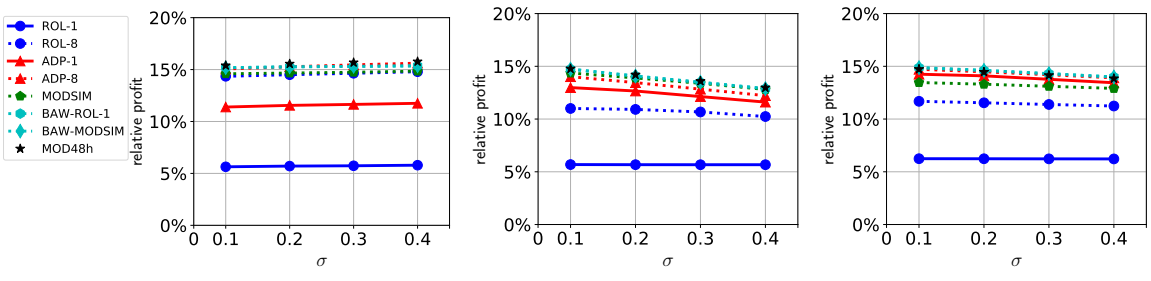

(a) $Z = 9$ (b) $Z = 16$ (c) $Z = 25$

Figure 3.7: Stochastic evaluation of solution approaches and benchmarks in a 9 zones- (SMALL), 16 zones- (MEDIUM) and 25 zones-setting (LARGE), $DSR = 1/3$.

3.5.2 Different Price Sets

In this section, we analyze the impact of the price sets on the performance of the different solution approaches and benchmarks. For this purpose, we use a common standard demand pattern (SMALL, $DSR = 1/3$). Furthermore, in each instance we use 0.30 €/min as base price. We conduct two experiments (see Table 3.2). First, we investigate 20 different price sets with three prices each. The intervals between prices are the same within a price set, but differ between price sets. We use intervals of 0.01 €/min, 0.02 €/min up to 0.2 €/min (see Table 3.2). Second, we investigate the impact of the number of prices on the performance. Here, the intervals are the same for each price set, but we increase the number of price points to five, seven and nine. Price sensitivities change in accordance with prices.

Note that we exclude the ADP benchmarks for this analysis due to the high effort of estimating the parameters in pre-processing. Thus, we focus on the solution approaches MODSIM, BAW-ROL-1 and BAW-MODSIM and on the benchmarks ROL-8 and MOD48h only.

experiment 1: different intervals			**experiment 2: different number of prices**		
price interval	price set	sensitivity factors	number of prices	price set	sensitivity factors
0.01 €/min	$\{0.29, 0.30, 0.31\}$	$\{1.04, 1, 0.96\}$	3	$\{0.24, 0.30, 0.36\}$	$\{1.25, 1, 0.75\}$
0.02 €/min	$\{0.28, 0.30, 0.32\}$	$\{1.08, 1, 0.92\}$	5	$\{0.18, 0.24, 0.30, 0.36, 0.42\}$	$\{1.50, 1.25, 1, 0.75, 0.50\}$
0.03 €/min	$\{0.27, 0.30, 0.33\}$	$\{1.12, 1, 0.87\}$	7	$\{0.12, 0.18, 0.24, 0.30, 0.36, 0.42, 0.48\}$	$\{1.75, 1.50, 1.25, 1, 0.75, 0.50, 0.25\}$
0.04 €/min	$\{0.26, 0.30, 0.34\}$	$\{1.17, 1, 0.83\}$	9	$\{0.06, 0.12, 0.18, 0.24, 0.30, 0.36, 0.42, 0.48, 0.54\}$	$\{2.00, 1.75, 1.50, 1.25, 1, 0.75, 0.50, 0.25, 0\}$
0.05 €/min	$\{0.25, 0.30, 0.35\}$	$\{1.21, 1, 0.79\}$			
0.06 €/min	$\{0.24, 0.30, 0.36\}$	$\{1.25, 1, 0.75\}$			
0.07 €/min	$\{0.23, 0.30, 0.37\}$	$\{1.29, 1, 0.71\}$			
0.08 €/min	$\{0.22, 0.30, 0.38\}$	$\{1.33, 1, 0.67\}$			
0.09 €/min	$\{0.21, 0.30, 0.39\}$	$\{1.37, 1, 0.62\}$			
0.10 €/min	$\{0.20, 0.30, 0.40\}$	$\{1.42, 1, 0.58\}$			
0.11 €/min	$\{0.19, 0.30, 0.41\}$	$\{1.46, 1, 0.54\}$			
0.12 €/min	$\{0.18, 0.30, 0.42\}$	$\{1.50, 1, 0.50\}$			
0.13 €/min	$\{0.17, 0.30, 0.43\}$	$\{1.54, 1, 0.46\}$			
0.14 €/min	$\{0.16, 0.30, 0.44\}$	$\{1.58, 1, 0.42\}$			
0.15 €/min	$\{0.15, 0.30, 0.45\}$	$\{1.62, 1, 0.37\}$			
0.16 €/min	$\{0.14, 0.30, 0.46\}$	$\{1.67, 1, 0.33\}$			
0.17 €/min	$\{0.13, 0.30, 0.47\}$	$\{1.71, 1, 0.29\}$			
0.18 €/min	$\{0.12, 0.30, 0.48\}$	$\{1.75, 1, 0.25\}$			
0.19 €/min	$\{0.11, 0.30, 0.49\}$	$\{1.79, 1, 0.21\}$			
0.20 €/min	$\{0.10, 0.30, 0.50\}$	$\{1.83, 1, 0.17\}$			

Table 3.2: Overview over different price lists.

Figure 3.8 illustrates the results for different intervals between the prices and different number of prices in the price set. On the vertical axis, the mean value of the relative profit increases with respect to BASE. On the horizontal axis, the interval between the prices (see Figure 3.8a) or the number of prices (see Figure 3.8b) in the price set is varied.

In Figure 3.8a the relative profit of all solution approaches and benchmarks, except of MODSIM, tends to increase with the difference between the prices in the price set up to the difference

of 0.14 €/min, after which it decreases. This shows that the prices should be chosen reasonably. The relative profit of MODSIM increases until the difference of 0.08 €/min. Thereafter, the profit curve drops sharply. We assume that this is due to the difference between the discrete price points $(p^{(1)}, p^{(2)}, p^{(3)})$. MODSIM, which converts the continuous prices of the simplified model into discrete prices, calculates larger price differences between the continuous and the discrete price. Thus, if the price difference between price points is greater than 0.08 €/min, the larger the price difference, the worse the results of MODSIM. In reality, however, differences of 0.05 and 0.06 €/min are observed for Share Now.

In addition, in Figure 3.8b the relative profit also increases as the number of price points in the price set increases. The profit increase is degressive. Furthermore, ROL-8, MODSIM, BAW-ROL-1, BAW-MODSIM and MOD48h perform similarily well for three and five price points, whereas ROL-8, BAW-MODSIM and MOD48h perform better than MODSIM and BAW-ROL-1 for seven and nine price points.

With regards to the worse performance of BAW-ROL-1 compared to BAW-MODSIM, the first step of calculating vehicle distributions seems to be decisive. More precisely, BAW-MODSIM, which has a suitable solution approach MODSIM to determine the vehicle distributions, performs better than BAW-ROL-1, which has the benchmark ROL-1 to determine the vehicle distributions.

From this we can conclude that BAW-MODSIM is the best practicable solution approach. It provides similar results as MOD48h and ROL-8.

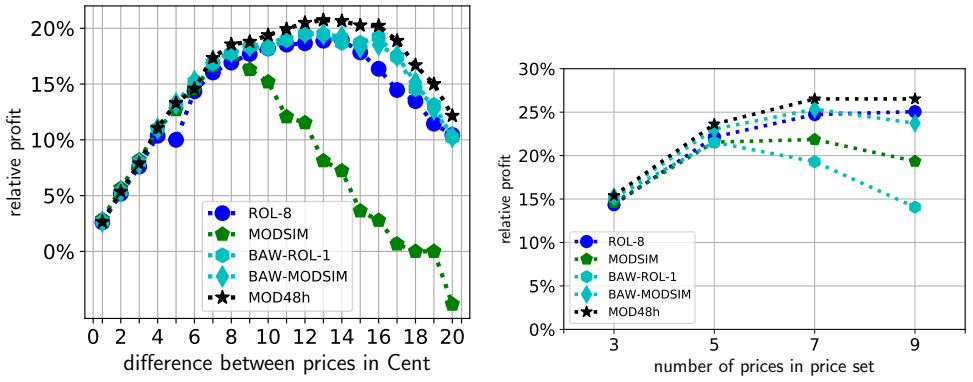

(a) Different intervals in the price sets

(b) Different number of prices in the price sets

Figure 3.8: Sensitivity analysis of varying intervals between prices and number of prices in price set in a 9 zones-setting (SMALL), $DSR = 1/3$.

3.5.3 Pricing for One Week without Operator-Based Relocation

In this section, we examined the determination of prices for an entire week without operator based relocation. For this purpose, we assume that each day has the same demand pattern. For this study, we look at the relative average profit for a day compared to the profit of pricing with BASE, the course of rentals, and the price structure.

3.5.3.1 Profit

First, we consider the relative average profit per day for one week (see Figure 3.9a), which is relative to the average profit per day of BASE. It is obvious that supply-side network effects have to be taken into account. This can be seen in the difference between myopic pricing ROL-1 and anticipative pricing ROL-8, MODSIM, BAW-ROL-1, BAW-MODSIM or MOD48h. Second, we consider the relative profit per day for one week (see Figure 3.9b), which is relative to the profit of BASE at the first day. Similar to the observation above, the profit of MODSIM, BAW-ROL-1, BAW-MODSIM, ROL-8 and MOD48h is similar and higher than the profit of ROL-1. It is also obvious that the order of the different solution approaches and benchmarks with regard to profit does not change over the seven days. In addition, we note that the profit is highest on the first day compared to the following days for all solution approaches and benchmarks (see Figure 3.9b). However, this shows that operator-based relocation can be worthwhile.

Considering computational times, MOD48h needs 336.44 h, ROL-8 needs 8.46 h, while BAW-ROL-1 needs 7.6 min, BAW-MODSIM 7 min and MODSIM 0.07 min to calculate prices (for a more detailed analysis see Section 3.4.3.4)

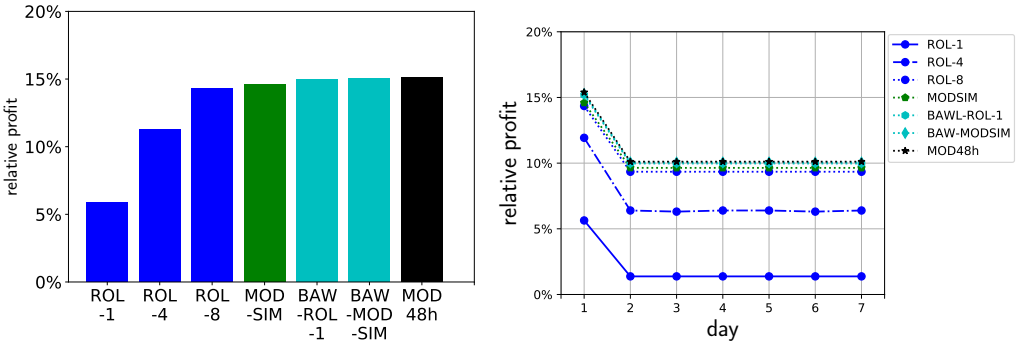

(a) Average relative profit of a day for a whole week

(b) Relative profit for each day of the week

Figure 3.9: Profit for a week without operator-based relocation in a 9 zones-setting (SMALL), $DSR = 1/3$.

3.5.3.2 Pricing Decisions

We examine the pricing decisions (see Figure 3.10). Except for the first day, we see a repeating price pattern for each day. Moreover, it is obvious that the myopic pricing approach (ROL-1, Figure 3.10a) leads to a clearly different price table than the solution approaches and benchmarks that include supply-side network effects (ROL-8, MODSIM, BAW-ROL-1, BAW-MODSIM, MOD48h). However, there are also differences between them. For example, ROL-8 (see Figure 3.16c) sets high and low prices less frequently than MODSIM, BAW-ROL-1, BAW-MODSIM and MOD48h (see Figure 3.10). The different price tables can be explained by the different pricing decisions on the first day, which probably lead to different vehicle distributions on the first day and thus different stable price patterns for days 2-7.

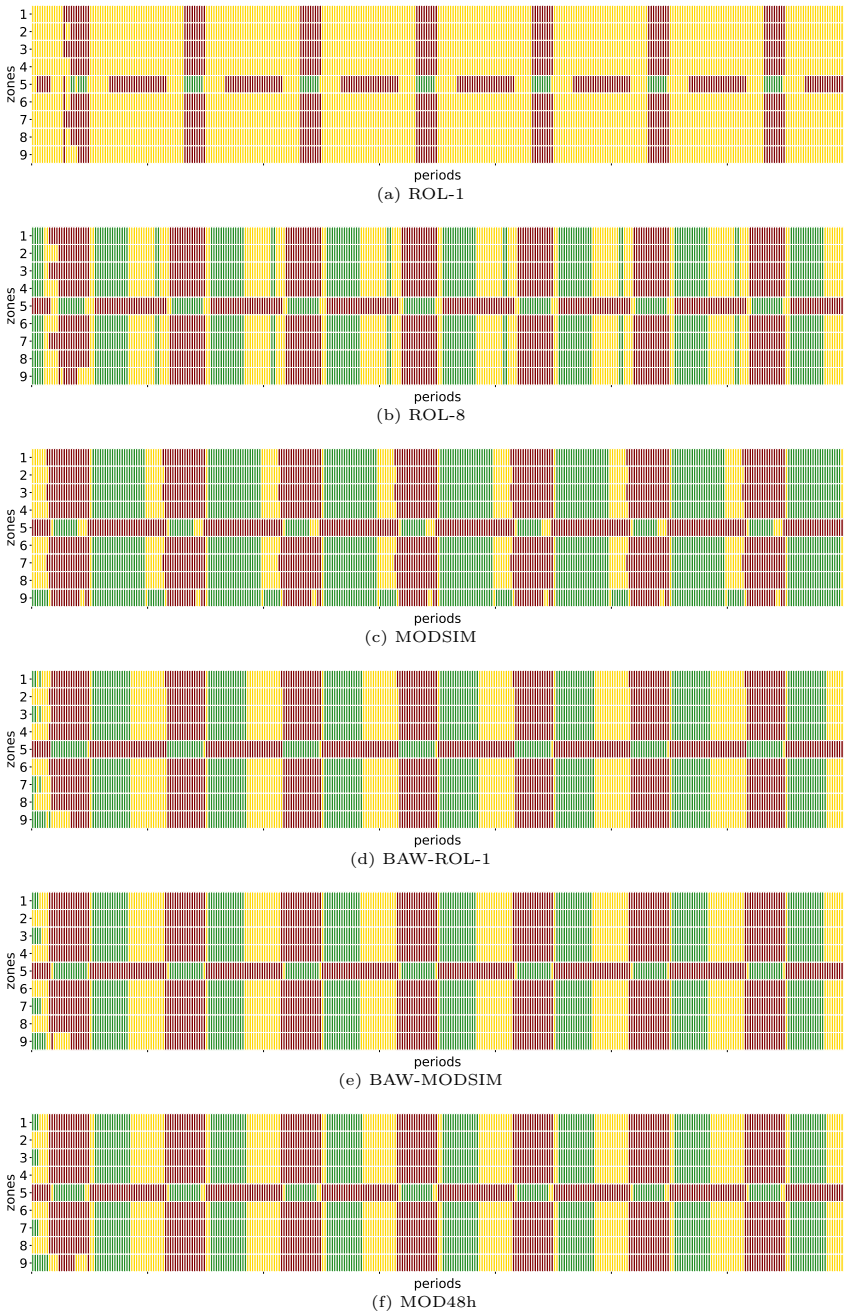

(a) ROL-1

(b) ROL-8

(c) MODSIM

(d) BAW-ROL-1

(e) BAW-MODSIM

(f) MOD48h

Figure 3.10: Pricing for one week with different solution approaches and benchmarks in a 9 zones-setting (SMALL), $DSR = 1/3$
Green: low price, yellow: base price, red: high price.

3.5.3.3 Rentals

We examine rentals over the seven days (see Figure 3.11). Again, we note that after the initial day, the rental course over the following days is identical. Furthermore, we observe that BASE and the myopic pricing approach (ROL-1) result in numbers of rentals that fluctuate clearly more than for the others. Furthermore, ROL-8, MODSIM, BAW-ROL-1, BAW-MODSIM, MOD48h are similar.

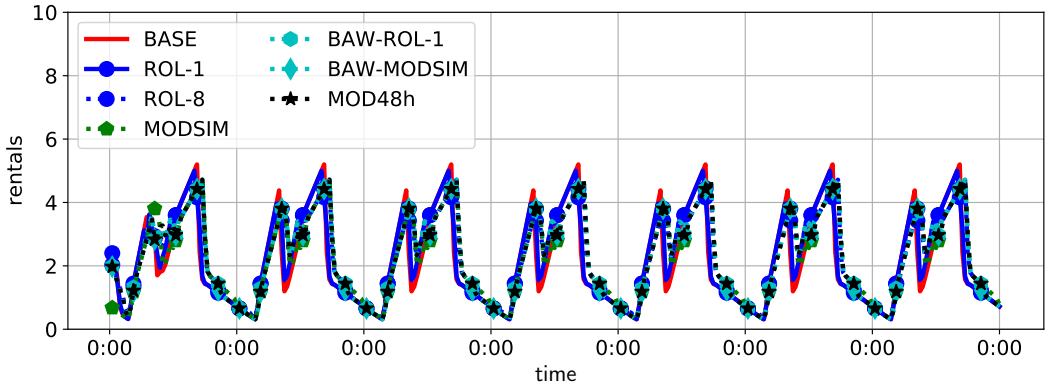

Figure 3.11: Rentals over seven days in a 9 zones-setting (SMALL), $DSR = 1/3$.

We can therefore conclude the following:

1. Each solution approach and each benchmark creates a (daily) regular rental pattern (see Figure 3.11) and pricing (see Figure 3.10) after the first day. These regular patterns (for day 2 to day 7) can be identified by the equal contribution margins (see Figure 3.9b).

2. The consideration of supply-side network effects in solution approaches and benchmarks is useful and leads to clearly higher profits, even in longer periods. The consideration of these supply-side network effects can be observed in the price tables (see Figure 3.10).

3. The solution approaches MODSIM, BAW-ROL-1 and BAW-MODSIM provide the same results as the benchmarks ROL-8 or MOD48h (see Figure 3.9a), but need less computational time.

3.5.4 Impact of a Start Solution

In Section 3.4.3, we notice that even for some instances ($Z = 25$, $DSR = 2/3$ and $Z = 25$, $DSR = 3/3$), there are no results for MOD48h since the solver does not find a feasible solution within the given time limit of 48 h. Therefore, we wanted to investigate two aspects in this section: First, whether a start solution improves the solution quality and second, whether and how a start solution affects the computational time. We use the BASE solution as a start solution in all instances.

	Difference in profit increase with respect to BASE in %								
	$Z = 9$			$Z = 16$			$Z = 25$		
	$DSR = 1/3$	$DSR = 2/3$	$DSR = 3/3$	$DSR = 1/3$	$DSR = 2/3$	$DSR = 3/3$	$DSR = 1/3$	$DSR = 2/3$	$DSR = 3/3$
ROL-4	0.02	0.00	0.00	0.00	0.37	0.09	-0.04	-0.15	-0.04
ROL-8	0.02	0.00	0.00	-0.06	-0.02	-0.09	-0.33	-0.01	0.04
MOD48h	0.00	0.00	0.00	0.07	0.02	0.25	0.30		
ADP-1	0.00	0.00	-0.06	0.00	-0.04	0.00	0.00	0.00	0.02
ADP-4	0.00	0.00	0.00	0.00	0.04	0.14	0.00	-0.01	-0.01
ADP-8	0.00	0.00	0.00	-0.07	0.05	0.01	-0.04	0.00	-0.04
BAW-ROL-1	-0.01	0.00	0.00	0.00	0.04	0.00	0.00	0.00	0.00
BAW-MODSIM	0.00	0.00	0.00	0.00	-0.04	0.00	0.00	0.00	-0.05

(a) Profit with and without start solution

	Difference in computational time in min								
	$Z = 9$			$Z = 16$			$Z = 25$		
	$DSR = 1/3$	$DSR = 2/3$	$DSR = 3/3$	$DSR = 1/3$	$DSR = 2/3$	$DSR = 3/3$	$DSR = 1/3$	$DSR = 2/3$	$DSR = 3/3$
BASE	0.0	0.0	0.0	0.0	0.0	0.0	0.0	0.0	0.0
ROL-4	0.04	-0.18	-0.12	-0.98	-1.44	-4.50	2.91	8.10	11.36
ROL-8	-23.55	-1.25	-0.75	-5.94	-91.07	-87.91	-84.10	-91.59	265.08
MOD48h	2723.46	1.00	0.42	-0.16	0.08	0.00	0.06		
ADP-1	0.14	0.07	-9.94	-3.89	-7.61	22.76	3.05	0.00	0.01
ADP-4	0.04	-0.05	-9.64	-3.71	-7.72	-36.43	-30.74	0.00	-0.01
ADP-8	-6.45	-2.90	0.46	47.06	-89.43	-1394.14	73.93	40.21	7.44
BAW-ROL-1	0.46	0.83	0.13	-15.44	-3.46	-2.24	16.17	21.76	65.43
BAW-MODSIM	0.21	-0.07	0.10	-9.42	-4.92	-2.51	-30.54	63.86	74.60

(b) Computational time with and without start solution

Table 3.3: Comparison regarding profit and computational time provided by solution approaches and benchmarks with and without start solution.

The comparison leads to the following findings: All applied solution approaches and benchmarks with a start solution result in no noticeable improvement of the results regarding profit (see Table 3.3a). Notably, the start solution has a positive effect on the computational time for most instances (a reduction of computational time up to 92 min, see Table 3.3b). However, a start solution can also have negative effects on the computational time for some instances. For example, for MOD48h at the smallest instance ($Z = 9$, $DSR = 1/3$), it has a clearly negative time effect (+ 46 h).

Nevertheless, the use of a start solution results in solutions for MOD48h in all instances within the time limit. From this it can be concluded that it makes sense to use BASE as a start solution. This applies in particular to real instances.

3.6 Conclusion

In this paper we propose two different solution approaches for the problem of origin-based differentiated pricing for SMSs, which maximize the profit by setting spatially and temporarily differentiated origin-based minute prices. Although origin-based pricing is the most practicable variant of differentiated pricing, only one paper in the current literature focuses on differentiated origin-based pricing in SMSs.

The first solution approach is a simplified mathematical model and formulated as a fluid approximation (simplified model, MODSIM). The second one is a backwards algorithm (BAW), which computes the vehicle distribution for every period with an appropriate straightforward solution approach in a first step. We apply a myopic solution approach (BAW-ROL-1) and a relaxed solution approach (BAW-MODSIM) for this step. In the second step, we calculate the prices backwards based on the calculated vehicle distributions in the first step.

Extensive computational experiments and the sensitivity analysis with a varying number of zones, demand patterns, overall demand levels, varying price sets and pricing for one week without operator-based relocation show the stability of the results from our solution approaches MODSIM, BAW-ROL-1 and BAW-MODSIM.

In the computational study, the proposed solution approaches perform similarly well as the best performing benchmarks ADP-8, ROL-8 and MOD48h with considerably shorter computational time without having to calculate additional parameters (as with ADP-8). Additionally, they show a considerable improvement with regard to profit over the myopic benchmark (ROL-1, up to 10 percentage points). In the instance (SMALL, $DSR = 1/3$) where the optimal solution can be determined, we can show that the proposed, anticipative solution approaches (MODSIM, BAW-ROL-1, BAW-MODSIM) find a solution close to optimality. Finally, the resulting price tables show high similarity to the optimal price tables, in contrast to the price tables from the myopic pricing approach (ROL-1). This shows that, in contrast to the myopic solution approach, our approaches, just like other benchmarks (ADP-8, ROL-8, MOD48h), take supply-side networks into account. We also show that the proposed solution approaches need clearly less computational time in comparison to the benchmarks ADP-4, ADP-8 and MOD48h.

In the sensitivity analysis, we investigate the stability of the solutions from our solution approaches and benchmarks in regards to four aspects. First, we investigate the stability of the results against a background of an environment with different degrees of stochasticity of the demand. The solution approaches MODSIM, BAW-ROL-1 and BAW-MODSIM are robust against stochasticity of demand. The order of the different solution approaches and benchmarks with respect to profit does not change in most cases. Second, we study the effect of different price sets on the performance of the different solution approaches and benchmarks. We find that MODSIM is only useful for the difference between the discrete prices up to 0.08 €/min, and that MODSIM and BAW-ROL-1 lose performance when the price set has more than five price points. For settings with price sets containing more than five price points, we recommend BAW-MODSIM. Third, we study the determination of prices for an entire week without operator-based relocation. Even in this long considered period the consideration of supply-side network effects is useful and leads to clearly higher profits for the anticipative solution approaches (MODSIM, BAW-ROL-1, BAW-MODSIM) and the benchmarks (ROL-8, MOD48h). Fourth, we study the

impact of a start solution. The implementation of a start solution does not noticeably improve the results regarding profit (except for MOD48h, where now always a feasible solution exists). However, in most cases, it has a positive effect on the computational time.

To conclude, we propose different pricing approaches (MODSIM, BAW-ROL-1, BAW-MODSIM) that can be used for profit maximization in SMSs by considering supply-side network effects with clearly shorter computational times. These pricing approaches do not require a pre-processing for estimating parameters in advance, are straightforward to apply and equal in profit to comparable but more complex benchmarks (e.g. ADP-8).

3.A Price Proportion for Different Scenarios

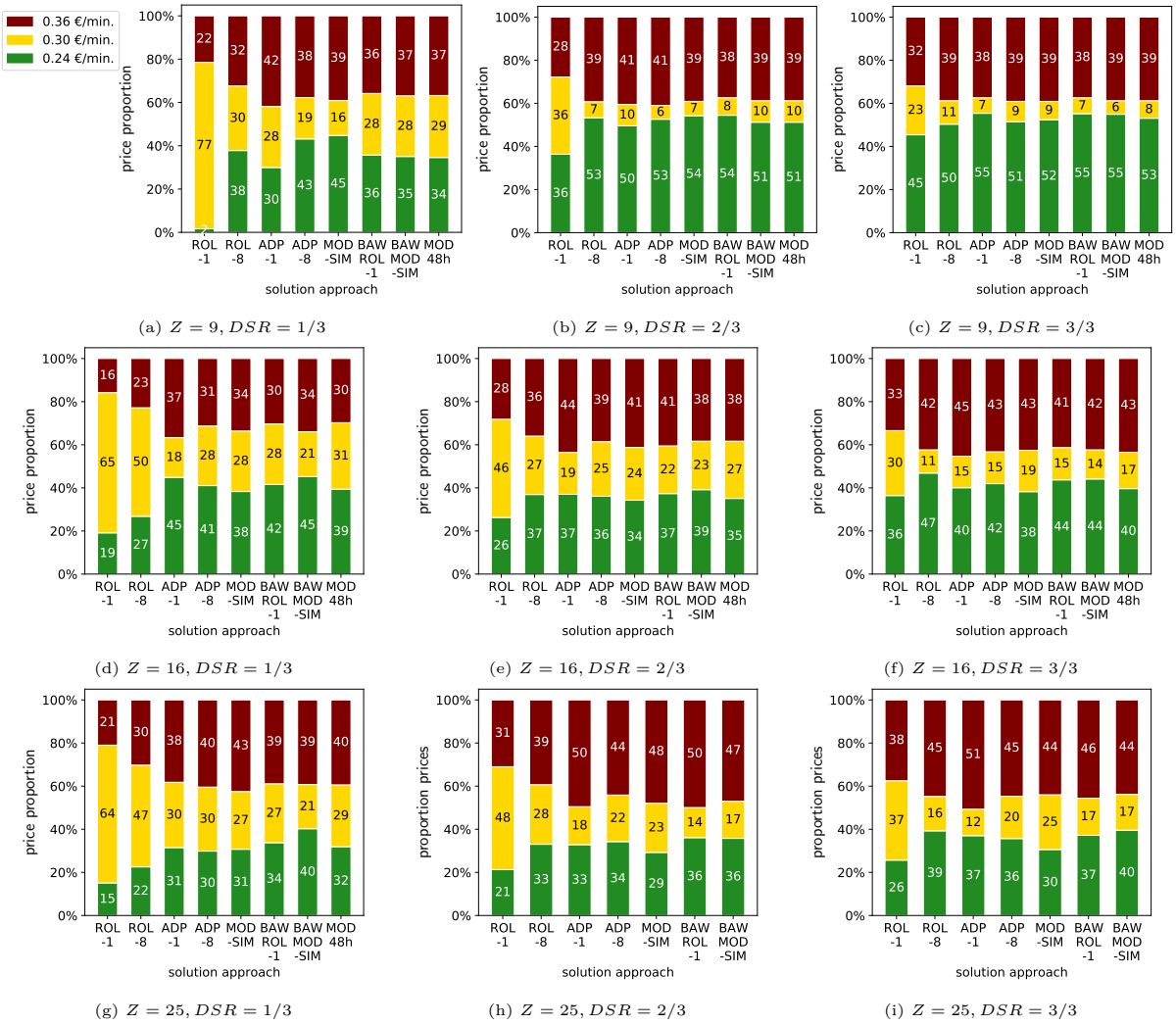

(a) $Z = 9, DSR = 1/3$ (b) $Z = 9, DSR = 2/3$ (c) $Z = 9, DSR = 3/3$

(d) $Z = 16, DSR = 1/3$ (e) $Z = 16, DSR = 2/3$ (f) $Z = 16, DSR = 3/3$

(g) $Z = 25, DSR = 1/3$ (h) $Z = 25, DSR = 2/3$ (i) $Z = 25, DSR = 3/3$

Figure 3.12: Price proportion in a 9 zones- (SMALL), 16 zones- (MEDIUM) and 25 zones-setting (LARGE)
Green: low price, yellow: base price, red: high price.

3.B Profit for Different Scenarios

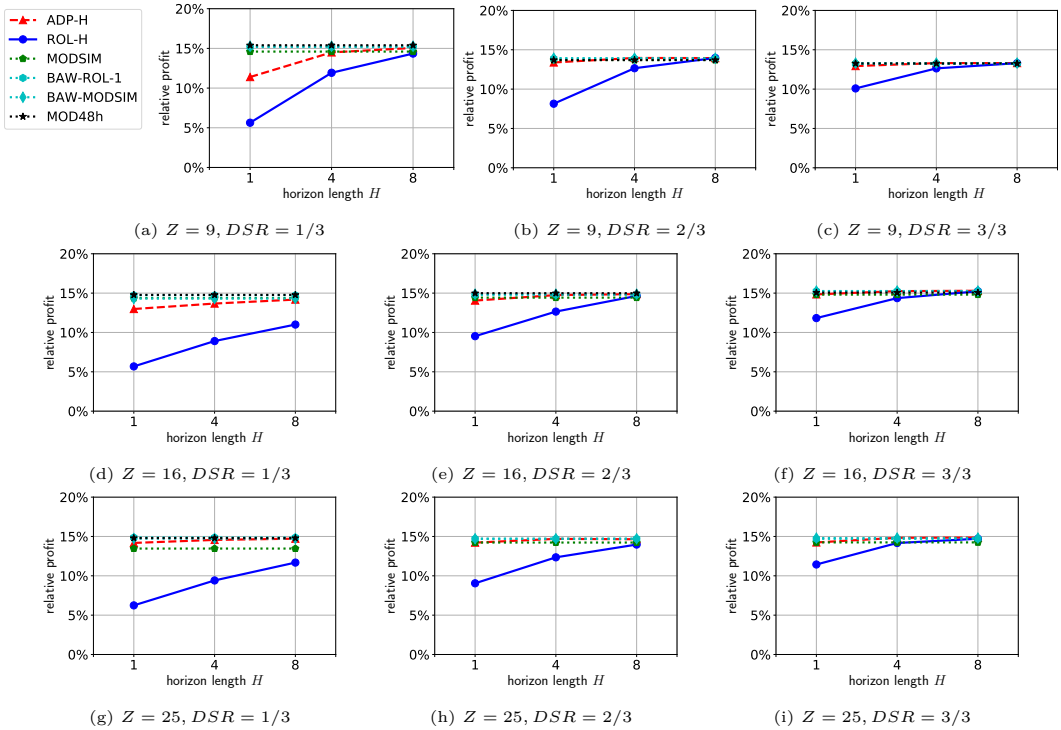

(a) $Z = 9, DSR = 1/3$ (b) $Z = 9, DSR = 2/3$ (c) $Z = 9, DSR = 3/3$

(d) $Z = 16, DSR = 1/3$ (e) $Z = 16, DSR = 2/3$ (f) $Z = 16, DSR = 3/3$

(g) $Z = 25, DSR = 1/3$ (h) $Z = 25, DSR = 2/3$ (i) $Z = 25, DSR = 3/3$

Figure 3.13: Relative profit increase in a 9 zones- (SMALL), 16 zones- (MEDIUM) and 25 zones-setting (LARGE).

3.C Computational Time for Different Scenarios

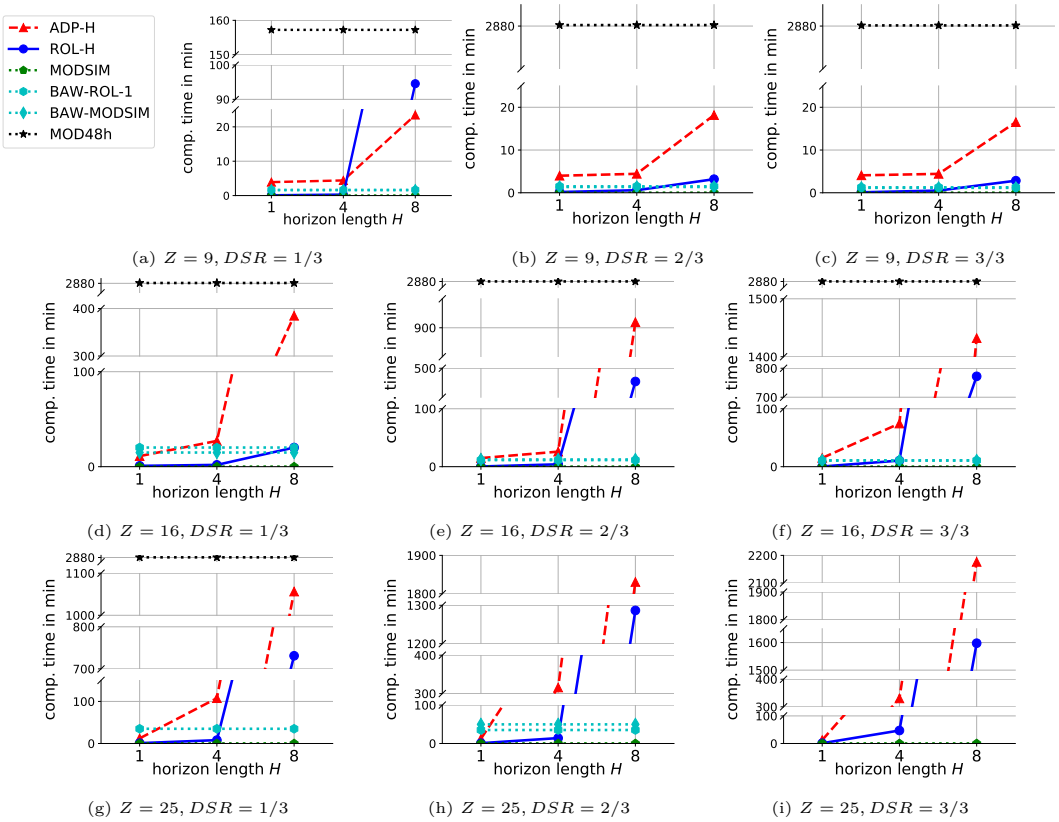

(a) $Z = 9, DSR = 1/3$ (b) $Z = 9, DSR = 2/3$ (c) $Z = 9, DSR = 3/3$

(d) $Z = 16, DSR = 1/3$ (e) $Z = 16, DSR = 2/3$ (f) $Z = 16, DSR = 3/3$

(g) $Z = 25, DSR = 1/3$ (h) $Z = 25, DSR = 2/3$ (i) $Z = 25, DSR = 3/3$

Figure 3.14: Computational time in a 9 zones- (SMALL), 16 zones- (MEDIUM) and 25 zones-setting (LARGE).

3.D Stochastic Demand

As a technical remark, note that in the stochastic demand model, demand realization $D_{ijt} < 0$ could potentially result in particular for high values of σ (see the corresponding discussion in Talluri and van Ryzin (2004, Chapter 7.3.4)). We correct for this by setting negative draws to 0. Note that the small positive bias resulting from this truncation is not relevant to our study, as for each degree of stochasticity, we use the same 1000 scenarios for all approaches we compare.

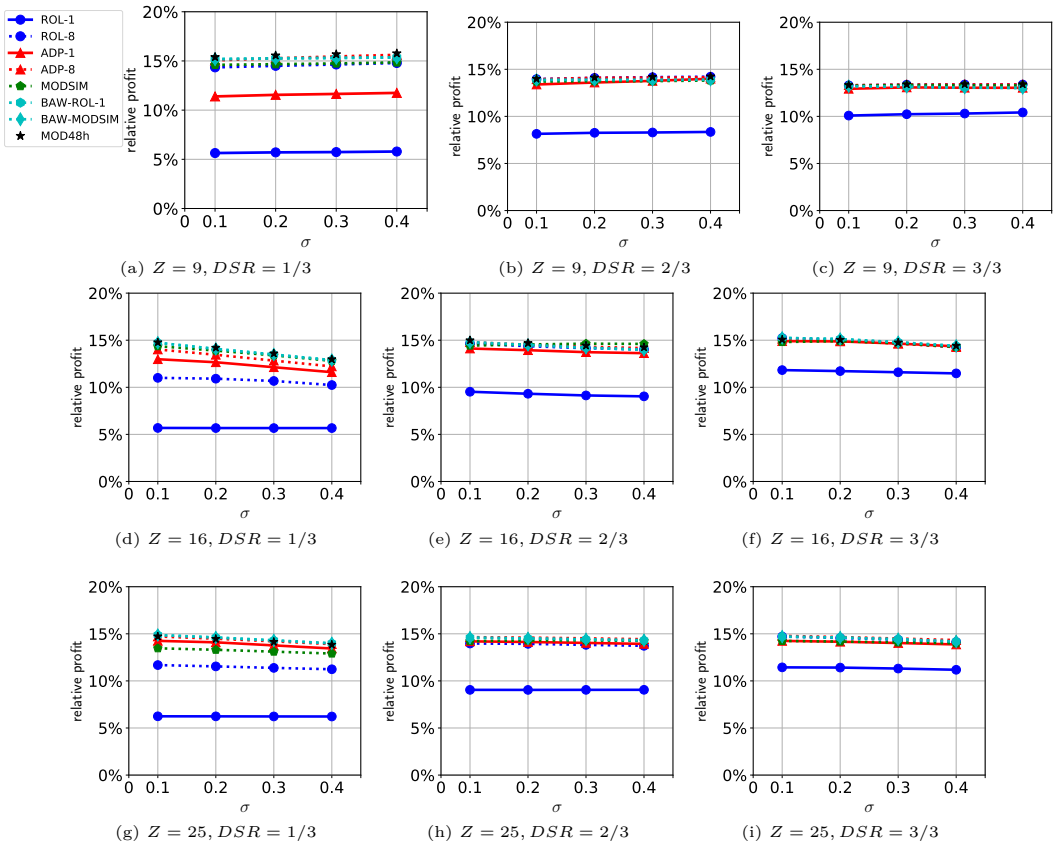

(a) $Z = 9, DSR = 1/3$ (b) $Z = 9, DSR = 2/3$ (c) $Z = 9, DSR = 3/3$

(d) $Z = 16, DSR = 1/3$ (e) $Z = 16, DSR = 2/3$ (f) $Z = 16, DSR = 3/3$

(g) $Z = 25, DSR = 1/3$ (h) $Z = 25, DSR = 2/3$ (i) $Z = 25, DSR = 3/3$

Figure 3.15: Pricing with different solution approaches in a 9 zones-setting (SMALL), $DSR = 1/3$.

3.E One Week Pricing

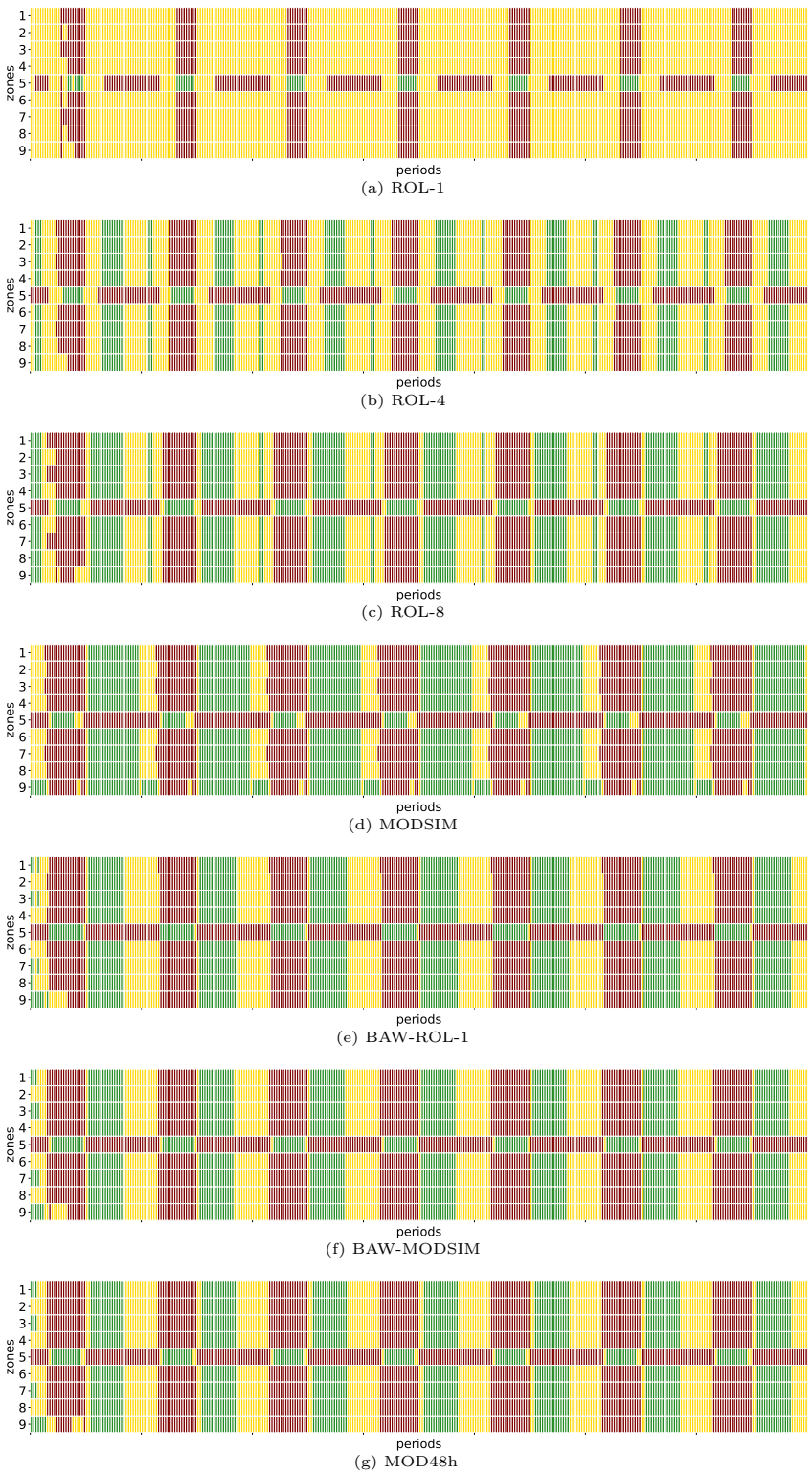

(a) ROL-1

(b) ROL-4

(c) ROL-8

(d) MODSIM

(e) BAW-ROL-1

(f) BAW-MODSIM

(g) MOD48h

Figure 3.16: Pricing for one week with different solution approaches in a 9 zones-setting (SMALL) $DSR = 1/3$
Green: low price, yellow: base price, red: high price.

3.F Stochastic Evaluation

	Mean profit increase with respect to BASE in %														
	$Z = 9$					$Z = 16$					$Z = 25$				
	$\sigma = 0$	$\sigma = 0.1$	$\sigma = 0.2$	$\sigma = 0.3$	$\sigma = 0.4$	$\sigma = 0$	$\sigma = 0.1$	$\sigma = 0.2$	$\sigma = 0.3$	$\sigma = 0.4$	$\sigma = 0$	$\sigma = 0.1$	$\sigma = 0.2$	$\sigma = 0.3$	$\sigma = 0.4$
BASE	0.0	0.0	0.0	0.0	0.0	0.0	0.0	0.0	0.0	0.0	0.0	0.0	0.0	0.0	0.0
ROL-1	6.24	5.71	5.73	5.79	5.78	9.05	5.67	5.67	5.67	5.61	11.44	6.24	6.23	6.22	6.22
ROL-4	9.41	12.06	12.16	12.29	12.36	12.35	8.84	8.78	8.45	8.15	14.17	9.24	9.07	8.90	8.74
ROL-8	11.68	14.50	14.64	14.79	14.83	13.97	10.91	10.67	10.24	9.83	14.71	11.54	11.38	11.24	11.09
ADP-1	14.25	11.55	11.65	11.75	11.81	14.20	12.66	12.13	11.60	11.00	14.25	14.10	13.77	13.44	13.12
ADP-4	14.57	14.59	14.79	15.03	15.20	14.67	13.20	12.57	11.95	11.35	14.82	14.36	14.05	13.72	13.40
ADP-8	14.72	15.27	15.46	15.62	15.72	14.65	13.45	12.83	12.22	11.64	14.78	14.48	14.20	13.91	13.60
MODSIM	13.46	14.67	14.74	14.85	14.97	14.23	13.90	13.39	12.80	12.26	14.25	13.30	13.11	12.90	12.69
BAW-ROL-1	14.87	15.26	15.31	15.36	15.37	14.59	14.08	13.48	12.88	12.32	14.70	14.61	14.30	13.99	13.66
BAW-MODSIM	14.73	15.36	15.41	15.47	15.49	14.71	13.62	12.97	12.34	11.73	14.80	14.41	14.06	13.72	13.36

(a) $DSR = 1/3$

	Mean profit increase with respect to BASE in %														
	$Z = 9$					$Z = 16$					$Z = 25$				
	$\sigma = 0$	$\sigma = 0.1$	$\sigma = 0.2$	$\sigma = 0.3$	$\sigma = 0.4$	$\sigma = 0$	$\sigma = 0.1$	$\sigma = 0.2$	$\sigma = 0.3$	$\sigma = 0.4$	$\sigma = 0$	$\sigma = 0.1$	$\sigma = 0.2$	$\sigma = 0.3$	$\sigma = 0.4$
BASE	0.0	0.0	0.0	0.0	0.0	0.0	0.0	0.0	0.0	0.0	0.0	0.0	0.0	0.0	0.0
ROL-1	8.14	8.26	8.29	8.35	8.28	9.53	9.31	9.13	9.04	8.99	9.05	9.04	9.05	9.05	9.07
ROL-4	12.65	12.84	12.91	12.99	12.98	12.65	12.43	12.20	12.05	11.99	12.35	12.30	12.26	12.22	12.17
ROL-8	13.96	14.09	14.16	14.22	14.14	14.64	14.37	14.15	14.02	13.97	13.97	13.93	13.82	13.73	13.63
ADP-1	13.69	13.59	13.77	14.00	14.10	14.42	13.94	13.73	13.62	13.55	14.23	14.13	14.03	13.93	13.84
ADP-4	13.87	14.00	13.98	13.99	13.90	14.79	14.44	14.15	13.96	13.85	14.59	14.57	14.46	14.35	14.24
ADP-8	13.93	14.10	14.12	14.16	14.07	14.87	14.53	14.31	14.16	14.06	14.71	14.60	14.52	14.43	14.34
MODSIM	13.38	13.73	13.74	13.80	13.77	14.12	14.55	14.63	14.61	14.60	14.20	14.29	14.30	14.25	14.18
BAW-ROL-1	13.96	13.88	13.87	13.89	13.82	14.80	14.50	14.20	13.99	13.84	14.67	14.51	14.41	14.31	14.22
BAW-MODSIM	13.94	13.94	13.94	13.97	13.90	14.79	14.62	14.33	14.12	13.99	14.65	14.64	14.53	14.43	14.33

(b) $DSR = 2/3$

	Mean profit increase with respect to BASE in %														
	$Z = 9$					$Z = 16$					$Z = 25$				
	$\sigma = 0$	$\sigma = 0.1$	$\sigma = 0.2$	$\sigma = 0.3$	$\sigma = 0.4$	$\sigma = 0$	$\sigma = 0.1$	$\sigma = 0.2$	$\sigma = 0.3$	$\sigma = 0.4$	$\sigma = 0$	$\sigma = 0.1$	$\sigma = 0.2$	$\sigma = 0.3$	$\sigma = 0.4$
BASE	0.0	0.0	0.0	0.0	0.0	0.0	0.0	0.0	0.0	0.0	0.0	0.0	0.0	0.0	0.0
ROL-1	10.09	10.23	10.30	10.42	10.45	11.83	11.72	11.60	11.48	11.51	11.44	11.41	11.31	11.18	11.08
ROL-4	12.64	12.78	12.74	12.73	12.64	14.36	14.31	14.08	13.64	13.30	14.17	14.09	13.93	13.73	13.55
ROL-8	13.29	13.37	13.39	13.38	13.30	15.23	15.03	14.69	14.25	13.95	14.71	14.56	14.37	14.13	13.90
ADP-1	13.26	13.08	13.04	13.03	12.95	14.81	14.87	14.64	14.34	13.98	14.25	14.16	14.02	13.87	13.75
ADP-4	13.20	13.24	13.17	13.13	13.06	15.25	15.04	14.73	14.35	14.02	14.70	14.67	14.52	14.35	14.21
ADP-8	13.31	13.38	13.40	13.39	13.30	15.26	14.95	14.63	14.26	13.81	14.80	14.66	14.50	14.34	14.18
MODSIM	12.93	13.33	13.30	13.29	13.21	14.90	14.90	14.69	14.28	13.84	14.25	14.18	14.09	13.99	13.89
BAW-ROL-1	13.31	13.14	13.06	13.01	12.94	15.25	15.12	14.78	14.40	14.04	14.82	14.60	14.42	14.18	13.95
BAW-MODSIM	13.31	13.24	13.17	13.13	13.06	15.14	15.05	14.68	14.20	13.79	14.78	14.70	14.55	14.39	14.21

(c) $DSR = 3/3$

Table 3.4: Mean profit increase in a 9 zones- (SMALL), 16 zones- (MEDIUM) and 25 zones-setting (LARGE) for different $DSRs$. For all analyses, the half-width of the 95% confidence interval was at most ± 0.16 percentage points.

Bibliography

Angelopoulos, A., Gavalas, D., Konstantopoulos, C., Kypriadis, D., Pantziou, G., 2016. Incentivization schemes for vehicle allocation in one-way vehicle sharing systems. *2016 IEEE Internat. Smart Cities Conf. (ISC2)*, 1–7.

Barth, M., Todd, M., Xue, L., 2004. User-based vehicle relocation techniques for multiple-station shared-use vehicle systems. Working paper, *Transp. Res. Board 80th Annual Meeting.*

Brendel, A.B., Brauer, B., Hildebrandt, B., 2016. Toward user-based relocation information systems in station-based one-way car sharing. *AMCIS Proc.*, 1–10.

Chemla, D., Meunier, F., Pradeau, T., Wolfler Calvo, R., Yahiaoui, H., 2013. Self-service bike sharing systems: Simulation, repositioning, pricing. Working paper, CERMICS, École des Ponts ParisTech, Champs-sur-Marne, France.

Clemente, M., Fanti, M.P., Iacobellis, G., Nolich, M., Ukovich, W., 2017. A decision support system for user-based vehicle relocation in car sharing systems. *IEEE Transact. Syst., Man and Cybernetics: Syst.* 48(8), 1283–1296.

Côme, E., 2014. Model-based count series clustering for bike sharing systems usage mining: A case study with the Vélib' system of Paris. *ACM Transact. Intell. Syst. Technol.*, 1–27.

DeMaio, P., 2009. Bike-sharing: History, impacts, models of provision, and future. *J. Public Transp.* 12(4), 41–56.

Destatis, 2017. Anteil von Fahrzeugen für New Mobility Dienste am gesamten Fahrzeugabsatz in den USA, China und der europäischen Union im Zeitraum der Jahre 2015 bis 2025. Accessed February 17, 2023,https://de.statista.com/statistik/daten/studie/796395/umfrage/prognose-des-fahrzeugabsatzes-fuer-new-mobility-service-nach-regionen/.

Dötterl, J., Bruns, R., Dunkel, J., Ossowski, S., 2017. Towards dynamic rebalancing of bike sharing systems: An event-driven agents approach. *EPIA Conf. Artificial Intell.*, 309–320.

Di Febbraro, A., Sacco, N., Saeednia, M., 2012, One-way carsharing. *Transp. Res. Record* 2319(1), 113–120.

Ferrero, F., Perboli, G., Vesco, A., Caiati, V., Gobbato, L., 2015a. Car-sharing services – Part A taxonomy and annotated review. Working paper, Istituto Superiore Mario Boella, Turin, Italy.

Ferrero, F., Perboli, G., Vesco, A., Musso, S., Pacifici, A., 2015b. Car-sharing services – Part B business and service models. Working paper, Istituto Superiore Mario Boella, Turin, Italy.

Fishman, E., Washington, S., Haworth, N., 2013. Bike share: A synthesis of the literature. *Transp. Rev.* 33(2), 148–165.

Guon G., Kang, M., 2022. Rebalancing and charging scheduling with price incentives for car sharing systems. *Transact. Intell. Transp. Syst.* 23(10), 18592-18602.

Haider, Z., Nikolaev, A., Kang, J.E., Kwon, C., 2018. Inventory rebalancing through pricing in public bike sharing systems. *Eur. J. Oper. Res.* 270(1), 103–117.

Huang, K., Kun, A., Rich, J., Ma, W., 2020. Vehicle relocation in one-way station-based electric carsharing systems: A comparative study of operator-based and user-based methods. *Transp. Res. Part E: Logist. Transp. Rev.* 142.

Illgen, S., Höck, M., 2019. Literature review of the vehicle relocation problem in one-way car sharing networks. *Transp. Res. Part B: Methodological* 120, 193–204.

Jiao, Z., Ran, L., Liu, X., Zhang, Y., Qiu, R.G., 2020. Integrating price-incentive and trip-selection policies to rebalance shared electric vehicles. *Serv. Sci.* 12(4), 148–173.

Jorge, D., Correia, G.H.D.A., 2013. Carsharing systems demand estimation and defined operations: A literature review. *Eur. J. Transp. Infrastructure Res.* 13(3), 201–220.

Jorge, D., Molnar, G., Correia, G.H.D.A., 2015. Trip pricing of one-way station-based carsharing networks with zone and time of day price variations. *Transp. Res. Part B: Methodological* 81, 461–482.

Kaspi M., Raviv T., Tzur M., Galili, H. 2016. Regulating vehicle sharing systems through parking reservation policies: Analysis and performance bounds. *Eur. J. Oper. Res.* 251(3), 969–987.

Laporte, G., Meunier, F., Wolfler Calvo, R., 2015. Shared mobility systems. *4OR* 13(4), 341–360.

Laporte, G., Meunier, F., Wolfler Calvo, R., 2018. Shared mobility sytems: An updated survey. *Ann. Oper. Res.* 271(1), 105–126.

Lippoldt, K., Niels, T., Bogenberger, K., 2018. Effectiveness of different incentive models in free-floating carsharing systems: A case study in Milan. *IEEE Intell. Transp. Syst. Conf. (ITSC)*, 1179–1185.

Lu, R., Correia, G.H.D.A., Zhao, X., Liang, X., Lv, Y., 2021. Performance of one-way carsharing systems under combined strategy of pricing and relocations. *Transp. B: Transp. Dyn.* 9(1), 134–152.

Pantuso, G., 2020. Formulations of a carsharing pricing and relocation problem. *Internat. Conf. Comput. Logist.*, 295–310.

Pantuso, G., 2022. Exact solutions to a carsharing pricing and relocation problem under uncertainty. *Comput Oper. Res.*, 295–310.

Pfrommer, J., Warrington, J., Schildbach, G., Morari, M., 2014. Dynamic vehicle redistribution and online price incentives in shared mobility systems. *IEEE Transact. Intell. Transp. Syst.* 15(4), 1567–1578.

Ren, S., Luo, F., Lin, L., Hsu, S.C., Li, X.I., 2019. A novel dynamic pricing scheme for a large-scale electric vehicle sharing network considering vehicle relocation and vehicle-grid-integration. *Internat. J. Prod. Econ.* 218, 339–351.

Ricci, M., 2015 Bike sharing: A review of evidence on impacts and processes of implementation and operation. *Res. Transp. Bus. Manag.* 15, 28–38.

Ruch, C., Warrington, J., Morari, M., 2014. Rule-based price control for bike sharing systems. *2014 European Control Conf. (ECC)*, 708–713.

Schiffer, M., Hiermann, G., Rüdel, F., Walther, G., 2021. A polynomial-time algorithm for user-based relocation in free-floating car sharing systems. Ruch, C., Warrington, J., Morari, M., 2014. Rule-based price control for bike sharing systems. *Transp. Res. Part B: Methodological* 143, 65–85.

Soppert, M., Steinhardt, C., Müller, C., Gönsch, J., 2022. Differentiated pricing of shared mobility systems considering network effects. *Transp. Sci.* 56(5), 1279–1303.

Stokkink, P., Geroliminis, N., 2021. Predictive user-based relocation through incentives in one-way car-sharing systems. *Transp. Res. Part B: Methodological* 149, 230–249.

Talluri, K.T., van Ryzin, G.J., 2004. The theory and practice of revenue management (Springer, Boston, MA).

Wagner, S., Willing, C., Brandt, T., Neumann, D., 2015. Data analytics for location-based services: Enabling user-based relocation of carsharing vehicles. *Proc. Internat. Conf. Inf. Syst. (ICIS)* 3, 279–287.

Wang, L., Ma, W., 2019. Pricing approach to balance demands for one-way car-sharing systems. *2019 IEEE Intell. Transp. Syst. Conf. (ITSC)*, 1697–1702.

Waserhole, A., Jost, V., 2012. Vehicle sharing system pricing regulation: A fluid approximation. Working paper, ENSTA ParisTech, Palaiseau, France.

Xu, M., Meng, Q., Liu, Z., 2018. Electric vehicle fleet size and trip pricing for one-way car-sharing services considering vehicle relocation and personnel assignment. *Transp. Res. Part B: Methodological* 111, 60–82.

Ruiyou Zhang, R., Kan, H., 2018. Dynamic trip pricing considering car rebalances for station-based carsharing services. *IEEE Chinese Control Decis. Conf. (CCDC)*, 1608-1613

Chapter 4

Matching Functions for Free-Floating Shared Mobility System Optimization to Capture Maximum Walking Distances

4.1 Introduction

Shared mobility systems (SMSs) such as car sharing and bike sharing systems have become an integral part of the inner-city mobility. Globally, the shared mobility market today has a size of approximately 250 bn. USD and is projected to grow annually by around 25% the next years (Data Bridge Market Research, 2021). Among the two general concepts of free-floating (FF) and station-based (SB) systems (Lu, Chen, and Shen, 2017), especially FF SMSs experienced considerable growth during the last decade (Shaheen, Cohen, and Jaffee, 2018). The decisive difference between FF SMSs and SB SMSs is that pick-up and drop-off locations for vehicles are not limited to certain predefined locations – the *stations* in an SB SMS. Instead, in an FF SMS, vehicles are *free-floating* within some predefined operating area and can be dropped-off (and picked-up) at any publicly accessible location.

The optimization of SMSs, e.g. with regard to pricing and relocation, has been studied extensively in the literature, summarized e.g. in review papers on car sharing by Ferrero et al. (2015a) and on SMSs in general by Laporte, Meunier, and Wolfler Calvo (2018); Ataç, Obrenović, and Bierlair (2021). However, in the body of works addressing operational optimization problems with endogenous modeling of rentals, FF SMSs – despite their dominance in practice – have not been adequately considered. Instead, up to now, FF SMSs are treated like SB SMSs (compare e.g. Jorge, Molnar, and de Almeida Correia (2015); Haider et al. (2018) for SB SMSs and Lu et al. (2021); Hardt and Bogenberger (2021) for FF SMSs). However, as it turned out in a close collaboration with Share Now, Europe's largest FF car sharing provider operating in 16 cities in 8 countries (Share Now, 2021), ignoring the difference between both concepts in the optimization models can result in an overestimation of rentals in the FF SMS, suboptimal decisions and substantial profit losses. In this work, we address and solve this fundamental issue of inaccurate rentals modeling in FF SMS optimization models.

To give an idea of the causes of this issue, we first need to consider how SMS optimization models are usually formulated: Regarding space, it is the state-of-the-art approach in literature and practice to discretize the operating area of an FF SMS into *zones* – the counterpart of *stations* in an SB SMS (e.g. Weikl and Bogenberger (2016); Neijmeijer et al. (2020)). Regarding time, the considered time frame is discretized into *periods* for both SB and FF SMSs. The SMSs are described and optimized on this level of aggregation, i.e. relevant data (e.g. demand) is collected, and optimization models are formulated on this *location*-period level (station-period in SB SMSs, zone-period in FF SMSs). Typically, these optimization models are mixed-integer (linear) programs based on network flow formulations for both SB (e.g. Jorge, Molnar, and de Almeida Correia (2015)) and FF (e.g. Lu, Chen, and Shen (2017)) SMSs.

Now, a central component of these optimization models is the formalization on the location-period level how rentals realize in dependence of the number of available vehicles and the number of arriving customers – i.e., how supply and demand *match*. The existing SB and FF SMS optimization models rely on the implicit assumption that rentals are determined by the *minimum of supply and demand*. While the realization of rentals can be modeled well with this *matching function* in an SB SMS, applying the same simplified assumption to FF SMSs can cause substantial errors. Consider e.g. a *station*-period combination in an SB SMS with one (expected) available vehicle and one (expected) arriving customer. In this SB SMS, it is valid to assume

that one (expected) rental realizes. For the same situation in an FF SMS in contrast, an accurate matching function must differ: When the zone is large, the available vehicle is not necessarily within reach of the customer, because the *zone* has a spatial expansion and customers have a maximum willingness-to-walk (e.g. Herrmann, Schulte, and Voß (2014)). Thus, *at most* one – for a large zone, much less than one – (expected) rental results. Note that we explicitly write "(expected)", because even though realizations of supply, demand and rentals are discrete values in reality, they can be (and often are) *modeled* continuously.

A presumably simple solution is to apply a finer spatial discretization scheme to the FF SMS, i.e. to define many small zones such that a customer can reach any vehicle in the respective zone, and then use the matching function to determine rentals as in an SB SMS. This, however, simply substitutes the problem of a vehicle being too far away in a large zone by other problems, which become more severe with decreasing zone size: Most importantly, defining many small zones is problematic, because observed data points of demand and supply that in reality resulted in a rental are more likely to be assigned to neighboring zones such that there would not be a matching in the FF SMS model. This aggregation error is related to the *modifiable areal unit problem* (see, e.g., Manley (2019)) which summarizes that statistical results, such as mean values, variance, and correlations do depend on the specific discretization scheme. Typical discretization schemes in literature and practice use zones in the order of several square kilometers (e.g. Weikl and Bogenberger (2016)) and for these zone area sizes, the described issue regarding the supply-demand matching due to the customers' maximum walking distance indeed prevails. These larger zone area sizes also have the practical advantage that the typically resulting fifty to hundred zones have a count which is still manageable for the staff of the SMS provider and that the optimization models which scale with the zone count do not grow too large. All of the named aspects already show that the decision on appropriate discretization schemes (including count, size and shape of zones) for FF SMSs is very complex. In fact, there is no single best definition of the discretization scheme. Thus, in our work, we consider a certain discretization scheme *as given*, and we address the search for accurate matching functions for FF SMSs that adapt to the given circumstances.

Clearly, any matching process can be replicated arbitrarily exact with stochastic simulations that consider discrete supply, demand, and resulting rentals. However, we are interested in *analytical* functions that output expected rentals (continuous values) and that can be integrated in the existing SMS optimization models from the literature. Therefore, to solve the issue of inaccurate matching modeling in FF SMS optimization models, we first formulate a general matching function that replicates the matching process within an FF SMS and incorporates its specific characteristics. Based on this, we then formally derive two novel matching functions which are specifically suited for FF SMS optimization models. We also formalize what is assumed in the existing literature so far by a third matching function and show that only the two novel matching functions can widely be applied to FF SMSs, and that their integration in FF SMS optimization models improves decision making.

To properly distinguish our work from the literature, two streams are of particular importance. First, matching functions have a long history in *macroeconomics*, mostly focusing on labor markets and with the intention to explain unemployment (e.g. Petrongolo and Pissarides

(2001)). Some extensions also consider matching functions in transportation systems, such as taxi systems (e.g. Buchholz (2019)). However, as we discuss in more detail in Section 4.2, matching functions that incorporate the specifics of FF SMSs have not been discussed yet. Moreover, in contrast to this literature stream, our focus eventually lies on the formulation of optimization models, such that we have a different view on matching functions and their requirements: For example, the matching functions' linearizability and integrability in an overall FF SMS optimization model is of particular importance in our case, but irrelevant in the existing literature. Second, the development of *matching functions* for FF SMSs in our work must not be mixed up with the development of so-called *matching algorithms* in *platform-based SMSs* such as *on-demand ride-hailing*, like Uber or Lyft (e.g. Yan et al. (2020)). In the latter, a *central platform* faces the problem to *assign* customer requests most efficiently to available drivers. Since the customer's GPS coordinates are shared with the driver after the assignment happened, the ride realizes with certainty and, thus, there is no need for *matching functions* in the sense explained above. In contrast to the matching algorithms in platform-based SMSs, the provider of the SMSs that we consider *cannot explicitly* decide on the *assignment* of vehicles to customers as customers choose vehicles themselves. Instead, the *matching functions* formalize how many rentals are expected to realize within some location-period combination, given supply, demand, and other relevant parameters.

The contributions of this paper are as follows:

- To the best of our knowledge, we are the first to reveal the necessity to formulate SB and FF SMS optimization models differently. We show that more sophisticated matching functions improve FF SMSs models and the decisions resulting from optimization.
- Second, we derive two novel matching functions for FF SMSs, which take into account the customers' sequential arrival, their maximum walking distance, and the size of the zone. These functions differ regarding their mathematical properties and can be integrated in different types of optimization models – one into the widespread linear network flow-based SMS optimization models, allowing to adapt a variety of existing SB SMS optimization models to FF SMSs.
- Third, we formalize a third matching function that reflects the assumptions made (implicitly) in the SMS optimization literature, i.e. that (expected) rentals correspond to the minimum of (expected) supply and demand. We demonstrate that this benchmark does not yield accurate rentals estimations for FF SMSs in general. Our analytical investigation of this function's properties shows that this shortcoming cannot be remedied by artificially partitioning zones for which data is given into multiple smaller zones.
- Fourth, in a computational study, we demonstrate that the rental prediction accuracy of the novel functions in an FF SMS is substantially higher than the benchmark function. This is because the novel matching functions adapt to the given circumstances, in particular to different zones sizes.
- Fifth, in a case study based on real-life data, we integrate one of the novel matching functions into an existing pricing optimization framework and demonstrate significant profit increases that can be ascribed solely to the more accurate matching modeling.

Overall, this work primarily contributes to the literature on FF SMS optimization from the operations research stream of literature. We build a bridge between the optimization of SB and FF SMSs, in the sense that, by the approaches presented in this paper, existing optimization approaches that were specifically designed for SB SMSs can straightforwardly be generalized to make them applicable for FF SMSs as well.

The remainder of the paper is structured as follows. In Section 4.2, we review the related literature. Section 4.3 discusses the novel as well as the benchmark matching functions. Section 4.4 contains the numerical study considering the rentals prediction accuracy. In Section 4.5, we assess the importance of accurate matching modeling in optimization problems by considering a pricing optimization case study. Section 4.6 covers managerial insights, concludes the paper and gives an outlook.

4.2 Literature

The literature on SMS optimization is broad and covers decision making at strategic, tactical and operational levels (Laporte, Meunier, and Wolfler Calvo, 2018). Various review papers on bike sharing (DeMaio, 2009; Fishman, Washington, and Haworth, 2013; Ricci, 2015) and car sharing (Jorge and Correia, 2013; Ferrero et al., 2015a,b; Brendel and Kolbe, 2017; Illgen and Höck, 2019; Golalikhani et al., 2021a,b) summarize the literature. Our work contributes to the tactical (e.g. fleet sizing) and operational (e.g. relocation or pricing) levels where matching functions are (implicitly) used and, as we will see, more advanced matching functions are required for FF SMSs.

Until now, matching functions for SMSs and the necessity of modeling FF SMSs differently than SB SMSs has not been discussed in the literature. On the contrary, the literature is divided on whether *any* differences need to be made between optimization models of SB and FF SMSs and we explore these views in Section 4.2.1. In Section 4.2.2, we provide an overview on SMS optimization problems with a focus on the wide spread approaches formulated as time-expanded networks. These works are relevant because existing assumptions regarding matching can be concluded from their optimization models and these works are the ones where our novel matching functions can be integrated in. In Section 4.2.3, we review the literature on matching functions from macroeconomics. In Section 4.2.4, we briefly review two other related literature streams, namely agent-based FF SMS simulations and empirical studies, as these works implicitly provide insights regarding relevant parameters for matching functions.

Note that, as explained in Section 4.1, we do not consider *platform-based* mobility offers like on-demand ride-hailing that *assign* customer requests to vehicles (e.g. Boysen, Briskorn, and Schwerdfeger (2019); Yan et al. (2020)), because the nature of these problems differs fundamentally from those in the SMSs that we consider (car sharing etc.).

4.2.1 Station-Based vs. Free-Floating Shared Mobility System Optimization

SB SMSs have a relatively long history in practice – the first SB car sharing system was installed in 1948 in Switzerland (called Sefage) (Shaheen, Sperling, and Wagner, 1998). In contrast, the concept of FF SMSs, which today largely relies on the usage of mobile phones and GPS tracking only became technically realizable much later and arguably was first put into practice with an FF car sharing system in 2008 in Germany (Ciari, Bock, and Balmer, 2014) (called car2go which ten years later became Share Now). This temporal delay of FF SMSs is reflected in the literature, where the majority of papers consider SB SMSs. For example, in the general survey paper on SMSs, Laporte, Meunier, and Wolfler Calvo (2015) entirely focus on SB SMSs, while their updated survey a few years later explicitly differs between SB and FF SMSs (Laporte, Meunier, and Wolfler Calvo, 2018).

Regarding the optimization of these SMSs, there are different views in the literature on whether SB and FF SMSs can be considered identical or not: Some authors state that SB and FF SMSs can be treated *identically*. As stated in Section 4.1, this view is based on the fact that the state-of-the-art approach in literature and practice regarding the modeling of FF SMSs is to discretize the operating area into zones (e.g. Weikl and Bogenberger (2016); Neijmeijer et al.

(2020)). Thus, it is tempting to equate stations and zones. For example, in their review paper on relocations in one-way car sharing, Illgen and Höck (2019) argue that "free-floating operation areas are usually partitioned into smaller zones that serve as virtual stations, such that the VReP [vehicle relocation problem] can be applied perfectly for relocations that occur between those zones instead of from station to station". Similarly, Lu et al. (2021) who consider combined relocation and pricing on the performance of one-way car sharing systems, implicitly state that SB and FF SMSs can be considered identically, as they use the decisive terms "stations" and "zones" interchangeably.

The only researchers we know of who represent a *more differentiated* view are from Bogenberger's group. Weikl and Bogenberger (2015) e.g. consider relocation optimization for FF SMSs. On the one hand, they state that from a technical viewpoint, SB SMS optimization models can be transferred to FF SMSs by "dividing the operating area into station-like zones." On the other hand, they state that "transferring the existing relocation models for station-based systems to free-floating car sharing systems is however restricted" and they give multiple reasons related to the considered relocation problem (see also Weikl and Bogenberger (2013)). The authors e.g. argue that zone-level relocation decisions are not specific enough for FF SMSs because vehicles have specific positions. Another argument concerns the optimization model, since zones of FF SMSs "do not have strict capacity limits" in contrast to stations in SB SMSs. To address these issues, the authors define "macroscopic zones" which are separated into "microscopic zones". The relocation decisions on macroscopic level are determined by optimization while the decisions on microscopic level are rule-based. Note that in the models of Weikl and Bogenberger (2013) and Weikl and Bogenberger (2015), the issue of accurate matching modeling does not arise, because the optimal number of vehicles per zone which is affected by the relocation decisions is given and rentals are not modeled endogenously (see also Section 4.2.2).

In our work, we demonstrate that SB and FF SMS optimization models indeed need to differ. While Weikl and Bogenberger (2015) focus on relocation, in this paper we address the essential issue of matching modeling, which is necessary for all optimization models in which rentals are endogenously modeled. We in particular show that once that data is collected on some defined zone level, artificially subdividing this zone into multiple sub-zones which correspond to stations of an SB SMS does not address the issue of inaccurate rentals predictions (Section 4.3).

4.2.2 Network Flow-Based Shared Mobility System Optimization Models

The dynamically changing, imbalanced distribution between available and demanded vehicles is a well-known challenge of SMSs (Jorge and Correia, 2013; Lippoldt, Niels, and Bogenberger, 2019; Molnar and Correia, 2019). Most tactical and operational optimization approaches seek to address this problem in order to optimize for the actual service- or monetary-related goal. To that end, the proposed approaches typically consider the interaction of supply and demand over the entire SMS by modeling the system with a time-expanded network, where rentals and relocations are described by flows. Note that not all network flow-based SMS models consider rentals *endogenously*. For example, papers on relocation typically consider the desired number of vehicles at different spatio-temporal network nodes as given, and model only the operator-based vehicle movements (=relocations) to serve this demand as network flows. The matching

functions in this work determine the user-based vehicle movements (=rentals) in dependence of supply, demand and other parameters. Accordingly, they are only relevant for optimization models with endogenous rentals which we focus on in the following.

Among these works, we identify three groups. First, works that consider SB SMSs (e.g. Jorge, Molnar, and de Almeida Correia (2015); Haider et al. (2018)), second, works that consider FF SMSs (e.g. Lu, Chen, and Shen (2017); Lu et al. (2021); Hardt and Bogenberger (2021)), and third, works that consider SMSs in general (e.g. Correia and Antunes (2012); Soppert et al. (2022)), by speaking of *locations* instead of *stations* or *zones*. Among the first and second group, several works do not use the term *station-based* or *free-floating* explicitly, but their problem description and modeling where they use the terms *station* or *zone* allows to classify them.

To the best of our knowledge, the issue of supply and demand matching in FF SMSs has not been addressed in any of these works, or elsewhere in the literature. Still, the above works model the relation between supply, demand, and rentals, such that assumptions regarding the matching modeling within a specific location-period are implicitly revealed: All of the above-named works use the concept that rentals are the minimum of demand and supply. Other parameters that may affect the matching are not considered. To the best of our knowledge, there are only two works in the above-named groups (Hardt and Bogenberger (2021); Soppert et al. (2022)) that explicitly model (expected) rentals to *equal* the minimum of (expected) supply and (expected) demand (always add "(expected)" in the following). All other works formulate constraints that only *limit* rentals to this minimum because they propose optimistic optimization models in the sense that the operator can deny a rental although there is supply and demand (see Soppert et al. (2022) for further discussions).

To summarize the SMS literature regarding matching modeling, one can conclude from the optimization models that it is current practice to (explicitly or implicitly) assume that rentals are determined by the minimum of supply and demand and this simplistic assumption is applied to both SB and FF SMSs. With regard to the three groups in the literature identified above, our contribution is to develop matching functions that allow to apply SB SMS models to FF SMS models (first group) and to improve FF and unspecified SMS models (second and third group).

Even if supply and demand matching has not been considered explicitly, the above works impose requirements on the matching functions that we develop. For one thing, the matching functions need to be compatible with a spatio-temporal discretization and shall be seamlessly integratable into these SMS models. More specifically, the matching functions' in- and output need to be compatible with the overall SMS models from literature. For another, many approaches are formulated as linear optimization problems. Therefore, linear matching functions that retain the linearity of the overall model have an additional value for the generalizability of existing literature.

4.2.3 Matching Functions

Analytical formulations that describe the formation of new relationships, i.e. *matches*, from unmatched agents are denoted as (*aggregate*) *matching functions* and have originally been discussed in macroeconomics, often in the context of stylized (labor) markets. The motivation to

formulate these matching functions is to explain "coordination failures" that e.g. "explain the existence of unemployment" (despite job availability) through "the modeling of *frictions*" which derive e.g. from "information imperfections" or "heterogeneities" (Petrongolo and Pissarides, 2001). In their survey paper on matching functions, Petrongolo and Pissarides (2001) state that for labor markets the simplest matching function m is of the form $M = m(U, V)$, where M is the number of jobs that result during a given time interval in dependence of unemployed workers U and vacant jobs V. Different underlying mechanisms of the matching process, called *microfoundations*, are assumed that lead to different matching functions. For example, the earliest works by Butters (1977) and Hall (1979) formulate matches based on an urn-ball microfoundation, where (in labor market context) workers randomly send applications (balls) to job vacancies (urns). Under the simplest assumption that "U workers know exactly the location of job V vacancies", that workers "send one application each", and that "a vacancy [...] selects an applicant at random", the resulting matching function becomes $M = V \cdot [1 - (1 - 1/V)^U]$ which can be approximated by $M = V \cdot [1 - e^{-U/V}]$ (Petrongolo and Pissarides, 2001).

In the context of transportation, the matching between customers and drivers in taxi systems has been analyzed by Bian (2018), Buchholz (2019), Fréchette, Lizzeri, and Salz (2018) as well as Ata, Barjesteh, and Kumar (2019). The matching functions of the first two are based on the works named above, have the same structural form, and are only slightly modified, e.g. by a "location specific parameter" (Bian, 2018) that allows to calibrate to spatial heterogeneities. A particular matching function that holds "in the absence of frictions" is $M = \min(U, V)$ (Petrongolo and Pissarides, 2001), also denoted as "perfect matching" (Bian, 2018) or "frictionless matching" (Buchholz, 2019), which in the latter is used to describe the search process by taxis for customers at airports.

In contrast, Fréchette, Lizzeri, and Salz (2018) as well as Ata, Barjesteh, and Kumar (2019) use fundamentally different approaches to derive matching functions for taxi systems. Fréchette, Lizzeri, and Salz (2018) picture different areas of a city where each area consists of a grid of locations that represent street corners. A matching function is approximated through a simulation in which customers and drivers appear randomly on these locations. Customers wait for some time before they leave and whenever a driver arrives at a location where a customer is waiting a match realizes. Ata, Barjesteh, and Kumar (2019) propose an analytical approach in which they draw the number of customers and drivers each from a Binomial distribution and then derive the expected number of matches by taking the minimum of both values. To find a tractable approximation, the authors use the Normal distribution and linear approximations to obtain the eventual matching function.

To the best of our knowledge, matching functions for FF SMSs have not yet been discussed in the literature. In our work, we fill this gap by deriving matching functions which are based on FF SMSs specifics (*microfoundations*), such as zone sizes and customers' willingness-to-walk. These parts of our work contribute to the matching functions literature. However, since we focus on FF SMS *optimization* – during development of the functions as well as in a pricing optimization case study – we overall see our contribution with regard to the SMS optimization literature from operations research. E.g. other than in the matching function literature, additional properties for the newly developed functions, like e.g. the integrability into optimization

models, are of particular interest in our work. In Section 4.3, we establish the connection between the developed matching functions and literature and e.g. discuss under which conditions the frictionless matching mentioned above can be applied to FF SMSs.

4.2.4 Further Related Literature Streams

The first related literature stream uses agent-based simulations to derive insights on SMSs. Typical applications are e.g. the evaluation of SMSs within a multi-commodity transportation network (Ciari, Balac, and Axhausen, 2016; Li et al., 2018; Heilig et al., 2018), the impact of specific (parking) pricing rules (Ciari, Balac, and Balmer, 2015; Balac, Ciari, and Axhausen, 2017), or the interplay of competing SMS providers (Balac et al., 2019). Because of the system's description on agent level, including customer behavior and exact vehicle positioning, matching is indeed considered in these simulations. However, an analytical formalization of the matching, in particular on location-period level, as required for the integration into network flow-based optimization problems, is not given. Another application of agent-based simulations is to serve as a heuristic solution approach for network flow optimization problems that we consider in our work (see e.g. Cocca et al. (2019)), but also in this case no analytical formulations of the matching is provided.

The second related literature stream deals with empirical studies on FF SMS. These works provide requirements for and relevant parameters of suitable matching functions. From several studies one can conclude that matching functions have to consider spatio-temporal differences of an SMS. For example, Reiss and Bogenberger (2016) simulate a bike sharing system based on empirical data and identify different demand patterns for weekdays and weekends, as well as for different locations and times of the day. Hardt (2018) also reports different spatio-temporal demand patterns and furthermore identifies differences regarding the resulting rentals, drop-offs, and availabilities within the operating area. Regarding relevant parameters on the customers' decision for the matching functions in FF SMSs, literature especially mentions the distance/walking time to the vehicles as well as the pricing. For example, Wu et al. (2019) investigate the user behavior with a stated-choice experiment considering for example walking time, willingness to pay, and socio-demographical features. Niels and Bogenberger (2017) analyze app openings and booking data from a car sharing system. Among other results, they report a high influence of the distance to available vehicles on the customers' decision.

4.3 Modeling Rentals in FF SMS Optimization Problems

In this section, we propose and discuss two novel analytical matching functions to model rentals in FF SMS optimization problems. Further, we formalize a third one which reflects the matching as it is currently assumed in the SMS optimization literature and which will serve as a benchmark later in the computational study. In Section 4.3.1, we begin by discussing the required output as well as reasonable inputs for the matching functions. Section 4.3.2 presents a generic stylized matching process and a corresponding generic matching function on which all specific matching functions are based. In Section 4.3.3, we systematically derive the different functions, along with their specific underlying assumptions. Section 4.3.4 discusses mathematical properties and Section 4.3.5 the potential of being integrated into linear optimization problems for each of the matching functions.

4.3.1 Output and Inputs

We begin by stating the *output* of the matching functions: As discussed in Sections 4.1 and 4.2.2, SMS optimization models are typically formulated based on network flow formulations, consisting of multiple locations and periods. In these SMS models, vehicle movements, i.e., rentals and relocations, have a certain location-period origin as well as a certain location-period destination. To fit in these network flow SMS models, a compatible matching function's output simply needs to quantify the (expected) number of rentals r that originate in a certain location and period. Conversely, it is not determined by the matching function how the rentals that realize in a specific origin split into different destinations, as this can be covered by other components of the overall SMS network flow model (see Section 4.3.5).

We continue with stating reasonable *inputs* for the matching functions: Clearly, the rentals depend on the number of available vehicles and arriving customers in a given location and period. Therefore, these quantities, which we denote as a and d, are inputs. However, when considering the realization of rentals in an FF SMS, two additionally necessary parameters become immediately apparent, namely the maximum distance that customers are willing to walk and the size of the zone. With a maximum walking distance in the order of several hundred meters (e.g. Herrmann, Schulte, and Voß (2014); Niels and Bogenberger (2017)), and a typical zone size of several square kilometers (e.g. Weikl and Bogenberger (2016); Müller, Correia, and Bogenberger (2017)), it is clear that an available vehicle is not necessarily within reach of a customer, even if the customer and vehicle are in the same zone. In order to formalize the matching functions based on these two additional parameters, we define A_w as the size of the area within walking distance and A_z as the size of the zone. The matching functions therewith become a function of the discussed inputs and parameters, meaning $r = r_{A_w,A_z}(a, d)$.

4.3.2 Preliminaries: Generic Matching

4.3.2.1 Stylized Matching Process

As discussed above, matching functions for network flow-based SMS optimization models require to describe the rentals r on *location-period level*, given a and d. In contrast, the actual matching

process in reality is independent of the artificial spatio-temporal discretization and underlies dynamics that take place *within* the period. In this section, we therefore introduce a stylized matching process that considers the requirements imposed by the discretization in the SMS model as well as the intent to formalize analytical functions that replicate the real matching process as accurately as possible. We take the following assumptions for the stylized matching process on location-period level:

- All vehicles a become available *at the beginning* and customers d arrive sequentially *during* the period. More precisely, the a vehicles are first distributed over the zone. Second, the d customers arrive sequentially and potentially rent one of the vehicles each. Both a and d have zero variance, meaning that these are deterministic values in the matching process. We assume homogeneity of the zone, such that the exact locations of vehicles and customers are drawn from a uniform distribution. To formalize the process and in particular its intermediate states, we denote the *remaining* customers to arrive during a period as $\hat{d}$ and the remaining available vehicles as $\hat{a}$.
- Each of the remaining available vehicles belongs to a corresponding part of the zone, meaning that the vehicle would be within reach for an arriving customer from this part. We say that a vehicle *covers* a part of the zone area and we denote the size of the area that is covered by $\hat{a}$ vehicles all together as $A_{\hat{a}}$. The size of the marginally covered area by the $\hat{a}^{\text{th}}$ vehicle is denoted as $\Delta A_{\hat{a}}$. The matching functions differ in their assumption how the vehicles are spatially distributed and how additional vehicles cover additional parts of the zone.

  Note that it is reasonable to define the marginal coverage of a *vehicle* $\Delta A_{\hat{a}}$ in dependence of the walking area A_w of a *customer*: As stated above, we assume homogeneity of a zone such that the probability of any location within the zone to lie within A_w is equal. Considering a situation with one available vehicle, the probability that this vehicle is located within the reachable area of the customer A_w is equivalent to the probability that the customer arrival location lies within the area A_w which is covered by the vehicle. The latter is in line with the assumption that vehicles are available from the beginning of a period and that customers arrive sequentially.
- For every arriving customer, there is a certain probability that a rental realizes. Clearly, this probability depends on the remaining available vehicles $\hat{a}$ in the zone, the customer's walking area A_w as well as the zone area size A_z. Since $\hat{a}$ and therewith $A_{\hat{a}}$ may change over the matching process, also this matching probability, which we denote by $P_{A_w,A_z}(\hat{a})$, generally differs for each of the customers. We assume that a rental realizes if the customer arrival position lies within the (currently) covered zone area $A_{\hat{a}}$. Considering the uniform distribution for a customer's exact arrival position, the probability of a matching $P_{A_w,A_z}(\hat{a})$ therewith is equal to the proportion of the covered area to the entire zone area, meaning $P_{A_w,A_z}(\hat{a}) = \frac{A_{\hat{a}}}{A_z}$. The matching process ends if all customers have arrived or if all vehicles have been rented.

  Note that drawing exact positions from the uniform distribution corresponds to assuming homogeneity of the zone. We define a zone as the smallest considered spatial unit within

an FF SMS for which data is aggregated or given. This implies that no information on a more disaggregate level is available which would justify separating a (heterogeneous) zone into multiple (homogeneous) ones. Later, in the numerical study, we vary the zone size which corresponds to different given levels of spatial data aggregation and we evaluate the matching functions with regard to their adaptability to these different circumstances.

4.3.2.2 Generic Matching Function

Given the above assumptions, the matching process within a location-period combination can be formalized by the following generic matching function

$$r_{A_w,A_z}(\hat{a},\hat{d}) = P_{A_w,A_z}(\hat{a}) \cdot (1 + r_{A_w,A_z}(\hat{a}-1,\hat{d}-1)) + (1 - P_{A_w,A_z}(\hat{a})) \cdot r_{A_w,A_z}(\hat{a},\hat{d}-1) \quad \forall \hat{a},\hat{d} \in \mathbb{Z} \tag{4.1a}$$

$$r_{A_w,A_z}(\hat{a},0) = 0 \quad \forall \hat{a} \in \mathbb{Z} \tag{4.1b}$$

$$r_{A_w,A_z}(0,\hat{d}) = 0. \quad \forall d \in \mathbb{Z} \tag{4.1c}$$

The inter-dependencies between the possible rental realizations and the changing zone coverages are formulated by a recursion over the customer arrivals (4.1a). For every arriving customer, the probability that a rental realizes is $P_{A_w,A_z}(\hat{a})$. In case of a match, one rental is counted and the number of available vehicles is reduced by one. With probability $\bar{P}_{A_w,A_z}(\hat{a}) = 1 - P_{A_w,A_z}(\hat{a})$, no rental takes place such that the subsequent customer (if existent) has the same number of vehicles available, i.e. $\hat{a}$. Independent of the outcome, the number of customers to come is reduced by one, i.e. $\hat{d} \leftarrow \hat{d} - 1$. The boundary conditions (4.1b) and (4.1c) ensure that the number of rentals is zero if either supply or demand are zero. Note that (4.1) is a discrete function in $\hat{a}$ and $\hat{d}$ but that its output of *expected* rentals in general takes continuous values. In reality, of course, realizations of supply, demand, and rentals are discrete but since matching functions, meaning (4.1) as well as all introduced in the following, are *models* that aim at replicating reality, continuous outputs are reasonable or even desired if interpreted as expected values (see Section 4.3.5).

In the context of an overall network flow SMS model, (4.1) would then be integrated to calculate the resulting rentals for a specific location-period combination with corresponding vehicle count a and arriving customers d, i.e., by evaluating $r_{A_w,A_z}(a,d)$.

4.3.3 Derivation of Matching Functions

Based on the previously described generic matching process, we derive three matching functions in this section. The decisive difference between the functions is the rate with which an additional vehicle covers the area of the zone. Consequently, we denote the three functions as

- *degressive coverage rate* matching function (DCR) (Section 4.3.3.1),
- *constant coverage rate* matching function (CCR) (Section 4.3.3.2), and
- *infinite coverage rate* matching function (ICR) (Section 4.3.3.3).

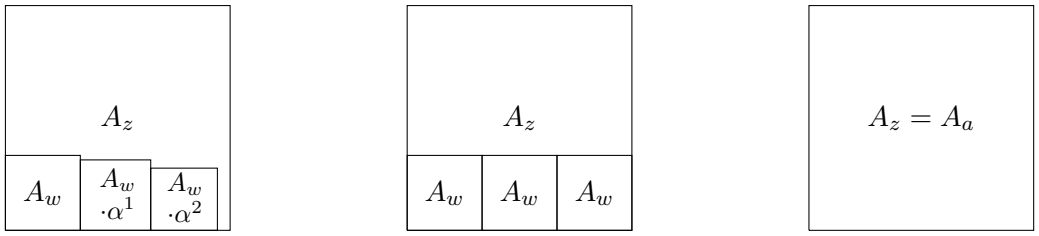

(a) DCR, $\alpha = (1 - \frac{A_w}{A_z})$, $A_{a=3} = A_w \cdot (1 + \alpha + \alpha^2)$

(b) CCR, $\lambda = \mu = 1$, $A_{a=3} = 3 \cdot A_w$

(c) ICR, $A_{a \geq 1} = A_z$

Figure 4.1: Illustrative representation of coverage by matching functions

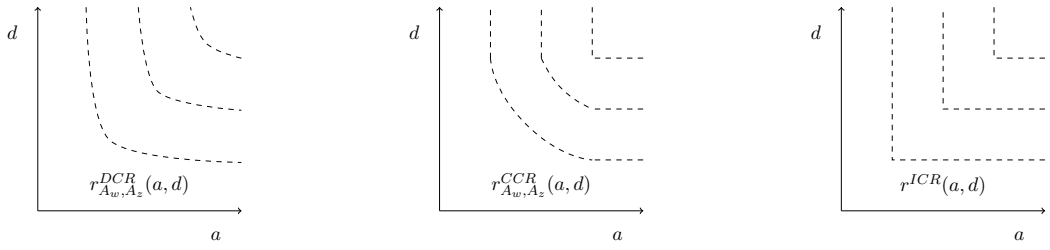

(a) DCR

(b) CCR

(c) ICR

Figure 4.2: Schematic iso-rental curves for different matching functions and a specific A_w, A_z with $A_w < A_z$

The assumptions of the DCR come closest to the real matching process, but also the other two functions, especially the CCR, have a range of validity, and other advantages compared to the DCR.

4.3.3.1 The Degressive Coverage Rate matching function (DCR)

The DCR results from the generic matching function (4.1) by further specifying the matching probability $P_{A_w,A_z}(\hat{a})$. The underlying assumption of the DCR is that each part of the zone is equally likely to belong to the area covered by a vehicle. Thus, the area covered by an additional vehicle comprises a part that is newly covered (marginally covered area) and a part that is already covered by the other vehicles (and wasted in this sense). More formally, the DCR assumes that, for a given available vehicle count $\hat{a}$, the additionally covered area $\Delta A_{\hat{a}+1}$ by one additional vehicle, meaning by the $(\hat{a}+1)^{st}$ vehicle, is a fraction of A_w. This fraction is the ratio of the not covered zone area with $\hat{a}$ vehicles $\bar{A}_{\hat{a}} = A_z - A_{\hat{a}}$ to the entire zone area, meaning $\Delta A_{\hat{a}+1} = A_w \cdot \frac{\bar{A}_{\hat{a}}}{A_z}$.

Proposition 1. *Assuming $\Delta A_{\hat{a}+1} = A_w \cdot \frac{\bar{A}_a}{A_z}$, the matching probability is $P_{A_w,A_z}(\hat{a}) = (1 - (1 - \frac{A_w}{A_z})^{\hat{a}})$ and the DCR is defined by*

$$\textbf{DCR:} \quad r^{DCR}_{A_w,A_z}(\hat{a},\hat{d}) = (1 - (1 - \frac{A_w}{A_z})^{\hat{a}}) \cdot (1 + r^{DCR}_{A_w,A_z}(\hat{a}-1,\hat{d}-1)) + (1 - \frac{A_w}{A_z})^{\hat{a}} \cdot r^{DCR}_{A_w,A_z}(\hat{a},\hat{d}-1) \qquad \forall \hat{a},\hat{d} \in \mathbb{Z} \qquad (4.2a)$$

$$r^{DCR}_{A_w,A_z}(\hat{a},0) = 0 \qquad \forall \hat{a} \in \mathbb{Z} \qquad (4.2b)$$

$$r^{DCR}_{A_w,A_z}(0,\hat{d}) = 0. \qquad \forall \hat{d} \in \mathbb{Z} \qquad (4.2c)$$

We prove Proposition 1 in Appendix 4.B. Figure 4.1a illustrates the marginal coverage of the DCR for $a = 3$ vehicles. The $\hat{a}^{th}$ vehicle additionally covers $A_w \cdot (1 - \frac{A_w}{A_z})^{\hat{a}-1}$. In Figure 4.2a,

the DCR iso-rental curves are schematically depicted, indicating which a, d combinations lead to the same number of rentals. For every a, d combination, an increase of one of the quantities always results in a higher-level curve, but the increase depends on the ratio of a and d. If a is larger than d, an increase of a causes a smaller increase of rentals r than if a and d are identical or if d is even larger than a, and vice versa..

Remark. Note that for formal reasons $A_w \leq A_z$ is required such that the matching probability does not exceed one. Naturally, $A_w \geq 0$ also holds. For $A_w > A_z$ the entire zone is always covered by the remaining available vehicles such that every arriving customer results in a rental as long as at least one vehicle is available. In this case, the matching process is rather trivial and, as we discuss later, it is covered by the ICR, the state-of-the-art matching function. This also holds for the following sections, in particular for the CCR which is discussed next.

4.3.3.2 The Constant Coverage Rate matching function (CCR)

The CCR is derived from the generic matching function (4.1) in two steps. The first step concerns the assumption regarding the marginal coverage by an additional vehicle and, as the name suggests, the CCR assumes a constant marginal coverage. More precisely, the marginal coverage for the $(\hat{a}+1)^{st}$ vehicle is $\Delta A_{\hat{a}+1} = \min(A_z - A_{\hat{a}}, A_w \cdot \lambda)$ with $\lambda \in [0,1]$, meaning that each additional vehicle additionally covers the same fraction of the walking area $A_w \cdot \lambda$ until the residual of the zone's covered area is smaller than this $A_w \cdot \lambda$, such that the next vehicle covers this residual. The factor λ allows to formulate a constant marginal coverage which implicitly considers the potential overlap of the area covered by the individual vehicles (as for the DCR). In Appendix 4.C, we show that for an expected number of available vehicles $\bar{a}$, for example determined by historic data, λ can be analytically approximated by

$$\lambda \approx \frac{1-(1-\frac{A_w}{A_z})^{\bar{a}}}{\frac{A_w}{A_z}} \cdot \frac{1}{\bar{a}}. \tag{4.3}$$

With this assumption for $\Delta A_{\hat{a}+1}$, the covered area by $\hat{a}$ vehicles becomes $A_{\hat{a}} = \min(A_z, A_w \cdot \lambda \cdot \hat{a})$, and $P_{A_w,A_z}(\hat{a}) = \frac{\min(A_z, A_w \cdot \lambda \cdot \hat{a})}{A_z}$ in (4.1a).

In the second step to derive the CCR, the additional assumption is taken that all customers have identical matching probabilities, such that the former recursive formulation simplifies to

$$r_{A_w,A_z}(a,d) = \min(\frac{\min(A_z, A_w \cdot \lambda \cdot \mu \cdot a)}{A_z} \cdot d, a, d), \qquad \forall a, d \in \mathbb{Z} \tag{4.4}$$

with $\mu \in [0,1]$. The fraction in the first argument of the (outer) min()-operator in (4.4) represents the average matching probability for every of the d arriving customers. μ allows to formulate the average covered area $A_w \cdot \lambda \cdot \mu \cdot a$, which is a fraction of $A_w \cdot \lambda \cdot a$. In the recursive formulations, the boundary conditions ensured that rentals can not exceed a or d. In the explicit (4.4), this is ensured by the second and third argument of the min()-operator. (4.4) can be simplified to the final CCR

$$\textbf{CCR:} \qquad r^{CCR}_{A_w,A_z}(a,d) = \min(\frac{A_w}{A_z} \cdot \lambda \cdot \mu \cdot a \cdot d, a, d). \qquad \forall a, d \in \mathbb{Z} \tag{4.5}$$

Clearly, μ has to depend on the amount of customers arriving. We show in Appendix 4.C, that

for an expected amount of customers $\bar{d}$, the parameter μ can be analytically approximated by

$$\mu \approx \frac{1}{\bar{d}} \cdot \sum_{i=1}^{\bar{d}} (1 - \frac{A_w \cdot \lambda}{A_z})^{i-1}. \tag{4.6}$$

Figure 4.1b illustrates the marginal coverage of the CCR for $\lambda = \mu = 1$ and $a = 3$ vehicles. Every vehicle additionally covers $A_w \cdot \lambda \cdot \mu$. In Figure 4.2b, the iso-rental curves of the CCR are schematically depicted. In contrast to the DCR, for large values of a and/or d, an increase of these quantities does not result in an increase of the rentals r.

4.3.3.3 The Infinite Coverage Rate matching function (ICR)

As the name suggests, the ICR assumes an infinite coverage by every additional vehicle (no friction). More precisely, the marginal coverage for the $(\hat{a}+1)^{st}$ vehicle is $\Delta A_{\hat{a}+1} = \min(A_z - A_{\hat{a}}, A_z)$, meaning that the entire zone is covered as long as there is at least one vehicle available. With this assumption, $P_{A_w,A_z}(\hat{a}) = 1$ for every arriving customer as long as there is at least one vehicle available. Then, the ICR in dependence of a and d can be formalized by

$$\textbf{ICR:} \qquad r^{ICR}_{A_w,A_z}(a,d) = r^{ICR}(a,d) = \min(a,d). \qquad \forall a,d \in \mathbb{Z} \tag{4.7}$$

Figure 4.1c illustrates the coverage of the zone according to the ICR for $a \geq 1$ vehicles, showing that the entire zone is covered. In Figure 4.2c, the iso-rental curves of the ICR are schematically depicted. If a is greater or equal to d, an increase of a does not result in an increase of the rentals r, and vice versa. The iso-rental curves demonstrate that the ICR follows the characteristics of a Leontief production (Fandel, 1991, Chapter 4).

Regarding the relation between the matching functions, one can state the following: When the first argument in the min()-operator in (4.5) is not restrictive, the CCR (4.5) and the ICR (4.7) become identical. This first argument is not restrictive if $\lambda \cdot \mu \cdot \frac{A_w}{A_z} \cdot a \geq 1$ or $\lambda \cdot \mu \cdot \frac{A_w}{A_z} \cdot d \geq 1$. Further, the ICR is a special case of the DCR: When $A_w = A_z$, $P_{A_w,A_z}(\hat{a}) = 1$ for every customer in the DCR (4.2) such that rentals realize until all vehicles are taken, or all customers have arrived – exactly as in the ICR (4.7). In the schematic depiction of iso-rental curves of the DCR in Figure 4.2a, the curves take the form of the ICR in Figure 4.2c if $P_a = 1$ for every customer. As stated in Section 4.3.3.1, the DCR is not defined for $A_w > A_z$. Similarly, the derivation of λ and μ for the CCR in Section 4.3.3.2 assumes $A_w \leq A_z$. However, more general formulations of these two matching functions that would also capture the case of $A_w > A_z$ would return rentals as for $A_w = A_z$, i.e. like the ICR, because $A_w = A_z$ already captures the case where the entire zone is covered by the available vehicles.

Remark. As discussed in Sections 4.1 and 4.2.2, it is current practice in the SMS optimization literature to determine rentals for a specific location-period combination by the minimum of the available vehicles and arriving customers (also known as "perfect/frictionless matching", see Section 4.2.3). Literature applies this (implicit) assumption to model both SB as well as FF SMSs. The ICR (4.7) is the formalization of this assumption such that the ICR could be considered as the state-of-the-art matching function, even if not discussed as such in the SMS literature. Clearly, since the ICR does not consider A_w and A_z, the ICR in general overestimates the actual matching when applied to model an FF SMS for which $A_w < A_z$. In the numerical

studies in Section 4.4, we use the ICR as a benchmark to evaluate the DCR and CCR.

Note that in an SB SMS, where available vehicles and arriving customers refer to a specific station, the issue of overestimating rentals due to the neglection of spatial parameters A_w and A_z described above does not occur. Note further that the link between SB and FF SMSs in the context of matching modeling can be established by considering an extreme case of the zone area size: A station of an SB SMS can be considered as a zone in an FF SMS of infinitely small size – a point zone. In this point zone, the expected rentals can be correctly described by the ICR (4.7).

4.3.4 Properties

In this section, we discuss mathematical properties of the three matching functions $r^M_{A_w,A_z}(a,d)$ with $M \in \{DCR, CCR, ICR\}$. This analysis is common in the matching function literature, as it allows to assess the plausibility of the derived functions by verifying desirable properties and to analytically derive limitations of the functions' applicability. Properties 1 and 2 can be considered as standard boundary conditions for matching functions. Properties 3 and 4 are related to the special case of "perfect/ frictionless" matching (see Section 4.2.3) in FF SMSs. Properties 5 and 6 are specific for matching functions in FF SMSs, while especially the latter also impacts the formulation of overall optimization models for FF SMSs – a particularly relevant aspect in our work (see also Section 4.3.5).

Property 1 – Zero rentals boundary conditions. *If either demand or supply are zero, no rentals realize. Formally, we have* $r^M_{A_w,A_z}(a,d) = 0$ *if* $a = 0$ *or* $d = 0$.

This property verifies an intuitive boundary condition: The absence of available vehicles or customers. Clearly, the DCR, the CCR, and the ICR fulfill this property.

Property 2 – Supply and demand limits. *If the number of available vehicles becomes infinitely large, the realized rentals equal demand, and vice versa. Formally, we have* $r^M_{A_w,A_z}(a,d) = d$ *for* $a \to \infty$ *and* $r^M_{A_w,A_z}(a,d) = a$ *for* $d \to \infty$*, respectively.*

This property verifies an intuitive boundary condition in the abundance of available vehicles or customers. Clearly, the CCR and the ICR fulfill this property. For the DCR, consider that if $a \to \infty$, also $\hat{a} \to \infty$ and that the probability of a matching $P_{A_w,A_z}(\hat{a}) = (1 - (1 - \frac{A_w}{A_z})^{\hat{a}}) \to 1$ in (4.2a), for realistic parameters where $A_w \leq A_z$. If this is true for every arriving customer d, $r^M = d$. For $d \to \infty$, the recursion in (4.2a) is executed until all vehicles a are taken because we have $P_{A_w,A_z}(\hat{a}) > 0 \, \forall \hat{a} > 0$.

Property 3 – Matching with certainty for entire zone coverage. *If the vehicles cover the entire zone area, the next arriving customer certainly finds a vehicle and a rental results. Formally, we have* $\frac{\partial}{\partial d} r^M_{A_w,A_z}(a,d) = 1$ *if* $A_a = A_z$.

This intuitive property covers constellations in which matching in an FF SMS works as matching in SB SMS. For the DCR, $A_a = A_z$ requires the special case that $A_z = A_w$, and in this case, $P_{A_w,A_z}(a) = 1$ for every arriving customer, as long as there is at least one vehicle available. For the CCR, $A_a = A_z$ means that $A_w \cdot \lambda \cdot \mu \cdot a = A_z$ such that the first argument of the

min()-operator is not restrictive and an additional demand results in an additional rental. The ICR fulfills this property by definition.

Property 4 – No matching for zero zone coverage. *If the vehicles cover an infinitely small zone area or the zone area grows to infinity, there is no matching. More precisely, every additional customer results in zero additional rentals. Formally, we have* $\frac{\partial}{\partial d} r^{M}_{A_w,A_z}(a,d) = 0$ *for* $A_a \to 0$ *or* $A_z \to \infty$.

This property is the opposite of the aforementioned one. Compared to the walking distance, distances are so long that there are no rentals.

For the DCR, both of the extreme cases result in $P_{A_w,A_z}(a) \to 0$ such that an additional customer does not increase the expected rentals. For the CCR, the first argument of the min()-operator becomes zero such this property is fulfilled. The ICR does not fulfill this property and in contrast predicts an additional rental for every customer, given an available vehicle, no matter what sizes A_w and A_z take.

Property 5 – Supply and demand symmetry. *The matching function is symmetric regarding supply and demand. Formally, we have* $r^{M}_{A_w,A_z}(a,d) = r^{M}_{A_w,A_z}(d,a)$.

Obviously, the CCR and the ICR both fulfill this property. We prove symmetry of the DCR in Appendix 4.D.

It follows from the proof, that the DCR can be formulated by interchanging $\hat{a}$ and $\hat{d}$ in (4.2) which yields

$$\begin{aligned} r^{DCR}_{A_w,A_z}(\hat{d},\hat{a}) &= (1-(1-\frac{A_w}{A_z})^{\hat{d}}) \cdot (1 + r_{A_w,A_z}(\hat{d}-1,\hat{a}-1)) \\ &\quad + (1-\frac{A_w}{A_z})^{\hat{d}} \cdot r^{DCR}_{A_w,A_z}(\hat{d},\hat{a}-1) && \forall \hat{a},\hat{d} \in \mathbb{Z} && \text{(4.8a)} \\ r^{DCR}_{A_w,A_z}(\hat{d},0) &= 0 && \forall \hat{d} \in \mathbb{Z} && \text{(4.8b)} \\ r^{DCR}_{A_w,A_z}(0,\hat{a}) &= 0. && \forall \hat{a} \in \mathbb{Z} && \text{(4.8c)} \end{aligned}$$

The intuition of this alternative DCR formulation (4.8) is exactly inverse to the one described in Section 4.3.2.1: A customer covers a certain fraction of the zone and every part of the zone is equally likely to belong to the marginally covered area by an additional customer. The positions where the available vehicles are located are sequentially drawn at random from a uniform distribution. For each drawn vehicle, the probability that it is rented is determined by the respective proportion of the covered zone at the time it is drawn. As for the DCR formulation (4.2), the process ends if either the rentals realized equal the initial customer count, or if all vehicle appearances were drawn.

Property 6 – Independence to zone partitioning. *For the ICR, the expected number of rentals does not change if a homogeneous zone is artificially sub-divided into multiple sub-zones. Formally, if a zone of zone area size* $\hat{A}_z$ *is partitioned into* Z *sub-zones,* $r^{ICR}_{A_w,\hat{A}_z}(a,d) = Z \cdot r^{ICR}_{A_w,\hat{A}_z/Z}(\frac{a}{Z},\frac{d}{Z})$ *holds*

Property 6 states that artificially partitioning a zone into multiple sub-zones does not change the overall expected number of rentals for the ICR. Consider that the collected data on the

zone level is given by a, d, and $\hat{A}_z$. A_w is also given. When data is collected on this zone level, the only reasonable assumption is that this zone is homogeneous, such that a and d would be divided proportionally to obtain the respective quantities for the Z smaller sub-zones, i.e. $\frac{a}{Z}$ and $\frac{d}{Z}$. Consequently, the resulting rentals for the ICR in each sub-zone are the rentals of the original zone divided by Z. Since there are Z of these sub-zones, overall, the amount of rentals remains the same.

This property is the reason for the fact that the issue of inaccurate matching modeling cannot be simply solved by partitioning a zone artificially into multiple smaller sub-zones of the 'right' size for the ICR (see the corresponding statement in Section 4.1). This property is illustrated with a numerical example in Appendix 4.I. Note that an analogous property holds for the DCR and CCR, which considers the probabilities of all combinations of possible discrete distributions of a and d over the sub-zones and then applies the matching functions on these sub-zones.

4.3.5 Integration in Linear Optimization Problems

As described in Sections 4.1 and 4.2.2, a lot of work has been done in the literature to cover the various SMS optimization problems based on network flow modeling. Mostly, the resulting formulations are mixed-integer linear programs (MILP). As explained, our work particularly focuses on the optimization models of FF SMSs and in this section, we therefore discuss whether the introduced matching functions can be linearized *losslessly*, such that an exact integration in a typical MILP is possible.

The decisive characteristic of spatio-temporal network flow formulations, illustrated in Figure 4.14 in Appendix 4.A, is a set of constraints that describe the flow conservation in the network. With discrete locations $i, j, k \in \mathcal{Z}$, and periods $t \in \mathcal{T}$, the flow conservation constraints can be formulated as

$$\sum_{i \in \mathcal{Z}} r_{ijt} + s_{jt} = \sum_{k \in \mathcal{Z}} r_{jk(t+1)} + s_{j(t+1)} \qquad \forall j \in \mathcal{Z}, t \in \mathcal{T}, \tag{4.9}$$

where r_{ijt} describe the rentals from location i to j in period t, and s_{jt} describe the vehicles that remain unused at location j in period t. Now, the number of rentals originating at a location i, given by $r_{it} = \sum_{j \in \mathcal{Z}} r_{ijt}$, are assumend to realize according to a specific matching function, depending on the number of available vehicles a_{it} and the arriving customers $d_{it} = \sum_{j \in \mathcal{Z}} d_{ijt}$. Therefore, the logic of the matching functions to determine r_{it} has to be formulated by means of additional constraints within the MILP formulation. Note that additional constraints are required to derive the i-j-t-specific rentals r_{ijt} from the r_{it}-values, but this is out of scope of the matching itself.

Note further that, in contrast to d_{it}, the quantities r_{it} and a_{it} are decision variables in the MILP. In certainty equivalent formulations (based on expected values), these decision variables are continuous, meaning $a_{it}, r_{it} \in \mathbb{R}_0^+ \; \forall i \in \mathcal{Z}, t \in \mathcal{T}$. In the following, we therefore discuss for each of the initial matching functions from Section 4.3.3, whether the range of values $\mathbb{Z}$ for a_{it} and d_{it} can be replaced by $\mathbb{R}_0^+$, how the functions are formulated for a specific i-t-combination, and whether a lossless integration in a MILP formulation is possible.

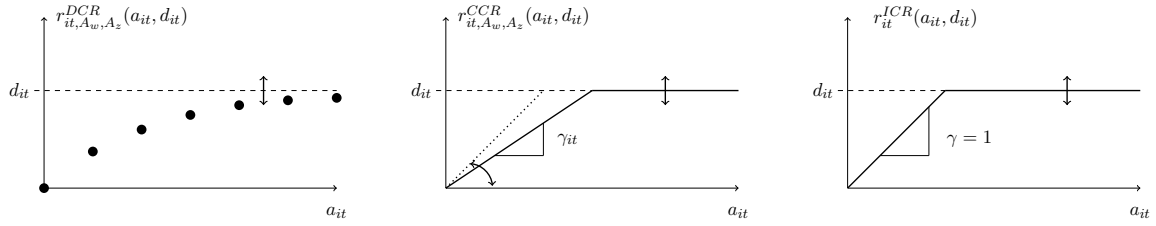

(a) DCR (4.10) (b) CCR (4.13) (c) ICR (4.14)

Figure 4.3: Schematic representation of matching functions

4.3.5.1 DCR

For a specific *i-t* combination, the DCR (4.2) becomes

$$r^{DCR}_{it,A_w,A_z}(\hat{a}_{it},\hat{d}_{it}) = (1-(1-\frac{A_w}{A_z})^{\hat{a}_{it}}) \cdot (1 + r^{DCR}_{it,A_w,A_z}(\hat{a}_{it}-1,\hat{d}_{it}-1)) + (1-\frac{A_w}{A_z})^{\hat{a}_{it}} \cdot r^{DCR}_{it,A_w,A_z}(\hat{a}_{it},\hat{d}_{it}-1) \qquad \forall \hat{a}_{it},\hat{d}_{it} \in \mathbb{Z} \qquad (4.10a)$$

$$r^{DCR}_{it,A_w,A_z}(\hat{a}_{it},0) = 0 \qquad \forall \hat{a}_{it} \in \mathbb{Z} \qquad (4.10b)$$

$$r^{DCR}_{it,A_w,A_z}(0,\hat{d}_{it}) = 0. \qquad \forall \hat{d}_{it} \in \mathbb{Z} \qquad (4.10c)$$

Due to the recursive formulation of the DCR (4.10) which is only defined for *discrete* values $\hat{a}_{it},\hat{d}_{it} \in \mathbb{Z}$, the range of values for $\hat{a}_{it}$ and $\hat{d}_{it}$, and therewith also for $r^{DCR}_{it,A_w,A_z}(\hat{a}_{it},\hat{d}_{it})$, cannot be replaced by the *continuous* range $\mathbb{R}^+_0$. Figure 4.3a depicts (4.10) schematically (for $A_w < A_z$). For a given demand level d_{it}, it illustrates how the realized rentals $r^{DCR}_{it,A_w,A_z}(a_{it},d_{it})$ depend on the number of initially available vehicles a_{it}. Every additional vehicle increases the expected rentals with decreasing margin such that the demand is the limit of the function.

Clearly, since for a given a_{it},d_{it}, (4.10) is a discrete function in $a_{it} \in \mathbb{Z}\ \forall i \in \mathcal{Z}, t \in \mathcal{T}$, the DCR can not be losslessly linearized and integrated in a MILP formulation. Note, however, that the DCR may find application in (non-linear) optimization approaches with discrete $a_{it} \in \mathbb{Z}$, such as for example in an approach based on a Markov decision process (MDP).

As for any function, an approximate linearization is possible in principle also for the DCR. However, the question is how accurate such a linearization is and, in the context of a MILP, how this impacts the number of decision variables and constraints. A reasonable way to linearize the DCR would be to define a piece-wise linear function with supporting points for every $a_{it} \in \mathcal{Z}$, for which the exact r_{it} is known. This would correspond to a function that connects the dots in Figure 4.3a. While this is possible in theory, it would require a large number of additional auxiliary variables in a MILP in order to determine which piece of this function is active. Thus, we do not see this as a promising path.

4.3.5.2 CCR

In the CCR (4.5), the range of values for a,d, and $r^{CCR}_{A_w,A_z}(a,d)$ can be replaced by $\mathbb{R}^+_0$. For a specific *i-t* combination, the CCR becomes

$$r^{CCR}_{it,A_w,A_z}(a_{it},d_{it}) = \min(\lambda \cdot \mu \cdot \frac{A_w}{A_z} \cdot d_{it} \cdot a_{it}, a_{it}, d_{it}). \qquad \forall a_{it},d_{it} \in \mathbb{R}^+_0 \qquad (4.11)$$

Since λ, μ, A_w, A_z and d_{it} are parameters, one can pre-compute whether the first or the second argument of the min()-operator is smaller. We define this i-t-specific pre-computed parameter as

$$\gamma_{it} = \min(\lambda \cdot \mu \cdot \frac{A_w}{A_z} \cdot d_{it}, 1) \tag{4.12}$$

and therewith obtain

$$r^{CCR}_{it,A_w,A_z}(a_{it}, d_{it}) = \min(\gamma_{it} \cdot a_{it}, d_{it}), \qquad \forall a_{it}, d_{it} \in \mathbb{R}^+_0 \tag{4.13}$$

which is schematically depicted in Figure 4.3b. It illustrates that for the CCR (4.13), the number of expected rentals $r^{CCR}_{it,A_w,A_z}(a_{it}, d_{it})$ is a piece-wise linear function of a_{it} with two pieces, where d_{it} determines the height of the horizontal second piece. As long as $a_{it} \leq \frac{d_{it}}{\gamma_{it}}$, an increase of a_{it} results in the same marginal increase of rentals. This marginal increase is determined by the slope parameter γ_{it}, determined with (4.12) or tuned (based on simulations or the DCR) to obtain an overall good fit for a certain range of expected a_{it}, d_{it}. For $a_{it} > \frac{d_{it}}{\gamma_{it}}$, an increase of a_{it} does not increase $r^{CCR}_{it,A_w,A_z}(a_{it}, d_{it})$.

The CCR (4.13) can be losslessly linearized and integrated in a MILP formulation with a set of auxiliary variables and corresponding constraints. Depending on the actual a_{it}, these constraints determine which part of the piece-wise linear function needs to be active. The model (4.44)-(4.58) in Appendix 4.F that we apply in the case study in Section 4.5 is an example of a CCR integrated into a MILP for a differentiated pricing optimization problem.

4.3.5.3 ICR

In the ICR (4.7), the range of values for a, d, and $r^{ICR}(a, d)$ can be replaced by $\mathbb{R}^+_0$. For a specific i-t combination, the ICR (4.7) becomes

$$r^{ICR}_{it}(a_{it}, d_{it}) = \min(a_{it}, d_{it}), \qquad \forall a_{it}, d_{it} \in \mathbb{R}^+_0 \tag{4.14}$$

which is schematically depicted in Figure 4.3c. Like for the CCR, the number of expected rentals $r^{ICR}_{it}(a_{it}, d_{it})$ in the ICR is a piece-wise linear function of the initially available vehicles count a_{it} with two pieces where d_{it} determines the height of the horizontal second piece. In contrast to the CCR, the slope of the first piece is $\gamma_{it} = 1$ such that every additional a_{it} results in a rental, as long as $a_{it} \leq d_{it}$.

Analogously to the CCR, a set of auxiliary variables and corresponding constraints enables a lossless integration of (4.14) in a MILP. Examples for the integration of the ICR in SMS optimization problems are Hardt and Bogenberger (2021) for relocation and Soppert et al. (2022) for pricing.

4.4 Computational Study

In this section, we evaluate the rental prediction accuracy of the three matching functions DCR, CCR, and ICR introduced in Section 4.3.3. We consider two general settings, i.e. the *single zone single period* setting and the *multiple zones multiple periods* setting, discussed in Section 4.4.1 and 4.4.2, respectively. The subsections for each setting are organized as follows. We begin with an introduction of the setting (4.4.1.1 resp. 4.4.2.1), followed by the description of a simulation which serves as a benchmark (4.4.1.2 resp. 4.4.2.2), the parameter configurations (4.4.1.3 resp. 4.4.2.3), and the evaluation metrics (4.4.1.4 resp. 4.4.2.4). The last subsections discuss the results (4.4.1.5 resp. 4.4.2.5).

4.4.1 Single Zone Single Period Setting

4.4.1.1 Setting

The *single zone single period* (SZSP) setting is a stylized setting where the FF SMS, as the name suggests, consists of one single zone and one single period. The purpose of this setting is to isolate the assessment of the rental prediction accuracy, and to eliminate potential effects that would result from replicating a real FF SMS consisting of more than one zone and multiple periods. For each considered *parameter configuration*, characterized by a given number of available vehicles a at the beginning of the period, a given number of customers to arrive d, and a specific choice of walking area A_w and zone area A_z size, $r^M_{A_w,A_z}(a,d)$ is evaluated for the different matching functions $M \in \{DCR, CCR, ICR\}$. The outputs are compared to a benchmark from a stochastic dynamic simulation, described next.

4.4.1.2 Simulation Benchmark

The simulation of the SZSP-setting is consistent with the generic matching process described in Section 4.3.2, i.e. vehicles are available at the beginning of the considered period, while customers arrive sequentially during the period. For each considered parameter configuration, we derive the benchmark by performing multiple simulation runs $n \in \mathcal{N} = \{1, 2, \ldots, N\}$ that each yield a rental observation r_n.

At the beginning of each simulation run n, a given number of available vehicles a is distributed within a squared zone of size A_z. In line with the assumptions from Section 4.3.2.1, a zone is homogeneous and consequently, the location of each vehicle is drawn from a uniform distribution. A given number of customers then arrive sequentially and their respective point of appearance is drawn from a uniform distribution as well. The customers have a maximum walking distance (corresponding to A_w) and the assumption is that if there is at least one vehicle within reach, the closest one is rented. This vehicle is then removed and the rental is recorded. Independent of the actual rental outcome, the number of customers to come is reduced by one and the process is repeated until all d customers have arrived. The simulation process for one simulation run is summarized as pseudo code in Algorithm 6 in Appendix 4.E.

To clarify the setup, consider Figure 4.4 that depicts a single simulation run of the SZSP-setting with $A_z = 1$ km^2 in retrospective. The $a = 10$ initially available vehicles are represented

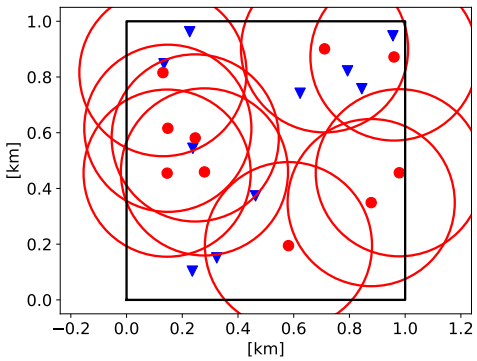

Figure 4.4: Run of SZSP-scenario with $A_z = 1$ km^2 in retrospective ($a = 10$, $d = 10$)

as blue triangles, and the $d = 10$ customers, that arrived sequentially during the run, are represented by red dots with their respective walking area, depicted as red circles. One of the vehicles, the one in the lower left corner of the zone, was out of reach for all customers. Consequently, this vehicle has not been rented in this simulation run. Note, however, that even though all other vehicles lay within at least one of the red circles, they were not necessarily rented, because the respective customer might have taken a different vehicle. Since Figure 4.4 does not show the temporal sequence of the run, some of the vehicles depicted have not been available for the customers that arrived rather late. In fact, only $r_n = 6$ rentals realized in this particular run.

Note that Figure 4.4 shows that parts of the walking area may lay outside of the zone. The actual area of the zone which is within reach of a customer therewith is smaller than the walking area. For the benchmark simulation, we exclude this effect by the following mechanism: Whenever a part of the walking area protrudes beyond the zone boundary, this part is displaced to the other side of the zone. The effect is that the entire walking area actually lies within the zone. Thus, our zone has a limited size, but effectively no border, like the surface of a sphere.

4.4.1.3 Parameter Configurations and Scenarios

We consider the following parameter settings, with every potential combination of values defining a valid parameter configuration:

- Available vehicles ($\mathcal{V}_{SZSP}$): a is selected from the discrete set $\mathcal{V}_{SZSP} = \{0, 1, \ldots, 10\}$.
- Arriving customers ($\mathcal{D}_{SZSP}$): d is selected from the discrete set $\mathcal{D}_{SZSP} = \{0, 1, \ldots, 10\}$.
- Walking area size (A_w): A_w is kept constant at $A_w = \pi \cdot (0.3\text{km})^2 = 0.28$ km^2. The radius of 0.3km represents a realistic maximum walking distance (Herrmann, Schulte, and Voß, 2014).
- Zone area size ($\mathcal{A}_z$): A_z is selected from the discrete set $\mathcal{A}_z = \{0.5 \text{ km}^2, 1 \text{ km}^2, 2 \text{ km}^2, 4 \text{ km}^2\}$, representing the typical range of zone size values from literature (e.g. Weikl and Bogenberger (2016); Müller, Correia, and Bogenberger (2017)) and practice.

We use the term SZSP-*scenario* to refer to parameter settings having the same value of A_z, i.e., we group all resulting parameter configurations for a specific A_z to belong to one scenario. Note that in this stylized setting there is no supply or demand uncertainty, meaning that a and d

have no variance within a scenario but are deterministic values. We perform $N = 100$ simulation runs for every parameter setting.

4.4.1.4 Evaluation Metrics

We use the following metrics to assess the rentals prediction accuracy:

- Rentals (RT): The expected absolute rentals RT predicted by the matching functions are simply $\bar{r} = r^M_{A_w,A_z}(a,d)$ with $M \in \{DCR, CCR, ICR\}$. With regard to the simulation benchmark, the corresponding value is obtained from averaging over the simulations runs, i.e., $\bar{r}_N = \frac{1}{N}\sum_{n\in\mathcal{N}} r_n$.
- Rentals' mean error (RT^{ME}): The mean absolute error RT^{ME} between the expected rentals $\bar{r}$ predicted by a matching function and the N observations of the simulation benchmark r_n is $RT^{ME} = \bar{r} - \bar{r}_N$.
- Rentals' mean relative error (RT^{MRE}) [%]: The mean relative error RT^{MRE} between the expected rentals $\bar{r}$ predicted by a matching function and the N observations of the simulation benchmark r_n is $RT^{MRE} = (\bar{r} - \bar{r}_N)/\bar{r}_N \cdot 100$.

4.4.1.5 Results

We begin by investigating the predicted and observed absolute rentals RT on an aggregate level. Therefore, we consider Figure 4.5 which provides a first impression of how the different matching functions predict rentals and how the rentals observed in the simulation benchmark depend on supply, on demand, as well as on the zone area size. In each of the subfigures, the vertical axis of the surface plot represents expected and observed rentals RT for the matching functions and the simulation benchmark, respectively. The horizontal axes represent $a \in \mathcal{V}_{SZSP}$ and $d \in \mathcal{V}_{SZPZ}$, respectively. The two rows depict the results of the SZSP-scenarios $A_z = 1$ km^2 and $A_z = 2$ km^2. The respective graphs for all scenarios, i.e. for all $A_z \in \mathcal{A}_z$, are depicted in Figure 4.16 in Appendix 4.G. The columns depict the mean of the simulation benchmark (SIM), and the expected rentals predicted by DCR, CCR, and ICR. From considering Figure 4.5, the following observations can be made, which partly relate to the properties discussed in Section 4.3.4.:

- For all matching functions, the surfaces are bounded to $RT = 0$ for all a-d combinations where $a = 0$ or $d = 0$ (see Property 1). All graphs increase monotonically in a and in d, which is reasonable, since additional vehicles/ additional customers can never, ceteris paribus, decrease but may increase the (expected) rentals.
- While the surfaces of the DCR resemble the SIM benchmarks in their general shape of being strictly concave in a and d, especially the ICR but also the CCR differ as they both run into saturation if one of the inputs is fixed and the other increased (see Property 2). The ICR has the characteristic shape of a Leontief production, consisting of two planes that intersect on the diagonal between a- and d-axis. The CCR takes this shape for large values of a and d. On this a-d-diagonal, the surface of SIM and DCR is strictly concave. The ICR grows linearly on this diagonal and for the CCR, the first part of the diagonal

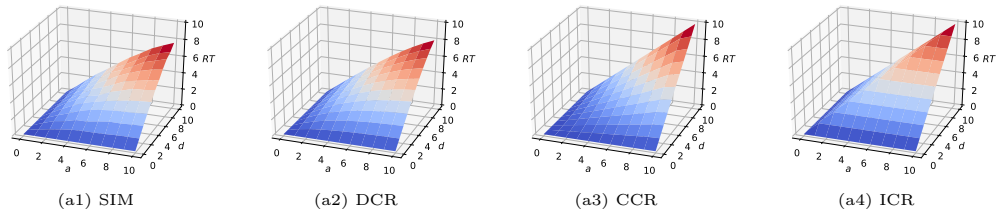

(a1) SIM (a2) DCR (a3) CCR (a4) ICR

(a) $A_z = 1$ km^2

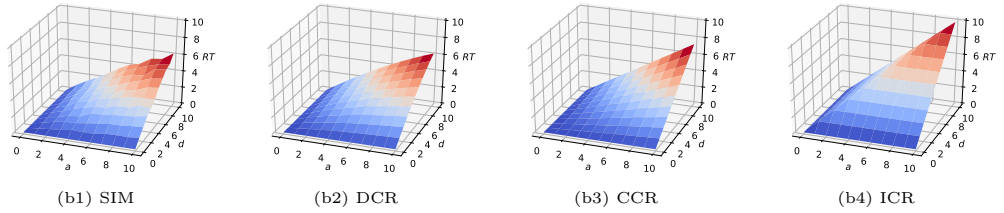

(b1) SIM (b2) DCR (b3) CCR (b4) ICR

(b) $A_z = 2$ km^2

Figure 4.5: Exemplary mean (SIM) and predicted (DCR, CCR, ICR) rentals RT in two SZSP-scenarios.

is strictly convex and then grows linearly from some point on. For all matching functions, the surfaces are symmetric on the diagonal between a- and d-axis (see Property 5).

- Comparing the respective observed and predicted rentals for $a = 10$ and $d = 10$ reveals, that all matching functions overestimate the SIM results at this point, but that the DCR prediction is better than the ICR and CCR. Considering the surfaces overall, as well as the concave and convex shapes of the surfaces on the diagonal discussed above, indicates that the DCR approximates the SIM best, followed by the CCR and then the ICR.

We continue the discussion of results by comparing the rental curves RT for specific values of the demand $\hat{d}$, depicted in Figure 4.6. These graphs which are common to depict matching functions can be thought of as corresponding vertical cuts through the surface plots in Figure 4.5. Again, the two rows depict the SZSP-scenarios with $A_z = 1$ km^2 and $A_z = 2$ km^2. The respective graphs for all $A_z \in \mathcal{A}_z$, are depicted in Figure 4.17 in Appendix 4.G. The columns correspond to different demands $\hat{d}$. The simulation (SIM) results are depicted by a black solid line, the results of ICR in dashed blue, CCR in dotted red, and DCR in dotdashed green. The following observations can be made:

- As illustrated in Figure 4.3 in Section 4.3.5, the DCR is strictly concave in a, while both ICR and CCR take the form of a piece-wise linear function with a positive slope piece anchored at the origin and a second horizontal piece.
- The expected rentals predicted by the DCR are almost identical to the average SIM results, for all a-$\hat{d}$ combinations and all A_z. The characteristic strictly concave shape of SIM is perfectly modeled by the DCR. The CCR underestimates SIM for small values of a and $\hat{d}$. For large values, it overestimates this benchmark. As above, for large a and $\hat{d}$, the CCR and the ICR do not differ (see Figures 4.17(a2)-4.17(a4) in Appendix 4.G).
- The ICR overestimates the SIM rentals for all a-$\hat{d}$ combinations. The difference grows in the size of the zone A_z and for a certain A_z it reaches its maximum at $a = \hat{d}$. Moreover,

this maximum difference grows in $\hat{d}$. This can be explained as follows: The ICR assumes a perfect matching, which is appropriate if the zone size A_z equals the walking area. However, when the zone becomes larger, the probability that an available vehicle is actually in walking distance to a customer decreases. The maximum is at $a = \hat{d}$ because at this value, each customer needs to find a vehicle for the ICR to be exact. By contrast, imagine $d = a + 1$, then we have an additional customer and the ICR prediction is still realized if one customer cannot reach a vehicle.

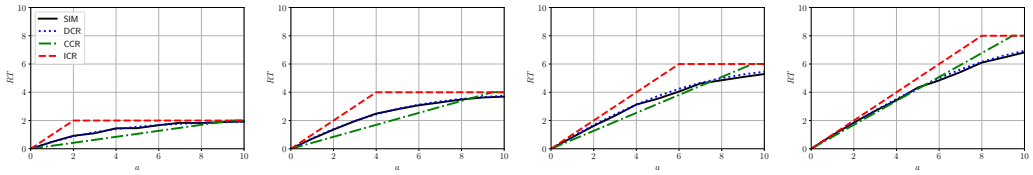

(a1) $\hat{d} = 2$ (a2) $\hat{d} = 4$ (a3) $\hat{d} = 6$ (a4) $\hat{d} = 8$

(a) $A_z = 1$ km^2

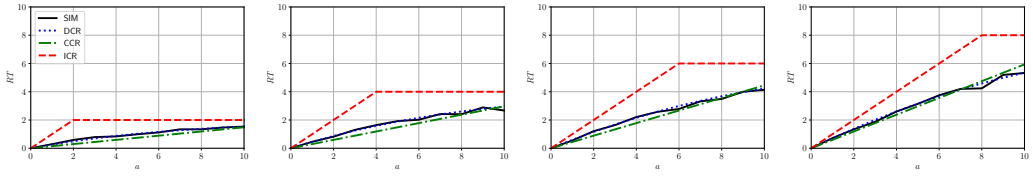

(b1) $\hat{d} = 2$ (b2) $\hat{d} = 4$ (b3) $\hat{d} = 6$ (b4) $\hat{d} = 8$

(b) $A_z = 2$ km^2

Figure 4.6: Exemplary mean (SIM) and predicted (DCR, CCR, ICR) rentals RT in two SZSP-scenarios.

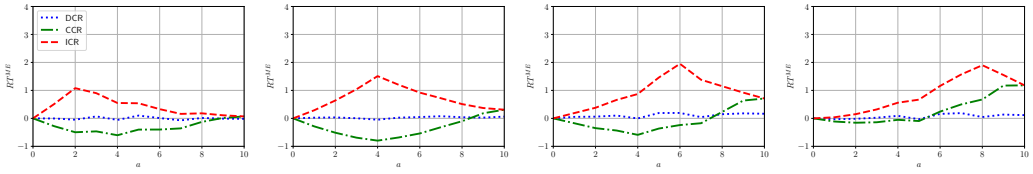

(a1) $\hat{d} = 2$ (a2) $\hat{d} = 4$ (a3) $\hat{d} = 6$ (a4) $\hat{d} = 8$

(a) $A_z = 1$ km^2

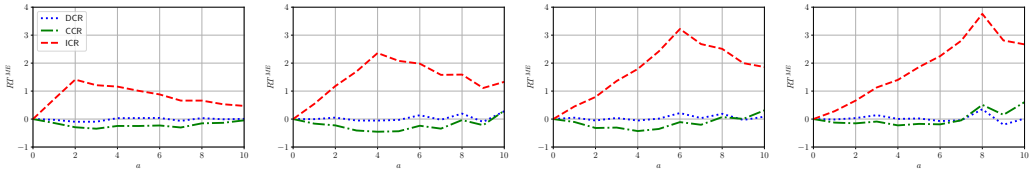

(b1) $\hat{d} = 2$ (b2) $\hat{d} = 4$ (b3) $\hat{d} = 6$ (b4) $\hat{d} = 8$

(b) $A_z = 2$ km^2

Figure 4.7: Exemplary mean absolute error RT^{ME} in two SZSP-scenarios.

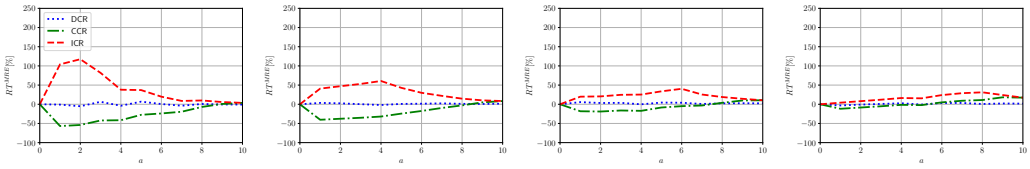

(a1) $\hat{d} = 2$ (a2) $\hat{d} = 4$ (a3) $\hat{d} = 6$ (a4) $\hat{d} = 8$

(a) $A_z = 1$ km^2

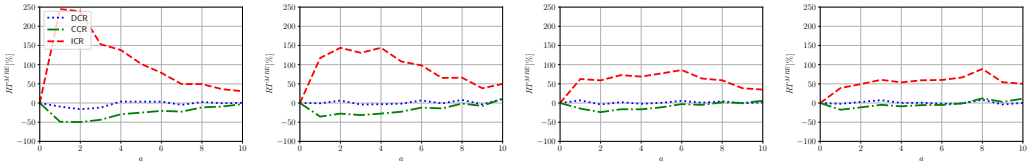

(b1) $\hat{d} = 2$ (b2) $\hat{d} = 4$ (b3) $\hat{d} = 6$ (b4) $\hat{d} = 8$

(b) $A_z = 2$ km^2

Figure 4.8: Exemplary mean relative error RT^{MRE} in two SZSP-scenarios.

In the following, we discuss the results based on the introduced metrics. Figure 4.7 and Table 4.3 in Appendix 4.G contains the values of RT^{ME} for the DCR, CCR, and ICR for all parameter configurations, grouped by SZSP-scenarios $A_z \in \mathcal{A}_z$. The corresponding RT^{MRE} are depicted in Figure 4.8 and Table 4.4 in Appendix 4.G.

- For the DCR, RT^{ME} takes both positive and negative values. The minimum RT^{ME} is between -0.06 ($A_z = 0.5$ km^2) and -0.20 ($A_z = 2$ km^2), i.e. -3.8% and -1.0% RT^{MRE}. The maximum RT^{ME} is between 0.19 ($A_z = 0.5$ km^2) and 0.40 ($A_z = 1$ km^2), i.e. 2.9% and 5.6% RT^{MRE}.
- For the CCR, RT^{ME} also takes both positive and negative values. The minimum RT^{ME} is between -0.06 ($A_z = 0.5$ km^2) and -0.80 ($A_z = 1$ km^2), i.e. -13.7% and -32.0% RT^{MRE}. The maximum RT^{ME} is between 0.85 ($A_z = 0.5$ km^2) and 2.20 ($A_z = 1$ km^2), i.e. 11.9% and 28.2% RT^{MRE}.
- For the ICR, RT^{ME} only takes values greater or equal to zero. The maximum RT^{ME} is 0.85 ($A_z = 0.5$ km^2) and it grows to 5.75 ($A_z = 4$ km^2), i.e. to 11.9% and 135.3% RT^{MRE}.

The above results demonstrate that in general, the ICR matching function is not suitable to predict rentals accurately in the stylized SZSP-setting that only considers one zone. In particular, they show that only the novel matching functions are capable to adapt to different zone area sizes. While the prediction error diminishes when the zone area size equals the walking area size and might be acceptable in our scenarios with ratios of walking area and zone area in the approximate range $\frac{A_w}{A_z} \geq \frac{1}{2}$, the ICR overestimates the observed rentals in the SIM benchmark substantially for smaller $\frac{A_w}{A_z}$. Since larger zone areas are commonly used in literature as well as practice and since using multiple smaller zones comes with several disadvantages (see Section 4.1), the ICR's applicability is limited. In contrast, the CCR considers A_w and A_z in the matching prediction and therewith is capable of predicting the rentals in the SZSP-setting much more accurately, especially for smaller ratios of $\frac{A_w}{A_z}$. The DCR predicts the rentals best in the SZSP-setting and in particular performs better than the CCR for ratios of around $\frac{A_w}{A_z} = \frac{1}{2}$. Overall, the adaptability of CCR and DCR to different zone sizes is the key advantage over

the ICR. As discussed in Section 4.3.5, the decisive disadvantage of the DCR is that it can not be losslessly integrated in a linear network flow SMS model, such that the DCR can not be considered in the following numerical results of the MZMP-setting.

4.4.2 Multiple Zones Multiple Periods Setting

4.4.2.1 Setting

The *multiple zones multiple periods* (MZMP) setting replicates an entire FF SMS with $Z = 59$ zones $\mathcal{Z} = \{1, 2, \ldots, Z\}$ and $T = 48$ periods $\mathcal{T} = \{0, 1, \ldots, T-1\}$ of 30 minutes each which together replicate one day. The purpose of this MZMP-setting is to assess how different matching functions affect the overall rental prediction accuracy when supply and demand interact in an entire FF SMS. In this setting, only the size of the zones A_z changes over the *parameter configurations*, replicating multiple FF SMSs with identical zone number but with different sizes of the operating area. Think of cities with the same number of inhabitants, but spread over areas of different sizes, i.e. with different densities. The MZMP-setting is based on a real-life FF SMS: The vehicle fleet is initially distributed over the zones in line with historical data from Share Now. Customers arrive according to a demand pattern over the different zones and periods, which is obtained from historical data as well. More precisely, for every zone $i \in \mathcal{Z}$, $\hat{a}_{i0}$ defines the initial vehicle count and for every zone-zone-period combination (i-j-t combination with $i, j \in \mathcal{Z}, t \in \mathcal{T}$), the demand d_{ijt} is given.

Due to the non-disclosure agreement with our practice partner, we do not state these parameters above explicitly. However, the following general statements regarding the data used can be made. Data sources for estimating the demand are primarily the realized app openings as well as the realized rentals. Every data point of an app opening contains information regarding location and time. Clearly, not every single app opening can be counted as an individual demand, e.g. because a customer might simply check a payment history or might check vehicle availability multiple times before the actual booking. However, with much data and experience, the provider can estimate the actual demand from these app openings. These data points are then mapped to a given discretization scheme, meaning to zone-period combinations. Average values over multiple identical days can then be derived. To obtain the demand data for every zone-zone-period combination, i.e. the expected destinations for the demand originating at a certain zone-period, the proportions of rentals that realize can be used as a proxy for the demand proportions. Clearly, rentals only reflect the served (constrained) demand, which is why unconstraining techniques can come into place (see e.g. Talluri and van Ryzin (2004, Chapter 9.4)). Similar to the demand on zone-period level, the initial vehicle count can be obtained by mapping and averaging data points of available vehicles to the respective zone-period.

As in the SZSP-setting, the benchmark in the MZMP-setting stems from a stochastic dynamic simulation, with the difference that the rentals that evolve over one entire day throughout the entire SMS are considered. The latter also implies that, in contrast to the SZSP-setting, the matching functions can no longer be directly evaluated for a given parameter configuration. Therefore, to evaluate the matching functions, we integrate the two functions which can be losslessly linearized – the CCR and the ICR – in an FF SMS model that is based on a linear network flow formulation, as described in Section 4.3.5. In each zone-period combi-

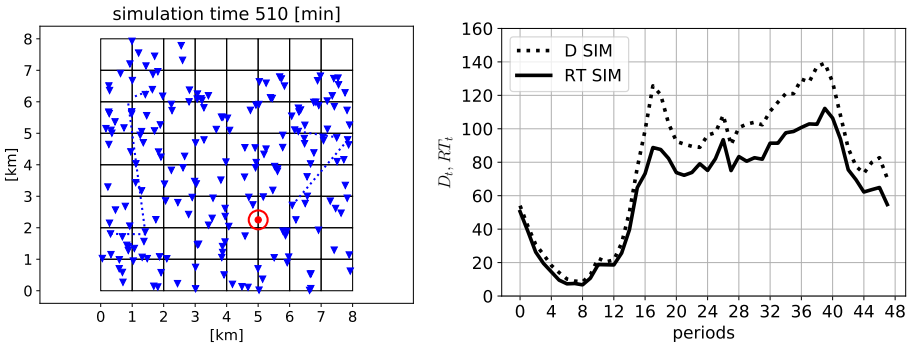

(a) Snapshot of simulation

(b) Course of demand and mean rentals over periods

Figure 4.9: Scenario with MZMP and $Z = 59$, $A_z = 1$ km^2, $A_o = 59$ km^2

nation, the rentals realize according to the respective matching function $r^{CCR}_{it,A_w,A_z}(a_{it}, d_{it})$ and $r^{ICR}_{it,A_w,A_z}(a_{it}, d_{it})$. The constraints of the network flow formulation ensure that these rentals r^M_{it} with $M \in \{CCR, ICR\}$ split into the different r^M_{ijt} in proportion to the given demand pattern, meaning $r^M_{ijt} = \frac{d_{ijt}}{d_{it}} \cdot r^M_{it}\ \forall i, j \in \mathcal{Z}, t \in \mathcal{T}$. Therewith, the rentals that realize over all zones and periods according to a specific matching function can be derived.

4.4.2.2 Simulation Benchmark

For a specific parameter configuration of the MZMP-setting, we derive the respective benchmark by performing multiple simulation runs $n \in \mathcal{N} = \{1, 2, \ldots, N\}$ that each yield a rental observation $r_{ijt,n}$ for every zone-zone-period combination (i-j-t combination with $i, j \in \mathcal{Z}, t \in \mathcal{T}$). Primarily, we consider the observed rentals on the period-level, meaning $r_{t,n} = \sum_{i\in\mathcal{Z}} \sum_{j\in\mathcal{Z}} r_{ijt,n}$.

At the beginning of each run, the vehicle fleet is initialized according to the initial spatial vehicle distribution $\hat{\mathbf{a}}_0 = [\hat{a}_{i0}]_{Z\times 1}$. Each zone then exactly contains the number of vehicles as defined in $\hat{\mathbf{a}}_0$, and the precise location within a zone for each of the vehicles is randomly determined from the uniform distribution. The customer arrival process follows a Poisson process $\mathbf{P}_{\lambda_t}$ in which the intensity λ_t varies for the periods and equals the demand in the respective period, meaning $\lambda_t = \sum_{i\in\mathcal{Z}} \sum_{j\in\mathcal{Z}} d_{ijt}/30$ (unit of λ_t is [1/min]). The inter-arrival time $\Delta\tau$ until a new customer arrives is sampled from the exponential distribution $\Delta\tau \sim \text{Exp}(\lambda_t)$. Whenever a customer arrives in period t, the customer's origin zone i is determined by roulette wheel selection, i.e. the probability for arrival in i is $P^{origin}_{it} = \sum_{j\in\mathcal{Z}} d_{ijt} / \sum_{i\in\mathcal{Z}} \sum_{j\in\mathcal{Z}} d_{ijt}$ (see previous section for demand pattern d_{ijt}). The customer's exact origin location is determined by uniform distribution of positions within the origin zone. All available vehicles within the walking distance of 0.3km are determined and, if there is at least one vehicle within reach, the customer chooses the closest one for rental. Note that, in contrast to the assumptions in the SZSP-setting (end of Section 4.4.1.2), customers may now cross the border of a zone and take a vehicle from a neighboring one. If there is no vehicle within reach, the customer leaves the system without further consideration. In case of a rental that originates at a certain i-t-combination, the destination zone is again determined by roulette wheel selection, i.e. the probability for destination zone j is $P^{destination}_{jt} = d_{ijt} / \sum_{k\in\mathcal{Z}} d_{ikt}$. All rentals have a duration of 15 min. and immediately become available as soon as a rental is terminated. Note that here, in contrast to the SZSP-simulation, not all vehicles are necessarily available at the beginning of a period. The customer's exact

destination location is determined by uniform distribution of positions within the destination zone. This process of customer arrival sampling and potential rental determination is executed until the cumulated arrival time over all customers exceeds the considered day $\tau_{max} = 48 \cdot 30$ [min]. One simulation run is depicted as pseudo code in Algorithm 5.

To clarify the setup, consider Figure 4.9a that depicts a snapshot of a single simulation run. In the simulation, the zones are squares of the same size and in this particular parameter configuration, $A_z = 1$ km^2 for all zones. Note that since the considered FF SMS consists of 59 zones, the five zones represented in the top row on the right are out of the simulation's scope. The vehicles are represented as blue triangles, and the currently rented vehicles are depicted at the rental origin with a dotted line that ends at the rental destination. One customer arrived in the considered instance, represented by the red dot with walking area, depicted as red circle. For this particular customer, no available vehicle was within reach. Figure 4.9b depicts the demand and the resulting rentals averaged over all N runs in the course of the day. More specifically, the dotted black curve represents the aggregate demand over all zones for every single period $t \in \mathcal{T}$, meaning $d_t = \sum_{i \in \mathcal{Z}} \sum_{j \in \mathcal{Z}} d_{ijt}$. The solid black curve represents the mean aggregate rentals over all zones for every single period $t \in \mathcal{T}$, meaning $\bar{r}_{t,N} = \frac{1}{N} \sum_{n \in \mathcal{N}} r_{t,N}$. This rentals curve for various parameter configurations serves as a benchmark to evaluate the rentals prediction of the matching functions qualitatively.

Algorithm 5 MZMP simulation (one run $n \in \mathcal{N}$)

- initialize simulation time $\tau = 0$
- initialize rental count $r_{t,n} = 0 \, \forall t \in \mathcal{T}$
- distribute vehicles randomly according to $\hat{\mathbf{a}}_0$
- initialize set of available vehicles $\mathcal{V}^{available}$ with all vehicles
- initialize set of currently rented vehicles $\mathcal{V}^{rented} = \emptyset$

while $\tau < \tau_{max}$ **do**
- draw inter-arrival time $\Delta\tau$ from exponential distribution $\Delta\tau \sim \text{Exp}(\lambda_t)$
- update simulation time $\tau \leftarrow \tau + \Delta\tau$
- **if** vehicles in $\mathcal{V}^{rented}$ have arrival time $< \tau$ **then**
  - remove respective vehicles from $\mathcal{V}^{rented}$
  - add respective vehicles to $\mathcal{V}^{available}$
- **end if**
- determine current period t
- determine customer's origin zone i with probabilities $P_{it}^{origin} \, \forall i \in Z$
- determine customer's exact origin location within origin zone i by uniform distribution
- determine distances to vehicles in $\mathcal{V}^{available}$
- **if** at least one vehicle in walking distance **then**
  - choose closest vehicle from $\mathcal{V}^{available}$
  - remove chosen vehicle from $\mathcal{V}^{available}$
  - add chosen vehicle to $\mathcal{V}^{rented}$
  - record rental: $r_{t,n} \leftarrow r_{t,n} + 1$
  - determine destination zone j with probabilities $P_{jt}^{destination} \, \forall j \in Z$
  - determine customer's exact destination location within j destination zone by uniform distribution
- **end if**

end while

4.4.2.3 Parameter Configurations and Scenarios

We consider the following parameter values:

- Available vehicles ($\mathcal{V}_{MZMP}$): The initial fleet distribution $\mathcal{V}_{MZMP}$ remains constant over all studies and it is chosen according to real-life data. The overall fleet size is $\sum_{j \in \mathcal{Z}} \hat{a}_{i0} =$

201 and for the individual zones, the initial vehicle count lays in the interval $\hat{a}_{i0} \in [0, 10] \, \forall i \in \mathcal{Z}$.

- Arriving customers ($\mathcal{V}_{MZMP}$): The pattern of arriving customers $\mathcal{V}_{MZMP}$ remains constant over all studies and it is chosen according to real-life data. The d_{ijt} values vary in the interval $d_{ijt} \in [0, 18] \, \forall i, j \in \mathcal{Z}, t \in \mathcal{T}$.
- Walking area size (A_w): As in the SZSP-setting, the size of the reachable area by walking is kept constant at $A_w = \pi \cdot (0.3\text{km})^2 = 0.28$ km^2.
- Zone area size ($\mathcal{A}_z$): We obtain four scenarios by considering the sizes of the zone area $\mathcal{A}_z = \{0.5 \text{ km}^2, 1 \text{ km}^2, 2 \text{ km}^2, 4 \text{ km}^2\}$. This can be considered as *different cities* with the same fleet and demand, but spread over operating areas of *different size*, i.e. $A_o = 29.5$ km^2 to $A_o = 236$ km^2. Note that the number of zones remains identical in each scenario. In Appendix 4.I, in contrast, we consider a setting in which a given operating area is partitioned into a different number of multiple zones.

We perform $N = 100$ simulation runs for every variant, meaning for every matching function in each parameter configuration (here equivalent to scenario).

4.4.2.4 Evaluation Metrics

Analogous to the SZSP-setting, we use several metrics to assess the rentals prediction accuracy. Different from above, all metrics here are time-specific:

- Rentals (RT_t): The period-specific absolute rentals RT_t are determined as follows for the simulation and the matching functions. The mean observed rentals in the simulation for a specific period t are $\bar{r}_{t,N} = \frac{1}{N} \sum_{n \in \mathcal{N}} \sum_{i \in \mathcal{Z}} \sum_{j \in \mathcal{Z}} r_{ijt,n}$. The predicted rentals by the network flow-based model with integrated matching function for a specific period t are $\bar{r}_t = \sum_{i \in \mathcal{Z}} \sum_{j \in \mathcal{Z}} r_{ijt}$.
- Rentals mean error (RT_t^{ME}): The period-specific mean absolute error RT_t^{ME} between the predicted rentals by the network flow-based model with integrated matching function $\bar{r}_t$ and the mean observed rentals in the simulation $\bar{r}_{t,N}$ is $RT_t^{ME} = \bar{r}_t - \bar{r}_{t,N}$.
- Rentals mean relative error (RT_t^{MRE}) [%]: The period-specific mean relative error RT_t^{MRE} between the predicted rentals by the network flow-based model with integrated matching function $\bar{r}_t$ and the mean observed rentals in the simulation $\bar{r}_{t,N}$ is $RT^{MRE} = (\bar{r}_t - \bar{r}_{t,N})/\bar{r}_{t,N} \cdot 100$.

4.4.2.5 Results

Figure 4.10 depicts the mean rentals RT_t for the simulation benchmark (SIM) and the predicted rentals by the two linear network flow formulations with CCR and ICR in the course of the day for the four MZMP-scenarios with $A_z = 0.5$ km^2, 1 km^2, 2 km^2, and 4 km^2. In Figures 4.11, 4.12 and Tables 4.5, 4.6 in Appendix 4.H, the corresponding mean errors RT_t^{ME} and mean relative errors RT_t^{MRE} are depicted. The most relevant results can be summarized as follows:

- The rental curves follow the typical demand pattern with two peaks around 8:00 and 19:00.

- Despite the identical demand pattern in all scenarios, the SIM benchmark of RT_t (solid black) varies substantially. As the city considered becomes less dense (mimicked by increasing c.p. A_z), the number of rentals quickly decreases (by a factor of more than 10) from $A_z = 0.5$ to $A_z = 4$. This can be explained as follows: For small A_z (dense cities), customers' walking area is comparatively larger. This increases the matching probability because – given the same number of vehicles in the operating area – they can walk to more vehicles. By contrast, with large A_z (low density), the available vehicles are spread over large distances and customers more often do not find a vehicle in their walking distance.
- The predicted ICR rentals are identical in all scenarios, because the ICR is independent of A_z (see (4.7)). While for $A_z = 0.5$ km^2, the overall rental curve incidentally resembles the SIM benchmark, it increasingly overestimates the benchmark with growing A_z. Already for $A_z = 1$ km^2, the ICR rental predictions are far from the SIM benchmark. The mean error RT_t^{ME} lies between [-17.7, 10.7] for $A_z = 0.5$ km^2, [1.5, 48.2] for $A_z = 1$ km^2, [4.7, 86.3] for $A_z = 2$ km^2, and [6.0, 105.2] for $A_z = 4$ km^2. In the periods between morning and evening peak, the mean relative error RT_t^{MRE} lies in the range of [-19.3%, 14.0%] for $A_z = 0.5$ km^2, [18.9%, 92.9%] for $A_z = 1$ km^2, [21.7%, 478.7%] for $A_z = 2$ km^2, and [870.8%, 2199.6%] for $A_z = 4$ km^2.
- The CCR rentals curve resembles the the SIM benchmark for all A_z (densities). The mean error RT_t^{ME} lies between [-17.2, 8.7] for $A_z = 0.5$ km^2, [-8.7, 41.0] for $A_z = 1$ km^2, [-2.9, 4.2] for $A_z = 2$ km^2, and [-3.1, 1.0] for $A_z = 4$ km^2. In the periods between morning and evening peak, the mean relative error RT_t^{MRE} lies in the range of [-19.2%, 11.2%] for $A_z = 0.5$ km^2, [-13.7%, 2.2%] for $A_z = 1$ km^2, [-11.3%, 30.5%] for $A_z = 2$ km^2, and [-32.9%, 24.1%] for $A_z = 4$ km^2. In comparison to the ICR, the curve changes with varying zone size A_z, demonstrating the CCR's capability to adapt to scenarios with high and low density also in the MZMP-setting.

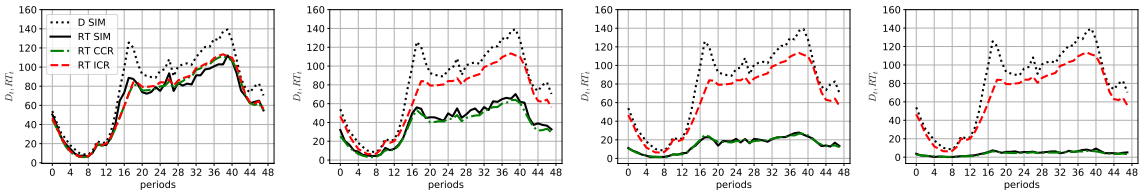

(a) $Z = 59$, $A_z = 0.5$ km^2, $A_o = 29.5$ km^2

(b) $Z = 59$, $A_z = 1$ km^2, $A_o = 59$ km^2

(c) $Z = 59$, $A_z = 2$ km^2, $A_o = 118$ km^2

(d) $Z = 59$, $A_z = 4$ km^2, $A_o = 236$ km^2

Figure 4.10: Mean (SIM) and predicted (CCR, ICR) rentals RT in MZMP-scenarios with different zone and operating area sizes A_z, A_o

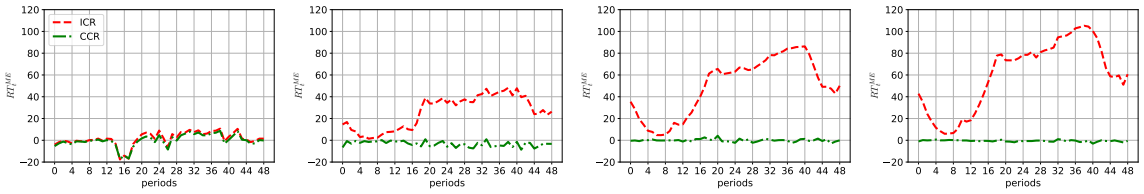

(a) $Z = 59$, $A_z = 0.5$ km^2, $A_o = 29.5$ km^2

(b) $Z = 59$, $A_z = 1$ km^2, $A_o = 59$ km^2

(c) $Z = 59$, $A_z = 2$ km^2, $A_o = 118$ km^2

(d) $Z = 59$, $A_z = 4$ km^2, $A_o = 236$ km^2

Figure 4.11: Mean absolute error RT_t^{ME} in MZMP-scenarios with different zone and operating area sizes A_z, A_o

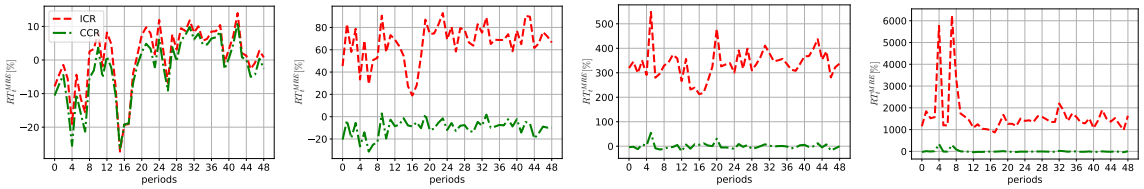

(a) $Z = 59$, $A_z = 0.5$ km^2, $A_o = 29.5$ km^2

(b) $Z = 59$, $A_z = 1$ km^2, $A_o = 59$ km^2

(c) $Z = 59$, $A_z = 2$ km^2, $A_o = 118$ km^2

(d) $Z = 59$, $A_z = 4$ km^2, $A_o = 236$ km^2

Figure 4.12: Mean relative error RT_t^{MRE} in MZMP-scenarios with different zone and operating area sizes A_z, A_o

As in the SZSP-setting, also the above results in the MZMP-setting demonstrate that the ICR in general is not suitable to predict rentals accurately and that the CCR in contrast is capable of adapting to different densities. For the $A_z = 0.5$ km^2 scenario (high density), both ICR and CCR provide good rentals predictions. For larger A_z (low density), however, the ICR substantially overestimates the SIM benchmark by a factor of approximately 2 in the $A_z = 1$ km^2 scenario and up to a factor of approximately 20 in the $A_z = 4$ km^2 scenario, while the error RT_t^{MRE} of CCR remains in a relatively narrow range of up to approximately 30% at the most. It may be tempting to wrongly think that $A_z = 0.5$ km^2 always, meaning for all possible instances, is a good value for the ICR. Certainly, the results (SZSP- and MZMP-setting) show that smaller zones which are closer to the walking area are favorable over larger zones with regard to the overall rental prediction accuracy that can be obtained when applying the ICR. However, since customers and vehicles in neighboring zones do not match in network flow formulations with discrete zones (as in the MZMP-setting), rentals that realize in reality are increasingly neglected when having multiple smaller zones. This means that the increased accuracy *within* a zone might be overcompensated by a reduced accuracy *across* zones. The specific results depend on the actual homogeneity of the zones and whether they can in fact be considered as disjunct zones for which there are indeed no customers crossing the borders.

4.5 Pricing Optimization Case Study

In this section, we evaluate the performance of the CCR and ICR matching functions in an FF SMS optimization problem. To that end, we present a pricing optimization case study based on Share Now data and assess whether more accurate rental predictions can result in better pricing decisions and eventually higher profits (more precisely contribution margin). The problem that we consider is a differentiated pricing problem for SMS that was discussed in Soppert et al. (2022) and for which a MILP, based on a network flow formulation, with ICR matching function was proposed. We adapt the MILP formulation by integrating the CCR. For the different instances considered in this case study, we derive pricing solutions with both of the MILP models and evaluate them in a simulation study.

The differentiated pricing problem and its original as well as the adapted mathematical modeling are introduced in Section 4.5.1. Section 4.5.2 discusses the setup of the simulation study we use to evaluate the different pricing solutions. In Section 4.5.3, we introduce the considered parameter configurations as well as the metrics we use. Section 4.5.4 discusses the obtained results.

4.5.1 Problem Statement and Mathematical Modeling

The *origin-based differentiated pricing problem* (OBDPP) in SMSs, as defined in Soppert et al. (2022), is a pricing problem in which spatially and temporally differentiated minute prices have to be determined, to maximize the contribution margin of an SMS. More precisely, an SMS is discretized into Z different locations $\mathcal{Z} = \{1, 2, \ldots, Z\}$ and the considered time span of one day is discretized into T periods $\mathcal{T} = \{0, 1, \ldots, T-1\}$. For every *i-t* combination with $i \in \mathcal{Z}, t \in \mathcal{T}$, a minute price p_{it} is to be chosen from a given price set $\mathcal{P} = \{p^1, p^1, \ldots, p^M\}$ with corresponding price indices $\mathcal{M} = \{1, 2, \ldots, M\}$. *Origin-based* refers to the fact that, in contrast to a *trip-based* pricing mechanism for example, all rentals that begin in a certain *i-t* combination, are charged with the same minute price p_{it}. Note that *differentiated* (=*static*), in contrast to *dynamic* (see Agatz et al. (2013)), refers to a pricing approach where prices do not depend on components of the current state of the system that are unobservable by the clients, such as current fleet distribution, but can be pre-computed and pre-published. The OBDPP assumes supply and demand matching according to the ICR.

The OBDPP can be modeled by a MILP which is based on a deterministic network flow formulation where expected vehicle movements are represented by flows in a spatio-temporal network, as depicted in Figure 4.14. Vehicle flows consist of actual rentals r^m_{ijt} from location $i \in \mathcal{Z}$ to $j \in \mathcal{Z}$ in period $t \in \mathcal{T}$ and at price p^m with index $m \in \mathcal{M}$ (solid arcs), or unused vehicles s_{it} that remain in the same location $i \in \mathcal{Z}$ at period $t \in \mathcal{T}$ (dashed arcs). For every *i-j-t* combination, the respective basic demand d_{ijt} is assumed to scale with the *i-j-t*-specific sensitivity factor f^m_{ijt}, depending on the price p^m, to the actual demand $d^m_{ijt} = d_{ijt} \cdot f^m_{ijt}$. The main components of the OBDPP MILP formulation are as follows:

- An objective function that maximizes the contribution margin from rentals that realize at different prices over the entire spatio-temporal network, meaning $\sum_{i,j \in \mathcal{Z}} \sum_{t \in \mathcal{T}} \sum_{m \in \mathcal{M}} r^m_{ijt} \cdot l_{ij} \cdot (p^m - c)$, where l_{ij} is the average rental duration and c is variable cost per minute.

- Flow conservation constraints of the form (4.9) as described in Section 4.3.5 which ensure that the fleet of vehicles remains constant in every period and that, for a certain i-t-combination, the available vehicles either remain unused or get rented.
- Constraints ensuring that for p_{it} exactly one of the prices from the price list $\mathcal{P}$ is chosen for every i-t-combination. If price p^m is chosen, the respective binary variable y_{it}^m is one.
- A set of constraints that determines the realization of rentals. The overall rentals for every i-t combination are determined according to the ICR. These rentals split into the i-j-t-specific rentals, proportionally according to the demand, as described in Appendix 4.F.

The constraints in the OBDPP MILP formulation that ensure rentals realization according to the ICR can easily be replaced by corresponding constraints for the CCR. We state the resulting full MILP formulation in Appendix 4.F. The constraints that are new compared to Soppert et al. (2022) are (4.49)-(4.54). To differentiate in the following, we denote the original problem by OBDPP-ICR and the adapted with CCR matching function by OBDPP-CCR. For solving the OBDPP-CCR, we use the decomposition solution approach described in Soppert et al. (2022) which builds on the idea to solve multiple smaller MILPs instead of the original one. The algorithm is implemented in Python 3.7 and all MILPs are solved with Gurobi 9.0.2. As in the original paper, the algorithm runs for 48 hours. The simulation evaluation takes approximately 8 hours without any parallelization. Given that the considered pricing problem (in Soppert et al. (2022) and, thus in this case study) is a differentiated (=static) pricing problem, these computation times do not pose a restriction for application in practice.

4.5.2 Simulation Evaluation

To evaluate and compare the performance of the optimization results, i.e., of the prices obtained from either optimizing using OBDPP-ICR or OBDPP-CCR, we perform a simulation study. Each run of the simulation reflects a potential real-world evolvement of the system over the considered day given the calculated pricing solutions. In essence, the simulation is in line with the one we used to calculate the simulation benchmarks for the MZMP-setting in Section 4.4.2.2. We only need to adapt it to allow for different prices and their effect on the demand. As described, the customer arrival process in the MZMP simulation follows a Poisson process $\mathbf{P}_{\lambda_t}$ with intensity λ_t that depends on the demand in the respective period. According to the assumption in the OBDPP, described in Section 4.5.1, the demand now depends on the chosen prices. Therefore, λ_t has to be calculated according to the pricing solution, meaning $\lambda_t = \sum_{i \in \mathcal{Z}} \sum_{j \in \mathcal{Z}} d_{ijt}^m / 30$, where $d_{ijt}^m = d_{ijt} \cdot f_{ijt}^m$ and f_{ijt}^m depends on the price p_{it} (see Section 4.4.2.1 for demand pattern d_{ijt}). Accordingly, the probability for an arriving customer in period t to arrive in zone i has to be updated to $P_{it}^{origin} = \sum_{j \in \mathcal{Z}} d_{ijt}^m / \sum_{i \in \mathcal{Z}} \sum_{j \in \mathcal{Z}} d_{ijt}^m$. In case of a rental originating in a certain i-t-combination, the probability to have target zone j is $P_{jt}^{destination} = d_{ijt}^m / \sum_{k \in \mathcal{Z}} d_{ikt}^m$. Every pricing solution is evaluated with $N = 100$ simulation runs.

4.5.3 Parameter Configurations, Scenarios, and Evaluation Metrics

The case study builds on the MZMP-setting introduced in Section 4.4.2.1. The number of zones and periods, the initial vehicle distribution, and the overall demand pattern are chosen as in the MZMP-setting. Again, we consider the two scenarios with $A_z \in \{0.5\ \text{km}^2, 1\ \text{km}^2, 2\ \text{km}^2, 4\ \text{km}^2\}$ (high to low density with operating area sizes of $A_o = 29.5\ \text{km}^2$ to $A_o = 236\ \text{km}^2$). The additional parameters are chosen according to Soppert et al. (2022), that is, prices of $p^1 = 24$ cent/min, $p^2 = 30$ cent/min, $p^3 = 36$ cent/min, denoted as *low*, *base*, and *high* price. The corresponding price sensitivities are $f^1_{ijt} = 1.25, f^2_{ijt} = 1, f^3_{ijt} = 0.75\ \forall i, j \in \mathcal{Z}, t \in \mathcal{T}$ (derived from a conjoint analysis and A/B tests). Variable costs of $c = 7.5$ cent/min make up 25% of the base price. The rental time is $l_{ij} = 15$ min. Note that for these parameters, one rental realizes a contribution margin per minute of 20.625 cent/min for price p^1, 22.5 cent/min for price p^2, and 21.375 cent/min for price p^3. Thus, in a myopic optimization when there is enough supply to serve the demand, the base price p^2 would be chosen.

The results obtained by a uniform pricing with the base price, that is, without price differentiation, (BASE) serve as a benchmark for the ones by a price optimization (OPT) with OBDPP-ICR or OBDPP-CCR. In addition to the metrics defined in Section 4.4.2.4, we consider the following metrics:

- Relative rentals increase ($RT^{rel}\,[\%]$): The RT^{rel} between rental observations with optimized pricing RT_n^{OPT} and the rental observations with base pricing RT_n^{BASE} is defined as $RT^{rel} = (\sum_{n=1}^{N} RT_n^{OPT} - \sum_{n=1}^{N} RT_n^{BASE}) / \sum_{n=1}^{N} RT_n^{BASE} \cdot 100$.
- Relative revenue increase ($RV^{rel}\,[\%]$): The RV^{rel} between revenue observations with optimized pricing RV_n^{OPT} and revenue observations with base pricing RV_n^{BASE} is defined as $RV^{rel} = (\sum_{n=1}^{N} RV_n^{OPT} - \sum_{n=1}^{N} RV_n^{BASE}) / \sum_{n=1}^{N} RV_n^{BASE} \cdot 100$.
- Relative contribution margin increase ($CM^{rel}\,[\%]$): The CM^{rel} between contribution margin observations with optimized pricing CM_n^{OPT} and the contribution margin observations with base pricing CM_n^{BASE} is defined as
  $CM^{rel} = (\sum_{n=1}^{N} CM_n^{OPT} - \sum_{n=1}^{N} CM_n^{BASE}) / \sum_{n=1}^{N} CM_n^{BASE} \cdot 100$.
- Proportion of prices ($PR_m^{prop}\,[\%]$): For a particular price p^m, the PR_m^{prop} defines the proportion of this price to all prices of a certain pricing solutions, i.e.,
  $PR_m^{prop} = \sum_{i=1}^{Z} \sum_{t=0}^{T-1} y_{it}^m / (Z \cdot T) \cdot 100$.

Note that $RT_n^{(\cdot)}$, $RV_n^{(\cdot)}$, and $CM_n^{(\cdot)}$ denote the respective quantity observed in one entire simulation run, meaning the sum over all zones and periods.

4.5.4 Results

In Table 4.1, the results for the evaluated pricing solutions, generated by OBDPP-ICR and OBDPP-CCR for MZMP-scenarios with $A_z = 0.5\ \text{km}^2, 1\ \text{km}^2, 2\ \text{km}^2, 4\ \text{km}^2$ are summarized. Table 4.7 in Appendix 4.H additionally depicts the corresponding confidence intervals that demonstrate the statistical significance of the respective CM^{rel} results.

- The PR_m^{prop} results for all scenarios demonstrate, that the prices in the solution obtained with the OBDPP-ICR are higher on average than those obtained with the OBDPP-CCR.

A_z [km^2]	OBDPP-	PR_m^{prop}			change w.r.t. BASE		
		low	base	high	RT^{rel}	RV^{rel}	CM^{rel}
0.5	ICR	17.1%	62.8%	20.1%	-4.3%	-0.1%	1.2%
	CCR	19.9%	61.1%	19.0%	-3.7%	0.6%	2.1%
1	ICR	17.1%	62.8%	20.1%	-3.4%	0.4%	1.6%
	CCR	34.1%	54.0%	11.1%	1.8%	3.6%	4.2%
2	ICR	17.1%	62.8%	20.1%	-3.2%	0.6%	1.8%
	CCR	16.3%	80.3%	3.5%	3.5%	4.3%	4.6%
4	ICR	17.1%	62.8%	20.1%	-5.7%	-1.9%	-0.6%
	CCR	0.0%	98.9%	1.1%	-1.3%	0.7%	1.4%

Table 4.1: Simulation results of pricing solutions from OBDPP-ICR and -CCR with different $A_z \in \mathcal{A}_z$.

For $A_z = 0.5$ km^2, the difference in the price levels is smaller than 2 percentage points, but it grows with increasing A_z up to almost 20 percentage points for $A_z = 4$ km^2. Exemplary, the two pricing solutions of OBDPP-ICR and OBDPP-CCR for $A_z = 2$ km^2 are depicted in Figure 4.13. Clearly, the OBDPP-ICR solution contains more high prices around the morning and evening demand peak, meaning around the periods 16 and 36. Only few of the zones, for example zone 7 and zone 49 have relatively many high prices in both solutions.

- As a consequence of the higher prices in the OBDPP-ICR solution, fewer rentals (RT^{rel}) realize in the simulation. The decrease in rentals depends on the scenario and lies between 0.6 percentage points for $A_z = 0.5$ km^2 and to 6.7 percentage points for $A_z = 2$ km^2.
- The revenue (RV^{rel}) obtained by the OBDPP-CCR solution is higher than the one resulting from the OBDPP-ICR in all scenarios. The gap lies in the range of 0.7 percentage points for $A_z = 0.5$ km^2 and 3.7 percentage points for $A_z = 2$ km^2.
- Most importantly, the contribution margin CM^{rel}, which is the objective of the pricing optimization, is significantly higher with the OBDPP-CCR pricing solution than with the OBDPP-ICR. The difference lies between 0.9 percentage points ($A_z = 0.5$ km^2) and 2.8 ($A_z = 2$ km^2) percentage points. Remember that for $A_z = 0.5$ km^2, the overall rentals prediction of ICR was very accurate. The fact that even here an increase of 0.9 percentage points by using the CCR is possible shows that this coincidental overall accuracy does not necessarily translate to good decisions. First, errors at the zone level may cancel out. Second, supply and demand are endogeneous in the optimization model, and, thus, zones which have the "appropriate" parameter combination in the ICR may no longer have in the optimal solution.

To summarize the results of the case study, the OBDPP-CCR with improved matching modeling compared to the OBDPP-ICR yields pricing solutions that generate significantly higher contribution margins. The overestimation of rentals by the ICR causes the OBDPP-ICR to predict too many rentals in general and therewith also too many rentals when high prices are set. The optimal pricing solution according to the OBDPP-ICR therefore sets too many high prices which cause a reduction of rentals and a decrease in contribution margin when compared to the optimal pricing solution according to the OBDPP-CCR. These results demonstrate that an accurate matching modeling that considers the specific characteristics of FF SMS is highly relevant for optimizing operations. Certainly, the specific results of an instance depend on the

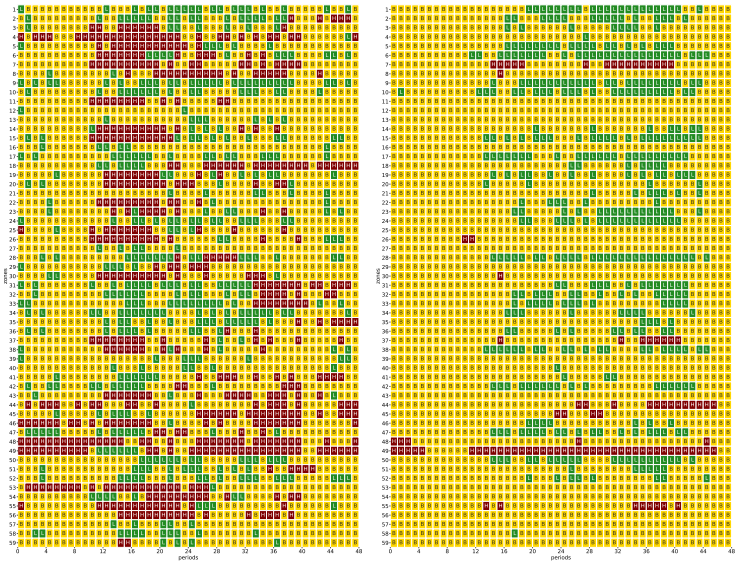

(a) OBDPP-ICR (b) OBDPP-CCR

Figure 4.13: Low (L), base (B), and high (H) prices in case study scenario with $A_z = 2$ km^2

many parameters (demand pattern, price sensitivities, etc.) but considering the results obtained in the SZSP-setting (Section 4.4.1), the MZMP-setting (Section 4.4.2) and in this case study, it seems clear that the overestimation of rentals with the OBDPP-ICR is the root cause of too high prices and the reduced profit.

4.6 Managerial Insights and Conclusion

In this paper, motivated by the insights gained in a close collaboration with Europe's largest FF car sharing provider Share Now, we examined the modeling of supply and demand matching in FF SMSs. Despite the fact that the realization of rentals is central to the accuracy of an SMS model, matching functions for SMSs have not been discussed in the literature yet and as a consequence, optimization models for SB and FF SMSs have been identical in this regard. With the development of matching functions that consider the central influencing factors specifically relevant for FF SMSs, such as customers' maximum walking distance and zone sizes, our work builds a bridge between the optimization models for SB and those for FF SMSs. This allows to adapt optimization models designed for SB to FF SMSs.

In the following, we structure the conclusions from our findings and the related managerial insights according to two central aspects, namely (1) the development and the analytical as well as computational assessment of accurate matching functions for FF SMSs and (2) the integration of the functions into FF SMS optimization approaches and the investigation of benefits that result from that.

With regard to (1), the methodological approach of developing accurate matching functions for FF SMSs was to formalize a generic, stylized matching process first and, based upon this, to systematically derive three matching functions in a second step. According to their assumptions regarding how vehicles cover the zone area, we termed the matching functions *degressive*, *constant*, and *infinite coverage rate* matching function (DCR, CCR, and ICR). While the DCR and CCR are novel matching functions, the ICR with its extremely simplified assumptions can be considered as the state-of-the-art matching function, even if not explicitly discussed as such in the SMS literature. In an extensive computational study, we compared the rental prediction accuracy by the matching functions in two settings – the first considering the rentals realization process isolated in a single zone and single period, and the second covering an entire FF SMS network consisting of multiple zones and periods.

The numerical results in the single zone single period setting revealed that the ICR in general overestimates rental: The maximum relative rental prediction errors lie in the range of 10% to more than 100%, depending on the zone size. With the CCR and DCR, the rentals prediction is a lot more accurate: For the CCR, the relative rental prediction errors lie in the range of -30% to 30% and for the DCR in the range of -5% to 5%. In the setting with multiple zones and multiple periods, the relative rental prediction error with the ICR can (in one period) grow up to 100%-500% for medium sized and above 2000% for larger zones. For the CCR, the maximum relative rental prediction error in the relevant periods where many vehicles move lies between -15% and 30% for medium sized and between -30% and 25% for larger zones. These results support the finding that the ICR cannot accurately describe matching in an FF SMS in general and that novel matching functions, like the CCR and DCR are required.

Besides the numerical analyses, we also investigated the matching functions analytically. Most importantly, we demonstrated that only the CCR and DCR have a rentals limit value of zero when the walking distance approaches zero or the zone area grows infinitely large. This demonstrates mathematically that these two functions behave meaningfully with regard to the spatial parameters relevant in FF SMS. Among other theoretical results, we also showed ana-

lytically that the ICR is a special case of the CCR and DCR for extreme cases of large walking distance and/or small zone area size, meaning that in such situations, even the ICR could have some validity for FF SMS.

Several important insights can be concluded from these numerical and analytical results. First, to accurately describe the matching between supply and demand in an FF SMS, multiple relevant parameters have to be considered. Besides the sheer number of available vehicles and arriving customers, the zone size, the customers' maximum willingness-to-walk, successively arriving customers as well as the decreasing marginal zone coverage by additional vehicles play a decisive role. Second, the results show that only the DCR and CCR are suitable for modeling FF SMSs in general, because they do consider all of the above parameters explicitly or implicitly. The ICR in contrast has the structural problem to neglect these additionally relevant parameters and to severely overestimate rentals. Third, the necessity for more comprehensive matching functions depends on the zone sizes and the area within walking distance of the customers. All of the above insights reveal that the previously mentioned and so far unconsidered aspect of matching modeling is indeed central for managing FF SMSs and that matching modeling needs to be considered in the modeling and control of FF SMSs.

Regarding the second central aspect of our work, (2) the integration of the matching functions into FF SMS optimization approaches and the investigation of resulting benefits, we demonstrated that the CCR, opposed to the DCR, can easily be losslessly linearized. Given the vast literature on SMS optimization that use linear network flow-based formulations, this allows the adaptation of the many existing optimization approaches to be generalized such that they can be applied to both SB as well as FF SMSs. To analyze the potential benefits resulting from that, as an example, we considered a pricing optimization approach from literature in a case study based on real data from Share Now.

The numerical results from the case study show that, compared to the pricing solution with the ICR, in the pricing solution from the CCR model high prices are chosen a lot less frequently, i.e. by a factor of 20. Low prices are chosen a lot more frequently, i.e. by a factor of 2 in the CCR pricing solution, such that the different matching functions do actually impact the decision making. The better pricing decisions with the CCR cause significant contribution margin gains over the overall too high prices caused by the overestimation of rentals in the ICR pricing solution. The difference in the resulting contribution margin increase with respect to the base price benchmark was up to 3 percentage points (corresponding to an increase by factors of 1.8 to 2.6) with the pricing solution obtained by the CCR, compared to the ICR – an effect than can be solely ascribed to the more accurate matching modeling (and, thus, in a sense comes for free, compared to marketing or a fleet increase).

The main insight to derive from the pricing optimization case study is that the more accurate matching modeling of the CCR also effects the decision making in a way that benefits the overall objective. Since other FF SMS optimization problems, such as relocation or fleet sizing problems, also rely on accurate rental predictions, it is clear that they would also be affected by an overestimation of rentals. Therefore, it is a managerial task to assess the potential problem of rental overestimation based on the findings in this work and to initiate the recommended adaptations if necessary.

Taking the presented results and insights with regard to (1) and (2) into account, we believe that there are promising directions for future work. First, the consideration of *inter-zone movements* by customers as well as boundary effects at the borders of an operating area might yield improvement potential when considered in the matching modeling. Second, an *empirical study* that focuses on matching in FF SMS would have the potential to identify additional relevant factors, such as for example zone-specific characteristics like its shape or its street network. Third, it would be insightful to investigate how FF SMSs could be modeled accurately in a *spatially (and temporally) continuous* manner, with the intention to circumvent the limitations that inevitably come with the current state-of-the-art approach of spatial (and temporal) discretization. For the latter, continuous optimization techniques might be suitable. Finally, while we considered specific discretization schemes as given in our work, the complex question regarding the discretization itself is an important topic for future research.

4.A Illustration Spatio-Temporal Network

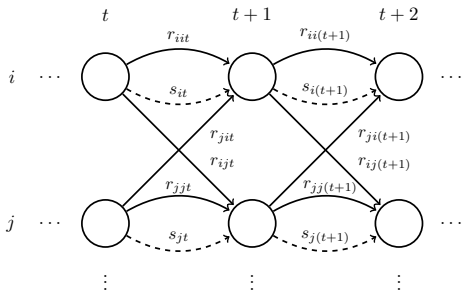

Figure 4.14: Spatio-temporal network

4.B DCR Proof

Proof. If the zone does not contain any vehicles, $A_0 = 0$ and $\bar{A}_0 = A_z$, such that the first vehicle, according to the assumption, covers

$$\Delta A_1 = A_w \cdot \frac{A_z}{A_z} = A_w. \tag{4.15}$$

The remaining uncovered area with one vehicle is $\bar{A}_1 = A_z - A_w$ and the additionally covered area by the second vehicle is

$$\Delta A_2 = A_w \cdot \frac{A_z - A_w}{A_z} = A_w \cdot (1 - \frac{A_w}{A_z}). \tag{4.16}$$

The $\hat{a}^{th}$ vehicle additionally covers

$$\Delta A_{\hat{a}} = A_w \cdot (1 - \frac{A_w}{A_z})^{\hat{a}-1} \; \forall \hat{a} \in \mathbb{Z}^+. \tag{4.17}$$

The total covered area $A_{\hat{a}}$ by $\hat{a}$ vehicles then is

$$A_{\hat{a}} = \sum_{n=1}^{\hat{a}} \Delta A_n = \sum_{n=0}^{\hat{a}-1} \Delta A_{n+1} = A_w \cdot \sum_{n=0}^{\hat{a}-1} (1 - \frac{A_w}{A_z})^n \tag{4.18a}$$

$$= A_w \cdot \frac{1 - (1 - \frac{A_w}{A_z})^{\hat{a}}}{1 - (1 - \frac{A_w}{A_z})} = A_z \cdot (1 - (1 - \frac{A_w}{A_z})^{\hat{a}}), \tag{4.18b}$$

where the fourth equation stems from reformulating the partial sum of the geometric series (with $A_w \neq 0$). Therewith, $P_{A_w,A_z}(\hat{a}) = \frac{A_{\hat{a}}}{A_z} = (1 - (1 - \frac{A_w}{A_z})^{\hat{a}})$ and substituting this in (4.1a) yields (4.2a). □

4.C CCR Parameter Approximation

In this section, we show that the parameters λ and μ, which we introduced in Section 4.3.3.2 can be analytically approximated.

We begin with λ. Following the DCR assumption of degressive coverage of the zone by

additional vehicles according to $\Delta A_a = A_w \cdot (1 - \frac{A_w}{A_z})^{a-1}$, one can reformulate A_a as follows.

$$A_a = \sum_{i=1}^{a} \Delta A_i = A_w \cdot \sum_{i=1}^{a} (1 - \frac{A_w}{A_z})^{i-1} \tag{4.19}$$

$$= A_w \cdot \sum_{i=0}^{a-1} (1 - \frac{A_w}{A_z})^{i} = A_w \cdot \frac{1 - (1 - \frac{A_w}{A_z})^{a}}{1 - (1 - \frac{A_w}{A_z})} \tag{4.20}$$

$$= A_w \cdot \frac{1 - (1 - \frac{A_w}{A_z})^{a}}{\frac{A_w}{A_z}} \tag{4.21}$$

For a known average available vehicle count $\bar{a}$, for example obtained from historical data or preliminary tests in an optimization model, we can formulate

$$A_a \approx A_w \cdot \lambda \cdot a, \tag{4.22}$$

where

$$\lambda = \frac{1 - (1 - \frac{A_w}{A_z})^{\bar{a}}}{\frac{A_w}{A_z}} \cdot \frac{1}{\bar{a}}. \tag{4.23}$$

Note that (4.21) could clearly be further simplified but the way we define λ and use it in (4.22) allows to interpret λ as the fraction of A_w which is in average covered by every additional vehicle.

In the following we derive μ which allows to formulate an average matching probability for every customer and the explicit formulation of the CCR (4.4). Therefore, we consider a certainty equivalent model of the matching process which can be formulated as

$$r_{A_w,A_z}(a,d) = \sum_{i=1}^{d} P_i = \sum_{i=1}^{d} \frac{\min(D_i, A_z)}{A_z}, \tag{4.24}$$

where P_i denotes the matching probability and D_i the area covered by the remaining available vehicles when the i^{th} customer arrives. In this expectation model, the coverage changes for every customer according to $D_{i+1} = D_i - P_i \cdot \Delta D$, where ΔD is the marginal coverage by one vehicle.

We first consider the case that $D_i \leq A_z$, such that the first argument of the min()-operator in (4.24) is restrictive, therewith $D_{i+1} = D_i \cdot (1 - \frac{\Delta D}{A_z})$, and the expectation model becomes

$$r_{A_w,A_z}(a,d) = \frac{D_1}{A_z} \cdot \sum_{i=1}^{d} (1 - \frac{\Delta D}{A_z})^{i-1}. \tag{4.25}$$

With $\Delta D = A_w \cdot \lambda$ and $D_1 = A_w \cdot \lambda \cdot a$ this yields

$$r_{A_w,A_z}(a,d) = \frac{A_w}{A_z} \cdot \lambda \cdot a \cdot \sum_{i=1}^{d} (1 - \frac{A_w \cdot \lambda}{A_z})^{i-1}, \tag{4.26}$$

where the last factor can be approximated by $\mu \cdot d$ with a known average $\bar{d}$ and

$$\mu \approx \frac{1}{\bar{d}} \cdot \sum_{i=1}^{\bar{d}} (1 - \frac{A_w \cdot \lambda}{A_z})^{i-1}, \tag{4.27}$$

such that (4.26) becomes

$$r_{A_w,A_z}(a,d) = \frac{A_w}{A_z} \cdot \lambda \cdot \mu \cdot a \cdot d. \tag{4.28}$$

Above, we considered that $D_i \leq A_z$ but with the constant coverage assumption $\Delta D = A_w \cdot \lambda$ this is not given in general such that the rentals could exceed the arriving customers. Furthermore, the assumption of an average matching probability neglects that all vehicles might be taken for some of the arriving customers such that the rentals could exceed the initial available vehicles count. Therefore, we need to introduce these two constraints back in the expectation model and obtain

$$r_{A_w,A_z}(a,d) = \min(\frac{A_w}{A_z} \cdot \lambda \cdot \mu \cdot a \cdot d, a, d), \tag{4.29}$$

which is exactly the CCR matching function in (4.5).

4.D Symmetry Proof of DCR

4.D.1 Idea of the Proof

To simplify notation in this outline, we use $r(a,d)$ and $r(d,a)$ instead of $r^{DCR}_{A_w,A_z}(\hat{a},\hat{d})$ and $r^{DCR}_{A_w,A_z}(\hat{d},\hat{a})$ here, so we prove $r(a,d) = r(d,a)$.

The proof is by induction over $n = a + d$. In the base cases, we show that $r(a,d) = r(d,a)$ for $n = 0$ and $n = 1$. This is straightforward, using the boundary conditions. In the induction step, we show that if $r(a,d) = r(d,a)$ for $n-2$ and $n-1$ (induction hypothesis), symmetry also holds for n.

The key idea of the proof is illustrated by the two subfigures in Figure 4.15. Each shows a grid of a-d combinations where every node represents the value of the respective $r(a,d)$. The dotted line on the diagonal represents the symmetry axis. The three dashed lines on the secondary diagonals illustrate the procedure of the induction: Every n has a corresponding secondary diagonal where symmetry holds, illustrated for $n = 0$, $n = 1$, and $n = 2$. The induction step can be interpreted as an upward shift of the secondary diagonal, using the previous secondary diagonals.

Illustratively, we need to prove equality of a node and its symmetric counterpart which results from mirroring the original node on the diagonal. Without loss of generality, we define nodes I and I′ to correspond to $r(a,d)$ and $r(d,a)$, respectively. We prove equality for these two (general) nodes I and I′. The other nodes denoted by roman numbers illustrate which nodes – in dependence of I and I′ – are used to show this equality. The proof consists of three steps:

(1) First, we show that node I can be expressed as a sum with summands corresponding to nodes III′, IV′, V′, and VI′ – the nodes within the dashed square in Figure 4.15a.

(2) Second, we analogously show that node I′ can be expressed as a sum with summands corresponding to nodes III, IV, V, and VI – the nodes within the dashed square in Figure 4.15b.

(3) Third, we show equality of the two resulting sums which completes the proof.

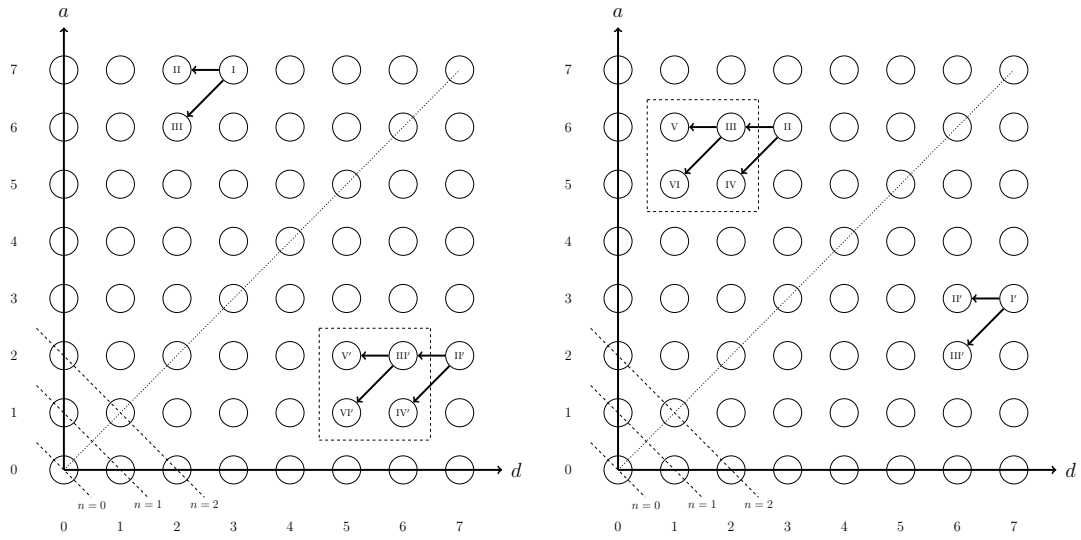

(a) Step one

(b) Step two

Figure 4.15: Illustration of the DCR symmetry proof (see Property 5)

More precisely, two different operations are performed (multiple times) within these three steps: Applying the recursion of the DCR and using the symmetry property in the induction hypothesis. In step (1) of the proof (consider the DCR (4.2a)), applying the recursion for $r(a, d)$ (I) yields a sum with two summands, one with $r(a, d-1)$ (II) and one with $r(a-1, d-1)$ (III), as illustrated in Figure 4.15a. Since the induction hypothesis supposes that the symmetry property holds for $n-1$ and $n-2$, nodes II and III have corresponding counterpart nodes II′ with $r(d-1, a) = r(a, d-1)$ and III′ with $r(d-1, a-1) = r(a-1, d-1)$. Subsequently applying recursion for both nodes II′ and III′ yields a sum with four summands, i.e. one each corresponding to nodes III′, IV′, V′, and VI′. Analogously in step (2) of the proof, starting with node I′ yields a sum with summands corresponding to nodes III, IV, V, and VI, as illustrated in Figure 4.15b. Finally, in step (3) of the proof, we then again use the induction hypothesis (twice) and show that the two resulting sums of $r(a, d)$ and $r(d, a)$ are equal. This completes the proof.

4.D.2 Formal Proof

To prove symmetry of the DCR (4.2), we need to show

$$r^{DCR}_{it,A_w,A_z}(\hat{a}_{it}, \hat{d}_{it}) = r^{DCR}_{it,A_w,A_z}(\hat{d}_{it}, \hat{a}_{it}). \tag{4.30}$$

To simplify notation, we use $r(a, d)$ and $r(d, a)$ instead of $r^{DCR}_{it,A_w,A_z}(\hat{a}_{it}, \hat{d}_{it})$ and $r^{DCR}_{it,A_w,A_z}(\hat{d}_{it}, \hat{a}_{it})$ here, so we need to show

$$r(a, d) = r(d, a). \tag{4.31}$$

Further, we introduce $\alpha = (1 - \frac{A_w}{A_z})$, such that the original DCR (4.2) results in

$$r(a,d) = (1-\alpha^a)\cdot(1+r(a-1,d-1)) + \alpha^a \cdot r(a,d-1) \tag{4.32}$$

$$r(a,0) = 0 \qquad \forall a \in \mathbb{Z} \tag{4.33}$$

$$r(0,d) = 0. \qquad \forall d \in \mathbb{Z} \tag{4.34}$$

The proof is performed by induction over $n = a + d$.

Base Cases: *$r(a,d) = r(d,a)$ for $a + d = 0$ and $a + d = 1$.*

$a + d = 0$: According to the boundary conditions (4.33) and (4.34), $r(a,d) = r(d,a) = 0$ if $a = d = 0$.

$a + d = 1$: According to the boundary conditions (4.33) and (4.34), $r(a,d) = r(d,a) = 0$ if $a = 0$ or $d = 0$.

Induction Hypothesis. *$r(a,d) = r(d,a)$ for $a + d = n - 2$ and $a + d = n - 1$, with $n \in \mathbb{Z}$.*

Induction Step. *If $r(a,d) = r(d,a)$ for $a + d = n - 2$ and $a + d = n - 1$, then $r(a,d) = r(d,a)$ for $a + d = n$ $\forall n \in \mathbb{Z}$.*

We first prove three lemmata which we then apply to prove the induction step.

Lemma 1.

$$\begin{aligned} &\alpha^{a-1} + \alpha^{a-1}\cdot r(a-2,d-2) - \alpha^{a-1}\cdot r(a-1,d-2) \\ &= \alpha^{d-1} + \alpha^{d-1}\cdot r(a-2,d-2) - \alpha^{d-1}\cdot r(a-2,d-1) \end{aligned} \tag{4.35}$$

According to the induction hypothesis, symmetry holds for $a + d = n - 2$, i.e. $r(a-1,d-1) = r(d-1,a-1)$. Starting with this, we show Lemma 1 by means of equivalent transformations.

$$\begin{aligned} & r(a-1,d-1) = r(d-1,a-1) \\ \iff \quad & (1-\alpha^{a-1})\cdot(1+r(a-2,d-2)) + \alpha^{a-1}\cdot r(a-1,d-2) \\ & = (1-\alpha^{d-1})\cdot(1+r(d-2,a-2)) + \alpha^{d-1}\cdot r(d-1,a-2) \\ \iff \quad & (1-\alpha^{a-1}) + (1-\alpha^{a-1})\cdot r(a-2,d-2) + \alpha^{a-1}\cdot r(a-1,d-2) \\ & = (1-\alpha^{d-1}) + (1-\alpha^{d-1})\cdot r(a-2,d-2) + \alpha^{d-1}\cdot r(d-1,a-2) \\ \iff \quad & \alpha^{a-1} + \alpha^{a-1}\cdot r(a-2,d-2) - \alpha^{a-1}\cdot r(a-1,d-2) \\ & = \alpha^{d-1} + \alpha^{d-1}\cdot r(a-2,d-2) - \alpha^{d-1}\cdot r(a-2,d-1) \qquad \square \end{aligned} \tag{4.36}$$

Lemma 2.

$$\begin{aligned} r(a,d) = {} & (1-\alpha^a) + (1-\alpha^{d-1}) \\ & + (1-\alpha^a)\cdot(1-\alpha^{d-1})\cdot r(d-2,a-2) \\ & + (1-\alpha^a)\cdot\alpha^{d-1}\cdot r(d-1,a-2) \\ & + \alpha^a\cdot(1-\alpha^{d-1})\cdot r(d-2,a-1) \\ & + \alpha^a\cdot\alpha^{d-1}\cdot r(d-1,a-1) \end{aligned} \tag{4.37}$$

We prove Lemma 2 by starting with the recursion of $r(a,d)$:

$$r(a,d) = (1-\alpha^a)\cdot(1+r(a-1,d-1)) + \alpha^a \cdot r(a,d-1) \tag{4.38}$$

We want so substitute $r(a-1,d-1)$ and $r(a,d-1)$ in (4.38) and therefore apply symmetry according to the induction hypothesis for $a+d=n-2$ and $a+d=n-1$:

$$\begin{aligned} r(a-1,d-1) &= r(d-1,a-1) \\ &= (1-\alpha^{d-1})\cdot(1+r(d-2,a-2)) + \alpha^{d-1}\cdot r(d-1,a-2) \end{aligned} \tag{4.39}$$

$$\begin{aligned} r(a,d-1) &= r(d-1,a) \\ &= (1-\alpha^{d-1})\cdot(1+r(d-2,a-1)) + \alpha^{d-1}\cdot r(d-1,a-1) \end{aligned} \tag{4.40}$$

We now substitute (4.39) and (4.40) in (4.38) and simplify the summands without $r(\cdot,\cdot)$:

$$\begin{aligned} r(a,d) &= (1-\alpha^a)\cdot\left[1+(1-\alpha^{d-1})\cdot(1+r(d-2,a-2)) + \alpha^{d-1}\cdot r(d-1,a-2)\right] \\ &\quad + \alpha^a\cdot\left[(1-\alpha^{d-1})\cdot(1+r(d-2,a-1)) + \alpha^{d-1}\cdot r(d-1,a-1)\right] \\ &= (1-\alpha^a) + (1-\alpha^a)\cdot(1-\alpha^{d-1}) + \alpha^a\cdot(1-\alpha^{d-1}) \\ &\quad + (1-\alpha^a)\cdot(1-\alpha^{d-1})\cdot r(d-2,a-2) \\ &\quad + (1-\alpha^a)\cdot\alpha^{d-1}\cdot r(d-1,a-2) \\ &\quad + \alpha^a\cdot(1-\alpha^{d-1})\cdot r(d-2,a-1) \\ &\quad + \alpha^a\cdot\alpha^{d-1}\cdot r(d-1,a-1) \\ &= (1-\alpha^a) + (1-\alpha^{d-1}) \\ &\quad + (1-\alpha^a)\cdot(1-\alpha^{d-1})\cdot r(d-2,a-2) \\ &\quad + (1-\alpha^a)\cdot\alpha^{d-1}\cdot r(d-1,a-2) \\ &\quad + \alpha^a\cdot(1-\alpha^{d-1})\cdot r(d-2,a-1) \\ &\quad + \alpha^a\cdot\alpha^{d-1}\cdot r(d-1,a-1) \end{aligned} \tag{4.41}$$

□

Lemma 3.

$$\begin{aligned} r(d,a) &= (1-\alpha^d) + (1-\alpha^{a-1}) \\ &\quad + (1-\alpha^d)\cdot(1-\alpha^{a-1})\cdot r(a-2,d-2) \\ &\quad + (1-\alpha^d)\cdot\alpha^{a-1}\cdot r(a-1,d-2) \\ &\quad + \alpha^d\cdot(1-\alpha^{a-1})\cdot r(a-2,d-1) \\ &\quad + \alpha^d\cdot\alpha^{a-1}\cdot r(a-1,d-1) \end{aligned} \tag{4.42}$$

The proof of Lemma 3 is analogous to Lemma 2, beginning with $r(d,a)$. □

Proof of Induction Step.
We show $r(a,d) = r(d,a)$, by means of equivalent transformations and by using Lemmata 1-3.

$$
\begin{aligned}
& r(a,d) \\
& = \textit{(Lemma 2)} \\
& (1-\alpha^a) + (1-\alpha^{d-1}) \\
& + (1-\alpha^a)\cdot(1-\alpha^{d-1})\cdot r(d-2,a-2) \\
& + (1-\alpha^a)\cdot\alpha^{d-1}\cdot r(d-1,a-2) \\
& + \alpha^a\cdot(1-\alpha^{d-1})\cdot r(d-2,a-1) \\
& + \alpha^a\cdot\alpha^{d-1}\cdot r(d-1,a-1) \\
& = \textit{(Rearrangement)} \\
& (1-\alpha^a) + (1-\alpha^{d-1}) \\
& + r(a-2,d-2) - \alpha^{d-1}\cdot r(a-2,d-2) - \alpha^a\cdot r(a-2,d-2) + \alpha^{a+d-1}\cdot r(a-2,d-2) \\
& + \alpha^{d-1}\cdot r(a-2,d-1) - \alpha^{a+d-1}\cdot r(a-2,d-1) \\
& + \alpha^a\cdot r(a-1,d-2) - \alpha^{a+d-1}\cdot r(a-1,d-2) \\
& + \alpha^{a+d-1}\cdot r(a-1,d-1) \\
& = \textit{(Use Lemma 1 to substitute summands with } \alpha^{d-1}\textit{)} \\
& (1-\alpha^a) + (1-\alpha^{a-1}) \\
& + r(a-2,d-2) - \alpha^{a-1}\cdot r(a-2,d-2) - \alpha^a\cdot r(a-2,d-2) + \alpha^{a+d-1}\cdot r(a-2,d-2) \\
& + \alpha^{a-1}\cdot r(a-1,d-2) - \alpha^{a+d-1}\cdot r(a-2,d-1) \\
& + \alpha^a\cdot r(a-1,d-2) - \alpha^{a+d-1}\cdot r(a-1,d-2) \\
& + \alpha^{a+d-1}\cdot r(a-1,d-1) \\
& = \textit{(Use Lemma 1 multiplied with } \alpha \textit{ to substitute summands with } \alpha^a\textit{)} \\
& (1-\alpha^d) + (1-\alpha^{a-1}) \\
& + r(a-2,d-2) - \alpha^{a-1}\cdot r(a-2,d-2) - \alpha^d\cdot r(a-2,d-2) + \alpha^{a+d-1}\cdot r(a-2,d-2) \\
& + \alpha^{a-1}\cdot r(a-1,d-2) - \alpha^{a+d-1}\cdot r(a-1,d-2) \\
& + \alpha^d\cdot r(a-2,d-1) - \alpha^{a+d-1}\cdot r(a-2,d-1) \\
& + \alpha^{a+d-1}\cdot r(a-1,d-1) \\
& = \textit{(Rearrangement)} \\
& (1-\alpha^d) + (1-\alpha^{a-1}) \\
& + (1-\alpha^d)\cdot(1-\alpha^{a-1})\cdot r(a-2,d-2) \\
& + (1-\alpha^d)\cdot\alpha^{a-1}\cdot r(a-1,d-2) \\
& + \alpha^d\cdot(1-\alpha^{a-1})\cdot r(a-2,d-1) \\
& + \alpha^d\cdot\alpha^{a-1}\cdot r(a-1,d-1) \\
& = \textit{(Lemma 3)} \\
& r(d,a)
\end{aligned}
\tag{4.43}
$$

This completes the proof. □

4.E SZSP Simulation

Algorithm 6 SZSP simulation (one run $n \in \mathcal{N}$)

- draw position for each of the a vehicles from uniform distribution
- initialize rental count: $r_n = 0$
- initialize customers to come $\hat{d} = d$
while $\hat{d} > 0$ **do**
  - draw arrival position of customer from uniform distribution
  - determine distance to vehicles
  if at least one vehicle in walking distance **then**
    - choose closest vehicle
    - remove chosen vehicle
    - record rental: $r_n \leftarrow r_n + 1$
  end if
  - reduce customers to come: $\hat{d} \leftarrow \hat{d} - 1$
end while

4.F The Origin-Based Differentiated Pricing Problem in Free-Floating Shared Mobility Systems

To allows for the optimization of FF SMSs, we in this section integrate the CCR in the origin-based differentiated pricing problem (OBDPP) in SMSs as defined by (Soppert et al., 2022) that assumes matching according to the ICR, here denoted as OBDPP-ICR. We denote the resulting problem with CCR (4.44)-(4.58) the OBDPP-CCR. Table 4.2 summarizes the nomenclature.

$$\max_{\mathbf{y},\mathbf{q},\mathbf{r},\mathbf{a},\mathbf{s}} \quad \sum_{t\in\mathcal{T}}\sum_{i\in\mathcal{Z}}\sum_{j\in\mathcal{Z}}\sum_{m\in\mathcal{M}} r_{ijt}^m \cdot l_{ij} \cdot (p^m - c) \tag{4.44}$$

s.t.

$$a_{it} = \sum_{j\in\mathcal{Z}}\sum_{m\in\mathcal{M}} r_{ijt}^m + s_{it} \qquad \forall i \in \mathcal{Z}, t \in \mathcal{T} \tag{4.45}$$

$$\sum_{i\in\mathcal{Z}}\sum_{m\in\mathcal{M}} r_{ijt}^m + s_{jt} = a_{j(t+1)} \qquad \forall j \in \mathcal{Z}, t \in \mathcal{T} \tag{4.46}$$

$$a_{i0} = \hat{a}_{i0} \qquad \forall i \in \mathcal{Z} \tag{4.47}$$

$$\sum_{m\in\mathcal{M}} y_{it}^m = 1 \qquad \forall i \in \mathcal{Z}, t \in \mathcal{T} \tag{4.48}$$

$$r_{ijt}^m \leq d_{ijt}^m \cdot y_{it}^m \qquad \forall i,j \in \mathcal{Z}, t \in \mathcal{T}, m \in \mathcal{M} \tag{4.49}$$

$$r_{ijt}^m \leq d_{ijt}^m / \sum_{k\in\mathcal{Z}} d_{ikt}^m \cdot \gamma_{it}^m \cdot a_{it} \qquad \forall i,j \in \mathcal{Z}, t \in \mathcal{T}, m \in \mathcal{M} \tag{4.50}$$

$$\sum_{j\in\mathcal{Z}} d_{ijt}^m \cdot y_{it}^m - \gamma_{it}^m \cdot a_{it} \leq \bar{M} \cdot q_{it}^m \qquad \forall i \in \mathcal{Z}, t \in \mathcal{T}, m \in \mathcal{M} \tag{4.51}$$

$$\sum_{j\in\mathcal{Z}} -d_{ijt}^m \cdot y_{it}^m + \gamma_{it}^m \cdot a_{it} \leq \bar{M} \cdot (1 - q_{it}^m) \qquad \forall i \in \mathcal{Z}, t \in \mathcal{T}, m \in \mathcal{M} \tag{4.52}$$

$$d_{ijt}^m \cdot y_{it}^m \leq r_{ijt}^m + \bar{M} \cdot q_{it}^m \qquad \forall i,j \in \mathcal{Z}, t \in \mathcal{T}, m \in \mathcal{M} \tag{4.53}$$

$$d_{ijt}^m / \sum_{k\in\mathcal{Z}} d_{ikt}^m \cdot \gamma_{it}^m \cdot a_{it} \leq r_{ijt}^m + \bar{M} \cdot (1 - q_{it}^m) + \bar{M} \cdot (1 - y_{it}^m) \qquad \forall i,j \in \mathcal{Z}, t \in \mathcal{T}, m \in \mathcal{M} \tag{4.54}$$

$$y_{it}^m, q_{it}^m \in \{0,1\} \qquad \forall i \in \mathcal{Z}, t \in \mathcal{T}, m \in \mathcal{M} \tag{4.55}$$

$$r_{ijt}^m \in \mathbb{R}_0^+ \qquad \forall i,j \in \mathcal{Z}, t \in \mathcal{T}, m \in \mathcal{M} \tag{4.56}$$

$$s_{it} \in \mathbb{R}_0^+ \qquad \forall i \in \mathcal{Z}, t \in \mathcal{T} \tag{4.57}$$

$$a_{it} \in \mathbb{R}_0^+ \qquad \forall i \in \mathcal{Z}, t \in \{0,1,\ldots,T\} \tag{4.58}$$

The central decision variables are $\mathbf{y} = [y_{it}^m]_{Z\times T\times M}$ where y_{it}^m is binary and takes the value 1, if and only if price p^m with $m \in \mathcal{M}$ was set in location $i \in \mathcal{Z}$ at period $t \in \mathcal{T}$. The continuous decision variables $\mathbf{a} = [a_{it}]_{Z\times(T+1)}$ describe the number of available vehicles for a certain *i-t* combination. $\mathbf{r} = [r_{ijt}^m]_{Z\times Z\times T\times M}$ is the vector of rentals where the continuous decision variable r_{ijt}^m describes the rentals at price p^m that realize from location i to location j during period t. $\mathbf{s} = [s_{it}]_{Z\times T}$ describes the vehicles that remain unused in a certain *i-t* combination and these decision variables are continuous as well. The vector of auxiliary decision variables $\mathbf{q} = [q_{it}^m]_{Z\times T\times M}$ is required to set the ensure the rentals realization according to the CCR (4.11).

The objective function (4.44) maximizes the contribution margin of the SMS. It considers the revenue which is generated by the rentals of duration l_{ij} at price p^m, minus the respective variable costs per minute c. Constraints (4.45) and (4.46) formulate the flow balance, where in

(4.45), for example, the available vehicles are either rented or remain in the same location. With Constraints (4.47), the vehicle count for all locations $i \in \mathcal{Z}$ is initialized by $\hat{a}_{i0}$. Constraints (4.48) ensure, that only one price can be set for a certain location-time combination.

All other constraints form the linearized CCR. Constraints (4.49) and (4.50) are the upper bounds and represent the horizontal, and the first piece, respectively, from Figure 4.3b. Note that if the first piece of the CCR is restrictive, meaning (4.50) is restrictive, the rentals split proportionally according to the demand, analogous to OBDPP-ICR. Note further that if a certain price is not set, (4.49) forces the respective rentals to be zero. The lower bounds on the rentals have to be set in dependence of which price is set and which part of the piece-wise linear function is active. Therefore constraints (4.51) and (4.52) ensure that the auxiliary variable q_{it}^m is 1, if and only if price p^m was set at the respective i-t combination and if and only if the first piece shall be active. In this case, when $q_{it}^m = 1$ and $y_{it}^m = 1$ the respective constraint (4.54) puts a lower bound on the rentals. If $q_{it}^m = 0$ and $y_{it}^m = 1$, the respective constraint (4.53) is active. The difference to the original OBDPP consists in the introduction of γ_{it}^m, the adaptation of the auxiliary variables $\mathbf{q}$, now dependent on m and with different meaning, and the respective constraints (4.50)-(4.54).

The original OBDPP-ICR was proven to be NP-hard (Soppert et al., 2022). Since the ICR is a special case of the CCR, obviously, also the OBDPP-ICR is a special case of the OBDPP-CCR. The OBDPP-CCR therewith is NP-hard as well.

(Decision) variables

a_{it}	vehicles available in i at t, $a_{it} \in \mathbb{R}_0^+$
r_{ijt}^m	vehicles rented from i to j during t when price m was set, $r_{ijt}^m \in \mathbb{R}_0^+$
s_{it}	vehicles not rented, meaning vehicles that remain in i during t, $s_{it} \in \mathbb{R}_0^+$
y_{it}^m	pricing decision variable, describing if price m is set in i at t, $y_{it}^m \in \{0,1\}$
q_{it}^m	auxiliary variable, $q_{it}^m \in \{0,1\}$

Sets

$\mathcal{Z}$	set of stations
$\mathcal{T}$	set of time periods
$\mathcal{M}$	set of price indices
$\mathbf{y}$	$= \{y_{it}^m \quad \forall i \in \mathcal{Z}, t \in \mathcal{T}, m \in \mathcal{M}\}$
$\mathbf{q}$	$= \{q_{it}^m \quad \forall i \in \mathcal{Z}, t \in \mathcal{T}, m \in \mathcal{M}\}$
$\mathbf{r}$	$= \{r_{ijt}^m \quad \forall i, j \in \mathcal{Z}, t \in \mathcal{T}, m \in \mathcal{M}\}$
$\mathbf{s}$	$= \{s_{it} \quad \forall i \in \mathcal{Z}, t \in \mathcal{T}\}$

Parameters and indices

$i, j, k \in \mathcal{Z}$	location index
$t \in \mathcal{T}$	period index
$m \in \mathcal{M}$	price index
p^m	price
f_{ijt}^m	sensitivity for price p^m for i-j-t combination
d_{ijt}	basic demand from i to j during t at base price
d_{ijt}^m	actual demand from i to j during t for price p^m, $d_{ijt}^m = d_{ijt} \cdot f_{ijt}^m$
$\hat{a}_{i0}$	initial number of available vehicles in i
c	variable costs per minute
l_{ij}	average duration of rental in minutes from i to j
M	sufficiently large number

Table 4.2: List of (decision) variables, sets, parameters and indices for the OBDPP-CCR (4.44)-(4.58)

4.G Single Zone, Single Period Setting - Additional Results

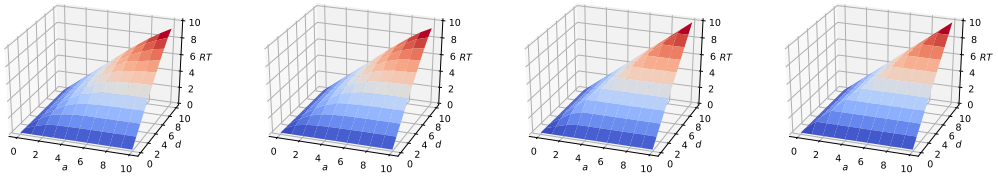

(a1) SIM (a2) DCR (a3) CCR (a4) ICR

(a) $A_z = 0.5$ km^2

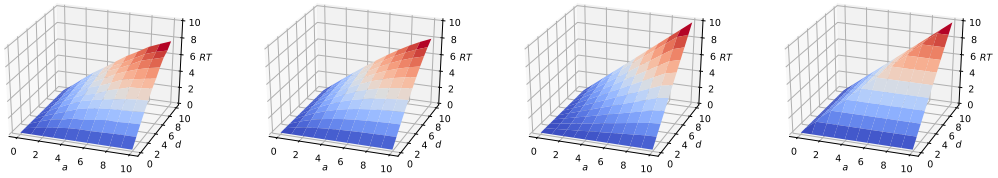

(b1) SIM (b2) DCR (b3) CCR (b4) ICR

(b) $A_z = 1$ km^2

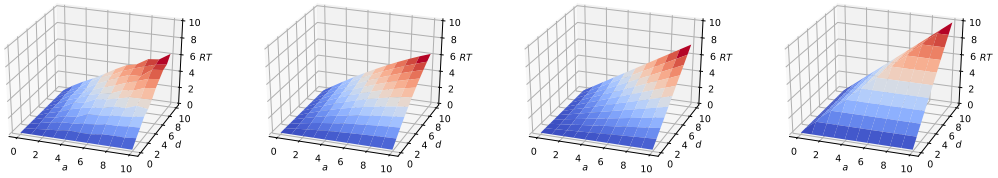

(c1) SIM (c2) DCR (c3) CCR (c4) ICR

(c) $A_z = 2$ km^2

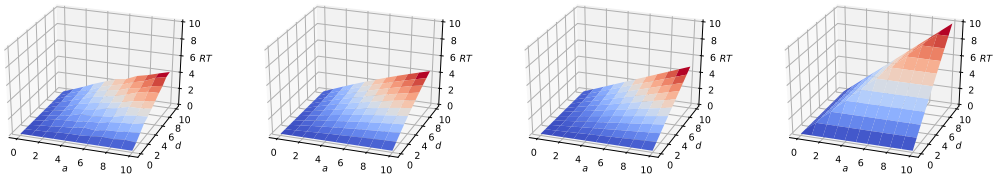

(d1) SIM (d2) DCR (d3) CCR (d4) ICR

(d) $A_z = 4$ km^2

Figure 4.16: Mean (SIM) and predicted (DCR, CCR, ICR) rentals RT in SZSP-scenarios with $A_z = 0.5$ km$^2, 1$ km$^2, 2$ km$^2, 4$ km^2

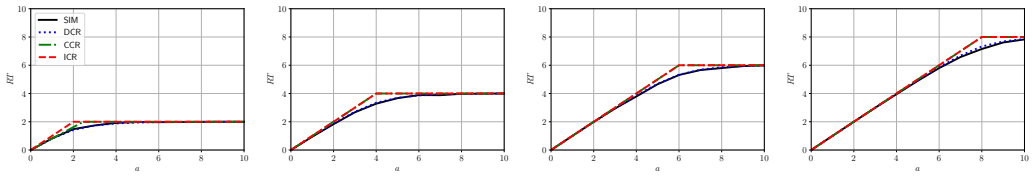

(a1) $\hat{d} = 2$ (a2) $\hat{d} = 4$ (a3) $\hat{d} = 6$ (a4) $\hat{d} = 8$

(a) $A_z = 0.5$ km^2

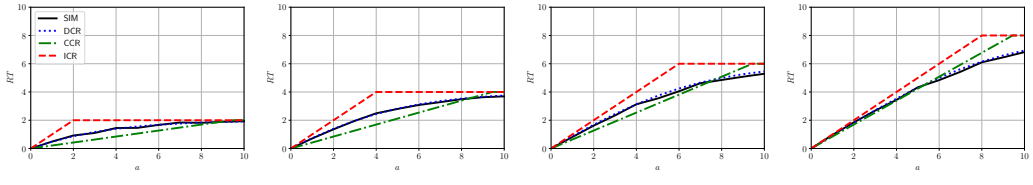

(b1) $\hat{d} = 2$ (b2) $\hat{d} = 4$ (b3) $\hat{d} = 6$ (b4) $\hat{d} = 8$

(b) $A_z = 1$ km^2

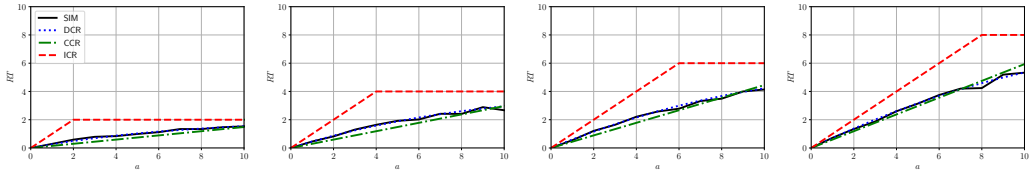

(c1) $\hat{d} = 2$ (c2) $\hat{d} = 4$ (c3) $\hat{d} = 6$ (c4) $\hat{d} = 8$

(c) $A_z = 2$ km^2

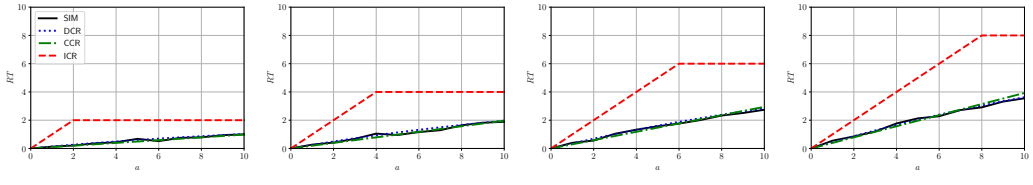

(d1) $\hat{d} = 2$ (d2) $\hat{d} = 4$ (d3) $\hat{d} = 6$ (d4) $\hat{d} = 8$

(d) $A_z = 4$ km^2

Figure 4.17: Mean (SIM) and predicted (DCR, CCR, ICR) rentals RT in SZSP-scenarios with $A_z = 0.5$ km$^2, 1$ km$^2, 2$ km$^2, 4$ km^2 and demand values $\hat{d} = 2, 4, 6, 8$

		d										
		0	1	2	3	4	5	6	7	8	9	10
a	0	0.00	0.00	0.00	0.00	0.00	0.00	0.00	0.00	0.00	0.00	0.00
	1	0.00	0.10	-0.03	-0.02	-0.01	-0.01	-0.01	0.01	0.00	0.00	0.00
	2	0.00	-0.01	-0.06	0.00	-0.04	-0.03	0.01	0.01	0.01	0.00	0.00
	3	0.00	0.03	0.15	0.06	0.04	0.04	0.00	0.00	0.02	0.01	0.00
	4	0.00	0.02	0.05	0.04	0.06	0.02	-0.03	0.06	-0.01	0.00	0.00
	5	0.00	0.01	0.06	-0.01	0.14	0.07	0.01	0.05	0.02	-0.01	0.00
	6	0.00	-0.01	-0.01	0.00	0.07	0.03	0.02	0.03	0.06	0.00	-0.02
	7	0.00	0.00	-0.01	-0.01	0.01	0.09	0.10	0.03	0.19	0.13	0.00
	8	0.00	0.00	0.00	0.00	0.02	0.04	0.06	0.11	0.18	0.07	0.03
	9	0.00	0.00	0.01	0.00	0.04	0.06	0.00	0.06	0.05	0.14	0.01
	10	0.00	0.00	0.00	0.01	0.00	0.00	0.00	0.04	0.07	0.10	0.05

(a) DCR - [-0.06,0.19]

		d										
		0	1	2	3	4	5	6	7	8	9	10
a	0	0.00	0.00	0.00	0.00	0.00	0.00	0.00	0.00	0.00	0.00	0.00
	1	0.00	-0.06	-0.03	0.06	0.03	0.01	0.00	0.01	0.00	0.00	0.00
	2	0.00	-0.01	0.14	0.26	0.08	0.02	0.03	0.02	0.01	0.00	0.00
	3	0.00	0.11	0.41	0.69	0.33	0.17	0.06	0.03	0.03	0.01	0.00
	4	0.00	0.06	0.17	0.33	0.72	0.33	0.11	0.12	0.02	0.01	0.00
	5	0.00	0.03	0.11	0.12	0.45	0.74	0.32	0.19	0.08	0.02	0.01
	6	0.00	0.00	0.01	0.06	0.21	0.34	0.69	0.34	0.20	0.06	0.01
	7	0.00	0.00	0.00	0.02	0.07	0.23	0.41	0.70	0.50	0.27	0.06
	8	0.00	0.00	0.00	0.01	0.05	0.10	0.20	0.42	0.85	0.39	0.17
	9	0.00	0.00	0.01	0.00	0.05	0.09	0.06	0.20	0.37	0.81	0.33
	10	0.00	0.00	0.00	0.01	0.00	0.01	0.03	0.10	0.21	0.42	0.72

(b) CCR - [-0.06,0.85]

		d										
		0	1	2	3	4	5	6	7	8	9	10
a	0	0.00	0.00	0.00	0.00	0.00	0.00	0.00	0.00	0.00	0.00	0.00
	1	0.00	0.53	0.16	0.06	0.03	0.01	0.00	0.01	0.00	0.00	0.00
	2	0.00	0.18	0.52	0.26	0.08	0.02	0.03	0.02	0.01	0.00	0.00
	3	0.00	0.11	0.41	0.69	0.33	0.17	0.06	0.03	0.03	0.01	0.00
	4	0.00	0.06	0.17	0.33	0.72	0.33	0.11	0.12	0.02	0.01	0.00
	5	0.00	0.03	0.11	0.12	0.45	0.74	0.32	0.19	0.08	0.02	0.01
	6	0.00	0.00	0.01	0.06	0.21	0.34	0.69	0.34	0.20	0.06	0.01
	7	0.00	0.00	0.00	0.02	0.07	0.23	0.41	0.70	0.50	0.27	0.06
	8	0.00	0.00	0.00	0.01	0.05	0.10	0.20	0.42	0.85	0.39	0.17
	9	0.00	0.00	0.01	0.00	0.05	0.09	0.06	0.20	0.37	0.81	0.33
	10	0.00	0.00	0.00	0.01	0.00	0.01	0.03	0.10	0.21	0.42	0.72

(c) ICR - [0.00,0.85]

		d										
		0	1	2	3	4	5	6	7	8	9	10
a	0	0.00	0.00	0.00	0.00	0.00	0.00	0.00	0.00	0.00	0.00	0.00
	1	0.00	0.02	0.05	-0.03	-0.07	-0.06	0.00	0.01	-0.02	-0.01	-0.01
	2	0.00	0.00	-0.05	0.07	-0.06	0.10	0.01	-0.07	0.01	-0.01	-0.02
	3	0.00	0.01	0.06	0.07	-0.08	-0.10	-0.08	-0.06	0.01	0.06	0.00
	4	0.00	0.03	0.03	0.00	-0.05	0.03	0.05	0.08	0.04	0.03	0.06
	5	0.00	0.00	-0.03	0.01	0.06	0.25	0.09	0.06	-0.09	0.04	0.02
	6	0.00	0.05	0.06	0.10	0.00	0.19	0.19	0.04	0.15	0.18	0.17
	7	0.00	0.05	0.01	0.11	0.07	0.15	0.07	0.08	0.08	0.09	0.10
	8	0.00	-0.03	-0.02	0.02	0.09	-0.03	0.16	0.19	0.05	0.14	0.12
	9	0.00	-0.02	-0.01	0.05	0.08	0.10	0.23	0.24	0.19	0.26	0.40
	10	0.00	0.05	0.00	0.00	0.10	0.11	0.10	0.18	0.14	0.24	0.30

(d) DCR - [-0.10, 0.40]

		d										
		0	1	2	3	4	5	6	7	8	9	10
a	0	0.00	0.00	0.00	0.00	0.00	0.00	0.00	0.00	0.00	0.00	0.00
	1	0.00	-0.15	-0.23	-0.34	-0.39	-0.34	-0.22	-0.15	-0.10	-0.01	0.03
	2	0.00	-0.28	-0.50	-0.46	-0.60	-0.40	-0.40	-0.36	-0.13	0.02	0.07
	3	0.00	-0.30	-0.47	-0.59	-0.77	-0.75	-0.61	-0.43	-0.15	0.13	0.15
	4	0.00	-0.29	-0.51	-0.69	-0.80	-0.68	-0.54	-0.32	-0.10	0.18	0.31
	5	0.00	-0.28	-0.53	-0.64	-0.65	-0.42	-0.46	-0.28	-0.16	0.31	0.39
	6	0.00	-0.17	-0.35	-0.43	-0.59	-0.36	-0.24	-0.17	0.23	0.64	0.71
	7	0.00	-0.11	-0.28	-0.26	-0.33	-0.19	-0.14	0.08	0.39	0.80	0.87
	8	0.00	-0.11	-0.16	-0.14	-0.05	-0.10	0.24	0.50	0.68	1.17	1.18
	9	0.00	-0.02	0.02	0.12	0.23	0.37	0.69	0.95	1.22	1.72	1.84
	10	0.00	0.09	0.09	0.15	0.35	0.48	0.64	0.95	1.20	1.68	2.20

(e) CCR - [-0.80,2.20]

		d										
		0	1	2	3	4	5	6	7	8	9	10
a	0	0.00	0.00	0.00	0.00	0.00	0.00	0.00	0.00	0.00	0.00	0.00
	1	0.00	0.74	0.56	0.34	0.19	0.13	0.14	0.11	0.05	0.04	0.03
	2	0.00	0.51	1.08	0.90	0.55	0.54	0.33	0.16	0.18	0.11	0.07
	3	0.00	0.38	0.89	1.46	0.96	0.66	0.48	0.35	0.31	0.27	0.15
	4	0.00	0.29	0.64	1.04	1.51	1.20	0.92	0.72	0.51	0.37	0.31
	5	0.00	0.19	0.41	0.77	1.23	1.93	1.36	1.01	0.61	0.55	0.39
	6	0.00	0.19	0.38	0.66	0.87	1.46	1.95	1.38	1.15	0.92	0.71
	7	0.00	0.15	0.24	0.52	0.71	1.10	1.41	1.89	1.46	1.13	0.87
	8	0.00	0.04	0.15	0.32	0.56	0.67	1.16	1.57	1.90	1.55	1.18
	9	0.00	0.03	0.11	0.26	0.42	0.61	0.97	1.28	1.60	2.14	1.84
	10	0.00	0.09	0.09	0.15	0.35	0.48	0.64	0.95	1.20	1.68	2.20

(f) ICR - [0.00,2.20]

		d										
		0	1	2	3	4	5	6	7	8	9	10
a	0	0.00	0.00	0.00	0.00	0.00	0.00	0.00	0.00	0.00	0.00	0.00
	1	0.00	0.02	0.01	0.02	-0.08	0.06	0.14	-0.03	-0.02	0.06	-0.04
	2	0.00	-0.03	-0.10	-0.09	0.03	0.04	0.04	-0.07	0.03	-0.01	0.01
	3	0.00	-0.03	0.07	0.00	0.14	-0.18	0.04	-0.02	0.04	0.06	-0.07
	4	0.00	0.00	0.05	-0.05	-0.05	-0.03	0.14	-0.02	0.19	-0.10	0.28
	5	0.00	-0.01	0.11	-0.15	0.08	-0.16	0.04	0.02	-0.02	0.17	0.34
	6	0.00	0.05	-0.05	0.04	-0.05	0.02	0.21	0.03	0.19	-0.03	0.09
	7	0.00	0.08	-0.04	0.09	0.04	0.06	0.12	0.03	0.01	-0.08	0.07
	8	0.00	-0.02	0.03	0.14	0.00	0.02	-0.07	-0.05	0.35	-0.20	0.02
	9	0.00	0.10	0.16	-0.01	-0.08	0.05	-0.04	0.00	0.06	0.13	0.35
	10	0.00	-0.05	0.02	0.14	0.11	0.02	-0.01	0.25	0.01	0.37	0.00

(g) DCR - [-0.20,0.37]

		d										
		0	1	2	3	4	5	6	7	8	9	10
a	0	0.00	0.00	0.00	0.00	0.00	0.00	0.00	0.00	0.00	0.00	0.00
	1	0.00	-0.05	-0.10	-0.13	-0.24	-0.10	-0.01	-0.17	-0.13	-0.02	-0.08
	2	0.00	-0.14	-0.29	-0.34	-0.25	-0.25	-0.23	-0.30	-0.15	-0.13	-0.05
	3	0.00	-0.18	-0.18	-0.32	-0.22	-0.55	-0.30	-0.31	-0.19	-0.08	-0.10
	4	0.00	-0.16	-0.23	-0.41	-0.45	-0.44	-0.24	-0.34	-0.04	-0.22	0.30
	5	0.00	-0.17	-0.18	-0.52	-0.33	-0.57	-0.33	-0.27	-0.21	0.11	0.44
	6	0.00	-0.10	-0.32	-0.30	-0.43	-0.35	-0.11	-0.20	0.07	0.01	0.31
	7	0.00	-0.06	-0.27	-0.20	-0.28	-0.23	-0.11	-0.10	0.01	0.09	0.45
	8	0.00	-0.13	-0.15	-0.09	-0.23	-0.17	-0.19	-0.05	0.51	0.15	0.61
	9	0.00	0.02	0.04	-0.15	-0.20	-0.01	0.00	0.17	0.41	0.70	1.18
	10	0.00	-0.09	-0.04	0.11	0.13	0.12	0.21	0.63	0.60	1.20	1.11

(h) CCR - [-0.57,1.2]

		d										
		0	1	2	3	4	5	6	7	8	9	10
a	0	0.00	0.00	0.00	0.00	0.00	0.00	0.00	0.00	0.00	0.00	0.00
	1	0.00	0.88	0.75	0.65	0.46	0.53	0.54	0.31	0.28	0.31	0.18
	2	0.00	0.71	1.41	1.21	1.16	1.01	0.88	0.66	0.66	0.53	0.47
	3	0.00	0.60	1.37	2.01	1.89	1.34	1.36	1.13	1.03	0.92	0.67
	4	0.00	0.54	1.18	1.70	2.36	2.08	1.98	1.58	1.59	1.11	1.33
	5	0.00	0.46	1.08	1.37	2.19	2.58	2.44	2.13	1.82	1.77	1.73
	6	0.00	0.45	0.79	1.36	1.79	2.42	3.22	2.68	2.51	2.00	1.86
	7	0.00	0.42	0.69	1.24	1.64	2.17	2.77	3.26	2.86	2.42	2.26
	8	0.00	0.28	0.66	1.13	1.40	1.86	2.25	2.80	3.76	2.81	2.67
	9	0.00	0.35	0.70	0.85	1.13	1.65	1.99	2.50	3.07	3.69	3.50
	10	0.00	0.17	0.48	0.88	1.16	1.41	1.76	2.44	2.66	3.52	3.69

(i) ICR - [0.00,3.76]

		d										
		0	1	2	3	4	5	6	7	8	9	10
a	0	0.00	0.00	0.00	0.00	0.00	0.00	0.00	0.00	0.00	0.00	0.00
	1	0.00	-0.01	0.03	-0.03	-0.02	0.04	-0.01	-0.09	0.02	-0.08	0.10
	2	0.00	0.01	0.05	0.02	0.05	-0.08	0.17	0.03	0.08	0.01	0.02
	3	0.00	0.02	-0.16	-0.05	0.06	0.01	0.10	-0.03	-0.03	0.02	-0.11
	4	0.00	-0.02	0.07	0.04	-0.12	0.18	0.16	0.21	0.02	0.00	0.07
	5	0.00	-0.04	0.04	-0.09	0.03	0.11	0.05	0.00	-0.14	0.07	0.09
	6	0.00	-0.04	0.13	-0.02	-0.01	0.04	0.12	0.13	0.06	0.11	0.09
	7	0.00	0.01	0.00	-0.03	-0.09	-0.02	0.09	0.02	-0.15	-0.16	0.05
	8	0.00	-0.11	0.02	0.08	-0.11	-0.10	0.11	0.00	0.13	0.02	0.08
	9	0.00	0.02	0.04	0.12	-0.01	0.03	0.13	0.04	0.07	-0.16	-0.12
	10	0.00	0.04	0.04	-0.03	-0.04	-0.07	0.16	0.01	0.11	0.10	0.10

(j) DCR - [-0.16,0.21]

		d										
		0	1	2	3	4	5	6	7	8	9	10
a	0	0.00	0.00	0.00	0.00	0.00	0.00	0.00	0.00	0.00	0.00	0.00
	1	0.00	-0.03	-0.01	-0.08	-0.07	-0.02	-0.08	-0.15	-0.03	-0.12	0.07
	2	0.00	-0.03	-0.01	-0.07	-0.05	-0.19	0.07	-0.06	0.00	-0.06	-0.02
	3	0.00	-0.03	-0.25	-0.17	-0.07	-0.12	-0.04	-0.15	-0.13	-0.04	-0.14
	4	0.00	-0.07	-0.03	-0.09	-0.26	0.03	0.02	0.09	-0.07	-0.05	0.07
	5	0.00	-0.10	-0.07	-0.22	-0.12	-0.04	-0.09	-0.11	-0.21	0.05	0.14
	6	0.00	-0.11	0.03	-0.16	-0.15	-0.10	0.01	0.05	0.03	0.14	0.21
	7	0.00	-0.05	-0.09	-0.15	-0.21	-0.13	0.01	-0.01	-0.12	-0.06	0.25
	8	0.00	-0.16	-0.06	-0.02	-0.20	-0.17	0.08	0.03	0.23	0.22	0.38
	9	0.00	-0.02	-0.03	0.06	-0.06	0.01	0.16	0.14	0.27	0.14	0.30
	10	0.00	0.01	0.00	-0.06	-0.04	-0.02	0.28	0.21	0.41	0.52	0.66

(k) CCR - [-0.26,0.66]

		d										
		0	1	2	3	4	5	6	7	8	9	10
a	0	0.00	0.00	0.00	0.00	0.00	0.00	0.00	0.00	0.00	0.00	0.00
	1	0.00	0.92	0.89	0.77	0.73	0.73	0.63	0.51	0.58	0.44	0.58
	2	0.00	0.87	1.79	1.64	1.56	1.32	1.48	1.25	1.21	1.06	1.00
	3	0.00	0.82	1.46	2.39	2.34	2.14	2.08	1.82	1.69	1.63	1.39
	4	0.00	0.73	1.58	2.32	2.95	3.05	2.84	2.71	2.36	2.18	2.11
	5	0.00	0.65	1.44	2.04	2.90	3.73	3.44	3.17	2.83	2.84	2.68
	6	0.00	0.60	1.44	1.96	2.67	3.43	4.24	3.99	3.67	3.49	3.26
	7	0.00	0.61	1.22	1.82	2.41	3.15	3.95	4.58	4.13	3.85	3.81
	8	0.00	0.45	1.15	1.80	2.23	2.87	3.72	4.28	5.09	4.68	4.45
	9	0.00	0.54	1.09	1.73	2.17	2.80	3.51	4.05	4.73	5.16	4.88
	10	0.00	0.52	1.02	1.47	2.00	2.52	3.33	3.77	4.48	5.10	5.75

(l) ICR - [0.00, 5.75]

Table 4.3: RT^{ME} in different SZSP-scenarios with varying A_z for DCR, CCR, and ICR
a) $A_z = 0.5$ km^2, b) $A_z = 1$ km^2, c) $A_z = 2$ km^2, d) $A_z = 4$ km^2

a \ d	0	1	2	3	4	5	6	7	8	9	10
0	-	-	-	-	-	-	-	-	-	-	-
1	-	20.3	-3.4	-2.3	-0.6	-0.6	-0.7	0.7	-0.1	-0.1	0.0
2	-	-1.1	-3.8	-0.1	-1.9	-1.6	0.4	0.5	0.3	-0.1	0.0
3	-	3.1	9.3	2.5	1.4	1.4	0.1	0.2	0.6	0.2	-0.1
4	-	2.6	2.9	1.4	1.9	0.7	-0.7	1.5	-0.2	0.0	-0.1
5	-	1.5	3.1	-0.4	4.1	1.7	0.2	1.1	0.4	-0.1	0.0
6	-	-0.7	-0.6	0.1	1.9	0.6	0.4	0.5	1.0	0.0	-0.3
7	-	-0.3	-0.5	-0.2	0.2	1.9	1.7	0.4	2.9	1.9	0.0
8	-	-0.1	-0.2	0.0	0.6	0.8	1.0	1.6	2.5	1.0	0.4
9	-	-0.1	0.4	-0.2	1.0	1.3	0.0	0.9	0.7	1.7	0.2
10	-	0.0	0.0	0.3	-0.1	0.0	0.0	0.5	0.9	1.2	0.5

(a) DCR - [-3.9, 20.3]

a \ d	0	1	2	3	4	5	6	7	8	9	10
0	-	-	-	-	-	-	-	-	-	-	-
1	-	8.7	10.4	-4.4	-9.2	-6.9	0.4	1.4	-2.1	-1.1	-0.6
2	-	-0.9	-5.2	6.4	-3.9	6.8	0.7	-3.8	0.8	-0.5	-0.8
3	-	1.8	5.4	4.8	-3.7	-4.5	-3.2	-2.2	0.5	2.1	-0.1
4	-	3.6	2.5	0.2	-1.9	0.9	1.5	2.4	1.1	0.8	1.7
5	-	0.0	-1.9	0.3	2.0	8.3	2.5	1.6	-2.1	0.8	0.3
6	-	6.6	3.8	4.3	-0.1	5.4	4.8	1.0	3.1	3.5	3.1
7	-	6.2	0.6	4.5	2.0	3.9	1.6	1.5	1.4	1.6	1.6
8	-	-3.1	-0.9	0.9	2.6	-0.7	3.3	3.5	0.8	2.1	1.7
9	-	-2.1	-0.5	1.7	2.2	2.2	4.5	4.2	2.9	3.8	5.6
10	-	5.9	0.2	-0.1	2.8	2.3	1.8	3.0	2.0	3.3	3.8

(d) DCR - [-9.2, 10.4]

a \ d	0	1	2	3	4	5	6	7	8	9	10
0	-	-	-	-	-	-	-	-	-	-	-
1	-	17.8	5.1	4.9	-15.5	13.5	30.3	-4.9	-2.1	8.2	-4.6
2	-	-9.4	-16.3	-11.9	3.8	3.6	3.5	-4.9	2.6	-0.6	0.4
3	-	-8.3	10.4	-0.1	12.4	-11.0	2.3	-0.8	2.0	3.0	-3.0
4	-	-0.8	6.4	-4.0	-3.3	-1.7	6.8	-1.0	8.1	-3.5	10.5
5	-	-1.2	11.5	-9.4	4.3	-6.6	1.4	0.9	-0.6	5.2	10.3
6	-	9.0	-4.2	2.3	-2.4	0.6	7.7	1.0	5.4	-0.8	2.1
7	-	13.1	-2.7	5.4	1.5	2.3	3.8	0.9	0.4	-1.8	1.4
8	-	-2.1	2.6	7.4	0.2	0.7	-1.9	-1.1	8.3	-3.9	0.3
9	-	14.8	12.4	-0.3	-2.8	1.4	-1.0	0.0	1.2	2.4	6.3
10	-	-5.8	1.1	6.6	3.9	0.5	-0.3	5.4	0.1	6.7	0.0

(g) DCR - [-16.3, 30.3]

a \ d	0	1	2	3	4	5	6	7	8	9	10
0	-	-	-	-	-	-	-	-	-	-	-
1	-	-11.6	24.0	-14.2	-5.9	13.7	-3.8	-18.1	5.6	-13.7	23.7
2	-	4.9	25.6	6.3	12.2	-12.1	33.5	4.6	10.0	0.8	2.0
3	-	9.7	-29.1	-8.7	9.1	1.5	10.4	-2.6	-2.7	1.6	-6.7
4	-	-5.9	17.6	5.9	-11.2	19.2	13.9	16.1	1.4	-0.1	3.9
5	-	-12.3	6.7	-9.1	3.0	8.5	3.2	-0.1	-6.3	3.1	3.8
6	-	-11.0	24.0	-2.3	-0.7	2.5	7.0	6.5	2.4	4.2	3.4
7	-	2.9	0.6	-2.6	-5.8	-1.2	4.5	0.8	-5.2	-5.1	1.6
8	-	-19.3	2.2	6.3	-6.0	-4.5	4.6	0.0	4.5	0.7	2.2
9	-	5.0	4.1	9.6	-0.6	1.2	5.1	1.3	2.2	-4.2	-2.9
10	-	8.2	4.1	-1.8	-1.8	-2.9	6.1	0.3	3.1	2.5	2.4

(j) DCR - [-29.1, 33.5]

a \ d	0	1	2	3	4	5	6	7	8	9	10
0	-	-	-	-	-	-	-	-	-	-	-
1	-	-13.7	-3.4	6.4	3.1	1.0	0.0	1.0	0.0	0.0	0.0
2	-	-1.1	9.6	14.9	4.2	1.0	1.5	1.0	0.5	0.0	0.0
3	-	12.4	25.8	29.9	12.4	6.0	2.0	1.0	1.0	0.3	0.0
4	-	6.4	9.3	12.4	22.0	9.0	2.8	3.1	0.5	0.3	0.0
5	-	3.1	5.8	4.2	12.7	17.4	6.8	4.0	1.6	0.4	0.2
6	-	0.0	0.5	2.0	5.5	7.3	13.0	6.0	3.4	1.0	0.2
7	-	0.0	0.0	0.7	1.8	4.8	7.3	11.1	7.7	4.0	0.9
8	-	0.0	0.0	0.3	1.3	2.0	3.4	6.4	11.9	5.1	2.2
9	-	0.0	0.5	0.0	1.3	1.8	1.0	2.9	4.8	9.9	3.8
10	-	0.0	0.0	0.3	0.0	0.2	0.5	1.4	2.7	4.9	7.8

(b) CCR - [-13.7, 29.9]

a \ d	0	1	2	3	4	5	6	7	8	9	10
0	-	-	-	-	-	-	-	-	-	-	-
1	-	-59.3	-51.9	-51.9	-47.7	-39.2	-26.1	-16.7	-10.8	-0.7	3.1
2	-	-56.8	-54.0	-42.3	-41.6	-27.5	-23.9	-19.4	-6.9	0.8	3.6
3	-	-48.8	-42.8	-38.1	-37.7	-32.1	-24.4	-16.1	-5.5	4.7	5.3
4	-	-40.4	-37.7	-35.2	-32.0	-24.4	-17.5	-9.6	-2.9	5.0	8.4
5	-	-34.6	-33.4	-28.8	-23.6	-13.8	-12.7	-7.1	-3.5	7.1	8.5
6	-	-21.6	-21.6	-18.6	-18.8	-10.3	-5.9	-3.8	4.8	12.5	13.4
7	-	-12.8	-15.8	-10.4	-9.9	-5.0	-3.1	1.5	7.0	13.6	14.2
8	-	-11.8	-8.4	-5.2	-1.5	-2.2	5.0	9.2	11.1	18.2	17.3
9	-	-1.8	0.8	4.3	6.5	8.5	13.7	16.6	19.1	25.0	25.7
10	-	9.9	4.7	5.3	9.6	10.6	11.9	15.7	17.6	23.0	28.2

(e) CCR - [-59.3, 28.2]

a \ d	0	1	2	3	4	5	6	7	8	9	10
0	-	-	-	-	-	-	-	-	-	-	-
1	-	-38.2	-40.6	-36.4	-45.0	-21.1	-3.2	-24.7	-17.6	-3.2	-9.5
2	-	-48.8	-49.7	-43.7	-29.3	-25.1	-20.5	-22.5	-11.4	-9.2	-3.0
3	-	-44.4	-29.3	-32.6	-19.8	-33.0	-18.6	-16.7	-9.6	-3.7	-4.5
4	-	-35.5	-27.6	-31.5	-27.6	-22.7	-11.9	-14.2	-1.5	-7.6	11.1
5	-	-31.3	-19.4	-31.7	-18.0	-23.4	-13.1	-9.5	-6.7	3.4	13.4
6	-	-19.1	-26.4	-18.6	-19.4	-13.7	-3.9	-6.1	2.0	0.2	7.5
7	-	-10.5	-20.7	-11.5	-12.0	-8.2	-3.5	-2.8	0.4	2.0	9.6
8	-	-17.6	-11.4	-4.8	-8.7	-5.5	-5.0	-1.1	12.0	2.9	11.4
9	-	2.7	2.7	-6.8	-6.9	-0.3	-0.1	3.9	8.3	13.2	21.4
10	-	-10.6	-2.4	5.0	4.5	3.3	5.0	13.9	11.1	21.8	17.6

(h) CCR - [-49.7, 21.8]

a \ d	0	1	2	3	4	5	6	7	8	9	10
0	-	-	-	-	-	-	-	-	-	-	-
1	-	-38.6	-10.7	-35.9	-27.2	-9.1	-20.4	-29.8	-6.5	-21.1	16.9
2	-	-24.4	-6.5	-18.1	-10.7	-27.8	13.3	-8.3	-0.5	-6.0	-1.8
3	-	-18.1	-45.4	-27.5	-10.7	-14.3	-3.9	-12.6	-10.0	-3.2	-8.5
4	-	-27.2	-6.5	-13.3	-25.2	3.4	1.6	6.6	-4.2	-2.9	3.9
5	-	-29.8	-12.3	-23.3	-10.7	-3.3	-5.6	-6.1	-9.5	2.3	5.8
6	-	-26.3	5.2	-15.0	-11.4	-6.2	0.5	2.6	1.2	5.7	7.5
7	-	-11.9	-11.9	-12.6	-13.5	-7.1	0.6	-0.6	-4.2	-1.8	7.8
8	-	-28.6	-7.6	-1.8	-11.2	-7.8	3.4	1.1	8.0	6.5	10.7
9	-	-3.9	-2.9	4.4	-3.4	0.5	6.5	4.9	8.1	3.6	7.3
10	-	2.3	0.2	-3.7	-1.8	-1.0	10.4	6.4	11.6	13.3	15.6

(k) CCR - [-45.4, 16.9]

a \ d	0	1	2	3	4	5	6	7	8	9	10
0	-	-	-	-	-	-	-	-	-	-	-
1	-	112.8	19.0	6.4	3.1	1.0	0.0	1.0	0.0	0.0	0.0
2	-	22.0	35.1	14.9	4.2	1.0	1.5	1.0	0.5	0.0	0.0
3	-	12.4	25.8	29.9	12.4	6.0	2.0	1.0	1.0	0.3	0.0
4	-	6.4	9.3	12.4	22.0	9.0	2.8	3.1	0.5	0.3	0.0
5	-	3.1	5.8	4.2	12.7	17.4	6.8	4.0	1.6	0.4	0.2
6	-	0.0	0.5	2.0	5.5	7.3	13.0	6.0	3.4	1.0	0.2
7	-	0.0	0.0	0.7	1.8	4.8	7.3	11.1	7.7	4.0	0.9
8	-	0.0	0.0	0.3	1.3	2.0	3.4	6.4	11.9	5.1	2.2
9	-	0.0	0.5	0.0	1.3	1.8	1.0	2.9	4.8	9.9	3.8
10	-	0.0	0.0	0.3	0.0	0.2	0.5	1.4	2.7	4.9	7.8

(c) ICR - [0.0, 112.8]

a \ d	0	1	2	3	4	5	6	7	8	9	10
0	-	-	-	-	-	-	-	-	-	-	-
1	-	284.6	127.3	51.5	23.5	14.9	16.3	12.4	5.3	4.2	3.1
2	-	104.1	117.4	81.8	37.9	37.0	19.8	8.7	9.9	5.8	3.6
3	-	61.3	80.2	94.8	47.1	28.2	19.0	13.2	11.5	9.9	5.3
4	-	40.8	47.1	53.1	60.6	42.9	29.9	22.0	14.6	10.2	8.4
5	-	23.5	25.8	34.5	44.4	62.9	37.4	25.3	13.9	12.4	8.5
6	-	23.5	23.5	28.2	27.8	41.2	48.1	29.9	23.7	18.1	13.4
7	-	17.6	13.6	21.0	21.6	28.2	30.7	37.0	26.4	19.3	14.2
8	-	4.2	8.1	11.9	16.3	15.5	24.0	28.9	31.1	24.0	17.3
9	-	3.1	5.8	9.5	11.7	13.9	19.3	22.4	25.0	31.2	25.7
10	-	9.9	4.7	5.3	9.6	10.6	11.9	15.7	17.6	23.0	28.2

(f) ICR - [3.1, 284.6]

a \ d	0	1	2	3	4	5	6	7	8	9	10
0	-	-	-	-	-	-	-	-	-	-	-
1	-	733.3	300.0	185.7	85.2	112.8	117.4	44.9	38.9	44.9	22.0
2	-	244.8	239.0	153.2	138.1	102.0	78.6	49.3	49.3	36.1	30.7
3	-	150.0	217.5	203.0	170.3	80.7	82.9	60.4	52.3	44.2	28.8
4	-	117.4	143.9	130.8	143.9	108.3	98.0	65.3	66.0	38.4	49.8
5	-	85.2	117.4	84.0	121.0	106.6	95.3	74.2	57.2	54.8	52.9
6	-	81.8	65.3	82.9	81.0	93.8	115.8	80.7	71.9	50.0	44.9
7	-	72.4	52.7	70.5	69.5	76.7	85.8	87.2	69.1	52.8	47.7
8	-	38.9	49.3	60.4	53.8	59.2	60.0	66.7	88.7	54.1	50.1
9	-	53.8	53.8	39.5	39.4	49.3	49.6	55.6	62.3	69.5	63.6
10	-	20.5	31.6	41.5	40.8	39.3	41.5	53.5	49.8	64.2	58.5

(i) ICR - [20.5, 733.3]

a \ d	0	1	2	3	4	5	6	7	8	9	10
0	-	-	-	-	-	-	-	-	-	-	-
1	-	1150.0	809.1	334.8	270.4	270.4	170.3	104.1	138.1	78.6	138.1
2	-	669.2	852.4	455.6	354.5	194.1	284.6	166.7	153.2	112.8	100.0
3	-	455.6	270.4	391.8	354.5	248.8	226.1	154.2	129.0	119.0	86.3
4	-	270.4	376.2	341.2	281.0	321.1	244.8	210.1	143.9	119.8	111.6
5	-	185.7	257.1	212.5	263.6	293.7	220.5	173.2	130.4	131.5	115.5
6	-	150.0	257.1	188.5	200.8	218.5	240.9	198.5	157.5	139.0	119.0
7	-	156.4	156.4	154.2	151.6	170.3	192.7	189.3	143.9	122.2	119.4
8	-	81.8	135.3	150.0	126.0	134.7	163.2	157.4	174.9	141.0	125.4
9	-	117.4	119.8	136.2	118.6	127.3	141.0	137.3	144.6	134.4	118.4
10	-	108.3	104.1	96.1	100.0	101.6	124.7	116.7	127.3	130.8	135.3

(l) ICR - [78.6, 1150.0]

Table 4.4: RT^{MRE}[%] in different SZSP-scenarios with varying A_z for DCR, CCR, and ICR
a) $A_z = 0.5$ km^2, b) $A_z = 1$ km^2, c) $A_z = 2$ km^2, d) $A_z = 4$ km^2

4.H Multiple Zones, Multiple Periods Setting - Additional Results

A_z [km^2]	M	0	1	2	3	4	5	6	7	8	9	10	11	12	13	14	15	16	17	18	19	20	21	22	23	24	25	26	27	28	29	30	31	32	33	34	35	36	37	38	39	40	41	42	43	44	45	46	47	∅
		period																																																
0.5	CCR	-5	-3	-1	-3	-4	-1	-1	-2	0	0	1	-1	0	-1	-4	-17	-14	-17	-6	-1	2	3	3	-2	5	-2	-9	3	0	5	6	8	6	7	5	5	6	7	9	-3	1	4	8	1	0	-3	-3	0	0
	ICR	-4	-2	0	-1	-3	0	-1	-1	0	0	2	0	2	1	-3	-18	-14	-17	-4	1	5	7	6	1	9	2	-6	6	3	8	7	10	7	9	6	6	9	9	11	-1	3	7	11	1	1	-2	-1	2	2
1	CCR	-7	-1	-3	-1	-2	-1	-2	-1	-1	0	-3	0	-1	-1	0	-3	-4	-3	-6	1	-5	-5	-2	-1	-6	-3	-7	-4	-4	-7	-8	-2	-5	1	-6	-5	-5	-5	-1	-6	-1	-9	-2	-2	-8	-6	-3	-3	-3
	ICR	15	17	10	8	3	4	1	2	2	5	7	8	8	10	13	10	9	16	30	39	34	34	36	39	34	37	32	36	38	35	35	41	42	47	41	43	45	46	48	41	48	40	41	34	24	25	28	24	26
2	CCR	0	0	-1	0	0	1	0	0	0	0	0	0	-1	0	-1	1	1	3	1	0	4	-1	-1	-1	-2	2	-1	1	-2	-1	0	1	1	0	0	0	0	-2	-1	1	1	-1	0	2	-1	1	-3	-1	0
	ICR	35	29	19	14	9	8	5	5	5	9	16	14	15	21	25	33	40	49	61	64	66	61	61	62	63	67	66	65	65	68	71	74	78	78	80	82	84	85	86	86	86	79	69	58	49	49	47	43	50
4	CCR	-1	0	0	0	1	0	0	0	0	0	0	0	-1	0	-1	-1	-1	-1	0	1	-1	-1	-2	-1	-1	-1	-1	0	0	-1	-1	-1	1	0	-1	0	0	-2	-2	0	-3	-1	0	-1	-1	0	-1	-2	-1
	ICR	43	35	24	17	12	8	6	6	7	10	19	17	18	25	33	43	54	64	78	79	73	73	74	75	78	78	81	76	81	83	84	85	95	95	96	99	103	104	105	104	100	94	82	67	59	58	60	51	61

Table 4.5: RT^{ME} in MZMP-scenarios with $A_z = 0.5\ \text{km}^2, 1\ \text{km}^2, 2\ \text{km}^2, 4\ \text{km}^2$ for matching functions (M) ICR and CCR

A_z [km^2]	M	0	1	2	3	4	5	6	7	8	9	10	11	12	13	14	15	16	17	18	19	20	21	22	23	24	25	26	27	28	29	30	31	32	33	34	35	36	37	38	39	40	41	42	43	44	45	46	47	∅
		period																																																
0.5	CCR	-11	-7	-4	-14	-26	-10	-16	-21	-5	-3	4	-5	1	-2	-11	-27	-19	-19	-7	-1	2	5	3	-2	6	-2	-9	4	0	6	7	10	6	8	5	5	6	7	8	-3	1	5	11	1	0	-5	-4	0	-4
	ICR	-8	-4	-1	-6	-19	-4	-12	-16	3	3	8	-2	8	5	-8	-27	-19	-19	-4	2	7	10	8	2	12	2	-7	8	3	9	9	12	8	10	6	6	8	9	10	-1	3	7	14	2	1	-3	-1	3	1
1	CCR	-21	-3	-19	-6	-27	-14	-31	-25	-23	3	-20	-3	-9	-7	-1	-8	-9	-5	-10	2	-12	-11	-5	-2	-12	-6	-13	-8	-8	-13	-14	-5	-8	2	-10	-9	-7	-8	-2	-9	-2	-14	-5	-6	-19	-15	-9	-10	-6
	ICR	45	83	58	79	33	68	29	51	53	91	58	73	69	63	55	27	19	28	54	87	74	75	83	93	69	81	58	79	78	66	64	83	75	89	65	69	69	69	74	59	77	65	90	90	62	66	76	72	67
2	CCR	-4	-2	-12	7	3	55	-8	-13	-12	-4	-3	5	-21	7	-10	8	6	12	3	0	31	-5	-5	-7	-11	9	-3	5	-11	-6	1	8	3	-2	1	1	-1	-9	-5	4	5	-3	-1	12	-5	7	-17	-9	0
	ICR	319	345	299	349	291	549	280	296	329	342	374	359	266	356	232	239	213	218	269	324	479	326	334	339	300	391	317	398	310	335	366	411	380	347	351	357	336	312	308	337	367	368	397	437	353	387	281	323	324
4	CCR	-28	9	-7	8	336	-11	-10	293	85	2	-15	-14	-38	-22	-25	-12	-10	-14	-4	11	-19	-22	-29	-11	-14	-13	-12	-6	-5	-12	-19	-21	24	10	-16	3	-4	-20	-18	-3	-33	-20	0	-14	-19	-3	-21	-38	1
	ICR	1158	1846	1520	1574	5766	1198	1192	6231	3336	1742	1597	1429	1084	1246	1040	1022	975	871	1255	1678	1267	1266	1167	1508	1401	1427	1352	1617	1586	1476	1349	1352	2200	1872	1396	1735	1582	1332	1283	1514	1068	1402	1901	1512	1365	1529	1241	981	1634

Table 4.6: RT^{MRE} [%] in MZMP-scenarios with $A_z = 0.5\ \text{km}^2, 1\ \text{km}^2, 2\ \text{km}^2, 4\ \text{km}^2$ for matching functions (M) ICR and CCR

4.I Artificial Zone Partitioning

This section illustrates Property 6, i.e., the *independence to zone partitioning*, which was introduced in Section 4.3.4. Consider an instance of the SZSP-setting (Section 4.4.1.1). The quadratic zone is comparably large to the walking areas with $A_z = 16 \cdot A_w$, as depicted in Figure 4.18a. The zone is assumed to be homogeneous and demand and supply in this zone are $d = 16$ and $a = 16$ (zero variance). As depicted in Figure 4.19 (left: 1 zone with $A_z = 16 \cdot A_w$), the simulation (SIM) yields 8.5 rentals on average. The DCR returns a similar result, the CCR slightly overestimates with around 10 rentals, while the ICR predicts 16 rentals.

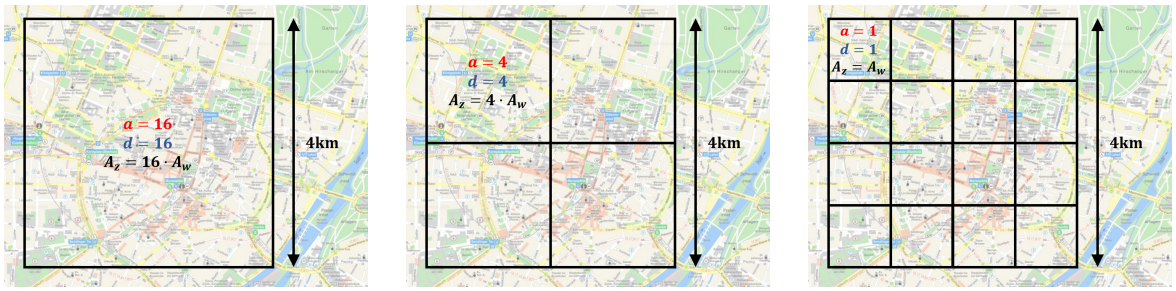

(a) 1 zone with $A_z = 16 \cdot A_w$ (b) 4 zones with $A_z = 4 \cdot A_w$ (c) 16 zones with $A_z = A_w$

Figure 4.18: Setting for artificial zone partitioning

We now *artificially partition* the zone into four smaller zones with each having a size of $A_z = 4 \cdot A_w$ (Figure 4.18b). Supply and demand are split homogeneously across the zones, i.e., $d = 4$ and $a = 4$ for each zone. To determine the overall rentals with the matching functions, the functions are evaluated on each individual zone and the result is multiplied by 4 (because of the 4 zones). As depicted in Figure 4.19 (middle: 4 zones with $A_z = 4 \cdot A_w$), the value from the SIM benchmark remains unchanged, because the artificial partitioning into smaller zones has no impact on the actual matching process on the original large zone. The overall rentals resulting from applying the DCR and CCR (both adapted to the zone size) on the four zones now both overestimate the actual rentals. The results for ICR remain unchanged compared to the previous results with one zone. This characteristic of the ICR is what is formalized as the *independence to zone partitioning* in Property 6. The reason for the overestimation of the DCR and CCR is that the friction regarding the supply-demand matching in the large zone is removed by assuming that supply and demand distributes proportionally across the smaller zones in which there is no friction.

In the last step of this analysis, the original zone is partitioned into 16 zones with each having a size of $A_z = A_w$ (Figure 4.18c). Again, supply and demand are split homogeneously across the zones, i.e., $d = 1$ and $a = 1$ for each zone. The effects are in principle the same as described for the four zones, but since $A_z = A_w$, the DCR and CCR now predict one rental per small zone and, thus 16 rentals overall, exactly as with the ICR (Figure 4.19 right: 16 zones with $A_z = A_w$).

This shows that one cannot improve rental prediction accuracy by artificially partitioning a zone for which supply and demand is given into multiple smaller zones and then apply the ICR. The predictions with the ICR do not change due to the "independence to zone partitioning" (Property 6) and the DCR and CCR only perform accurately on the original zone where the

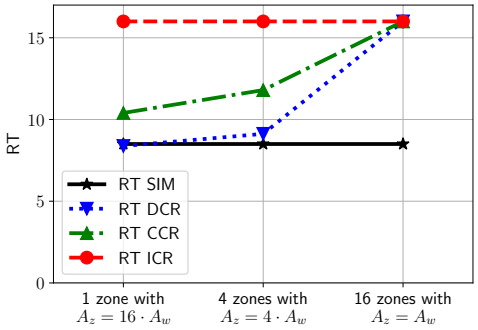

Figure 4.19: Results for artificial zone partitioning

friction is considered correctly. The difference between the studies performed in the SZSP- and the MZMP-setting (Sections 4.4.1.1 and 4.4.2.1) and the study in this section is that in the former, the operating area (one zone in the SZSP-setting) is *scaled* to different sizes while maintaining the number of zones, while here the operating area is *partitioned* into multiple zones.

4.J Case Study - Additional Results

A_z [km^2]	OBDPP-	*RT*		*RV*		*CM*	
		mean	c.i.	mean	c.i.	mean	c.i.
0.5	ICR	2908.3	±12.4	13651.2	±60.1	10379.4	±46.2
	CCR	2925.2	±12.3	13755.2	±57.9	10464.3	±44.2
1	ICR	**1788.5**	±11.8	**8365.4**	±55.9	**6353.3**	±42.8
	CCR	**1885.2**	±10.9	**8636.8**	±50.8	**6515.9**	±38.8
2	ICR	**698.7**	±6.4	**3267.2**	±30.8	**2481.2**	±23.5
	CCR	**747.4**	±6.2	**3388.5**	±29.0	**2547.7**	±22.0
4	ICR	**203.5**	±3.1	953.1	±14.7	724.2	±11.2
	CCR	**213.0**	±2.9	978.2	±13.5	738.5	±10.3

Table 4.7: Mean and 95% confidence interval for *RT*, *RV*, and *CM* of pricing solutions of OBDPP-ICR and OBDPP-CCR for MZMP-settings with $A_z = 0.5$ km^2, 1 km^2, 2 km^2, 4 km^2 evaluated in simulation. ICR-CCR pairs with non-overlapping confidence intervals are highlighted

Bibliography

Agatz N, Campbell AM, Fleischmann M, Van Nunen J, Savelsbergh M (2013) Revenue management opportunities for internet retailers. *J. Revenue Pricing Manag.* 12(2):128–138.

Ata B, Barjesteh N, Kumar S (2019) Spatial pricing: An empirical analysis of taxi rides in New York City. Working paper, The University of Chicago Booth School of Busines, Chicago, IL.

Ataç S, Obrenović N, Bierlair M (2021) Vehicle sharing systems: A review and a holistic management framework. *EURO J. Transp. Logist.* 100033.

Balac M, Ciari F, Axhausen KW (2017) Modeling the impact of parking price policy on free-floating carsharing: Case study for Zurich, Switzerland. *Transp. Res. Part C: Emerg. Technol.* 77:207–225.

Balac M, Becker H, Ciari F, Axhausen KW (2019) Modeling competing free-floating carsharing operators – A case study for Zurich, Switzerland. *Transp. Res. Part C: Emerg. Technol.* 98:101–117.

Bian B (2018) Spatial equilibrium, search frictions and efficient regulation in the taxi industry. Working paper, Pennsylvania State University, PA.

Boysen N, Briskorn D, Schwerdfeger S (2019) Matching supply and demand in a sharing economy: Classification, computational complexity, and application. *Eur. J. Oper. Res.* 278(2):578–595.

Brendel AB, Kolbe LM (2017) Taxonomy of vehicle relocation problems in car sharing. Working paper, University of Göttingen, Göttingen, Germany.

Buchholz N (2019) Spatial equilibrium, search frictions and efficient regulation in the taxi industry. Working paper, Princeton University, Princeton, NJ.

Burdett K, Shi S, Wright R (2001) Pricing and matching with frictions. *J. Pol. Econ.* 109(5):1060–1085.

Butters GR (1977) Equilibrium distributions of sales and advertising prices. *Rev. Econ. Studies* 44(3):465–491.

Ciari F, Bock B, Balmer M (2014) Modeling station-based and free-floating carsharing demand: Test case study for Berlin. *Transp. Res. Record* 2416(1):37–47.

Ciari F, Balac M, Balmer M (2015) Modelling the effect of different pricing schemes on free-floating carsharing travel demand: A test case for Zurich, Switzerland. *Transp.* 42(3):413–433.

Ciari F, Balac M, Axhausen KW (2016) Modeling carsharing with the agent-based simulation MATSim: State of the art, applications, and future developments. *Transp. Res. Record* 2564(1):14–20.

Cocca M, Giordano D, Mellia M, Vassio L (2019) Free floating electric car sharing design: Data driven optimisation. *Pervasive Mob. Comput.* 55:59–75.

Correia GHDA, Antunes AP (2012) Optimization approach to depot location and trip selection in one-way carsharing systems. *Transp. Res. Part E: Logist. Transp. Rev.* 48(1):233–247.

Data Bridge Market Research (2021) Global shared mobility market size forecast from 2021 to 2028. *Statista.* Accessed June 21, 2021, https://www.statista.com/statistics/1229457/shared-mobility-market-size-worldwide/.

DeMaio P (2009) Bike-sharing: History, impacts, models of provision, and future. *J. Public Transp.* 12(4):41–56.

Fandel G (1991) Theory of production and cost (Springer, Berlin, Germany).

Ferrero F, Perboli G, Vesco A, Caiati V, Gobbato L (2015a) Car-sharing services – Part A taxonomy and annotated review. Working paper, Istituto Superiore Mario Boella, Turin, Italy.

Ferrero F, Perboli G, Vesco A, Musso S, Pacifici A (2015b) Car-sharing services – Part B business and service models. Working paper, Istituto Superiore Mario Boella, Turin, Italy.

Fishman E, Washington S, Haworth N (2013) Bike share: A synthesis of the literature. *Transp. Rev.* 33(2):148–165.

Fréchette G, Lizzeri A, Salz T (2018) Frictions in a competitive, regulated market evidence from taxis. Working paper, National Bureau of Economic Research, Cambridge, MA.

Golalikhani M, Oliveira BB, Carravilla MA, Oliveira JF, Antunes AP (2021a) Carsharing: A review of academic literature and business practices toward an integrated decision-support framework. *Transp. Res. Part E: Logist. Transp. Rev.* 149 Article 102280.

Golalikhani M, Oliveira BB, Carravilla MA, Oliveira JF, Pisinger D (2021b) Understanding carsharing: A review of managerial practices towards relevant research insights. *Res. Transp. Bus. Manag.* Article 100653.

Haider Z, Nikolaev A, Kang JE, Kwon C (2018) Inventory rebalancing through pricing in public bike sharing systems. *Eur. J. Oper. Res.* 270(1):103–117.

Hall RE (1979) A theory of the nature of the natural unemployment rate. *J. Monetary Econ.* 5(2):153–169.

Hardt C (2018) Empirical analysis of demand patterns and availability in free-floating carsharing systems. *2018 21st Internat. Conf. Intelligent Transp. Systems (ITSC)*, 1186–1193.

Hardt C, Bogenberger K (2021) Dynamic pricing in free-floating carsharing systems - A model predictive control approach. *TRB 100th Annual Meeting Compendium of Papers.*

Heilig M, Mallig N, Schröder O, Kagerbauer M, Vortisch P (2018) Implementation of free-floating and station-based carsharing in an agent-based travel demand model. *Travel Beh. Soc.* 12:151–158.

Herrmann S, Schulte F, Voß S (2014) Increasing acceptance of free-floating car sharing systems using smart relocation strategies: A survey based study of car2go Hamburg. *Comp. Logist.*, Lecture Notes in Computer Sci., Vol. 8760 (Springer, London), 151–162.

Hu L, Liu Y (2016) Joint design of parking capacities and fleet size for one-way station-based carsharing systems with road congestion constraints. *Transp. Res. Part B: Methodol.* 93:268–299.

Illgen S, Höck M (2019) Literature review of the vehicle relocation problem in one-way car sharing networks. *Transp. Res. Part B: Methodol.* 120:193–204.

Jorge D, Correia GHDA (2013) Carsharing systems demand estimation and defined operations: A literature review. *Eur. J. Transp. Infrastructure Res.* 13(3):201–220.

Jorge D, Molnar G, Correia GHDA (2015) Trip pricing of one-way station-based carsharing networks with zone and time of day price variations. *Transp. Res. Part B: Methodol.* 81:461–482.

Laporte G, Meunier F, Wolfler Calvo R (2015) Shared mobility systems. *4OR* 13(4):341–360.

Laporte G, Meunier F, Wolfler Calvo R (2018) Shared mobility sytems: An updated survey. *Ann. Oper. Res.* 271(1):105–126.

Li Q, Liao F, Timmermans HJ, Huang H, Zhou J (2018) Incorporating free-floating car-sharing into an activity-based dynamic user equilibrium model: A demand-side model. *Transp. Res. Part B: Methodol.* 107(1):102–123.

Lippoldt K, Niels T, Bogenberger K (2018) Effectiveness of different incentive models in free-floating carsharing systems: A case study in Milan. *2018 21st Internat. Conf. Intelligent Transp. Systems (ITSC)*, 1179–1185.

Lippoldt K, Niels T, Bogenberger K (2019) Analyzing the potential of user-based relocations on a free-floating carsharing system in Cologne. *Transp. Res. Proc.* 37(9):147–154.

Lu M, Chen Z, Shen S (2017) Optimizing the profitability and quality of service in carshare systems under demand uncertainty. Available at SSRN.

Lu R, Correia GHDA, Zhao X, Liang X, Lv Y (2021) Performance of one-way carsharing systems under combined strategy of pricing and relocations. *Transportmetrica B* 9(1):134–152.

Manley D (2019) Scale, Aggregation, and the Modifiable Areal Unit Problem. In: Fischer M, Nijkamp P (eds), Handbook of Regional Sci. (Springer, Berlin), 1–15.

Molnar G, Correia GHDA (2019) Long-term vehicle reservations in one-way free-floating car-sharing systems: A variable quality of service model. *Transp. Res. Part C: Emerg. Technol.* 98(1):298–322.

Müller J, Correia GHDA, Bogenberger K (2017) An explanatory model approach for the spatial distribution of free-floating carsharing bookings: A case-study of German cities. *Sustainability* 9(7):1290.

Neijmeijer N, Schulte F, Tierney K, Polinder H, Negenborn RR (2020) Dynamic pricing for user-based rebalancing in free-floating vehicle sharing: A real-world case. *Internat. Conf. Comput. Logist.* 443–456.

Niels T, Bogenberger K (2017) Booking behavior of free-floating carsharing users. *Transp. Res. Record: J. Transp. Res. Board* 2650(1):123–132.

Petrongolo B, Pissarides CA (2001) Looking into the black box: A survey of the matching function. *J. Econ. Literature* 39(2):390–431.

Reiss S, Bogenberger K (2016) Optimal bike fleet management by smart relocation methods: Combining an operator-based with an user-based relocation strategy. *IEEE Intell. Transp. Syst. Conf. (ITSC)*, 2613–2618.

Ricci M (2015) Bike sharing: A review of evidence on impacts and processes of implementation and operation. *Res. Transp. Bus. Manag.* 15:28–38.

Share Now (2021) Overview on countries and cities. *share-now.com*. Accessed June 21, 2021, https://www.share-now.com/de/en/country-list/.

Sayarshad H, Tavassoli S, Zhao F (2012) A multi-periodic optimization formulation for bike planning and bike utilization. *Appl. Math. Modelling* 36(10):4944–4951.

Schuijbroek J, Hampshire RC, van Hoeve WJ (2017) Inventory rebalancing and vehicle routing in bike sharing systems. *Eur. J. Oper. Res.* 257(3):992–1004.

Shaheen S, Sperling D, Wagner C (1998) Carsharing in Europe and North American: Past, Present, and Future. *Transp. Quarterly* 52(3):35–52.

Shaheen S, Cohen A, Jaffee M (2018) Innovative mobility: Carsharing outlook. Technical Report, Transportation Sustainability Research Center, University of California, Berkeley, CA.

Soppert M, Steinhardt C, Müller C, Gönsch J (2022) Differentiated pricing of shared mobility systems considering network effects. *Transp. Sci.*, ePub ahead of print April 1, https://doi.org/10.1287/trsc.2022.1131.

Talluri KT, van Ryzin GJ (2004) The theory and practice of revenue management (Springer, Boston, MA).

Weikl S, Bogenberger K (2013) Relocation strategies and algorithms for free-floating car sharing systems. *IEEE Intell. Transp. Syst. Magazine* 5(4):100–11.

Weikl S, Bogenberger K (2015) A practice-ready relocation model for free-floating carsharing systems with electric vehicles – Mesoscopic approach and field trial results. *Transp. Res. Part C: Emerg. Technol.* 57:206–223.

Weikl S, Bogenberger K (2016) Integrated relocation model for free-floating carsharing systems. *Transp. Res. Record: J. Transp. Res. Board* 2563(1):19–27.

Wu C, Le Vine S, Sivakumar A, Polak J (2019) Traveller preferences for free-floating carsharing vehicle allocation mechanisms. *Transp. Res. Part C: Emerg. Technol.* 102:1–19.

Yan C, Zhu H, Korolko N, Woodard D (2020) Dynamic pricing and matching in ride-hailing platforms. *Nav. Res. Logist.* 67:705–724.

Chapter 5

Customer-Centric Dynamic Pricing for Free-Floating Shared Mobility Systems

5.1 Introduction

Vehicle sharing systems (VSSs), such as car sharing, bike sharing, or scooter sharing, are specific shared mobility systems (Mourad, Puchinger, and Chu, 2019) that allow users to flexibly and spontaneously rent vehicles for a short period of time (Ataç, Obrenović, and Bierlaire, 2021). In contrast to other popular shared mobility systems, VSSs enable individual trips (conducted by the user), whereas, for example, ride-hailing (e.g. Wang and Yang, 2019) requires connecting passengers with drivers in a two-sided market, and ride-pooling (e.g. Ke et al., 2020) as well as dial-a-ride (e.g. Qiu et al., 2018) concepts strive for shared trips.

There are three fundamental types of VSSs which, from the customers' view, decisively differ with regard to the degree of flexibility they offer. In *two-way station-based* systems, customers have to return vehicles to the pick-up station, whereas in *one-way station-based* systems, customers can pick-up and drop-off the vehicle at any station. *Free-floating* is the most flexible variant, as it allows customers to pick-up and drop-off vehicles at any public parking spot in the business area of the VSS provider (e.g. Chow and Yu, 2015). For this reason, free-floating VSSs have become a very popular type in urban areas (e.g. Statista, 2022). However, higher degrees of flexibility come with an important drawback: Due to unbalanced demand patterns and the oscillation of the demand intensity over the course of the day, vehicles accumulate at certain locations (usually the outskirts) over time, while other areas lack vehicles (usually downtown). This so-called "tide phenomenon" (spatio-temporal demand asymmetries (Côme, 2014; Jorge and Correia, 2013)) is even more pronounced for free-floating VSSs than for station-based one-way VSSs. The reason is that while demand and supply in a free-floating VSSs spread across the entire business area, they concentrate to rather few locations in station-based VSSs (Wagner et al., 2015).

Pricing is an established tool to counter these imbalances and to improve the system's profit. The idea is to nudge some customers to slightly adapt their travel plans, for example, to pick up a sharing vehicle at a low demand location instead of a high demand location. Thus, adequate pricing can achieve a vehicle availability that assures an appropriate service level.

Existing pricing approaches from the related literature on VSSs determine vehicle-specific prices, meaning that all customers are getting displayed the same (minute) price for a particular vehicle when checking prices at the same time. These approaches do not leverage on the detailed disaggregate information which is available in modern free-floating VSSs. Opposed to these approaches, a *customer-centric* pricing approach determines prices under consideration of the situation-specific information of each customer. As depicted in Figure 5.1a, this particularly comprises a customer's location as well as the information about the available vehicles within the customer's walking distance. Thus, in contrast to vehicle-specific pricing, customer-centric pricing may result in different prices for the same vehicle when customers are at different locations (Figure 5.1b). It can be considered as an application of choice-based revenue management (Strauss, Klein, and Steinhardt, 2018) with the particularity in free-floating VSSs that the consideration set of available vehicles is determined by the customer's location. The core idea of customer-centric pricing has successfully been applied to shared mobility systems other than VSSs, i.e., to mobility on demand services (Qiu et al., 2018). However, these mobility systems differ fundamentally from VSSs in that the provider operates a platform that receives requests

for the customers' desired trips and then matches demand to supply. This (moving) supply of vehicles may either be under full control of the provider (Ke et al., 2020) or it may be influenced by pricing as well, resulting in a two-sided market (Wang and Ma, 2019). Thus, these approaches are not directly applicable to our context, and in this work we propose such customer-centric dynamic pricing which is specifically tailored to free-floating VSSs.

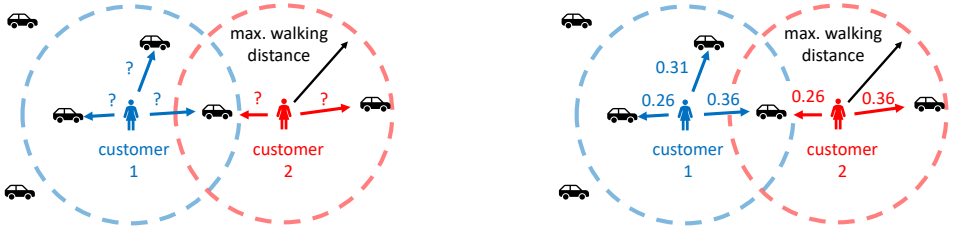

(a) Provider's pricing problem: The "?" indicate prices to be optimized online.

(b) Resulting customer's choice situation: Customers might see *different* prices for a vehicle.

Figure 5.1: Illustration of the first distinguishing feature of the developed pricing approach: *customer-centricity*.

In this work, we consider a profit-maximizing free-floating VSS provider's dynamic online pricing problem with a strong focus on applicability in practice, meaning that problem definition and solution approach design are based on the circumstances and requirements in practice. More precisely, whenever a customer considers prices in the mobile application, prices need to be determined based on the currently available information. For this problem, we develop a new pricing approach that is characterized by the following three distinguishing features:

- First, and most importantly, the pricing is *customer-centric*. As briefly described above, adopting the concept of customer-centricity means that prices are situation-specific for each customer. As a consequence, the online price optimization can leverage on detailed disaggregate information like the customer's location. This, in turn, allows to exploit that the location not only determines the vehicles within the customer's walking distance, but that the distance to a vehicle also impacts the customer's utility and, thus, the probability of choosing it. Due to the customer-centricity, the pricing approach can incorporate the customer choice behavior through an appropriate choice model. As stated above, this pricing can result in one specific vehicle having different prices for different customers, but this does not mean that pricing is *personalized*. More specifically, we do *not* use socio-demographic characteristics such as age or income to potentially exploit individual willingness-to-walk or individual price sensitivity. Only the location of the customer's device when she looks for vehicles is used to account for the impact of distance to different vehicles on customer utility. Thus, prices are identical for every customer who faces the same situation. Note, however, that – as for all pricing approaches in which locations of customers or vehicles are decisive – prices may indirectly be dependent on socio-demographic characteristics, e.g. because of location-dependent income levels.

- Second, within our pricing approach, prices can be varied (solely) based on location and time of a rental's start, denoted as *origin-based pricing*, in line with the business decision of Share Now. In particular, information on a rental's destination can not be used, because it is not available in reality: Asking customers for their destination beforehand

contradicts the spontaneous selling proposition of free-floating VSSs (Soppert et al., 2022). The alternative, i.e., displaying prices for all potential origin-destination (and -time) combinations in advance of a rental, is impracticable in general, given that free-floating VSS providers often discretize their business area into up to hundred zones. Note, however, that if zones (or stations in a station-based system) are aggregated to fewer categories, such as "incentivized rental (return) station" and "neutral station" which allow the customer to pre-calculate incurring rental prices based upon these zone categories (Chung, Freund, and Shmoys , 2018), this becomes practical.

- Third, for the provider, it is important *how* prices are determined. In this respect, our pricing approach is *anticipative* as it considers future profits based on dynamic programming. The papers using mathematical models largely rely on myopic optimization models. In addition, as we will discuss in-depth in Section 5.2, they can not be applied to the problem we consider for various other reasons. The ways we design the anticipation allows to use historical data that is readily available in practice.

This pricing approach takes into account the typical characteristics of free-floating VSS (pick-up and drop-off possible at any location within the business area). However, given that station-based VSSs can be considered as a special case of free-floating systems, the approach is applicable to both. The pricing problem and our approach's practical relevance is ensured by, among other things, close cooperation with Share Now, Europe's largest car sharing provider operating in eight countries and 16 cities (Share Now, 2021).

The contributions of our work are the following:

- We present a dynamic pricing approach for modern (free-floating) VSSs like car sharing and bike sharing, which is characterized by the three distinguished features mentioned above, i.e., it is *customer-centric*, *origin-based*, and *anticipative*.

- We formulate the pricing problem underlying our approach as a dynamic program which considers stochasticity of the VSS. We show that regarding the action space at each stage of the dynamic program, only vehicles within walking distance need to be considered, such that online pricing becomes tractable. Based on the dynamic programming formulation, we develop an approximate dynamic programming solution method for the online pricing problem. The approach incorporates a non-parametric regression which allows the approximation of future profits based on historical data. This enables the pre-calculation of state-values such that the numerical operations of the online pricing problem can be reduced to a minimum.

- We conduct several computational studies, including sensitivity analyses as well as a case study based on Share Now data from the city of Vienna. We consider a discrete set of five (see Sections 5.5.4 to 5.5.6) or three price points (see Section 5.6) as VSS providers aim for a transparent and easy-to-communicate pricing mechanism. These studies show that our new dynamic pricing approach dominates all of the considered benchmarks in terms of realized profit, including state-of-the-art approaches from the literature. Further,

these results are shown to be robust across the various considered settings and parameter variations, such as different VSSs sizes, overall demand levels, and customer preferences.

- We derive a number of relevant managerial insights from the computational studies. In particular, we show that our pricing approach is particularly effective when there is spatial variation in demand and that sophisticated anticipation of future states and profits is key. Another finding is that our pricing approach realizes higher profits compared to the benchmarks while maintaining the overall level of rentals, which is beneficial for service-oriented metrics of a VSS provider.

The remainder of the paper is organized as follows. In Section 5.2, we review the relevant literature. Section 5.3 formalizes the problem. Based on this, we develop the new dynamic pricing approach in Section 5.4. Section 5.5 contains the computational study with a discrete set of five price points. Section 5.6 presents the Share Now case study with the set of the three original price points. Section 5.7 concludes the paper and gives an outlook on future research. The appendix contains additional numerical results and a list of notation.

5.2 Related Literature

The literature on VSS optimization is broad, covering various types of systems, optimization problems, control approaches, and methodologies. General overviews on VSS optimization problems have been presented in survey papers on bike sharing (e.g. DeMaio, 2009; Fishman, Washington, and Haworth, 2013; Ricci, 2015), car sharing (e.g. Jorge and Correia, 2013; Ferrero et al., 2015a,b; Illgen and Höck, 2019; Golalikhani et al., 2021a,b), and VSSs in general (e.g. Laporte, Meunier, and Wolfler Calvo, 2015, 2018).

To define the scope of the following discussion of the related literature, please first note that VSSs are one specific type of shared mobility systems (Mourad, Puchinger, and Chu, 2019), with the latter also comprising other modern mobility concepts such as ride-hailing (e.g. Wang and Yang, 2019), ride-pooling (e.g. Ke et al., 2020), or dial-a-ride (e.g. Qiu et al., 2018). VSSs substantially differ from these other mobility concepts in terms of the service offered as well as in terms of the provider's operating tasks. For example, in contrast to ride-hailing where the provider operates a platform that connects passengers and drivers in a two-sided market for individual trips, providers of VSSs operate in a one-sided market with a fixed supply (fleet) of (non-autonomous) vehicles. Further, e.g., in dial-a-ride concepts, the provider is in charge of executing trips and, thus, strives for shared trips among passengers, whereas users in VSSs rent vehicles for individual trips and then drive these vehicles themselves. Due to these substantial differences in terms of mobility services and provider tasks, we exclude the other mobility concepts from our literature discussion and exclusively concentrate on VSSs. As a side remark, please note that the term "shared mobility system" is sometimes also used in a narrower sense as a synonym for VSS (e.g. Laporte, Meunier, and Wolfler Calvo, 2015, 2018).

Within the literature on VSS pricing, we further focus on the closest related works that address *dynamic* pricing in VSSs. Dynamic – in contrast to *differentiated* (or static) pricing for VSSs like in Waserhole and Jost (2012) or Ren et al. (2019) – means that the pricing is performed on-line and depends on the system's current state (e.g. vehicle locations) (Agatz et al., 2013).

Our presentation of the closest related literature is organized in two groups according to the methodology proposed. First, in Section 5.2.1, we summarize approaches in which prices are determined through *business rules*. Second, in Section 5.2.2, we present those which are based on *optimization*. For both groups, we distinguish further into approaches that are *anticipative* in contrast to the *myopic* ones. Please note that some of these works have another main focus than pricing, but we discuss them specifically with regard to their pricing mechanism. In Section 5.2.3, we briefly refer to other literature streams that are related only in a broader sense. Finally, in Section 5.2.4, we position our approach in the closest related literature on dynamic pricing for VSSs.

5.2.1 Rule-Based Approaches

Rule-based approaches propose business rules to derive prices, for example by comparing endogenously given thresholds to the current state of the system. Among them, a group of anticipative approaches incorporates expected future states of the VSS into the pricing decision. Threshold

values are usually compared with the ratio of future supply and demand at individual locations, which is derived from historical data and the system's current state (Brendel, Brauer, and Hildebrandt, 2016; Dötterl et al., 2017). Wagner et al. (2015) in contrast consider exogenously given rules based on expected idle times. These three works have in common that they propose an overall framework for dynamic pricing, of which the rule-based pricing approach is one component.

Other works that use business rules propose myopic approaches. Bianchessi, Formentin, and Savaresi (2013) compare the number of vehicles at a location with the mean value across all locations to determine prices. Zhang, Meng and David (2019) define prices by comparing the current number of vehicles with demand and propose a negative price that is linear in the undersupply of a rental's destination location. If there is no undersupply, the regular positive price applies. Barth, Todd, and Xue (2004) propose a system that, once it recognizes an imbalance, provides incentives for joint rides of independent customers in one car or splitting a party of customers into multiple cars. Mareček, Shorten, and Yu (2016) derive drop-off charges for vehicles depending on the intended destination location's distance to the nearest vehicle. Angelopoulos et al. (2016, 2018) propose two algorithms for promoting trips based on the priorities of vehicle relocations between locations. Chung, Freund, and Shmoys (2018) study the impact of an incentive program of New York City's bike sharing system and propose two myopic dynamic pricing approaches which are based on a performance metric that incorporates the estimated reduction of future out-of-stock events as well as the costs incurred by the incentives. Whereas the first considers each individual trip, the second determines decisions less frequently, i.e., for several periods. Neijmeijer et al. (2020) is difficult to classify regarding methodology. They formulate a MIP that minimizes deviations of idle times from a desired value plus the costs of incentives, but in the empirical evaluations of a scooter sharing system, they test the effect of two possible discounts on vehicles' idle times.

5.2.2 Optimization-Based Approaches

Optimization-based dynamic pricing approaches are characterized by having a formal objective metric that is maximized (profit, revenue, rentals, service, etc.) or minimized (costs, unsatisfied demand, etc.). Methodologically, these approaches comprise those built on mathematical optimization like mixed-integer programming as well as learning methods that iteratively improve the objective, like reinforcement learning.

A couple of these optimization-based approaches use anticipative models. Singla et al. (2015) design a complete architecture of an operational incentive system which comprises, among other components, an "Incentive Deployment Schema" that decides whether to offer an alternative station with incentives or not with the objective to align future demand and supply. They evaluate using a real world survey as well as simulations. Pfrommer et al. (2014) propose an approach that uses quadratic programming and combines user-based and operator-based relocation. Prices are recalculated each period in a rolling horizon fashion. Ruch, Warrington, and Morari (2014) build on Pfrommer et al. (2014) and investigate simplified variants that can be used to benchmark more complex approaches. Di Febbraro, Sacco, and Saeednia (2012) aim at balancing supply and demand at all locations. They suggest alternative drop-off locations

with a discount to customers. Assuming a given acceptance probability for these suggestions, a simulation evaluates the benefit for vehicle availability. Di Febbraro, Sacco, and Saeednia (2019) follow up on their earlier paper and formulate and test corresponding optimization models. Kamatani, Nakata, and Arai (2019) optimize thresholds by simulation-based optimization (Q-learning), while Clemente et al. (2017) propose a decision support system that uses a simulation-based heuristic (particle swarm optimization).

The remaining papers use myopic optimization. While they overall focus on user-based relocation, in one subsection Chemla et al. (2013) determine myopic prices period by period. They aim at a service-maximizing fleet distribution in bike-sharing systems through user-based relocation, where customer satisfaction is measured by successful and unsuccessful customer actions (available or non available bike, empty or full rack). They use a linear program to determine the number of customers who change their travel plans because of the price incentive to reach the given target inventory of vehicles for each location. Two papers do not directly solve a mathematical model, but use it as a basis to develop a heuristic. Haider et al. (2018) formulate a bi-level program, where the upper level determines prices and minimizes vehicle imbalance, while the lower level represents the cost-minimizing route choice of customers. The problem is transformed into a single-level problem and a heuristic is proposed that iteratively adjusts prices (and, in contrast to the bi-level program, contains some anticipation). Wang and Ma (2019) consider the objective of keeping inventory within a certain range for a period. For this purpose, they define lower and upper thresholds for each location. The number of rentals from or to a location can be affected by pickup and drop-off fees. They formulate a simple quadratic program to determine optimal dynamic pickup and drop-off fees and solve it with a genetic algorithm. Kanoria and Qian (2019) define a myopic and location-based dynamic pricing algorithm for a trip-based VSS with time-variant arrival rates, without knowledge of arrival rates and with a finite time horizon. The algorithm needs the information about the queue length of origin and destination and a partitioning of the business area into zones.

5.2.3 Further Literature

There are several further literature streams which have some similarities with the considered problem and the applied methods, but which we do not discuss in detail. In particular, this concerns the determination of relocation prices with an auction process for VSSs (Ghosh and Varakantham, 2017). Furthermore, we do not consider papers that do not describe the price setting process in detail. For example, Fricker and Gast (2016) show that user-based relocation is worthwhile, but they do not elaborate on how the prices are calculated.

Another stream of the literature investigates the steady state of stationary settings in mobility sharing concepts (including VSSs as considered in this work and ride-hailing applications), using techniques from closed-queuing networks. Waserhole and Jost (2016) maximize the number of trips taken, assuming time-invariant demand and zero travel time. Banerjee, Freund, and Lykouris, Thodoris (2022) extend this work by considering additional performance metrics and allowing non-zero travel time. Besbes, Castro, and Lobel (2021) focus on the single-location case of this setting. Benjaafar and Shen (2022) present an alternative solution approach with better performance bounds for several of the particular problems addressed in the above. Since

all of these works consider stylized steady-state settings with time-invariant arrival-rates, exact knowledge of arrival-rate and an infinite time horizon. The derived pricing policies are differentiated (static) (see Benjaafar and Shen, 2022), and, thus, not within the scope of our work. Further, they consider the systems on an aggregated level in which customer choices on a disaggregated level cannot be easily incorporated. Note that there are papers from this stream that differ from the aforementioned papers and use dynamic pricing. We have already mentioned an example (Kanoria and Qian , 2019) of this in Section 5.2.2.

5.2.4 Positioning in the Literature

Our approach is positioned as follows in the literature on dynamic pricing for VSSs. With regard to methodology, the pricing approach we propose is anticipative and optimization-based. Thus, it belongs to the first group of works named in Section 5.2.2. It substantially differs from the above-named closest related works in particular by incorporating the concept of customer-centricity. As explained in Section 5.1 and illustrated by Figure 5.1, this means that prices are situation-specific for each customer, considering in particular a customer's location, the available vehicles within walking distance and other situational characteristics that influence the customer choice behavior, like walking distances to these vehicle. Using this situation-specific information for each customer has also been applied in shared mobility systems other than VSSs, e.g. for mobility on demand services (Qiu et al., 2018). To adopt this idea to the particularities of free-floating VSSs, we design our approach using disaggregate demand modeling which is capable of capturing the uncertain choice behavior. More specifically, our approach is designed to incorporate discrete choice models (Train, 2009) in which the available vehicles within walking distance represent the discrete alternatives of the customer's consideration set that have individual choice probabilities. In the context of dynamic pricing in VSSs, we are not aware of any other comparable pricing approach.

As a consequence, our work also differs in terms of the mathematical modeling. Almost all of the closest related works which use mathematical models for determining prices use deterministic models (e.g. Chemla et al., 2013; Pfrommer et al., 2014; Wang and Ma, 2019). In contrast, our approach is built upon a stochastic dynamic model and uses approximate dynamic programming with a non-parametric value function approximation to become tractable and scalable.

With regard to the type of the VSS, there are a few papers that also consider free-floating systems, albeit with rule-based approaches. Di Febbraro, Sacco, and Saeednia (2012) and Di Febbraro, Sacco, and Saeednia (2019) are the only two optimization-based approaches. Their vehicle-specific pricing is based on aggregated demand modeling.

Further, our approach differs from most of the literature in that prices are origin-based, meaning that they only depend on time and location of a rental's start. Such origin-based pricing, as applied by Share Now, is the most practicable variant for free-floating VSSs (see Section 5.1 or Soppert et al., 2022) for differentiated pricing, and thus a popular business practice. Other variants are destination-based prices (e.g. target-specific discounts as in Singla et al., 2015) and trip-based prices (or other incentives as in Chung, Freund, and Shmoys , 2018), that depend on both origin and destination. Only Neijmeijer et al. (2020) in a rule-based approach consider origin-based pricing.

5.3 Model

In this section, we formally model the free-floating VSS provider's decision problem as a dynamic program. To do so, in Section 5.3.1, we give an overview on the sequence of events. In Sections 5.3.2 to 5.3.5, we explain how we choose the standard ingredients of dynamic programs: states, decisions, state transitions, and cost/revenue function. Based on this, we formally state the provider's optimization problem in Section 5.3.6.

5.3.1 Sequence of Events

We consider a free-floating VSS provider who operates a fleet of vehicles $\mathcal{C} = \{1, \dots, C\}$ which is distributed spatially across a continuous business area. At any given point in time, a vehicle $i \in \mathcal{C}$ is either *idle* (standing available) or *in use* (currently rented). The provider seeks to maximize his profit over a finite planning horizon (e.g. one day) by pricing.

We follow the standard approach in the literature on pricing and revenue management by which this planning horizon is discretized into micro periods $t \in \{0, \dots, T\} = \mathcal{T}$ and we have Δ micro periods per minute. These micro periods are w.l.o.g. so short that at most one customer request arrives and/or one rental terminates per period.

For every customer who opens the mobile application and requests prices, the provider has the ability to optimize and display prices. Hence, in this *online pricing problem*, the four *steps* within a micro period t are the following: (I) A customer may arrive, (II) if so, prices are determined by the provider, and (III) the customer chooses among the available vehicles under consideration of the offered prices. Finally, (IV) another moving vehicle that was previously rented (before period t) by another customer may return. One micro period of this process is illustrated in Figure 5.2, where decision nodes are represented as squares and stochastic nodes as circles.

Please note that in the following description, t denotes the current period, t' an earlier period, and t'' some future period, i.e., $t' < t < t''$. Further, for random variables, following conventional notation, the indices t', t, and t'' reflect when these random variables *realize* and, thus, become known to the provider.

Step I: At the beginning of period t, the system is in state S_t which contains information about idle and driving vehicles. Now, at the stochastic node (circle) in Step I, with probability λ_t a *customer* k_t *arrives*, i.e., she opens the mobile application and looks for available vehicles. The coordinates of the requesting customer's specific location in the business area are random variables (X_t^O, Y_t^O) which follow a given, time-dependent origin probability distribution $O(t)$. Realizations of these random variables, meaning the coordinates where a customer opens the mobile application, are denoted with (x_t^O, y_t^O).

Step II: The *provider optimizes the* $C \times 1$ *price vector* $\vec{\boldsymbol{p}}_{\boldsymbol{t}}$, visualized by the decision node (square).

Step III: Based on these prices, the *customer* k_t *decides* whether and which vehicle to rent. The vehicle chosen is denoted by the random variable I_t with realizations i_t. The *customer choice behavior* is formalized as follows: Customers have a (fixed) maximum willingness to walk $\bar{d}$ (assumed to be known), meaning that a customer only considers idle vehicles i_t for which the

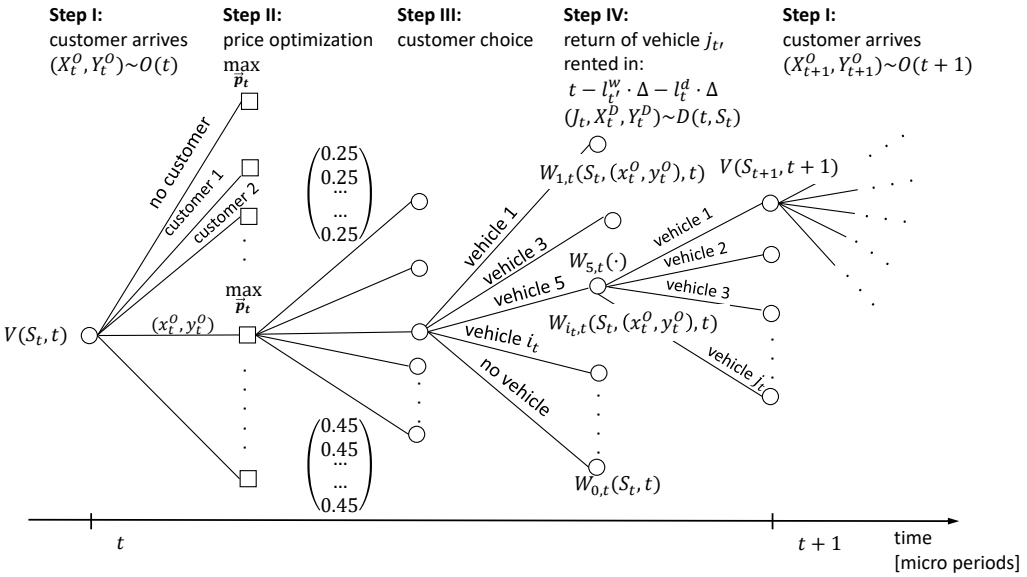

Figure 5.2: Illustration of dynamic pricing problem

walking distance $d_{i_t,t}$ between the customer's current location (x_t^O, y_t^O) and the idle vehicle is smaller than this radius, i.e., the consideration set is $\mathcal{C}_{t,(x_t^O,y_t^O)} = \{i_t \in \mathcal{C} \mid d_{i_t,t} \leq \bar{d} \wedge \tau_{i_t,t}^v = 0\}$ ($\tau_{i_t,t}^v$ is explained below in Section 5.3.2, it contains the information whether a vehicle is idle or in use). This is a well-known behavior of customers in VSSs and has been reported in multiple studies (e.g. Niels and Bogenberger, 2017). More technically, we assume that the customer's choice probability $q_{i_t,t}$ for vehicle $i_t \in \mathcal{C}_{t,(x_t^O,y_t^O)}$ follows a known choice model and depends on the prices and the distances of the vehicles within reach, i.e. $\mathcal{C}_{t,(x_t^O,y_t^O)}$ and $\vec{\boldsymbol{p}}_{\boldsymbol{t}}$. The probability of not choosing any of the available vehicles is denoted by $q_{0,t}$. Note that our problem formulation is generic in this regard, meaning that *arbitrary* choice models providing these probabilities can be used. In the numerical studies, we apply a multinomial logit model (e.g. Train, 2009). If she chooses a vehicle, the customer needs to walk there. This walking time l_t^w in minutes is a realization of L_t^W and depends on her distance to the vehicle. We assume a constant walking speed. As the chosen vehicle is stochastic, L_t^w is a random variable.

Step IV: Finally, in each micro period, w.l.o.g., at most one *rental may terminate*, which started in some period $t' < t$ *before* the current period t. More specifically, a customer who arrived at $t' = t - l_{t'}^w \cdot \Delta - l_t^d \cdot \Delta$ terminates her rental in t (see also Figure 5.3). Similar to the customer origin probability distribution $O(t)$, when and where a rental terminates is random. More technically, (J_t, X_t^D, Y_t^D) is a random variable which denotes that vehicle J_t (zero if none) is returned at location (X_t^D, Y_t^D). It follows a given *destination probability distribution* $D(t, S_t)$ that depends on the *state* S_t at the beginning of period t. The state definition is explained below. In particular, to capture typical traffic flow patterns, $D(t, S_t)$ may depend on where and when the currently driving customers have originated. Realizations of these random variables are denoted with j_t and $(x_t^D,\ y_t^D)$. The driving/rental time l_t^d in minutes is a realization of the random variable L_t^d, which follows a distribution $\rho(S_{t'})$ and depends on the stochastic travel speed and the travel distance from pick-up to drop-off location (X_t^D, Y_t^D) of the vehicle, all unknown to the provider before the rental ends at micro period t.

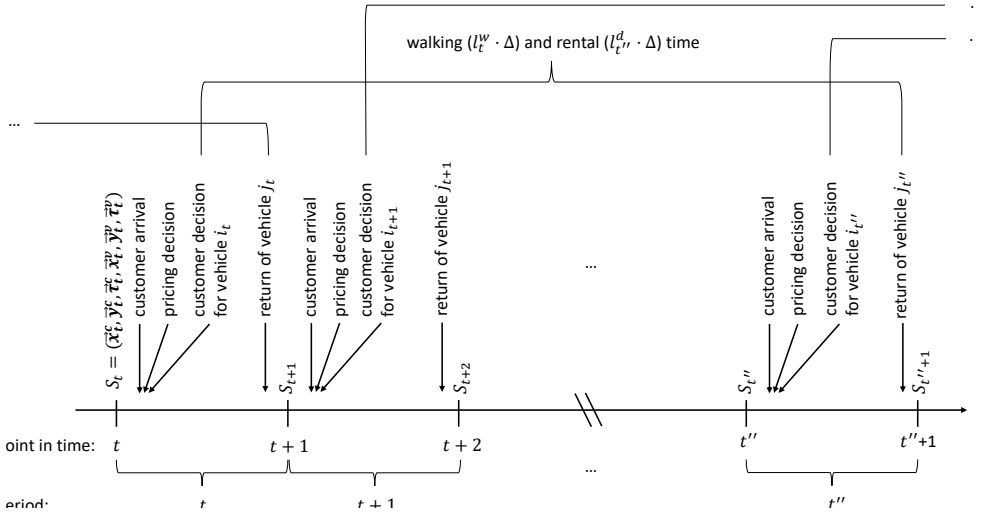

Figure 5.3: Sequence of events

5.3.2 State

The VSS's state $S_t = (\vec{x}_t^c, \vec{y}_t^c, \vec{\tau}_t^c, \vec{x}_t^v, \vec{y}_t^v, \vec{\tau}_t^v)$ at the beginning of period t consists of six vectors of dimension $C \times 1$, where the i_t-th element in each vector describes a property of the i_t-th vehicle of the fleet. The vectors $\vec{x}_t^v$ and $\vec{y}_t^v$ contain the coordinates of all vehicles of the fleet, i.e. $x_{i_t,t}^v$ and $y_{i_t,t}^v$ $\forall i_t \in \mathcal{C}, t \in \mathcal{T}$, respectively. More specifically, for an idle vehicle they contain the coordinates of its location at the current micro period t. For a rented vehicle, they contain where the currently driving customer picked up the vehicle. The vector $\vec{\tau}_t^v$ contains when the vehicle was picked up, with the value 0 indicating a vehicle standing idle. The vectors $\vec{x}_t^c$, $\vec{y}_t^c$, and $\vec{\tau}_t^c$ describe when and where the respective customers have requested the rental (i.e. for driving vehicles when and where the *customer* initially opened the mobile application).

5.3.3 Actions

Regarding the VSS provider's *pricing* decisions, we assume that the provider seeks to maximize profits by means of dynamic pricing. More precisely, when a customer opens the mobile application to look for available vehicles in micro period t, the VSS provider needs to optimize prices. As explained in Section 5.1, prices are *origin-based per-minute prices* and they are chosen from a discrete finite price set $\mathcal{M}$.

5.3.4 State Transitions

The transition function describes the evolution of the system from state S_t at the beginning of period t to state S_{t+1} at the beginning of period $t+1$. It depends on the current state S_t and the following *realizations* of random variables: the arriving customer's location (x_t^O, y_t^O), the chosen vehicle i_t (0 indicates the customer decides against renting a vehicle), and the returned vehicle j_t together with its return location (x_t^D, y_t^D) if (another) vehicle j_t rented before is returned (likewise, $j_t = 0$ indicates no vehicle is returned), i.e.,

$$S_{t+1} = S_{t+1}\big(S_t, (x_t^O, y_t^O), i_t, (x_t^D, y_t^D), j_t\big). \tag{5.1}$$

Please note that the probability distribution of the chosen vehicle I_t and therewith specific choices i_t depend on $\vec{\boldsymbol{p}}_{\boldsymbol{t}}$. Technically speaking, S_{t+1} is *probabilistically dependent* (Powell , 2011, Chapter 3) on the pricing decision $\vec{\boldsymbol{p}}_{\boldsymbol{t}}$. By contrast, j_t does not depend on $\vec{\boldsymbol{p}}_{\boldsymbol{t}}$, but solely on which vehicles are currently in use and when and where these rentals started (stored in $\vec{\boldsymbol{x}}^{\boldsymbol{c}}_{\boldsymbol{t}}, \vec{\boldsymbol{y}}^{\boldsymbol{c}}_{\boldsymbol{t}}, \vec{\boldsymbol{\tau}}^{\boldsymbol{c}}_{\boldsymbol{t}}, \vec{\boldsymbol{x}}^{\boldsymbol{v}}_{\boldsymbol{t}}, \vec{\boldsymbol{y}}^{\boldsymbol{v}}_{\boldsymbol{t}}, \vec{\boldsymbol{\tau}}^{\boldsymbol{v}}_{\boldsymbol{t}}$).

The transitions of the state vectors are as follows. When a customer selects a vehicle i_t, the respective entries of the vectors $\vec{\boldsymbol{x}}^{\boldsymbol{c}}_{\boldsymbol{t}}$ and $\vec{\boldsymbol{y}}^{\boldsymbol{c}}_{\boldsymbol{t}}$ are filled with the customer's origin location (x_t^O, y_t^O), the *origin* time is updated to $\tau^c_{i_t,t} = t$ and the rental start time is set to $\tau^v_{i_t,t} = t + l^w_t \cdot \Delta$. When vehicle i_t is returned, $x^v_{i_t,t}$ and $y^v_{i_t,t}$ change to the destination location (x_t^D, y_t^D) and the corresponding $\tau^v_{i_t,t}$ and $\tau^c_{i_t,t}$ change back to 0.

5.3.5 Cost/Revenue Structure

For each minute that a vehicle i_t is rented, the provider collects the corresponding revenue $p_{i_t,t}$. During the rental, when the customer drives, the provider incurs variable costs per minute of c (e.g. for fuel). Following common practice, we assume that the short time frame the customer needs to walk to the vehicle is free of charge. Thus, the profit resulting from renting out vehicle i_t to the customer who arrived in period t and will return it in period t'' is given by $(p_{i_t,t} - c) \cdot l^d_{t''}$, where $l^d_{t''}$ is the realization of $L^d_{t''} \sim \rho(S_t)$.

5.3.6 Dynamic Programming Formulation

In this subsection, we model the problem described previously as a Markov decision process and state the corresponding Bellman equation:

$$
\begin{aligned}
&V(S_t, t) = \\
&\lambda_t \cdot \mathop{\mathbb{E}}_{\substack{(X_t^O, Y_t^O) \\ \sim O(t)}} \Bigg[\max_{\vec{\boldsymbol{p}}_{\boldsymbol{t}}} \overbrace{\sum_{i_t \in \mathcal{C}_{t,(x_t^O, y_t^O)}} q_{i_t,t}(\vec{\boldsymbol{p}}_{\boldsymbol{t}}) \cdot \Big((p_{i_t,t} - c) \cdot \mathop{\mathbb{E}}_{L^d_{t''} \sim \rho(S_t)} [L^d_{t''}]}^{\text{customer arrives and chooses a vehicle}} \\
&\overbrace{+ \mathop{\mathbb{E}}_{\substack{(J_t, X_t^D, Y_t^D) \\ \sim D(t, S_t}} \Big[V\Big(S_{t+1}\big(S_t, (X_t^O, Y_t^O), i_t, (X_t^D, Y_t^D), J_t\big), t+1 \Big) \Big] \Big)}^{\text{customer arrives and chooses a vehicle}} \\
&\overbrace{+ q_{0,t}(\vec{\boldsymbol{p}}_{\boldsymbol{t}}) \cdot \mathop{\mathbb{E}}_{\substack{(J_t, X_t^D, Y_t^D) \\ \sim D(t, S_t}} \Big[V\Big(S_{t+1}\big(S_t, 0, 0, (X_t^D, Y_t^D), J_t\big), t+1 \Big) \Big]}^{\text{customer arrives and chooses no vehicle}} \Bigg] \\
&\overbrace{+ (1 - \lambda_t) \cdot \mathop{\mathbb{E}}_{\substack{(J_t, X_t^D, Y_t^D) \\ \sim D(t, S_t}} \Big[V\Big(S_{t+1}\big(S_t, 0, 0, (X_t^D, Y_t^D), J_t\big), t+1 \Big) \Big]}^{\text{no customer arrives}}
\end{aligned}
\tag{5.2}
$$

with the boundary condition $V(S_T, T) = 0 \, \forall S_T$. The Bellman equation recursively calculates the optimal expected profit from future rentals $V(S_t, t)$ for being in state S_t at the beginning of period t. Each micro period t corresponds to a stage in this dynamic program. In the following, we explain how the four steps (I-IV) within each stage (=micro period) are represented in (5.2).

In the first and the second line of (5.2), a customer arrives (Step I) with probability λ_t at a location (x_t^O, y_t^O) and in this case, the optimal price vector $\vec{\boldsymbol{p}}_{\boldsymbol{t}}$ for all available vehicles is

determined (Step II). The following customer choice process has different potential outcomes (Step III): With probability $q_{i_t,t}(\vec{\boldsymbol{p}}_{\boldsymbol{t}})$ (first line), vehicle i_t is chosen, and, in expectation a profit of $(p_{i_t,t} - c) \cdot \mathbb{E}_{L^d_{t'' \sim \rho(S_t)}}[L^d_{t''}]$ is obtained. Another vehicle j_t that was rented before micro period t may be returned at location (x^D_t, y^D_t) (Step IV) and the system evolves to the next state in micro period $t+1$ where expected future profit is $V\left(S_{t+1}\left(S_t, (x^O_t, y^O_t), i_t, (x^D_t, y^D_t), j_t\right), t+1\right)$.

With probability $q_{0,t}(\vec{\boldsymbol{p}}_{\boldsymbol{t}})$ (second line), no vehicle is chosen. Nonetheless a vehicle j_t may be returned at location (x^D_t, y^D_t), and the system evolves into the state in micro period $t+1$ with expected future profit $V\left(S_{t+1}\left(S_t, 0, 0, (x^D_t, y^D_t), j_t\right), t+1\right)$. The third line of the Bellman equation considers the case – occuring with probability $(1-\lambda_t)$ – in which no customer arrives, so again, only a vehicle may be returned at location (x^D_t, y^D_t). Hence, we have the same expected future profit as in the second line of the equation.

If a customer arrives in micro period t, the optimal prices need to be calculated. When doing so, the provider is aware of the customer's coordinates (x^O_t, y^O_t), which are thus deterministic for the problem of pricing. Obviously, profit-maximizing prices in (5.2) are given by

$$\begin{aligned}\vec{p}^{\,*}_t = \underset{\vec{p}_t}{\arg\max} \sum_{i_t \in \mathcal{C}_{t,(x^O_t, y^O_t)}} q_{i_t,t}(\vec{p}_t) \cdot \Big((p_{i_t,t} - c) \cdot \mathbb{E}_{L^d_{t'' \sim \rho(S_t)}}[L^d_{t''}] + W_{i_t}\big(S_t, (x^O_t, y^O_t), t\big) \Big) \\ + q_{0,t}(\vec{p}_t) \cdot W_0(S_t, t)\end{aligned} \tag{5.3}$$

with

$$W_{i_t,t}\big(S_t, (x^O_t, y^O_t), t\big) = \mathop{\mathbb{E}}_{\substack{(J_t, X^D_t, Y^D_t) \\ \sim D(t, S_t)}} \left[V\Big(S_{t+1}\big(S_t, x^O_t, y^O_t), i_t, (X^D_t, Y^D_t), J_t\big), t+1 \Big) \right] \quad \forall i_t \in \mathcal{C}_{t,(x^O_t, y^O_t)}, \tag{5.4}$$

$$W_{0,t}(S_t, t) = \mathop{\mathbb{E}}_{\substack{(J_t, X^D_t, Y^D_t) \\ \sim D(t, S_t)}} \left[V\Big(S_{t+1}\big(S_t, 0, 0, (X^D_t, Y^D_t), J_t\big), t+1 \Big) \right]. \tag{5.5}$$

Since the provider knows the customer's coordinates, he also knows her consideration set $\mathcal{C}_{t,(x^O_t, y^O_t)}$ and only the prices for the idle vehicles $i_t \in \mathcal{C}_{t,(x^O_t, y^O_t)}$ within reach of the current customer at location (x^O_t, y^O_t) need to be optimized, as the choice probabilities only depend on them (see Section 5.3.3 and Figure 5.1a). Thus, instead of the $C \times 1$ vector $\vec{\boldsymbol{p}}_{\boldsymbol{t}}$, a smaller price vector $\vec{\boldsymbol{p}}_{\boldsymbol{t},(\boldsymbol{x^O_t}, \boldsymbol{y^O_t})}$ with only $|\mathcal{C}_{t,(x^O_t, y^O_t)}| \times 1$ entries (a subset of the entries of the original price vector) needs to be optimized. More specifically, this new $\vec{\boldsymbol{p}}_{\boldsymbol{t},(\boldsymbol{x^O_t}, \boldsymbol{y^O_t})}$ contains the entries i of $\vec{\boldsymbol{p}}_{\boldsymbol{t},(\boldsymbol{x^O_t}, \boldsymbol{y^O_t})}$, for which $i \in \mathcal{C}_{t,(x^O_t, y^O_t)}$. Thus, the action space reduces from pricing all idle vehicles of the fleet to a handful and the online pricing problem becomes

$$\begin{aligned}\vec{p}^{\,*}_{t,(x^O_t, y^O_t)} = \underset{\vec{p}_{t,(x^O_t, y^O_t)}}{\arg\max} \sum_{i_t \in \mathcal{C}_{t,(x^O_t, y^O_t)}} q_{i_t,t}(\vec{p}_t) \cdot \Big((p_{i_t,t} - c) \cdot \mathop{\mathbb{E}}_{L^d_{t'' \sim \rho(S_t)}}[L^d_{t''}] + W_{i_t,t}\big(S_t, (x^O_t, y^O_t), t\big) \Big) \\ + q_{0,t}(\vec{p}_t) \cdot W_{0,t}(S_t, t).\end{aligned} \tag{5.6}$$

The dynamic program considers all steps (Step I-Step IV) in a micro period, i.e., at the beginning of the micro period, it is not yet clear if and where a customer arrives. Therefore, the outer expectation in (5.2) is over the location $(X^O_t, Y^O_t) \sim O(t)$ where the customer arrives. However, the supplier determines the prices of the reachable vehicles when the customer has

already arrived (Step II). Thus, when deciding on prices, the provider knows the location (x_t^O, y_t^O) of the customer and the expectation over $(X_t^O, Y_t^O) \sim O(t)$ can be dropped in (5.6).

5.4 Solution Method

In this section, we describe the solution method we propose for the considered problem. First, in Section 5.4.1, we derive a convexity result that allows us to obtain an efficient linear reformulation of the pricing problem. Then, in Section 5.4.2, we develop our approximate dynamic programming solution method. Section 5.4.3 contains the proposed non-parametric value function approximation, including a description how historical data is used.

5.4.1 Convexity of the Pricing Problem and Linear Reformulation

When solving the online pricing problem (5.6) by complete enumeration, the number of calculations that must be performed for each micro period t is of the order $\mathcal{O}(|\mathcal{M}|^{|\mathcal{C}_{t,(x_t^O,y_t^O)}|})$, implying that the calculation time in one single stage of the dynamic program increases exponentially with the number of reachable vehicles $|\mathcal{C}_{t,(x_t^O,y_t^O)}|$ and polynomially with the number of price levels $|\mathcal{M}|$. Further, given that the state space grows exponentially across the multiple stages, an alternative solution method is required to efficiently solve larger instances.

Under the assumption that demand follows a multinomial logit model (see Section 5.3.1) as it does in our numerical studies (see Section 5.5.4.2), the pricing problem at stage t (i.e. the one-stage optimization problem) can be formalized by the following fractional program(see, e.g., Davis, Gallego, and Topaloglu, 2013), using decision variables $z_{i_t,m}$ that equal 1 if the provider selects price level m for vehicle i_t:

$$\max \frac{1}{B_t + \sum_{i_t \in \mathcal{C}_{t,(x_t^O,y_t^O)}} \sum_{m \in \mathcal{M}} A_{i_t,t,m} \cdot z_{i_t,t,m}} \cdot \left[\sum_{i_t \in \mathcal{C}_{t,(x_t^O,y_t^O)}} \sum_{m \in \mathcal{M}} \left((p_{i_t,m} - c) \cdot \mathop{\mathbb{E}}_{L^d_{t''} \sim \rho(S_t)} [L^d_{t''}] + W_{i,t}\big(S_t, (x_t^O, y_t^O), t\big) \right) \cdot A_{i_t,t,m} \cdot z_{i_t,t,m} + B_t \cdot W_{0,t}(S_t, t) \right] \tag{5.7}$$

s.t.

$$\sum_{m \in \mathcal{M}} z_{i_t,t,m} = 1 \qquad \forall i_t \in \mathcal{C}_{t,(x_t^O,y_t^O)} \tag{5.8}$$

$$z_{i_t,t,m} \in \{0,1\} \qquad \forall i_t \in \mathcal{C}_{t,(x_t^O,y_t^O)}, m \in \mathcal{M} \tag{5.9}$$

In the objective function (5.7), $A_{i_t,t,m}$ denote given attraction values for each vehicle i_t and price level m, capturing the attractiveness of the corresponding alternative to the customer. The attraction values correspond to $e^{(u_{i_t,t})}$, with $u_{i_t,t}$ referring to the utility of alternative i_t in the underlying multinomial logit demand model. The attraction value for the no-choice alternative is B_t and corresponds to $e^{(u_{0,t})}$. Constraints (5.8) ensure that exactly one price level m is selected for each reachable vehicle i_t, and Constraints (5.9) define the variables $z_{i_t,t,m}$ as binary.

The structure of the fractional program (5.7)-(5.9) is identical to that of the product line and price selection problem analyzed by Chen and Hausman (2000). They show that its objective function is strictly quasi-convex in $z_{i_t,m}$. Further, the coefficient matrix of the model's Constraints (5.8) is totally unimodular (also see Lemma 2 in Chen and Hausman (2000)).

Consequently, the binary Constraints (5.9) can be LP-relaxed (i.e., $0 \leq z_{i_t,t,m} \leq 1 \quad \forall i_t \in \mathcal{C}_{t,(x_t^O,y_t^O)}, m \in \mathcal{M}$) and, due to the convexity of the resulting model, every local maximum is also a global maximum, allowing to solve the problem by standard nonlinear programming codes.

It is even possible to use linear programming to solve the problem, as we can linearize the objective of the relaxed fractional program by applying a Charnes-Cooper transformation (see, e.g. Stancu-Minasian , 1997). The idea is to substitute the reciprocal of the denominator, i.e., $(B_t + \sum_{m\in\mathcal{M}} \sum_{i_t \in \mathcal{C}_{t,(x_t^O,y_t^O)}} A_{i_t,t,m} \cdot z_{i_t,m})^{-1}$ in (5.7) by a new variable $v_t > 0$ and ensure correctness by additionally imposing the constraint:

$$B_t \cdot v_t + \sum_{i_t \in \mathcal{C}_{t,(x_t^O,y_t^O)}} \sum_{m\in\mathcal{M}} A_{i_t,t,m} \cdot \hat{z}_{i_t,t,m} = 1, \tag{5.10}$$

where the variable $\hat{z}_{i_t,t,m}$ substitutes $v_t \cdot z_{i_t,t,m}$.

After performing the latter substitution also in the existing constraints of the relaxed fractional program and removing redundant constraints, the following equivalent, linear reformulation for period t is obtained:

$$\begin{aligned} \max \sum_{i_t \in \mathcal{C}_{t,(x_t^O,y_t^O)}} \sum_{m\in\mathcal{M}} \Bigg((p_{i_t,m} - c) \cdot \mathop{\mathbb{E}}_{L^d_{t''}\sim\rho(S_t)} (L^d_{t''}) + W_{i_t}\big(S_t, (x_t^O, y_t^O), t\big) \Bigg) \\ \cdot A_{i_t,t,m} \cdot \hat{z}_{i_t,t,m} + (B_t \cdot v_t) \cdot W_{0,t}(S_t, t) \end{aligned} \tag{5.11}$$

s.t.

$$B_t \cdot v_t + \sum_{i_t \in \mathcal{C}_{t,(x_t^O,y_t^O)}} \sum_{m\in\mathcal{M}} A_{i_t,t,m} \cdot \hat{z}_{i_t,t,m} = 1 \tag{5.12}$$

$$\sum_{m\in\mathcal{M}} \hat{z}_{i_t,t,m} = v_t \qquad \forall i_t \in \mathcal{C}_{t,(x_t^O,y_t^O)} \tag{5.13}$$

$$\hat{z}_{i_t,t,m} \geq 0 \qquad \forall i_t \in \mathcal{C}_{t,(x_t^O,y_t^O)}, m \in \mathcal{M} \tag{5.14}$$

$$v_t \geq 0 \tag{5.15}$$

5.4.2 Approximate Dynamic Programming Solution Method

The state space as well as the outcome space of the dynamic program (5.2) depend on the coordinates of the arriving customer. Since the customer can arrive anywhere within the continuous business area, these coordinates are continuous. The same holds for the return location of a vehicle. Thus, state and outcome space are of infinite size. As a consequence, the dynamic program cannot be solved exactly (curse of dimensionality, see, e.g., Powell , 2011, Chapter 1.2).

We use approximate dynamic programming to obtain a tractable solution method and exploit the fact that we are only interested in the price decisions $\vec{p}^{\,*}_{t,(x_t^O,y_t^O)}$, i.e., the solution of (5.6).

In particular, we approximate the values $W_{i_t,t}, W_{0,t}$ of the stochastic nodes immediately *after a customer's decision* (Step III) and before a potential return of a vehicle becomes known (see Figure 5.2). This allows to reduce the size of the online pricing problem tremendously by only optimizing *one* period explicitly while still taking into account the customer choice behavior. Graphically, this corresponds to "trimming" the decision tree in Figure 5.2 after Step IV and capture the parts that are cut away by $W_{0,t}$ and $W_{i_t,t}$. The challenge, however, is to find

accurate approximations $\tilde{W}_{i,t}$, $\tilde{W}_{0,t}$ for $W_{i_t,t}$, $W_{0,t}$, respectively. Our approximation is based on the key simplification that V and, thus, W is *additive* in the values of all vehicles. The intuition here is that, since the overall revenue obtained is composed of the revenues realized by the individual vehicles, adding up the revenue-to-come from a certain point in time on for all vehicles – the vehicle values – yields the state value. Clearly, this is a simplification because the actual spatial vehicle distribution never perfectly matches the one observed in history such that potential interdependencies between vehicle values for the current vehicle distribution are neglected. However, this additivity assumption has a very favorable property with regard to runtime and, thus, implementation in practice: In order to calculate the optimal prices, we no longer need to consider *all* available vehicles of the fleet, but only the *reachable* ones. This is because the vehicles out of the customer's reach remain idle for any choice outcome and, thus — technically speaking — form a constant term in the online pricing problem (5.6) that can be neglected. Our results show that this value function approximation works well and that this policy provides in a small instance, the same results (=prices) as the theoretically optimal policy (TINY, see Sections 5.5.2 and 5.5.3).

For the same reason, we neglect the currently moving vehicles. Clearly, this also is an approximation, because, in reality, unreachable and moving vehicles obviously impact future revenues and may also alter a decision – e.g., if a vehicle is part of a large agglomeration of vehicles.

Clearly, a vehicle's value (=expected future profit until the end of the time horizon) depends on whether it remains standing *idle* at its current location or whether it *departs* to another location through a rental. Hence, for a certain vehicle i_t, we denote these approximate vehicle-specific values as $\tilde{w}_{i_t}^{idle}$ and $\tilde{w}_{i_t}^{depart}$, respectively. With this assumption, the approximated values $\tilde{W}_{i_t,t}$ and $\tilde{W}_{0,t}$, thus, can be obtained by

$$W_{i_t,t} \approx \tilde{W}_{i_t,t} = \sum_{j_t \in \mathcal{C}_{t,(x_t^O,y_t^O)} \setminus \{i_t\}} \tilde{w}_{j_t,t}^{idle} + \tilde{w}_{i_t,t}^{depart} \quad \forall i_t \in \mathcal{C}_{t,(x_t^O,y_t^O)}, \tag{5.16}$$

$$W_{0,t} \approx \tilde{W}_{0,t} = \sum_{j_t \in \mathcal{C}_{t,(x_t^O,y_t^O)}} \tilde{w}_{j_t,t}^{idle}. \tag{5.17}$$

The idea in (5.16) is that the value of the state after vehicle i_t has been chosen ($W_{i_t,t}$) is approximately the sum of the values of the remaining idling vehicles from the consideration set $\mathcal{C}_{t,(x_t^O,y_t^O)}$, plus the value of the departing (=chosen) vehicle i_t. Accordingly in (5.17), the state value when no vehicle was chosen ($W_{0,t}$) is approximately the sum of all idling vehicles from $\mathcal{C}_{t,(x_t^O,y_t^O)}$.

Hence, the online pricing problem (5.6) solved in Step II becomes

$$\vec{p}^{\,*}_{t,(x_t^O,y_t^O)} \approx \underset{\vec{p}_{t,(x_t^O,y_t^O)}}{\arg\max} \sum_{i_t \in \mathcal{C}_{t,(x_t^O,y_t^O)}} q_{i_t,t}(\vec{p}_t) \cdot \left((p_{i_t,t} - c) \cdot \mathbb{E}_{L_{t''}^d \sim \rho(S_t)}[L_{t''}^d] + \tilde{W}_{i_t,t}\right) + q_{0,t}(\vec{p}_t) \cdot \tilde{W}_{0,t}. \tag{5.18}$$

5.4.3 Non-parametric Value Function Approximation

In this subsection, we describe the specific approach for obtaining the values $\tilde{w}_{i_t,t}^{idle}$ and $\tilde{w}_{i_t,t}^{depart}$. We first give an overview of our approach in Section 5.4.3.1. Then, we present the details of

data selection and the kernel function used in Section 5.4.3.2.

5.4.3.1 General Idea

Based on the current time t and the location, a vehicle i_t is evaluated. This evaluation is performed for two different cases. First, for the case that vehicle i_t is chosen by the customer, departs and is dropped off at the destination after the rental time. Second, when the customer does not choose the vehicle and, thus, the vehicle remains idle at the current location. For the first case ($\tilde{w}_{i_t}^{depart}$), the value indicates the expected value of vehicle i_t after it has been chosen and parked by the customer. For the second case ($\tilde{w}_{i_t}^{idle}$), the value indicates the expected value of the vehicle after the customer has not chosen the vehicle and it is still idle at the same location.

More technically, the approximate vehicle values $\tilde{w}_{i_t,t}^{idle}$ and $\tilde{w}_{i_t,t}^{depart}$ for a vehicle i_t are determined by a non-parametric value function approximation (see Powell , 2011, Chapter 8.4 for an introduction to this technique). Building on this, our approach is as follows. The values $\tilde{w}_{i_t,t}^{idle}$ and $\tilde{w}_{i_t,t}^{depart}$ are calculated as weighted averages across corresponding data points k from historical and/or simulated data that reflects current system behavior. That is, for an idle vehicle, $\tilde{w}_{i_t,t}^{idle}$ is a weighted average of corresponding idle vehicle values $\hat{w}_k^{idle}$ in the data and $\tilde{w}_{i_t,t}^{depart}$ is a weighted average of corresponding departing vehicle values $\hat{w}_k^{depart}$ in the data. The values $\tilde{w}_{i_t,t}^{idle}$ and $\tilde{w}_{i_t,t}^{depart}$ depend on the location of the vehicle i_t and the time at which the vehicle i_t to be valuated is located. These approximate vehicle values are location and time dependent, i.e. they depend on a subset of the state. More specifically,

$$\tilde{w}_{i_t,t}^{s} = \sum_{k \in \mathcal{K}_{i_t}^{s}} \kappa_{k,i_t}^{s} \cdot \hat{w}_k^{s} \quad \forall i_t \in \mathcal{C}_{t,(x_t^O, y_t^O)}, s \in \{idle,\ depart\}, t \in \mathcal{T} \tag{5.19}$$

where κ_{k,i_t}^{idle} and κ_{k,i_t}^{depart} are the weights that capture how "similar" a specific data point k is to vehicle i_t (see next subsection for details). The sets $\mathcal{K}_{i_t,t}^{idle}$ and $\mathcal{K}_{i_t,t}^{depart}$ represent the sets of observations relevant to approximate the value of vehicle i_t (see next subsection for details).

To explain the process of obtaining these values $\hat{w}_k^{idle}$ and $\hat{w}_k^{depart}$ from data, we assume for the following illustration w.l.o.g. that the problem's time horizon is one day and that we dispose of data that only comprises one specific date. For each vehicle, we know over the day when and where it was standing idle, when it departed, and how much profit the corresponding rental generated, as well as when and where each rental terminated. Figure 5.4 illustrates such "paths" in the historical data, consisting of idle times (thick blue/red lines) and rentals (thin blue/red arrows) exemplarily for two vehicles (red and blue). For now, consider only the temporal dimension on the horizontal axis. The remainder of this figure (with the spatial dimension on the vertical axis) is explained in the next subsection. Thus, for any given point in time, we can determine the current status of each vehicle from this data, and the required values $\hat{w}_k^{idle}$ and $\hat{w}_k^{depart}$ capture the – loosely speaking – profit the vehicle generates from this point in time onwards until the end of the day.

Obviously, robustness improves with increased amount of data available, and, thus, one would combine data from multiple comparable historical/simulated dates, for example from multiple identical days of the week. Then, regarding a data's timestamps, only the time (and not the date) is relevant and observations from different dates are considered as different vehicles. Further, an implicit assumption to note here is that spatial vehicle distributions, demand patterns and, thus,

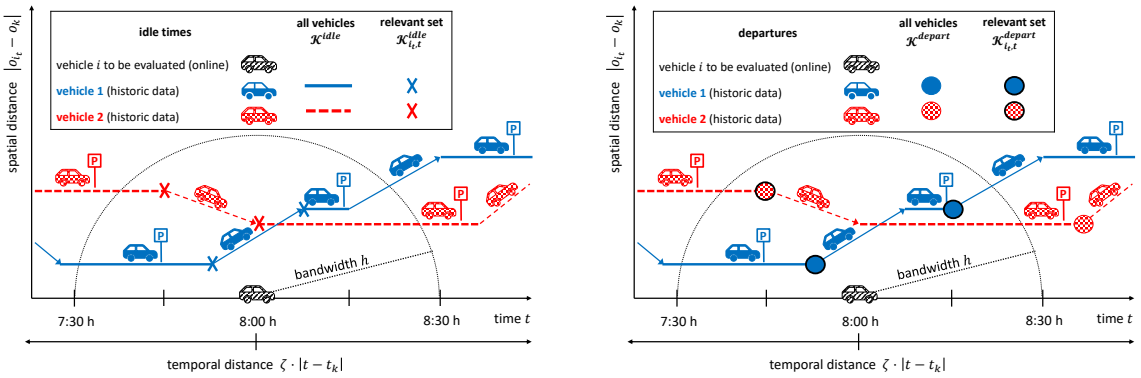

(a) Idle vehicles

(b) Departing vehicles

Figure 5.4: Illustration of historical data considered for evaluation of vehicle i_t

vehicle values are similar for comparable days and, even more important, to the situation when the pricing approach is applied. This, of course, is the case only to a certain extend, because the above-mentioned are endogeneous and an important point of pricing is to influence the vehicle distribution. To address this issue, the underlying database may be iteratively updated (see also the numerical results in Sections 5.5.3 and 5.5.7.2)

The described non-parametric value function approximation has two decisive benefits for practice. First, historical data can readily be used. Second, the approximate vehicle values can continuously be pre-computed such that they do not need to be determined in the moment the pricing problem (5.18) needs to be solved.

5.4.3.2 Data Collection, Data Selection and Kernel Function

The remaining part to fully specify our approach is the determination of the sets $\mathcal{K}^{idle}_{i_t,t}$ and $\mathcal{K}^{depart}_{i_t,t}$ relevant for the evaluation of vehicle i_t from the sets of all data points $\mathcal{K}^{idle}$ and $\mathcal{K}^{depart}$, as well as the weights $\kappa^{idle}_{i_t,k}$ and $\kappa^{depart}_{i_t,k}$.

Regarding *departing vehicles*, the set of all data points $\mathcal{K}^{depart} = \{(\hat{w}^{depart}_k, o_k, t_k)\}$ consists of collected data points k with location o_k and time t_k of the departure event. The value $\hat{w}^{depart}_k$ is the profit earned by this vehicle *after* the rental that started at t_k (this is necessary for consistency with (5.18)) until the considered time frame (one day in our case). Thus, a VSS provider can simply reconstruct this data from the observed historical vehicle movements, which are collected anyway for invoicing.

As mentioned above, one central idea is to approximate values for departing vehicles based on “similar" data points. Since all events in the free-floating VSS are characterized by a certain location and time, it is reasonable to integrate the spatial as well as the temporal dimension in the metric that measures “similarity". This implies that the vehicle values $\tilde{w}^{idle}_{i_t,t}$ and $\tilde{w}^{depart}_{i_t,t}$ are time- and location-dependent. To determine $\mathcal{K}^{depart}_{i_t}$ for a vehicle i_t whose value is to be approximated (with location $o_{i_t,t} = (x^v_{i_t,t}, y^v_{i_t,t})$ and at time t), we define the following filter:

$$\mathcal{K}^{depart}_{i_t,t} = \left\{ (\hat{w}^{depart}_k, o_k, t_k) \in \mathcal{K}^{depart} \;\middle|\; \zeta \cdot |t - t_k| + |o_{i_t,t} - o_k| \leq h \right\}. \tag{5.20}$$

where $|t - t_k|$ is some *temporal distance*, $|o_{i_t,t} - o_k|$ is some *spatial distance*, ζ is a scaling parameter, and h is a bandwidth. This idea of a spatio-temporal “similarity" and a bandwidth

h can be thought of as a (stretched) circle. It is illustrated in Figure 5.4b. The black (diagonally striped) vehicle at a certain location at 8:00 h is to be evaluated. The departure event data points are the red and blue circles. According to the filter, only data points (red and blue circles within the semicircle) within radius h (black dotted) are to be considered and marked by a black circle.

For the *idle vehicles*, this step is slightly more complex, because collected data points on idle vehicles $\mathcal{K}^{idle} = \{(\hat{w}_k^{idle}, o_k, \bar{t}_k)\}$ refer to the time *intervals* $\bar{t}_k$ when the vehicles stood idle (the horizontal thick lines in Figure 5.4a). For an interval $\bar{t}_k$, data point k has the future value $\hat{w}_k^{idle}$ that equals the profit earned by this vehicle after the interval until the end of the horizon (there is obviously no profit during the interval). To determine distance in time, we need to compare these intervals with the point in time t of the vehicle to evaluate. To do so, from each interval, we consider the point in time closest to t. More formally, the set of relevant observations to evaluate an idle vehicle i_t (depicted as red and blue crosses in the figure) is

$$\mathcal{K}_{i_t,t}^{idle} = \Bigg\{ (\hat{w}_k^{idle}, o_k, t_k) \;\Bigg|\; \exists\, (\hat{w}^{idle}, o_k, \bar{t}_k) \in \mathcal{K}^{idle} \;\wedge\; t_k = \underset{t_k''' \in \bar{t}_k}{\arg\min} |t_k''' - t| \;\wedge\; \zeta \cdot |t - t_k| + |o_{i_t,t} - o_k| \leq h \Bigg\}. \tag{5.21}$$

Next, the weights κ_{k,i_t}^s for every historical/simulated data point $k \in \mathcal{K}_{i_t,t}^s \; \forall s \in \{idle,\ depart\}$ are determined with a *kernel function* K. As described above, a scaling ensures that the weights sum to one. In particular, we use

$$\kappa_{i_t,k}^s = \frac{K_{i_t,k}^s}{\sum_{l=1}^{|\mathcal{K}_{i_t,t}^s|} K_{i_t,l}^s} \quad \forall k \in \mathcal{K}_{i_t,t}^s, s \in \{idle,\ depart\}. \tag{5.22}$$

The unscaled weights $K_{i_t,k}^s \forall s \in \{idle, depart\}$ can be determined using various kernel weighting functions, including the Gaussian, Uniform, Epanechnikov, or Bi-Weight kernel weighting functions. As kernel weighting function, we use the following Epanechnikov kernel function (Powell , 2011, Chapter 8.4.2)

$$K_{i_t,k}^s = \frac{3}{4} \cdot \left(1 - \left(\frac{d_{i_t,k}}{h}\right)^2\right) \quad \forall k \in \mathcal{K}_{i_t,k}^s, s \in \{idle,\ depart\} \tag{5.23}$$

with

$$d_{i_t,k} = \sqrt{(\zeta \cdot (t - t_k))^2 + (|o_{i_t,t} - o_k|)^2} \quad \forall k \in \mathcal{K}_{i_t,k}^s, s \in \{idle,\ depart\}. \tag{5.24}$$

5.5 Computational Studies

In this section, we evaluate the developed dynamic pricing approach in comparison to different benchmark approaches. To that end, we consider two different groups of settings. The first group only consists of one artificial, small setting (denoted TINY) that allows analytically solving the dynamic program by backward recursion to obtain the optimal prices (=policy) as a benchmark. The second group with its three settings SMALL, MEDIUM and LARGE allows to evaluate the approaches in more realistic instances.

The new pricing approach and the benchmark approaches are described in Section 5.5.1. Regarding TINY, Section 5.5.2 describes the setup and Section 5.5.3 describes the evaluation procedure and the results. The setup of the second group (i.e. SMALL, MEDIUM, LARGE) is described in Section 5.5.4, followed by the main results in Section 5.5.5 and additional sensitivity analyses in Section 5.5.6. In Section 5.5.7, we briefly analyze variations of the developed solution approach.

5.5.1 Pricing Approaches

We compare our developed pricing approach with nine benchmark approaches (see Table 5.1). First we describe the *customer-centric* pricing approaches:

- C-ANT: Our *customer-centric and anticipative* pricing approach determines dynamic prices for each customer by considering current and future (approximate) state values (see Section 5.4).
- OPT: Calculation of the optimal price for each arriving customer by backward recursion. As usual in dynamic programming, this pricing approach is only feasible for very small instances.
- C-MYOP: *Myopic* version of C-ANT without anticipation: $\tilde{w}^{idle}_{i_t,t} = \tilde{w}^{depart}_{i_t,t} = 0$ for all $i_t \in \mathcal{C}_{t,(x^O_t,y^O_t)}$, resulting in $\tilde{W}_{i_t,t} = \tilde{W}_{0,t} = 0$ for all $i_t \in \mathcal{C}_{t,(x^O_t,y^O_t)}$.
- C-HEUR: *Heuristic* improvement of C-MYOP. Instead of $\tilde{w}^{idle}_{i_t,t} = 0$, $\tilde{w}^{idle}_{i_t,t}$ equals the average profit per expected rental duration across all vehicles for all $i_t \in \mathcal{C}_{t,(x^O_t,y^O_t)}$. More specifically, no distinction is made in the valuation of the idle vehicles: $\tilde{w}^{idle}_{i_t,t} = \tilde{w}^{idle}\ \forall i_t$. Thus, in the price optimization (5.18), a rental is no longer "for free" (no opportunity cost) as in C-MYOP, but $\tilde{w}^{idle}_{i_t,t}$ now reflects that if vehicle i_t is not rented now, it obtains in expectation a profit of $\tilde{w}^{idle}_{i_t,t}$ during the expected rental time $\mathbb{E}_{L^d_{t''}\sim\rho(S_t,S_{t,d})}[L^d_{t''}]$ because it may be chosen by another customer already in the next period.

		focus of dynamic pricing		**uniform pricing**
		customer-centric	location-based	
foresight	anticipative	C-ANT, C-HEUR, OPT	L-ANT	BASE, LOW, HIGH
	myopic	C-MYOP	L-MYOP, RUBA	

Table 5.1: Overview of pricing approaches

In addition, we consider some pricing approaches that are *location-based*. Here we differentiate between approaches that are based on partitioning the business area into tiles and approaches that are based on business rules.

- RUBA: *Rule-based* pricing approach, in which the business area is partitioned into 1 km x 1 km *tiles* that can be thought of as stations, as it is common in the literature. To obtain prices for the vehicles in each tile, we follow the approach of Bianchessi, Formentin, and Savaresi (2013) who compare the number of vehicles in each tile to the average number of available vehicles in the entire business area. If the number of vehicles in a tile falls below the average number of available vehicles, the price of the vehicles in the tile is increased and the magnitude of the increase depends on the severity of the imbalance. Vice versa, if the number of idle vehicles rises above the average number of available vehicles, the price is decreased. Whereas in the original approach continuous prices are used, we require discrete prices for the considered problem. Thus, in a further step, the calculated continuous prices are discretized by rounding to the nearest price point.

- L-ANT: In a first step, the business area is also partitioned into 1 km x 1 km tiles. This location-based pricing approach determines dynamic prices for every tile and 1h-period (e.g. 1am-2am, 2am-3am, etc). At the beginning of each period, a Faure sequence is used to generate multiple realizations of artificial customer arrivals for each tile. C-ANT is then applied to determine the prices for the available vehicles for each artificial customer. The prices for the vehicles in a tile are then averaged and rounded to the next price point. All vehicles located in the tile obtain this price. This benchmark is anticipative but is not customer-centric, since it does not use the situation-specific information of the customer's location as in C-ANT. Therefore, by comparing the results of L-ANT to C-ANT's, the value of considering the location of the customer in anticipative pricing is isolated, i.e. the importance of customer-centric pricing can be quantified.

- L-MYOP: *Myopic* version of L-ANT without anticipation: This means that instead of C-ANT we use C-MYOP to determine the prices for the vehicles in the different tiles. This benchmark is neither anticipative nor customer-centric. Therefore, compared to C-MYOP, this benchmark can be used to measure the impact of considering the location of the customer in myopic pricing. Compared to the benchmark above, we see the value of anticipation in non-customer-centric (=location-based) pricing.

Regarding the relation between C-ANT and L-ANT, note that C-ANT dominates L-ANT in the (theoretical) case that the state value approximation is exact. In this case, C-ANT is the optimal policy. However, since state value approximations are not exact in general, both approaches are heuristics.

Last, we consider the following *uniform* pricing approaches. As they use only one price, they do not require a pricing decision from the provider.

- BASE: Constant uniform pricing, where $p_{i,t}$ is the median price from the set of price points (following our industry partner, we also call it *base* price) for all vehicles. Due to

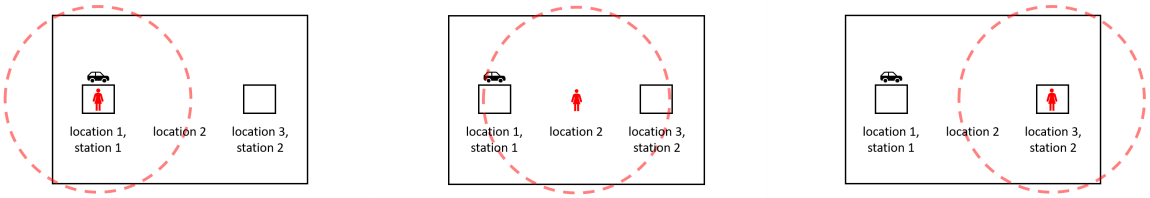

(a) Customer arrives at location 1 (b) Customer arrives at location 2 (c) Customer arrives at location 3

Figure 5.5: Locations and stations in artificial setting in the first micro period (TINY)

its wide adoption over all VSS types, this pricing approach can be considered as the de facto standard in practice.

- LOW: Constant uniform pricing, where $p_{i,t}$ is the *lowest* price for all $i \in \mathcal{C}$, $t \in \mathcal{T}$.
- HIGH: Constant uniform pricing, where $p_{i,t}$ is the *highest* price for all $i \in \mathcal{C}$, $t \in \mathcal{T}$.

Each pricing approach is evaluated in $N = 500$ simulation runs with common random numbers and we report average values.

5.5.2 Setup Artificial Setting

This artificial setting (denoted TINY) is set up such that it is still possible to optimally solve the dynamic program by backwards recursion. To that end, a spatial discretization of the business area is required such that the state space becomes finite. Thus, the setting can be considered as a station-based VSS. It consists of two *stations* where vehicles can be rented and returned, two micro periods, and one vehicle. The customer can arrive (i.e. open the app) at three possible *locations*, of which two (location 1 and 3) coincide with the two stations (see Figure 5.5). If the customer arrives at one station, the other is too far to walk to. Both stations are within reach of the customer if she arrives at location 2. The customer arrival probability for both micro periods is 80% for location 1, 10% for location 2, and 5% for location 3. With 5%, no customer arrives. The provider can set two different prices, i.e., the high price (0.46 €/min) or the low price (0.18 €/min).

The customer choice probability depends on the distance between customer and vehicle (positive correlation) and the price (negative correlation): If the vehicle is out of reach, the choice probability is 0. If the customer arrives at the station where the vehicle is located, she chooses the vehicle with 80% for the low price and with 30% for the high price. If the customer arrives at location 2 and the vehicle is located at one of the two stations, then she chooses the vehicle at the low price with 60% and at the high price with 20%.

The rental destination probabilities are set as follows: If the customer chooses the vehicle at station 1 (station 2), she terminates the rental at station 1 with probability 5% (50%) and at station 2 with 95% (50%). For simplicity, the walking time is neglected in this setting ($l_1^w = l_2^w = 0$) and the rental time is always one micro period ($l_1^d = l_2^d = 1/\Delta$). At the beginning of the first micro period, the vehicle is at station 1. Figure 5.18 in Appendix 5.A.1 shows the corresponding decision tree. The optimal policy always sets high prices in the first micro period and low prices in the second micro period.

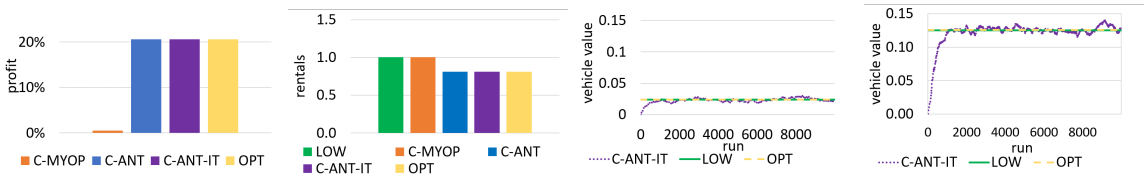

(a) Profit impr. over LOW (b) Rentals (c) $\tilde{w}_1^{depart}$ generated by (d) $\tilde{w}_1^{idle}$ generated by

Figure 5.6: Performance indices and vehicle value for station 1 and period 1

5.5.3 Simulation Procedure and Results Artificial Setting

In this subsection, we compare the results of LOW, C-ANT, and C-MYOP with OPT. For the evaluation of each approach, N=10,000 runs are simulated.

Regarding C-ANT, the required historical data is generated by simulating 10,000 runs with LOW. As the only vehicle is always at station 1 at the beginning of period 1, we obtain two vehicle values. In case the vehicle departs from station 1, it has an expected future profit (i.e. in period 2) of $\tilde{w}_1^{depart} = 0.0242$ €. In case it remains idle at station 1, we have $\tilde{w}_1^{idle} = 0.125$ €. As the vehicle is never at station 2 in period 1, no values are available or needed. The values for period 2 are $\tilde{w}_1^{idle} = \tilde{w}_2^{idle} = \tilde{w}_1^{depart} = \tilde{w}_2^{depart} = 0$, as no rentals can occur beyond this period.

Figure 5.6a depicts the profits as relative improvements over LOW. It shows that C-MYOP generates the same profit as LOW and that C-ANT generates the same profit as OPT, i.e., over 20% more profit than LOW. Further analyses (not shown here) reveal that both LOW and C-MYOP only set the low price. C-ANT and OPT also yield the same policy with a frequency of 44% for the low price and 56% for the high price. This is also reflected in the number of rentals, which are about 20% lower for C-ANT and OPT (Figure 5.6b). Overall, this shows that C-ANT can indeed yield the theoretically optimal policy. The optimality achieved by C-ANT in this small example cannot be generalized. However, it shows that in principle C-ANT can achieve optimality.

For C-ANT, the vehicle values were determined based on LOW runs. However, as discussed in Section 5.4.3.1, vehicle values reflect customer behaviour and are, thus, influenced by prices. If past pricing considerably deviates from current practice, iteratively updating the vehicle values based on new data is an alternative. To demonstrate this, we initialize the values $\tilde{w}^{idle}$ and $\tilde{w}^{depart}$ with 0, perform a simulation run, and then adjust the vehicle values. In doing so, we used a constant stepsize and weighted the previous vehicle value with 0.995 and the new vehicle value from the recent simulation run with 0.05. The vehicle values for the departing and idle vehicle at station 1 in period 1 in comparison to the vehicle values obtained by runs with LOW (as before) and OPT are shown in Figure 5.6c and Figure 5.6d.

Although the initialization is quite bad, we observe the values to quickly converge to the value obtained with the LOW or the OPT pricing. After 10,000 iterations we obtain the values $\tilde{w}^{idle} = 0.1263$ € and $\tilde{w}^{depart} = 0.025$ €, which – in this example – yield the same policy as described above. We will further investigate the value of iterative updating in a more realistic setting (Section 5.5.7.2).

Thus, we could show two things by comparing C-ANT with OPT: First, C-ANT can generate the same results as OPT if the vehicle values are well estimated. Second, we demonstrated how to iteratively update the vehicle values based on new data.

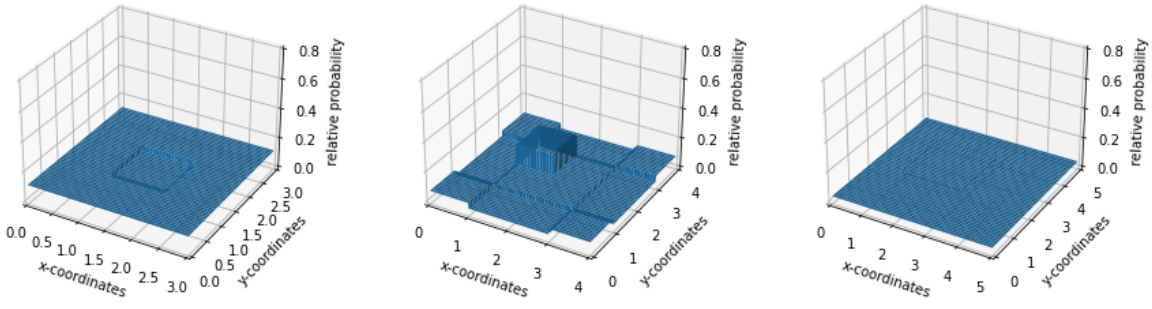

(a) 8:00 h, SMALL (b) 8:00 h, MEDIUM (c) 8:00 h, LARGE

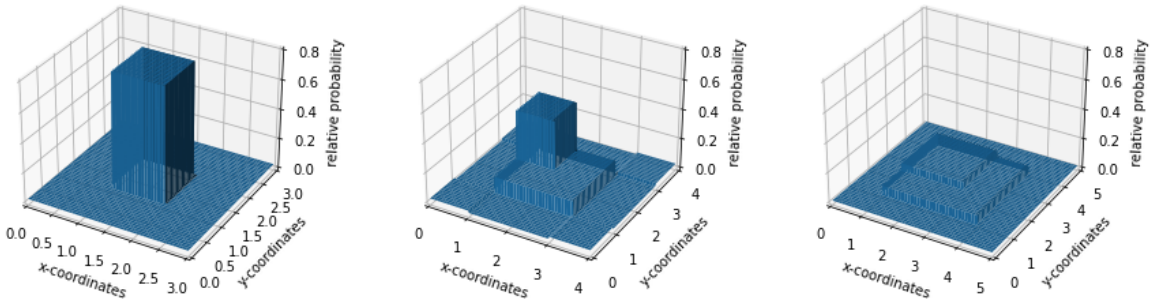

(d) 16:00 h, SMALL (e) 16:00 h, MEDIUM (f) 16:00 h, LARGE

Figure 5.7: Exemplary density (pdf) of customer arrivals (demand) over business area

5.5.4 Setup Realistic Settings

5.5.4.1 Settings and Parameters

We consider three *settings* that differ mainly in the size of the business area and the number of vehicles (SMALL, MEDIUM and LARGE). The area of the SMALL setting has a size of 9 km^2 and is equipped with 36 vehicles (MEDIUM 16 km^2 and 64 vehicles, LARGE 25 km^2 and 100 vehicles, all areas are square). The planning horizon is one day and at the beginning, all vehicles are randomly uniformly distributed across the business area. The demand patterns we use replicate what is observed in practice. Demand intensity varies over the course of the day with two peaks (Figure 6.5 in Appendix 5.A.2, see, e.g., Reiss and Bogenberger, 2016). Furthermore, in line with practice, there is also a spatial variation of demand, for example, between the city center and peripheral areas. This is modeled by the density (pdf) of the origin probability distribution $O(t)$ (see Section 5.3.1), which is exemplarily shown for all settings and two different times (8:00 h, 16:00 h) in Figure 5.7. Density here means that the demand for the respective time period is spread over the size of a certain area, e.g. the the city center (the very center of Figure 5.7a). In other words, integrating the demand densities displayed in Figure 5.7a over the whole business area yields a value of 1 (note that density values are rounded) which corresponds to the normalized demand value from Figure 5.7 for a certain period. The destination probability distribution for a customer who departed in the center is exemplarily shown for all settings and at two different times in Figure 5.23 in Appendix 5.A.4.

Each of the three settings is examined for three different overall demand levels, which differ in the *demand-supply-ratio* (DSR). The DSR is the maximum period demand (second peak) divided by the fleet size and we consider the values $\in \{\frac{1}{3}, \frac{2}{3}, 1\}$ by scaling demand appropriately.

The other parameters are constant throughout all three settings: We choose a presumably small number of possible prices ($M = 5$ price points). The reason is related to the practitioners' important pursuit for a transparent and easy to communicate pricing mechanism. In particular, a pricing mechanism with a small number of prices in comparison to infinite possibilities in a continuous range is much more transparent and easier to communicate to customers. These price points (prices for short) $p^m \in \mathcal{M}$ are predefined with regard to typical prices in practice: We chose a *base price* per minute of $p^3 = 0.35$ €/min and a price difference of 0.10 €/min to the so-called *low* and *high* prices, so that $p^1 = 0.25$ €/min and $p^5 = 0.45$ €/min. The other prices are $p^2 = 0.30$ €/min and $p^4 = 0.40$ €/min. Variable costs are $c = 0.07$ €/min. We calculate the travel time of a rental by drawing the speed from a realistic distribution for urban traffic. We then get the rental/driving time l_t^d as the product of the driving speed and the distance $d_{o_{i_t},(X_t^D,Y_t^D)}$. Further, we assume a willingness to walk of $\bar{d} = 500$ m.

The parameter $\bar{d}$ is assumed to be known and its estimation was performed based on two analyzes. In the first analysis, we conducted a literature search with regard to the maximum walking distance. For example, Singla et al. (2015); Herrmann, Schulte, and Voss (2014) show that below 20% and at most 20.43%, respectively, of the respondents were willing to walk more than 500 m. In the second analysis, we examined the data on customer choices from our practice partner which, amongst others, contains information on the distances to reachable vehicles. In particular, we analyzed two aspects. First, we analyzed the share of customers walking more than 500 m to a vehicle. This share is below 2%. Second, we examined the choice situations in which all of the available vehicles were located more than 500 m away. In this situation, the share of customers who chose one of these vehicles was close to 0. Thus, by combining the insights of literature and data, we decided to set the maximum walking distance to $\bar{d} = 500$ m.

Furthermore, we only consider the ten closest vehicles, as we observed from looking at the Share Now data that on average there are 4.3 vehicles within walking distance and the customer in average chooses the 2.1 nearest vehicle. Furthermore, an analysis of the distribution of the number of available vehicles shows that 90% of customers have seven or fewer vehicles available upon arrival. Only about 4% have ten or more vehicles available (see Figure 5.22).

5.5.4.2 Customer Choice Model

As described in Section 5.3.1, a customer at position (x_t^O, y_t^O) chooses among the vehicles $i \in \mathcal{C}_{t,(x_t^O,y_t^O)}$ within reach and may also decide not to rent (no choice option), which is denoted by $i_t = 0$. In the numerical study, customer choice behavior follows a multinomial logit model (see e.g. Train, 2009, Chapter 3). Accordingly, the choice probabilities $q_{i_t,t}$ depend on the alternatives' deterministic utilities $u_{i_t,t}$ for the customer (see Figure 5.21b in Section 5.A.3) :

$$q_{i_t,t} = \frac{e^{u_{i_t,t}}}{\sum_{n \in \mathcal{C}_{t,(x_t^O,y_t^O)} \cup \{0\}} e^{u_{n,t}}}. \tag{5.25}$$

The deterministic utility $u_{i_t,t}$ of a vehicle i_t depends on its price $p_{i_t,t}$ and its distance to the customer $d_{i_t,t}$ (see Figure 5.21a in Section 5.A.3):

$$u_{i_t,t} = \beta^{price} \cdot p_{i_t,t} + \beta^{distance} \cdot d_{i_t,t}. \tag{5.26}$$

The no-choice option has utility $u_{0,t} = ASC^{NoChoice}$ where $ASC^{NoChoice}$ stands for the alternative-specific constant for the no-choice option. These assumptions imply homogeneous customers and that customers decide solely based on current circumstances (myopic behavior). In particular, they do not act strategically (see, e.g., Gönsch et al., 2013; Gallego and Van Ryzin, 1997; Talluri and Van Ryzin , 2004, Chapter 5.1.4 for discussions of strategic or forward looking customers.)

The parameters for the one choice model which is fit across all locations are estimated with a maximum-likelihood estimation based on 200,000 observations of mobile application openings. Technically, we used the Python package PandasBiogeme 3.2.10 (Bierlaire, 2020). Among others, we used the likelihood ratio test and the Akaike information criterion to compare different model specifications. We tested attributes for the nearest vehicle, the time of the day, the different vehicle types used in practice, and displayed discount badges. However, their impact was minimal, so, in the end, we then implemented the above utility function with the two attributes with the biggest impacts on utility, i.e., price and distance, as one might intuitively expect. We can state that 60 meters of walking distance reduction approximately correspond to a price reduction of 0.10 €/min.

5.5.5 Main Results Realistic Settings

5.5.5.1 Profit

We first discuss profit, whose maximization is the objective of the optimization problem and obviously the most important metric from the provider's perspective. The results for all three settings and DSRs are summarized in Figure 5.8. All profits are presented as relative profit improvements over the BASE pricing approach.

We observe that C-ANT clearly provides the highest profit for all settings and DSRs. Compared to BASE, C-ANT shows profit improvements of up to 13.4%. The improvement over LOW is 22.9 to 32.7 percentage points, over HIGH 4.2 to 9.3, over C-MYOP 4 to 7.6, over C-HEUR 3.6 to 8, over RUBA 5.1 to 8.4, over L-MYOP 5.5 to 9.3, over L-ANT 0.5 to 2.3 percentage points. By contrast, LOW performs much worse than BASE. L-ANT always performs second best across all settings and DSRs with an improvement of 5.1-10.5 percentage over BASE. For the benchmarks HIGH, C-MYOP, L-MYOP, C-HEUR, and RUBA, there is no clear order.

The fact that C-ANT generates up to 7.6 percentage points higher profits than C-MYOP shows that including anticipation has substantial value. However, the comparison of C-ANT, L-ANT and C-HEUR shows that it is important *how* anticipation is done. A simple constant valuation for $\tilde{w}_i^{idle}$ as done in C-HEUR is not effective, since in some cases, e.g. in the SMALL setting with DSR=2/3, C-MYOP performs better than C-HEUR. The comparison between C-ANT and L-ANT shows the additional profit that C-ANT gains, because it is customer-centric, i.e., it has the advantage to take situation-specific customer information (location of customer and distance to each vehicle within walking distance) into account. C-ANT is up to 2.3 percentage points better than L-ANT.

We conclude that C-ANT dominates all other pricing approaches with regard to profit and that its anticipative and customer-centric design is key for the performance – with about three

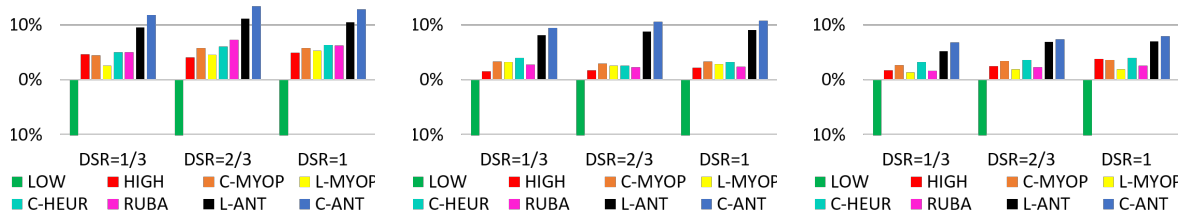

(a) SMALL (b) MEDIUM (c) LARGE

Figure 5.8: Profit improvement over BASE

quarters of C-ANT's improvement over simple heuristics such as L-MYOP coming from anticipation and one quarter from being customer-centric.

5.5.5.2 Prices

Now, we compare the prices resulting from the different pricing approaches. To that end, we consider results from the SMALL setting with all three DSRs. Figure 5.9 illustrates the average price across all areas during the day (we left out LOW, BASE, and HIGH that set constant prices), and Figure 5.24 in Appendix 5.A.6 shows the average price for different parts of the business area from C-ANT and C-MYOP. Figure 5.10 shows the relative frequency of prices for all approaches. The results for MEDIUM and LARGE are depicted in Appendix 5.A.7.

Regarding the average price curves (Figure 5.9), we observe two different groups of approaches. For both groups there is a similar pattern in the average prices, but the prices of the non-anticipative (myopic) pricing approaches fluctuate less than the anticipative pricing approaches. For example in Figure 5.9a, the average price of C-MYOP fluctuates between 0.35 and 0.40 €/min, whereas the average price of C-ANT fluctuates between 0.34 and 0.42 €/min. These results can be explained as follows: The anticipatives approaches (C-ANT, L-ANT, C-HEUR) attempt to incentivize the use of the vehicles in certain parts of the business area during the morning such that they become available in other parts with high demand later during the day. This explains the comparably low average prices of C-HEUR and especially C-ANT and L-ANT during the morning. On the other hand, the myopic approaches do not consider futures states and profits and, thus, set higher average prices during the morning hours which are more profitable in the short term but less profitable in the long term, as the profit results above show.

The difference in terms of pricing between anticipative and myopic approaches becomes even more apparent when considering the temporal *and* spatial differences of prices by C-ANT and C-MYOP in Figure 5.24 in Appendix 5.A.6. C-MYOP sets relatively high average prices in all parts of the business area throughout the entire day. In contrast, C-ANT varies prices in time and space. For example, in all peripheral parts, relatively low prices are set in the morning, while prices in the center at the same time are comparably high. Again, the purpose of this is to incentivize customers to drive vehicles from the outer areas to the center. In the center there is always high demand, so the price here is always quite high.

The discussed differences in price patterns between the pricing approaches can also be seen at the aggregate level by comparing the frequency of prices in Figure 5.10. While C-MYOP and L-MYOP do not set the lowest price, C-ANT also sets lowest prices. L-ANT, on the other hand, does also not use the lowest prices, but the share of second lowest prices is higher than for

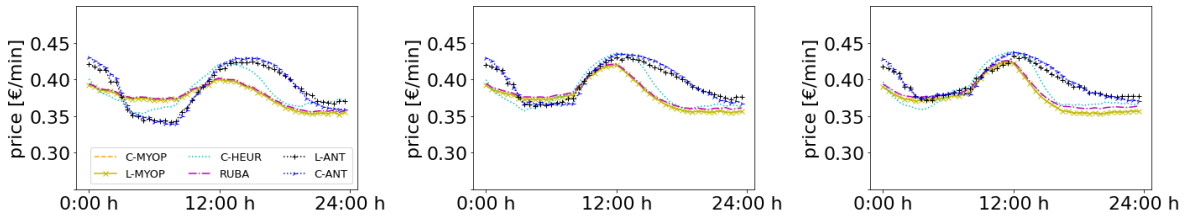

(a) DSR=1/3 (b) DSR=2/3 (c) DSR=1

Figure 5.9: Average prices over the course of the day (SMALL)

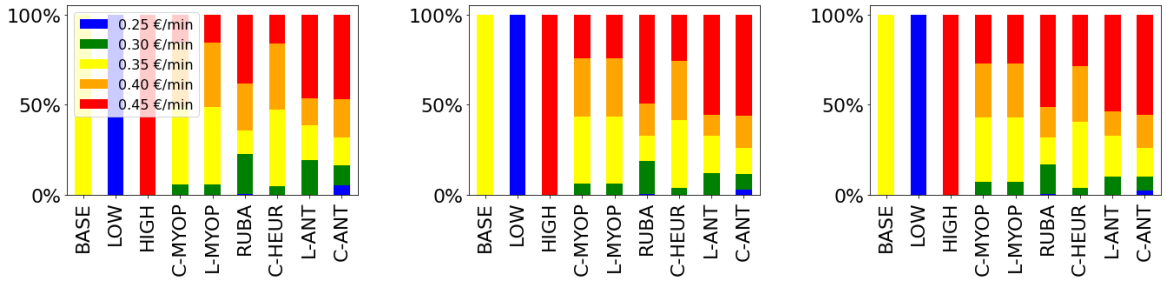

(a) DSR=1/3 (b) DSR=2/3 (c) DSR=1

Figure 5.10: Relative price frequency (SMALL)

L-MYOP. Thus, these lowest prices (C-ANT) and the higher share of lower prices (C-ANT and L-ANT) cannot be motivated by myopic considerations, but only by regard to future profits. The lower profits by the higher share of lower prices in the morning are overcompensated by profits from later rentals. This also works in the opposite direction: C-ANT and L-ANT also choose highest prices more often then C-MYOP and L-MYOP.

We conclude that lowest prices and the higher share of lower prices, especially during morning hours, can be used as an incentive for customers and allow to generate higher profits at highest prices later during the day when the vehicle distribution is better aligned with the demand. This only works when future profits are taken into account like it is done by C-ANT or L-ANT, because vehicle values are approximated more accurately – in particular their dependence on both location and time is considered. Taking the customer's location into account allows C-ANT to better tailor incentives to the customer.

5.5.5.3 Rentals

For the analysis of the rentals, we consider Figure 5.11, which shows the average hourly rentals for the different pricing approaches over the course of the day for different DSRs in the SMALL setting. The respective results for MEDIUM and LARGE are depicted in Appendix 5.A.7.

The rental curves resemble the demand curve (Figure 6.5) in that there is a minimum of rentals in the early morning and a maximum in the afternoon. As expected, the number of rentals increases in the DSR and the number of rentals is lowest (highest) for HIGH (LOW).

The rental curves for C-MYOP and L-MYOP are very similar to the rental curves for C-ANT and L-ANT. Thus, although they all have very similar aggregated rentals, C-ANT and L-ANT manage to obtain considerably higher profits. It is also interesting that the rental curve for C-ANT is very similiar to the rental curve of L-ANT, but C-ANT generates a considerably higher profit.

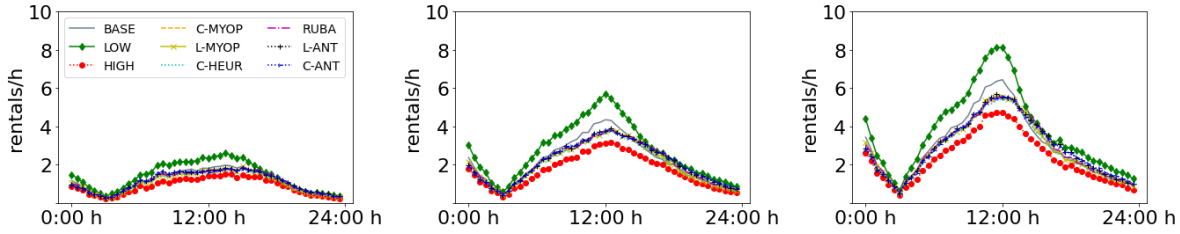

(a) DSR=1/3 (b) DSR=2/3 (c) DSR=1

Figure 5.11: Rentals over the course of the day (SMALL)

The rental curves of BASE lie above the ones for C-ANT, L-ANT, C-MYOP and L-MYOP for all DSRs. Three important insights can be drawn thereupon. First, myopic pricing (C-MYOP, L-MYOP) leads to a significant decrease in the number of rentals compared to BASE, but an improvement in profit. Second, including anticipation, as in C-ANT and L-ANT compared to the C-MYOP and L-MYOP, leads to similiar number of rentals and *at the same time* to an increase in profit. Thus, besides the increased profit, C-ANT and L-ANT arguably provides the same service to customers with a higher profit. Third, including customer's location as in C-ANT compared to L-ANT leads to a similar number of rentals, but a considerably higher profit.

5.5.5.4 Service-Oriented Metrics

In this section, we consider three metrics: the share of customers who have (1) *no available vehicle within reach*, the (2) *walking effort* by considering the share of customers who choose the nearest, second nearest, etc. vehicle, and the comparison of the (3) *spatial distribution of vehicles* at the beginning of the day and immediately before the afternoon peak. All results are obtained in the SMALL setting.

Regarding (1), Figure 5.13a shows that – as expected – the share of customers who cannot find an reachable vehicle increases for each pricing approach, as the overall demand level (DSR) increases. For each demand level, this share is highest (lowest) for LOW (HIGH). It is also noticeable that for the two pricing approaches C-ANT and L-ANT, this share is considerably lower than for BASE, C-MYOP, and L-MYOP. Overall, the results suggest that the service level improves with anticipation (C-ANT and L-ANT), because it leads to a lower share of customers who do not have a reachable vehicle within the walking distance.

Regarding (2), Figure 5.25 in Appendix 5.A.6 shows that most customers (>50%) take the nearest vehicle and then, to a decreasing extent, the second nearest, the third nearest, and then the others. Since these shares for the nearest (second nearest, etc.) vehicle hardly differ between the different pricing approaches, we conclude that the applied pricing approach has only a minor influence on the customers' walking distance. This implies that total customer experience does not suffer.

Regarding (3), Figure 5.12 shows the spatial vehicle distributions over the business area at the beginning of the day as well as at 17:30 (immediately before the afternoon peak) for BASE, C-MYOP, RUBA, L-ANT, and C-ANT in the SMALL setting with DSR=2/3. For illustrative purposes, we partitioned the 3 km x 3 km business area into 9 tiles and calculated the average

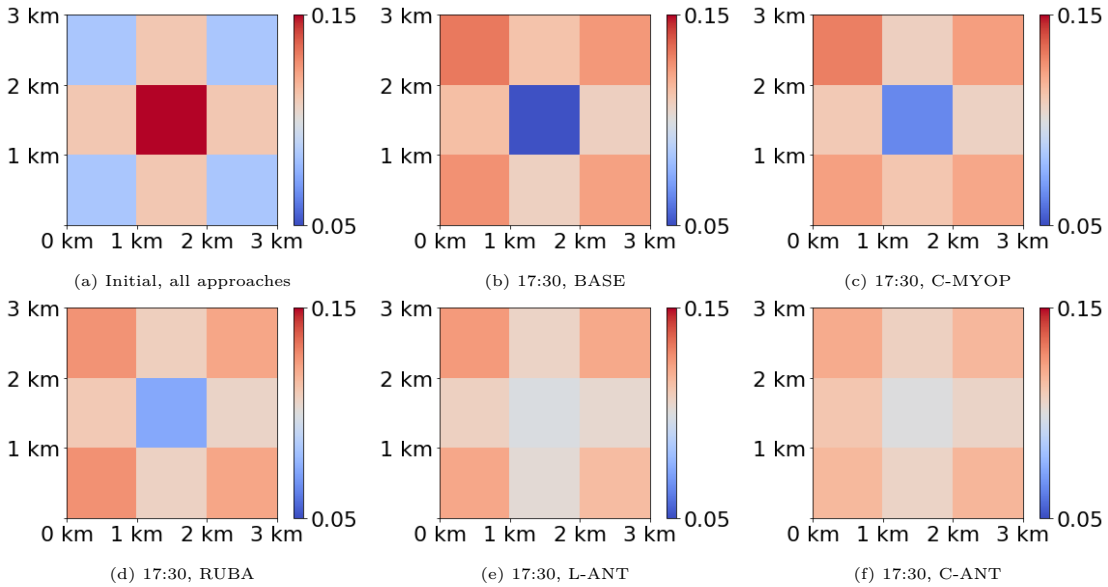

(a) Initial, all approaches (b) 17:30, BASE (c) 17:30, C-MYOP

(d) 17:30, RUBA (e) 17:30, L-ANT (f) 17:30, C-ANT

Figure 5.12: Vehicle distribution for different pricing approaches (SMALL, DSR=2/3)

share of idle vehicles in each tile. While at the start of the day 22% of the vehicles are in the center of the business area (Figure 5.12a) where demand is strongest in the afternoon, at 17:30h with BASE that number declined to 5%. By contrast, C-ANT manages to have 10% of vehicles in the center which explains the higher availability observed above.

5.5.6 Sensitivity Analysis Realistic Settings

We consider two aspects in more detail. We examine the robustness of the above results regarding changes in demand preferences which, for example, vary across cities and countries. To that end, first, we examine whether the dominance of C-ANT discussed above holds if the spatial and temporal variation of the demand intensity is less pronounced (Section 5.5.6.1). Second, we analyze the impact of customer preference variation regarding price sensitivity and disutility from walking in Section 5.5.6.2.

A common *standard demand pattern* serves as a basis for parameter variations throughout the sensitivity analysis. We use the demand pattern of the SMALL setting for DSR=2/3, depicted in the top right of Figure 5.20 in Appendix 5.A.2.

5.5.6.1 Variation of Spatial and Temporal Demand Intensity

5.5.6.1.1 Parameter Variations: In addition to the standard demand pattern, we define four additional *demand patterns* which range from spatial and temporally homogeneous demand intensity to spatially and temporally heterogeneous demand intensity (the standard demand pattern), as illustrated in Figure 5.20 in Appendix 5.A.2. In the most homogeneous demand pattern, there is no spatial and no temporal variation at all (bottom left in Figure 5.20 in Appendix 5.A.2). In the most heterogeneous demand pattern, there is a high spatial and temporal variation, as observed in practice (top right in Figure 5.20 in Appendix 5.A.2, *standard demand pattern*). More over, we also consider patterns with only spatial or temporal and intermediate variation.

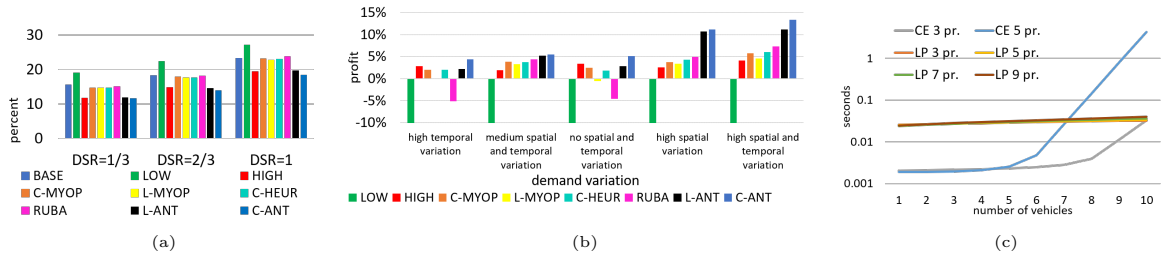

Figure 5.13: (a) Share of customers with no vehicle within walking distance (SMALL, DSR=2/3)
(b) Profit improvement over BASE (SMALL, DSR=2/3)
(c) Computational time of linear program (LP) and complete enumeration (CE) (SMALL, DSR=2/3) for the reachable vehicles within walking distance

5.5.6.1.2 Results: Regarding profit, there is a clear impact of spatial and temporal demand variation (Figure 5.13b). The superiority of C-ANT (and L-ANT) over the other benchmark pricing approaches is more pronounced the more spatial variation there is. When there is no spatial variation the difference between the anticipative and myopic approaches is considerably smaller. Thus, the spatial variation is the main driver of C-ANT's (and L-ANT's) advantage over C-MYOP (and L-MYOP): C-ANT (L-ANT) performs around 7 percentage points better than C-MYOP (L-MYOP) when there is only spatial variation or spatial and temporal variation but the approaches performs only around 2 percentage points better when there is only temporal variation. However, as the results for high spatio-temporal demand variation show, C-ANT (and L-ANT) leverages most on its anticipation when there is both high spatial *and* high temporal demand variation, as it is observed in practice. Overall, the dominance of C-ANT as discussed in Section 5.5.5 can be confirmed and C-ANT proves to be robust against changes in spatial and temporal demand variation. The main insight here is that more sophisticated pricing approaches are of particular value when there is more demand variation – especially spatial demand variation. For the analysis of rentals and prices we refer to Appendix 5.A.8.1. The most interesting insight there is that C-ANT only uses the low price with high spatial variation. This shows that it indeed sacrifices revenue to nudge customers to drive to "better" areas.

5.5.6.2 Variation of Customer Preferences

5.5.6.2.1 Parameter Variations: In this section, we again use the standard demand pattern. We define three *choice patterns* in which we alter the parameters $\beta^{distance}$ and β^{price} of the multinomial logit model which describes the customer choice behavior (see Section 5.5.4.2). As we cannot disclose the choice parameters estimated on Share Now data, we now use three new choice patterns (Table 5.2). The first choice pattern (*walking distance sensitive*) is similar to the real values we estimated on Share Now data. Here, a walking distance change of 1 km has a higher impact on the customer's utility than a price change of 1 €/min. In the second choice pattern (*price sensitive*), the price is more important for the customer than the walking distance. In the last parameter variation, the customer is both *walking distance and price sensitive*. Please note that also customers always care about distance and price, for simplicity, we name the patterns according to the more pronounced sensitivity. For each choice pattern, we vary the DSR as in Section 5.5.5.

choice pattern	$\beta^{distance}$	β^{price}	$ASC^{NoChoice}$
walking distance sensitive	-10	-7.5	-5
price sensitive	-7.5	-10	-5
walking distance and price sensitive	-10	-10	-5

Table 5.2: Parameter variations

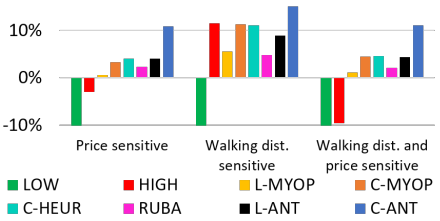

Figure 5.14: Profit impr. over BASE (SMALL, DSR=2/3)

5.5.6.2.2 Results: Regarding profit, we consider Figure 5.14. C-ANT clearly outperforms all other pricing approaches across all choice patterns and all DSRs. Compared to C-MYOP, C-ANT yields a profit increase of up to 7.6 percentage points. However, there are substantial differences in the results between the three choice patterns. For example, with price sensitive customers, the improvements of all approaches over BASE are slightly lower (C-ANT's is the highest at 10.8%). With walking distance sensitive customers, improvements reach up to 16.2%. Regarding an analysis of rentals and prices we again refer to Appendix 5.A.8.2.

In conclusion, we recommend C-ANT independent of customer preferences. It considerably improves profits and consistently provides the best result (significant at the 95% confidence level).

5.5.7 Variations of C-ANT

In the following, we briefly investigate straightforward variations of two aspects of C-ANT. First, in Subsection 5.5.7.1, we compare using the LP (5.11) - (5.15) from Section 5.4.1 and complete enumeration of all possible price combinations for the reachable vehicles to solve the pricing problem for each customer. Second, in Subsection 5.5.7.2, we look at the database used to approximate the vehicle values. As historical/simulated data depends on the pricing regiment active during that time, we consider iteratively updating the data base based on new data, as already investigated in the TINY example (see Section 5.5.3). Throughout this section, as in the sections above, we use the standard demand pattern (SMALL, DSR=2/3)

5.5.7.1 Comparison of Linear Program and Complete Enumeration

5.5.7.1.1 Experiment: We define four cases in which we alter the number of possible prices. For each case, we calculate the optimal prices in C-ANT using the linear program (LP, Section 5.4.1) and complete enumeration (CE).

5.5.7.1.2 Results: Figure 5.13c shows computational times with 3 to 9 price points for up to 10 vehicles within the walking distance.

With three prices, there is no considerably difference in computational time between CE and the LP. For five or more prices, however, it is clearly visible that computational time with CE increases in the number of vehicles within reach and explodes above seven vehicles. For eight or more vehicles, CE's computational time clearly exceeds the LP's runtime, which remains

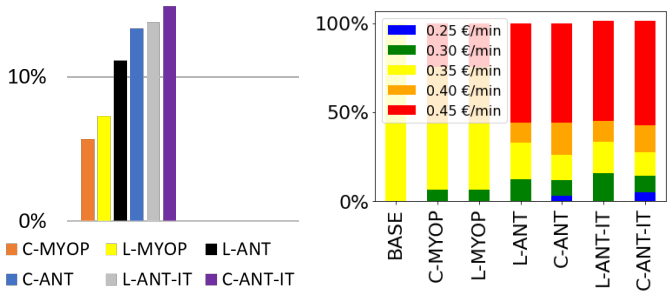

(a) Profit improvement over BASE (b) Relative price frequency

Figure 5.15: Comparison of iterative updating based on new data and static database (SMALL, DSR=2/3)

consistently below 0.1 seconds. In conclusion, we recommend to use the LP to determine the optimal prices, independent of the number of possible prices $|\mathcal{M}|$.

5.5.7.2 Iterative Updating of Historical Data

5.5.7.2.1 Experiment: In this analysis, we evaluate the impact of updating the historical data $\mathcal{K}^{idle}$ and $\mathcal{K}^{depart}$ (see Section 5.4.3.2) *iteratively* in batches based on new data. We denote these variants of C-ANT and L-ANT as C-ANT-IT and L-ANT-IT, respectively. This process is interesting for practical application, e.g. a provider may update the data after several weeks of applying the most recent parameterization of C-ANT-IT (L-ANT-IT). More specifically, of the 5,000 simulation runs in this analysis, a batch consists of 1,000 runs each, such that the data is updated five times. For the first 1,000 runs, C-ANT-IT and L-ANT-IT use the same historical data as C-ANT and L-ANT (from 1,000 runs with BASE). For the second 1,000 runs, the *entire* batch of the historical data (1,000 runs BASE) is replaced by the data collected from these first 1,000 runs and so on.

5.5.7.2.2 Results: The results show that the iterative update based on new data improves the performance of C-ANT-IT and L-ANT-IT compared to C-ANT and L-ANT by 3.7 and 2.6 percentage points, respectively (see Figure 5.15a). With regard to the amount of rentals realized, there are no differences between these four approaches. However, with regard to pricing, Figure 5.15b shows that the updating leads to a higher proportion of lower prices being set. Overall, this analysis shows that there is additional potential for the proposed solution approach when updating the historical data.

5.6 Case Study – Share Now in Vienna, Austria

In this section, we consider a real-world setting that reflects the origin-based dynamic pricing optimization of Share Now for a weekday in Vienna, Austria. This case study allows to conclude results and managerial insights from a real-world instance, as all parameters are based on real historical data which was collected over several months at Share Now. We introduce the scenario in Section 5.6.1 and discuss the results in Section 5.6.2.

5.6.1 Setting and Parameters

To respect the non-disclosure agreement, we do not share the exact origin and destination probability distributions $O(t)$ and $D(t, S_t)$, respectively. Instead, we present the course of the aggregate demand across the entire business area normalized to the maximum period demand (at base price) in Figure 5.16b. Demand parameters are obtained from data that Share Now recorded during six months in 2018. We unconstrained the constrained demand, i.e., the observed rentals, with the help of location- and time-specific app opening data which served as a proxy for the unconstrained demand. Such unconstraining is a standard issue in revenue management (see, e.g., Talluri and Van Ryzin , 2004, Chapter 9.4).

The demand curve (Figure 5.16b) shows two peaks at the rush hour times, in the morning at 8:30 h and in the evening at 18:30 h, with the lowest level during the night at 3:00 h. This pattern is typical for weekdays in cities in central and northern Europe. The demand-supply-ratio is approximately DSR=0.84, which is similar to the scenario with DSR=2/3 above. As is in reality at the time of data recording, we use three price points. All other parameters (walking speed, stochastic rental times, etc.) are as in the computational studies (Section 5.5.4.1). Regarding the customer choice modeling, we applied the same multinomial logit model including the utility function as described in Section 5.5.4.2, which has been estimated on real-life data. Due to the very good performance of the C-ANT pricing approach in the sensitivity analysis, only this pricing approach and some benchmarks (BASE, LOW, HIGH, C-MYOP) are used for the case study.

5.6.2 Results

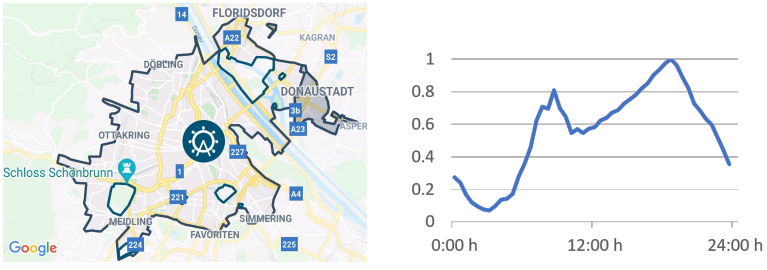

(a) Business area (b) Normalized demand

Figure 5.16: Share Now in Vienna, Austria

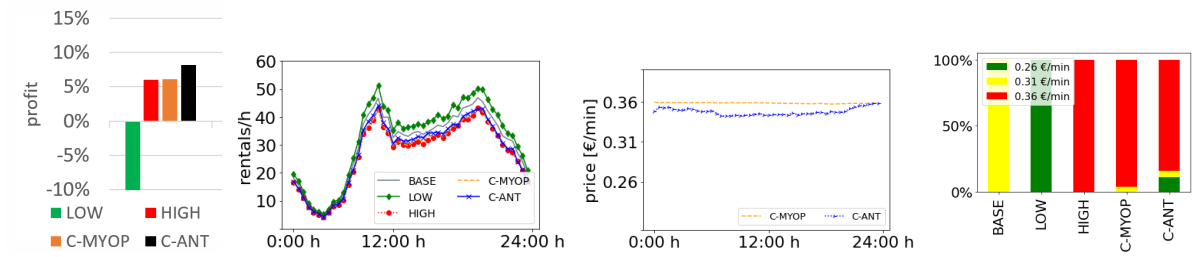

(a) Profit impr. over BASE

(b) Rentals over the course of the day

(c) Average prices over the course of the day

(d) Relative price frequency

Figure 5.17: Results for case study

We first consider the profit of the different approaches (Figure 5.17a). Again, LOW leads to a reduction in profit compared to BASE. The approaches HIGH and C-MYOP deliver almost identical profits. As in the numerical study, C-ANT obtains the best result. Compared to C-MYOP (6.1% better than BASE), C-ANT's solution is more than 2 percentage points better in profit.

Overall, the rental curves (Figure 5.17b) follow the general course of the demand curve, with less pronounced peaks. During the night, the difference between demand and rentals is smaller than during the day. This can be explained by the higher availability of vehicles during the night, implying that potential customers almost always find an available vehicle. During the day, in particular during peak times, the probability that demand results in a rental is lower due to the relatively high number of vehicles in use. Regarding the pricing approaches, Figure 5.17b shows that LOW leads to the most rentals. Just below this is the curve of BASE.

The average price per period (Figure 5.17c) of C-MYOP is always above the average price of C-ANT and very close to the high price. In addition, differences in the average price over all periods (not depicted here) of the *reachable* vehicles and the *chosen* vehicles are also apparent. While the average price of C-MYOP is higher for the chosen vehicles than for the reachable vehicles, it is vice versa for C-ANT. This indicates that C-ANT sets low prices for reachable vehicles due to anticipation, so that the probability of choosing these vehicles increases. The rental curves (Figure 5.17b) of HIGH and C-MYOP are almost identical and the rental curve of C-ANT is above them. This can also be seen in the frequency of the prices (Figure 5.17d). Thus, most (96%) of C-MYOP's prices are the high price. Comparing C-ANT and C-MYOP, the frequency of the base price is larger (5% C-ANT, 4% C-MYOP). Furthermore, low prices are also more frequent (10% C-ANT, 0% C-MYOP). Therefore, the case study confirms that C-ANT is a viable pricing approach that can handle real-world problem instances.

5.7 Conclusion

In modern free-floating VSSs, providers have access to disaggregate real-time data regarding the locations of vehicles as well as of customers who open the mobile application to look for available vehicles. In this work, we demonstrate that this information can be leveraged in dynamic pricing to increase profitability. The *anticipative customer-centric* dynamic pricing approach in VSSs takes customers' location as well as their behavior regarding walking distances and prices explicitly into consideration in the online price optimization. Thus, vehicles can have different prices for customers who are requesting the price information at the same time but from different locations. Further, the specific pricing approach that we consider relies on *origin-based* per-minute prices. This origin-based feature is decisive for practice, because the information of a customer's intended destination is usually not available and its enquiry would contradict the spontaneous nature of free-floating VSSs. The third distinguishing feature of the developed pricing approach is that it is *anticipative*, i.e., that future expected profits resulting from different spatial vehicle fleet distributions are taken into consideration.

We formally define the provider's online pricing problem as a Markov decision process and formulate the corresponding dynamic program by stating the corresponding Bellman equation. We show that in our approach, with regard to the action space of the pricing problem, only the vehicles within a customer's maximum walking distance have to be considered. Nevertheless, the dynamic program cannot be solved to optimality by classical backwards induction due to the curse of dimensionality which, in our case, is (above all) caused by the state space containing the location of every vehicle in the business area.

To solve the online pricing problem, we develop a solution method based on approximate dynamic programming. We approximate state values representing expected future profits that occur *after* the current customer's decision, such that the current customer's choice behavior can still be considered explicitly with a disaggregated choice model in the optimization – in our case by a multinomial logit model. We take the assumption that state values are additive in the vehicle values which represent the profits that individual vehicles are expected to realize until the end of the considered time horizon. As a consequence of this assumption, vehicles which are not part of the current customer's consideration set can be neglected for the calculation of the state values, as they do not change their state for any possible choice and, thus, do not influence the online pricing optimization. To approximate the vehicle values, we propose a non-parametric value function approximation. This type of approximation has two main benefits for implementation in practice. First, historical data can easily be used for the approximation and, second, approximate vehicle values can be pre-computed such that the numerical operations of the online pricing problem can be reduced to a minimum.

In an extensive computational study with varying size of business area and fleet as well as varying demand patterns and overall demand levels, we demonstrate the advantages of our dynamic pricing approach compared to various benchmarks, including one from the literature and a myopic variant of customer-centric dynamic pricing. The new pricing approach outperforms all benchmarks significantly and considerably. It improves profits by up to 13.4% compared to the de facto standard in practice of constant uniform prices, as well as up to 7.6 percentage points compared to myopic dynamic pricing. From the latter, we conclude that the accurate

approximation of our pricing approach is decisive for its performance. Compared to the benchmark from the literature, our approach obtains up to 8.4 percentage points more profit. Further, the numerical study demonstrates that the theoretical advantage of integrating the concept of customer-centricity in dynamic pricing compared to a location-based approach — in the case that state value approximations are exact — also applies when using the approximation that we propose. That is, considering situation-specific customer information like the position of the customer and distance to the vehicles within walking distance yields up to 2.3 percentage points more profit. The numerical results of a real-life case study based on Share Now data from Vienna also confirm the benefit of customer-centric and anticipative pricing and demonstrate the scalability of our approach. With regard to service level, we observe that anticipation in the pricing leads to an improvement, because there is a lower share of customers who do not have a reachable vehicle within the walking distance.

With a sensitivity analysis, we show that our results are robust regarding the decisive parameters of the customer choice behavior and we derive valuable managerial insights. We vary the influence of price and distance on the customers' utility of a vehicle and show that our pricing approach still always performs best in terms of profit. A detailed analysis indicates that this is because the new pricing approach leads to a higher variation of prices over different parts of the business area compared to a myopic pricing. The reason is the consideration of future vehicle locations and rentals. Thus, for example, our approach already raises prices in an area in the early morning if it anticipates a shortage of vehicles around noon. It would be very tedious to comprehensively mimic this anticipation with, e.g., simple pricing rules. An analysis of spatial and temporal variations in demand shows that spatial variation, in contrast to temporal variation, has a stronger effect on the importance of anticipation. For a VSS provider this means that if there is no spatial demand variation, it is not necessary to anticipate the future in the pricing and rather straightforward approaches are sufficient – even a uniform pricing may be appropriate. If, however, there are already small spatial differences, it is worthwhile to anticipate the future. Another important insight for VSS providers is that our dynamic pricing approach manages to increase profits while maintaining the overall number of rentals that realize. This is important, since many service-related metrics that strive for customer satisfaction are related to a high number of rentals.

The comparison of the linear program formulation (based on Charnes-Cooper transformations) to solve the pricing problem with complete enumeration shows that the former is substantially more efficient for five or more prices. We further demonstrate that an iterative update of the historical data based on new data improves the performance of the developed solution approach.

To summarize, our new customer-centric, origin-based, and anticipative dynamic pricing approach for free-floating VSSs performs considerably well in comparison to existing approaches in terms of the relevant performance metrics. The non-parametric value function approximation solution method provides a scalable means to successfully account for the future evolution of the VSS based on current decisions, and allows to integrate disaggregated historical and real-time data which is readily available in practice for modern free-floating VSSs. Currently, to prepare implementation in practice, the approach is tested by our practice partner Share Now in an

agent-based simulation (digital twin) which samples historical events on a disaggregated level, meaning with individual customer and vehicle events.

There are several reasonable paths for future research to extend this work. For example, in approximate dynamic programming, updating/stepsize rules often have an important impact on solution quality. Thus, there certainly is potential for additional improvements, given that there are several more sophisticated updating procedures than the applied batch update. Incorporating additional features such as idle-times in the vehicle value approximation may improve results and/or substitute vehicle values by another intuitive, often already available data source. Regarding the scope of the problem, a combined optimization of pricing and operator-based vehicle relocation seems natural.

5.A Appendix

5.A.1 Decision Tree for Artificial Setting (TINY)

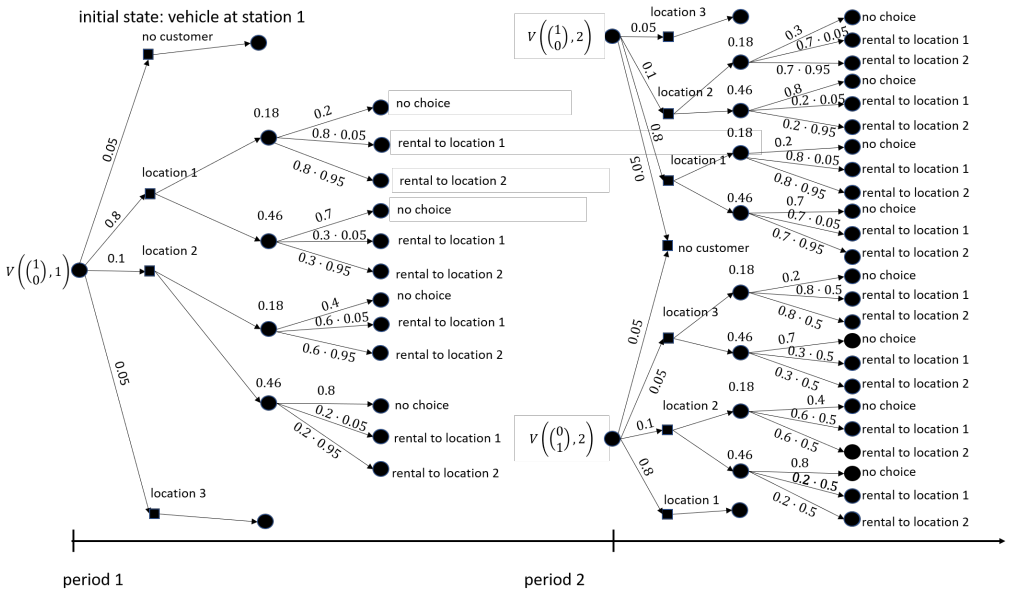

Figure 5.18: Decision tree for artificial setting (TINY). For better readability, the arrows between the first and second micro period are not displayed.

5.A.2 Demand Patterns

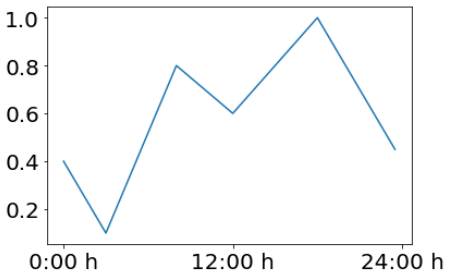

Figure 5.19: Normalized demand over the course of the day (SMALL, MEDIUM, LARGE)

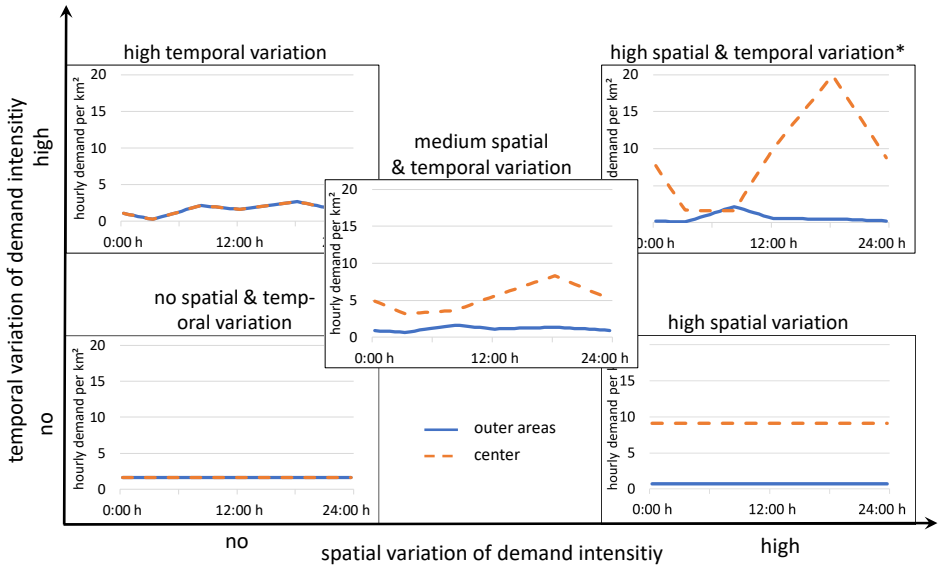

Figure 5.20: Demand patterns with differing degrees of temporal and spatial variation (areas as defined in Figure 5.24d, SMALL, DSR=2/3, *standard demand pattern (see Figures 5.7a, 5.7d))

5.A.3 Customer Choice: Figures of Utility and Probability Function

We plot utility and probability in dependence of prices and distances for a situation in which a customer has one vehicle within walking distance. (Figure 5.21). Figure 5.21a shows the utility for the different prices (low, base and high price) in Vienna. The utility is linear in price and distance, as described in Section 5.5.4.2. Figure 5.21b shows the probability for the different prices. This probability is a function of the utility of choosing a vehicle and the utility of no choice.

Due to the non-disclosure agreement we cannot display vertical and horizontal axes labels, because this information would reveal the exact utility function parameterization or the choice behavior, respectively.

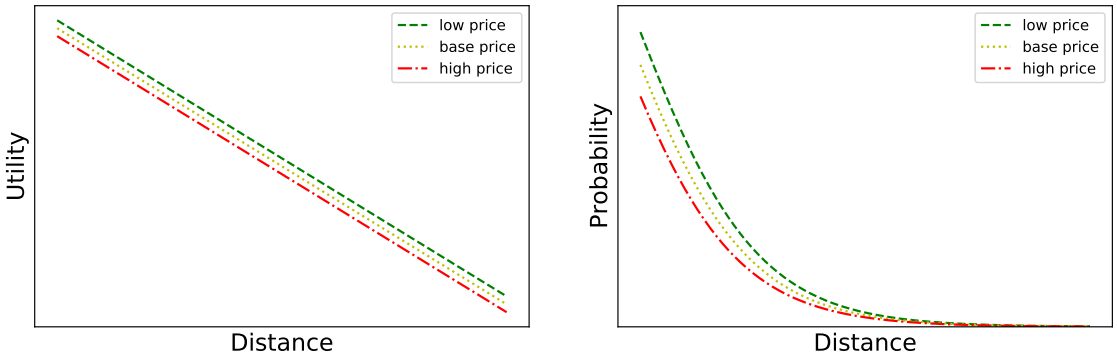

(a) Utility (b) Probability

Figure 5.21: Utility and probability in dependence of prices and distances

5.A.4 Distribution of number of reachable vehicles

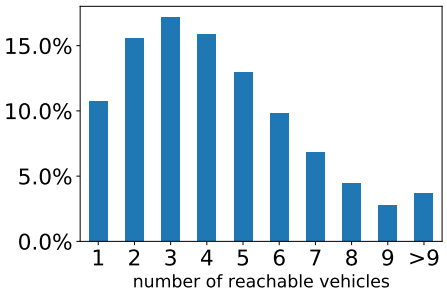

Figure 5.22: Distribution of number of reachable vehicles for an arriving customer in Vienna

5.A.5 Probability Density Functions

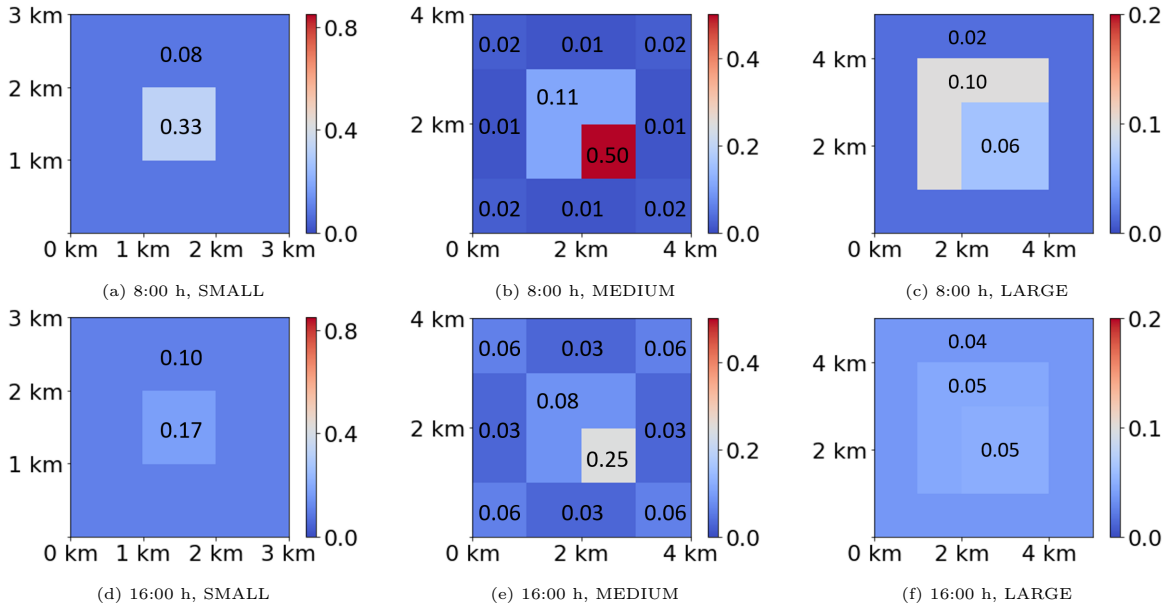

(a) 8:00 h, SMALL (b) 8:00 h, MEDIUM (c) 8:00 h, LARGE

(d) 16:00 h, SMALL (e) 16:00 h, MEDIUM (f) 16:00 h, LARGE

Figure 5.23: Density (pdf) of destinations over business area for a customer who departed in the center

5.A.6 Results for SMALL Setting

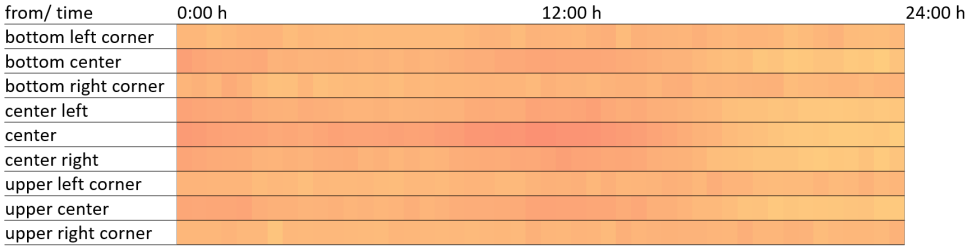

(a) Pricing C-MYOP

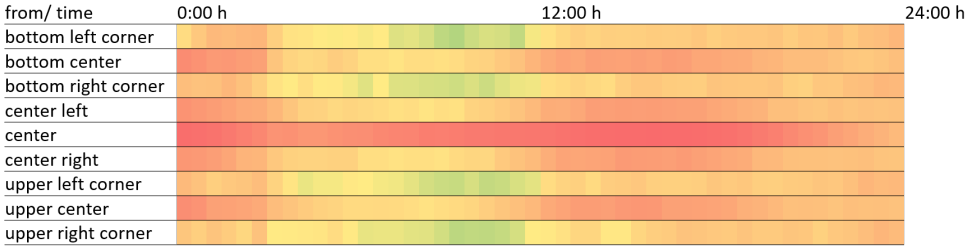

(b) Pricing C-ANT

(c) Legend

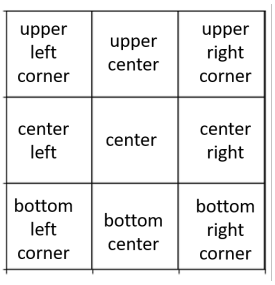

(d) Partitioning of business area (evaluation)

Figure 5.24: Average prices in different parts of the business area over the course of the day (SMALL, DSR=2/3)

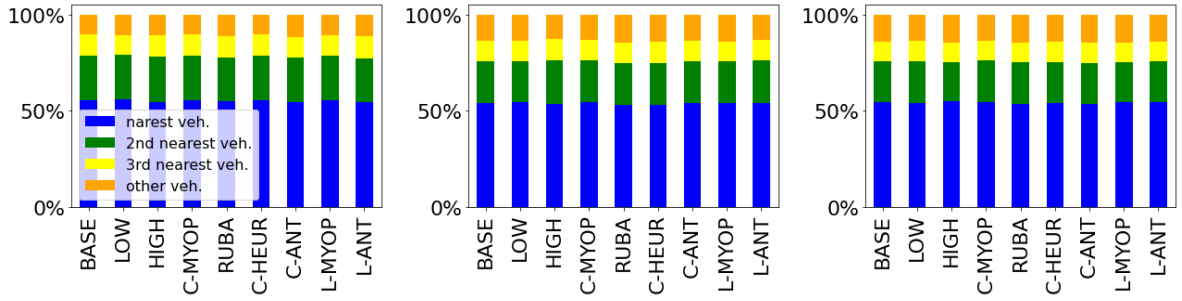

(a) DSR=1/3 (b) DSR=2/3 (c) DSR=1

Figure 5.25: Share of customers choosing the closest, the 2nd closest, the 3rd closest or another vesicle (SMALL)

5.A.7 Results for MEDIUM and LARGE Setting

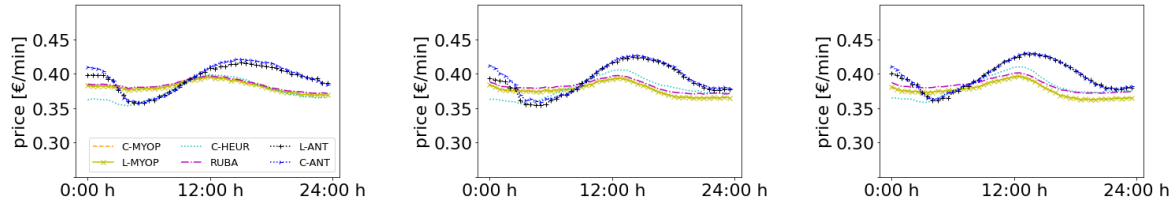

(a) DSR=1/3 (b) DSR=2/3 (c) DSR=1

Figure 5.26: Average prices over the course of the day (MEDIUM)

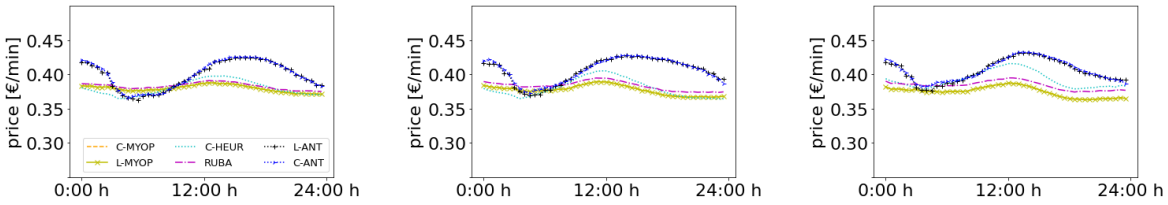

(a) DSR=1/3 (b) DSR=2/3 (c) DSR=1

Figure 5.27: Average prices over the course of the day (LARGE)

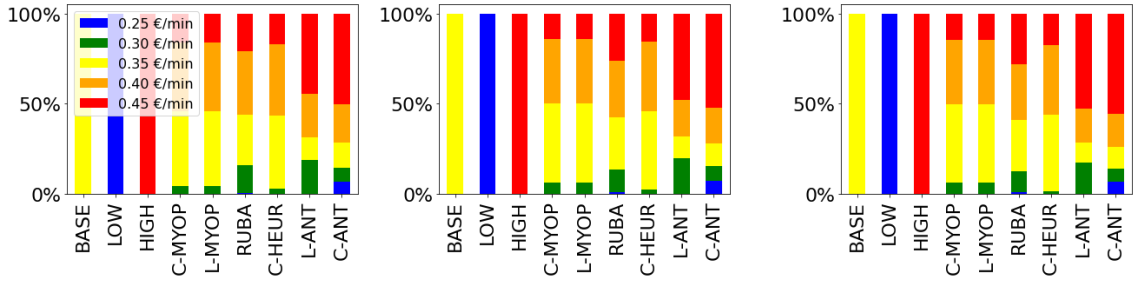

(a) DSR=1/3 (b) DSR=2/3 (c) DSR=1

Figure 5.28: Relative price frequency (MEDIUM)

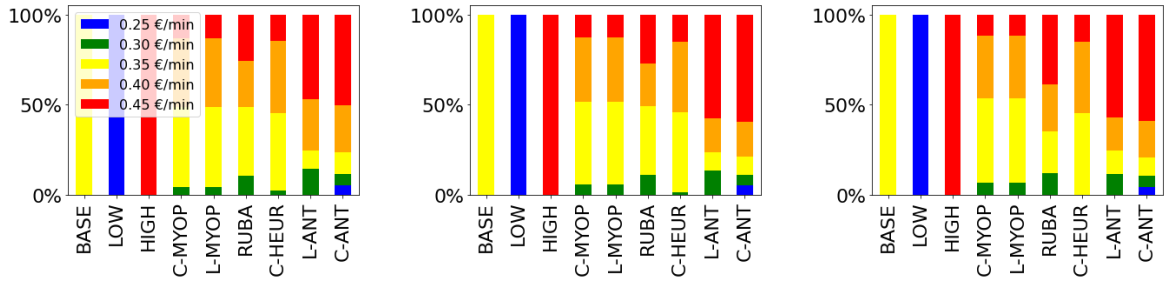

(a) DSR=1/3 (b) DSR=2/3 (c) DSR=1

Figure 5.29: Relative price frequency (LARGE)

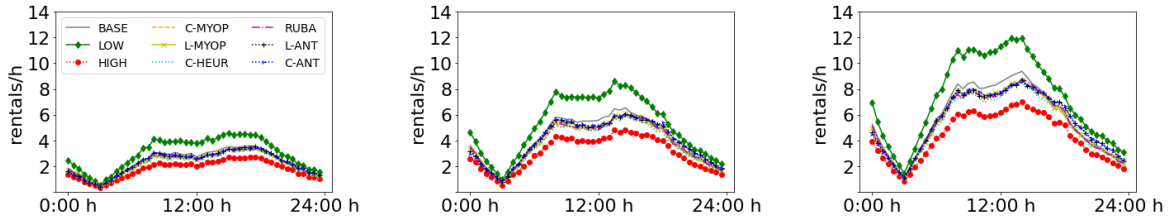

(a) DSR=1/3 (b) DSR=2/3 (c) DSR=1

Figure 5.30: Rentals over the course of the day (MEDIUM)

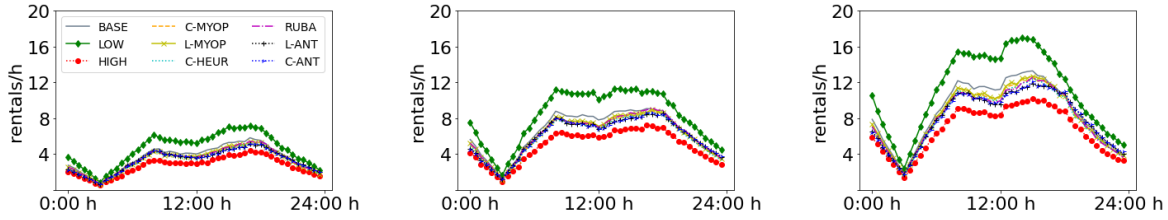

(a) DSR=1/3 (b) DSR=2/3 (c) DSR=1

Figure 5.31: Rentals over the course of the day (LARGE)

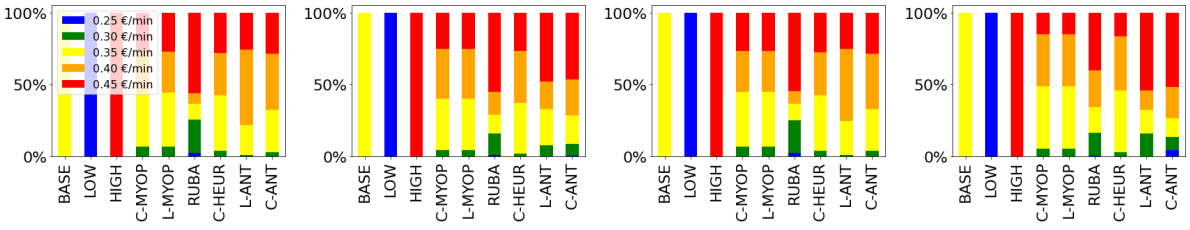

(a) High temporal variation (b) Medium spatial and temporal variation (c) No spatial and temporal variation (d) High spatial variation

Figure 5.32: Relative price frequency (SMALL, DSR=2/3)

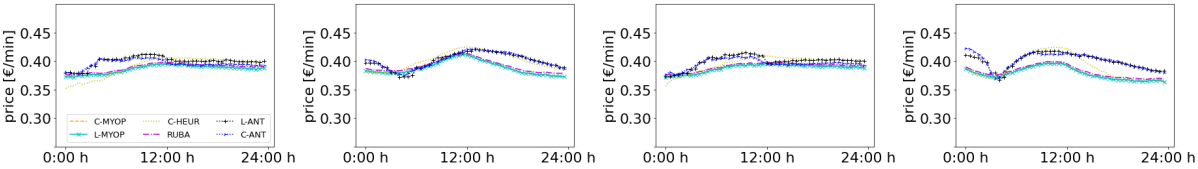

(a) High temporal variation (b) Medium spatial and temporal variation (c) No spatial and temporal variation (d) High spatial variation

Figure 5.33: Average prices over the course of the day (SMALL, DSR=2/3)

5.A.8 Sensitivity Analysis

5.A.8.1 Variation of Spatial and Temporal Demand Intensity

5.A.8.1.1 Additional Results: Regarding prices, we again depict the relative frequency of prices (Figure 5.32) as well as average prices over the day (Figure 5.33). As above, we observe that the pricing approaches without anticipation (C-MYOP, L-MYOP and RUBA), have relatively small price variation, compared to the ones with anticipation (C-ANT and L-ANT). However, the degree of price variation depends on the demand pattern. For example, with medium spatial and temporal demand variation, the average prices of C-ANT over the day have a pattern similar to the ones described in Section 5.5.5.2 and they fluctuate between 0.37 €/min and 0.42 €/min (Figure 5.33b) but there is almost no price fluctuation when there is no spatio-temporal demand variation (Figure 5.33c). Again, the spatial demand variation has higher influence on the results. When there is high spatial demand variation, prices of C-ANT fluctuate between 0.37 €/min and 0.42 €/min (Figure 5.33d), while with temporal demand fluctuation, average prices only fluctuate between 0.38 €/min and 0.41 €/min and no low prices are set (Figure 5.33d). Only in the setting with spatial variation, the anticipative pricing approach C-ANT uses low prices (with reduced profits) as an incentive for customers to increase the total profit in the VSS. L-ANT, however, does not use low prices. This indicates that the individual consideration of each customers is beneficial in the use of targeted incentives.

Regarding rentals, the hourly rentals depicted in Figure 5.34 confirm the results in Section 5.5.5.3 and the findings discussed above, in particular that with C-ANT (and L-ANT) a identical number of rentals realize compared to C-MYOP (and L-MYOP) when there is spatial demand variation.

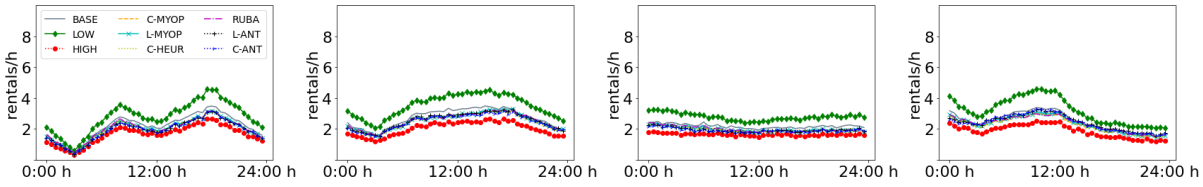

(a) High temporal variation (b) Medium spatial and temporal variation (c) No spatial and temporal variation (d) High spatial variation

Figure 5.34: Rentals over the course of the day (SMALL, DSR=2/3)

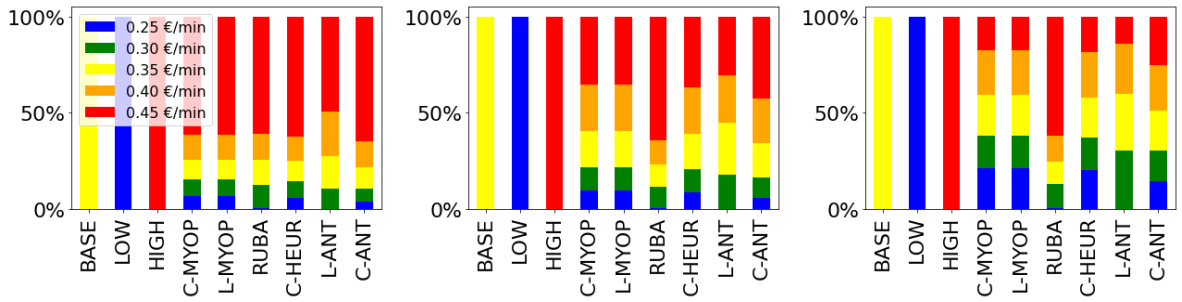

(a) Walking distance sensitive (b) Price sensitive (c) Walking dist. and price sensitive

Figure 5.35: Relative price frequency (SMALL, DSR=2/3)

5.A.8.2 Variation of Customer Preferences

5.A.8.2.1 Additional Results: Regarding prices, we once again consider the relative frequency of prices (Figure 5.35) and the average prices over the course of the day (Figure 5.36).

There are clear differences in the average price between the choice patterns. For example, the average prices vary the most for all pricing approaches in the choice pattern with price and distance sensitivity. For example, with C-ANT, the average price exceeds 0.40 €/min for all choice patterns around noon (10 a.m. til 1 p.m.). In the pattern with price and distance sensitivity, the average price for C-ANT falls below 0.30 €/min during the night. We do not see this variation in the other two choice patterns. The average price for C-ANT for the walking distance sensitive pattern does not fall below 0.32 €/min and the average price for the price sensitive pattern does not fall below 0.34 €/min. These differences are also evident when looking at the frequencies of prices. Comparing C-MYOP, L-MYOP C-HEUR, C-ANT and L-ANT for all patterns, the frequency of low prices is – as expected – largest in the pattern with walking distance and price sensitivity (21% for C-MYOP and L-MYOP, 20% for C-HEUR, 14% for C-ANT, 0% for L-ANT). It is lower in the pattern with price sensitivity (10% for C-MYOP and L-MYOP, 9% for C-HEUR, 6% for C-ANT, 0% L-ANT) and lowest with walking distance sensitivity (7% for C-MYOP and L-MYOP, 6% for C-HEUR, 4% for C-ANT, 0% for L-ANT). This shows that the optimization-based approaches succeed in adapting to customer behavior. By contrast, RUBA always has a similar frequency of prices.

The rental curves are depicted in Figure 5.37. Obviously rentals increase in demand (DSR). There are no clear differences between the three choice patterns.

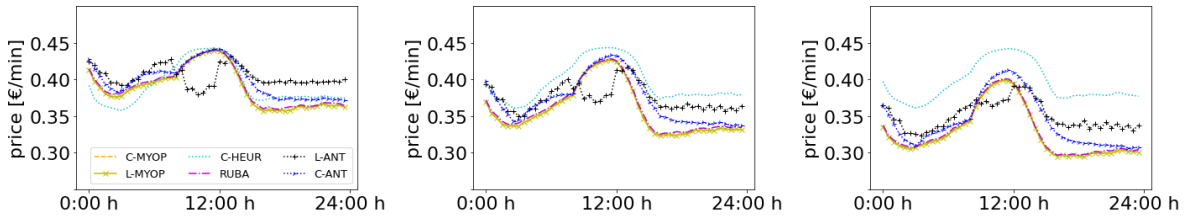

(a) Walking distance sensitive (b) Price sensitive (c) Walking dist. and price sensitive

Figure 5.36: Average prices over the course of the day (SMALL, DSR=2/3)

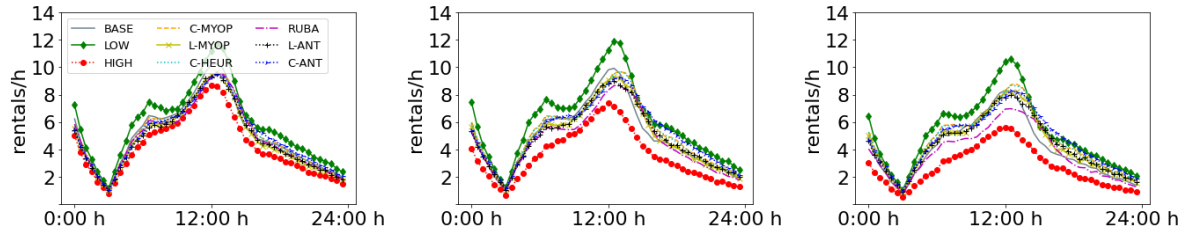

(a) Walking distance sensitive (b) Price sensitive (c) Walking dist. and price sensitive

Figure 5.37: Rentals over the course of the day (SMALL, DSR=2/3)

5.A.9 List of Notation

symbol	description
sets	
$\mathcal{C}$	fleet of vehicles $\mathcal{C} = 1, ..., C$
$\mathcal{C}_{t,(x_t^O, y_t^O)}$	reachable vehicles $\mathcal{C}_{t,(x_t^O, y_t^O)} \subset \mathcal{C}$
$\mathcal{K}^{depart}_{i_t,t}$	set of observations of departing vehicles to approximate the value of vehicle i_t
$\mathcal{K}^{idle}_{i_t,t}$	set of observations of idle vehicles to approximate the value of vehicle i_t
$\mathcal{M}$	set of discrete prices
$\mathcal{T}$	set of micro periods $\mathcal{T} = 1, ...T$
parameters, variables and functions	
C	number of vehicles
m	price point
N	number of simulation runs
c	variable costs per minute of a rental
T	number of micro periods
t	micro period
Δ	number of micro periods per minute
λ_t	arrival rate of customers in micro period t
$\bar{d}$	maximum walking distance (willingness-to-walk)
$d_{i_t,t}$	walking distance between customer (x_t^O, y_t^O) and vehicle i_t
k	data point in historical/simulated data
$d_{o_k,(X_t^D, Y_t^D)}$	spatial distance between the location of the vehicle i_t and its destination
$A_{i_t,t,m}$	attraction value for vehicle i_t in period t at price level m
B_t	attraction value for no choice alternative
$z_{i_t,t,m}$	binary, 1 if price level m chosen for vehicle i_t in period t
v_t	auxiliary variable for linearization
$u_{0,t}$	utility for no-choice option
$u_{i_t,t}$	utility for choosing vehicle i_t
β^{price}	coefficient for price
$\beta^{distance}$	coefficient for distance
$ASC^{NoChoice}$	alternative-specific constant, utility of no-choice alternative

Table 5.3: List of notation, part 1

symbol	description
$o_{i_t,t} = (x_{i_t,t}, y_{i_t,t})$	location of vehicle i_t at time t
o_k	location of data point k
h	bandwidth for Kernel Regression
t_k	time stamp of data point k
$\bar{t}_k$	time interval vehicle stood idle in data point k
ζ	scaling parameter for temporal/spatiol distance
$\tilde{w}^{depart}_{i_t,t}$	approximate vehicle value, i.e. future revenue of vehicle i_t if it departs in period t
$\tilde{w}^{idle}_{i_t,t}$	approximate vehicle value, i.e. future rev. of vehicle i_t if it remains idle in period t
κ^{idle}_{k,i_t},κ^{depart}_{k,i_t}	weight, captures similiarity of data point k to vehicle i_t
$K^{idle}_{i_t,k}$, $K^{depart}_{i_t,k}$	kernel function for data point k for vehicle i_t
$\vec{p}_t$	price vector including all vehicles for micro period t
$\vec{p}_{t,(x^O_t,y^O,t)}$	price vector including only vehicles reachable for customer at (x^O_t, y^O)
$p_{i_t,t}$	price for vehicle i_t in micro period t
$q_{i_t,t}(\vec{p}_t)$	probability that vehicle i_t is chosen
$q_{0,t}(\vec{p}_t)$	probability that no vehicle is chosen
distributions, random variables and realizations	
I_t	vehicle chosen by customer in period t
i_t	realization of I_t
J_t	vehicle dropped-of by customer in period t
j_t	realization of J_t
L^d_t	rental time
l^d_t	realization of L^d_t
L^w_t	walking time
l^w_t	realization of L^w_t
$O(t)$	origin probability distribution, $(X^O_t, Y^O_t) \sim O(t)$
$D(t, S_t)$	destination probability distribution, $(J_t, X^D_t, Y^D_t) \sim D(t, S_t)$
X^O_t, Y^O_t	coordinates the customer requesting a vehicle in period t
X^D_t, Y^D_t	destination coordinates of vehicle returned in period t
x^O_t, y^O_t	realization of X^O_t, Y^O_t
x^D_t, y^D_t	realization of X^D_t, Y^D_t
value functions	
$V(S_t, t)$	Bellman Equation, expected future revenue from state S_t in micro period t onwards
$W_{i_t,t}$	expected future revenue if customer in period t chooses vehicle i_t
$W_{0,t}$	expected future revenue if customer in period t chooses no vehicle
$\tilde{W}_{i_t,t}$	approximation of $W_{i_t,t}$
$\tilde{W}_{0,t}$	approximation of $W_{0,t}$
states	
S_t	$S_t = (\vec{x}^c_t, \vec{y}^c_t, \vec{\tau}^c_t, \vec{x}^v_t, \vec{y}^v_t, \vec{\tau}^v_t)$, state at the beginning of micro period t
S_{t+1}	$S_{t+1} = S_{t+1}(S_t, (x^O_t, y^O_t), i_t, (x^D_t, y^D_t), j_t)$ transition function, state at the beginning of micro period $t+1$
$\vec{x}^v_t$	vector containing x-coordinates of all vehicles
$\vec{y}^v_t$	vector containing y-coordinates of all vehicles
$x^v_{i,t}, y^v_{i,t}$	coordinates of vehicle i
$\vec{x}^c_t$	vector containing x-coordinates of arriving customer for each vehicle
$\vec{y}^c_t$	vector of y-coordinates of arriving customer for each vehicle
$x^c_{i_t,t}, y^c_{i_t,t}$	arrival (=app opening) coordinates of customer who chose vehicle i_t
$\vec{\tau}^v_t$	vector containing starting times for all vehicles
$\tau^v_{i_t,t}$	starting time of vehicle i_t
$\vec{\tau}^c_t$	vector containing customers' arriving (=app opening) times of all vehicles
$\tau^c_{i_t,t}$	arriving (=app opening) time of customer driving vehicle i_t

Table 5.4: List of notation, part 2

Bibliography

Agatz N, Campbell AM, Fleischmann M, Van Nunen J, Savelsbergh M (2013) Revenue management opportunities for internet retailers. *J. Revenue Pricing Manag.* 12(2):128–138.

Angelopoulos A, Gavalas D, Konstantopoulos C, Kypriadis D, Pantziou G (2016) Incentivization schemes for vehicle allocation in one-way vehicle sharing systems. *2016 IEEE Internat. Smart Cities Conf. (ISC2)* 1–7.

Angelopoulos A, Gavalas D, Konstantopoulos C, Kypriadis D, Pantziou G (2018) Incentivized vehicle relocation in vehicle sharing systems. *Transp. Res. Part C: Emerg. Technol.* 97:175–193.

Ataç S, Obrenović N, Bierlaire M (2021) Vehicle sharing systems: A review and a holistic management framework. *EURO J. Transp. Logist.* 10:100033.

Banerjee S, Freund D, Lykouris T (2022) Pricing and optimization in shared vehicle systems: An approximation framework. *Oper. Res.* 70(3): 1783-1805.

Barth M, Todd M, Xue L (2004) User-based vehicle relocation techniques for multiple-station shared-use vehicle systems. *Transp. Res. Board 80th Annual Meeting.*

Benjaafar S, Shen X (2022) Pricing in On-Demand (and One-Way) Vehicle Sharing Networks. Working paper, University of Minnesota, Minnesota.

Besbes O, Castro F, Lobel I (2021) Surge pricing and its spatial supply response. *Manag. Sci.* 67(3):1350–1367.

Bianchessi AG, Formentin S, Savaresi SM (2013) Active fleet balancing in vehicle sharing systems via feedback dynamic pricing. *IEEE Internat. Conf. Intell. Transp. Syst.* 1619–1624.

Bierlaire, MA (2020) A short introduction to PandasBiogeme. Technical Report, Transport and Mobility Laboratory, École Polytechnique Fédérale de Lausanne, Lausanne, Switzerland.

Brendel AB, Brauer B, Hildebrandt B (2016) Toward user-based relocation information systems in station-based one-way car sharing. *AMCIS Proc.* 1–10.

Chemla D, Meunier F, Pradeau T, Wolfler Calvo R, Yahiaoui H (2013) Self-service bike sharing systems: Simulation, repositioning, pricing. Working paper, CERMICS, École des Ponts ParisTech, Champs-sur-Marne, France.

Chen KD, Hausman WH (2000) Mathematical properties of the optimal product line selection problem using choice-based conjoint analysis. *Manag. Sci.* 46(2):327–332.

Chow Y, Yu JY (2015) Real-time bidding based vehicle sharing. *Proc. 2015 Internat. Conf. Auton. Agents and Multiagent Syst.* 1829–1830.

Chung H, Freund D, Shmoys D B (2018) Bike Angels: An analysis of Citi Bike's incentive program. *Proc. 1st ACM SIGCAS Conf. Comp. Sust. Soc.* 1-9.

Clemente M, Fanti MP, Iacobellis G, Nolich M, Ukovich W (2017) A decision support system for user-based vehicle relocation in car sharing systems. *IEEE Trans. Syst., Man and Cybernetics: Syst.* 48(8):1283–1296.

Côme E (2014) Model-based count series clustering for bike sharing systems usage mining: A case study with the Vélib' system of Paris. *ACM Transact. Intell. Syst. Technol.* 1–27.

Davis J, Gallego G, Topaloglu H (2013) Assortment planning under the multinomial logit model with totally unimodular constraint structures. Working paper, The University of Illinois at Urbana Champaign, Urbana and Champaign, Illinois.

DeMaio P (2009) Bike-sharing: History, impacts, models of provision, and future. *J. Public. Trans.* 12(4):3.

Dötterl J, Bruns R, Dunkel J, Ossowski S (2017) Towards dynamic rebalancing of bike sharing systems: An event-driven agents approach. *EPIA Conf. Artificial Intell.* 309–320.

Di Febbraro A, Sacco N, Saeednia M (2012) One-way carsharing. *Transp. Res. Record* 2319(1):113–120.

Di Febbraro A, Sacco N, Saeednia M (2019) One-way car-sharing profit maximization by means of user-based vehicle relocation. *IEEE Trans. Intell. Transp. Syst.* 20(2):628–641.

Ferrero F, Perboli G, Vesco A, Caiati V, Gobbato L (2015a) Car-sharing services – Part A taxonomy and annotated review. Working paper, Istituto Superiore Mario Boella, Turin, Italy.

Ferrero F, Perboli G, Vesco A, Musso S, Pacifici A (2015b) Car-sharing services – Part B business and service models. Working paper, Istituto Superiore Mario Boella, Turin, Italy.

Fishman E, Washington S, Haworth N (2013) Bike share: A synthesis of the literature. *Transp. Rev.* 33(2):148–165.

Fricker C, Gast N (2016) Incentives and redistribution in homogeneous bike-sharing systems with stations of finite capacity. *Euro J. Transp. Logist.* 5(3):261–291.

Gallego G, Van Ryzin G (1997) A multiproduct dynamic pricing problem and its applications to network yield management. *Oper. Res.* 45(1):24–41.

Ghosh S, Varakantham P (2017) Incentivizing the use of bike trailers for dynamic repositioning in bike sharing systems. *Proc. Internat. Conf. Automated Planning and Scheduling* 23:373-381.

Golalikhani M, Oliveira BB, Carravilla MA, Oliveira JF, Antunes AP (2021) Carsharing: A review of academic literature and business practices toward an integrated decision-support framework. *Transp. Res. Part E: Logist. Transp. Rev.* 138:23–45.

Golalikhani M, Oliveira BB, Carravilla MA, Oliveira JF, Pisinger D (2021) Understanding car-sharing: A review of managerial practices towards relevant research insights. *Res. Transp. Bus. Manag.* 41:100653.

Gönsch J, Klein R, Neugebauer M, Steinhardt C (2013) Dynamic pricing with strategic customers. *J. Bus. Econ.* 83(5):505–549.

Haider Z, Nikolaev A, Kang JE, Kwon C (2018) Inventory rebalancing through pricing in public bike sharing systems. *Eur. J. Oper. Res.* 270(1):103–117.

Herrmann S, Schulte F, Voß S (2014) Increasing acceptance of free-floating car sharing systems using smart relocation strategies: A survey based study of car2go Hamburg. *Internat. Conf. Computat. Logist.)* 151-162.

Illgen S, Höck M (2019) Literature review of the vehicle relocation problem in one-way car sharing networks. *Transp. Res. Part B: Methodol.* 120:193–204.

Jorge D, Correia G (2013) Carsharing systems demand estimation and defined operations: a literature review. *Eur. J. Transp. Infrastruct. Res.* 13(3).

Kamatani T, Nakata Y, Arai S (2019) Dynamic pricing method to maximize utilization of one-way car sharing service. *IEEE Internat. Conf. Agents (ICA)* 65–68.

Kanoria Y, Qian P (2019) Blind dynamic resource allocation in closed networks via mirror backpressure. Working paper, Columbia Business School, New York.

Ke J, Yang H, Li X, Wang H, Ye J (2020) Pricing and equilibrium in on-demand ride-pooling markets. *Transp. Res. Part B: Methodol.* 139: 411-431.

Laporte G, Meunier F, Wolfler Calvo R (2015) Shared mobility systems. *4OR* 13(4):341–360.

Laporte G, Meunier F, Wolfler Calvo R (2018) Shared mobility systems: An updated survey. *Ann. Oper. Res.* 271(1):105–126.

Marecek J, Shorten R, Yu JY (2016) Pricing vehicle sharing with proximity information. *2016 3rd MEC Internat. Conf. Big Data and Smart City (ICBDSC)* 1–7.

Mourad A, Puchinger J, Chu C (2019) A survey of models and algorithms for optimizing shared mobility. *Transp. Res. Part B: Methodol.* 123:323-346.

Neijmeijer N, Schulte F, Tierney K, Polinder H, Negenborn RR (2020) Dynamic pricing for user-based rebalancing in free-floating vehicle sharing: A real-world case. *Internat. Conf. Comput. Logist.* 443–456.

Niels T, Bogenberger K (2017) Booking behavior of free-floating carsharing users. *Transp. Res. Record: J. Transp. Res. Board* 2650(1):123–132.

Pfrommer J, Warrington J, Schildbach G, Morari M (2014) Dynamic vehicle redistribution and online price incentives in shared mobility systems. *IEEE Trans. Intell. Transp. Syst.* 15(4):1567–1578.

Powell, WB (2011) Approximate dynamic programming: Solving the curses of dimensionality, 2nd ed. (John Wiley & Sons, Hoboken, NJ).

Qiu H, Li R, Zhao J (2018) Dynamic pricing in shared mobility on demand service. Working paper, Cornell University, Ithaca, New York.

Reiss S, Bogenberger K (2016) Optimal bike fleet management by smart relocation methods: Combining an operator-based with an user-based relocation strategy. *IEEE Intell. Transp. Syst. Conf. (ITSC)* 2613–2618.

Ren S, Luo F, Lin L, Hsu SC, LI XI (2019) A novel dynamic pricing scheme for a large-scale electric vehicle sharing network considering vehicle relocation and vehicle-grid-integration. *Internat. J. Prod. Econ.* 218:339–351.

Ricci M (2015) Bike sharing: A review of evidence on impacts and processes of implementation and operation. *Res. Transp. Bus. Manag.* 15:28–38.

Ruch C, Warrington J, Morari M (2014) Rule-based price control for bike sharing systems. *2014 European Control Conf. (ECC)* 708–713.

Share Now (2021) Overview countries and cities. *Share Now.* Accessed February 25, 2021, https://www.share-now.com/de/en/country-list/.

Singla A, Santoni M, Bartók G, Mukerji P, Meenen M, Krause A (2015) Incentivizing users for balancing bike sharing systems. *Proc. Twenty-Ninth AAAI Conf. Artificial Intell. Pattern* 723–729.

Soppert M, Steinhardt C, Müller C, Gönsch J (2022) Differentiated pricing of shared mobility systems considering network effects. *Transp. Sci.* 45(5):1279-1303.

Stancu-Minasian IM (1997) Fractional programming: Theory, methods and applications, 1st ed. (Springer, Boston, MA).

Statista (2022) Number of carsharing users in Germany by variant from 2014 to 2022. Accessed August 29, 2022, https://de.statista.com/statistik/daten/studie/202416/umfrage/entwicklung-der-carsharing-nutzer-in-deutschland/.

Talluri KT, Van Ryzin GJ (2004) The theory and practice of revenue management, 1st ed. (Springer, Boston, MA).

Strauss AK, Klein R, Steinhardt C (2018) A review of choice-based revenue management: Theory and methods. *Eur. J. Oper. Res.* 271(2): 375-387.

Train K (2009) Discrete choice methods with simulation, 2nd ed. (Cambridge University Press, Cambridge, UK).

Wagner S, Willing C, Brandt T, Neumann D (2015) Data analytics for location-based services: Enabling user-based relocation of carsharing vehicles. *Proc. Internat. Conf. Inf. Syst. (ICIS)* 3:279–287.

Wang L, Ma W (2019) Pricing approach to balance demands for one-way car-sharing systems. *2019 IEEE Intell. Transp. Syst. Conf. (ITSC)* 1697–1702.

Wang H, Yang H (2019) Ridesourcing systems: A framework and review. *Transp. Res. Part B: Methodol.* 129: 122–155.

Waserhole A, Jost V (2012) Vehicle sharing system pricing regulation: A fluid approximation. Working paper, ENSTA ParisTech, Palaiseau, France.

Waserhole A, Jost V (2016) Pricing in vehicle sharing systems: Optimization in queuing networks with product forms. *EURO J. Transp. Logist.* 5(3):293–320.

Zhang J, Meng M, David Z (2019) A dynamic pricing scheme with negative prices in dockless bike sharing systems. *Transp. Res. Part B: Methodol.* 127:201–224.

Chapter 6

Dynamic Pricing for Shared Mobility Systems Based on Idle Time Data

6.1 Introduction

In recent years, the popularity and usage of shared mobility systems (SMSs) has grown rapidly. This is reflected, for example, in the evolution of car sharing users in Germany, which has increased steadily from only two hundred thousand users in 2011 to almost three million users in 2021 (Statista, 2021).

Independent of private or public ownership, SMS providers strive for maximizing the system's operational performance. In doing so, different metrics are analyzed. A popular one is the *idle time*, which is defined as "the amount of time between two consecutive rentals of one vehicle that is available for rent" (Neijmeijer et al., 2020). In other words, it is "the time between the rental and the prior return [...]" (Reiss and Bogenberger, 2015). According to Xie and Wang (2018), total operating time consists of idle time, maintenance time, and use time. Importantly, idle time "is not a characteristic of a specific [...] vehicle, but rather of the location where a rental ends. It reflects how supply and demand [...] match in the vicinity" (Wagner et al., 2015).

Using the idle time as a performance metric has various advantages. First, it is easy to measure, which is why historical idle time data is often available in practice. Since idle time is location- and time-specific and since spatial as well as temporal information can be measure on different levels of granularities, the specific idle time data available in practice varies. The second advantage of idle time data is that it includes latent demand (i.e. the demand that does not lead to rentals because, e.g., of supply shortages) as Neijmeijer et al. (2020) point out. Thus, it is an "honest" indicator which, unlike simply considering rentals, does not have to be adjusted to become meaningful. More specifically, observing a short idle time reveals the interplay between supply and a comparably high demand while observing a certain amount of rentals does not allow to conclude weather supply or demand was the limiting factor.

Due to these advantages, idle time is used for several purposes to analyze and control SMSs. Most frequently it is used as a metric for the analysis of the spatial differences in utilization (e.g. Reiss and Bogenberger, 2015) and the attractiveness of different zones (Lippoldt et al., 2018). Moreover, idle time is also used as part of an unconstraining technique to estimate unconstrained demand. As indicated above, while unconstrained demand is typically difficult to measure, idle times are not. For example, Mooney et al. (2019) uses the inverse of the idle time as a proxy for the demand. Furthermore, high idle times provide an indication for an accumulation of vehicles in a part of the business area with low demand. Thus, idle time is a reliable metric for operator-based relocation and used as the basis for rules of thumb in practice. For example, Göppel and Blumenstock (2012) report that at car2go, a vehicle was relocated if its idle time had exceeded a certain threshold (e.g. three days). Finally, another application is to use idle time (usually in combination with other metrics) to determine the attractiveness of a zone and then either combine a differentiated pricing approach with operator-based relocation (e.g. Reiss and Bogenberger, 2016b) or apply operator-based relocation only (e.g. Weikl and Bogenberger, 2015).

Another very important application for idle times in SMSs is in the context of dynamic pricing, which we focus on in this work. A few first business rules relying on exogeneously given idle time thresholds have been proposed in literature and practice: A straightforward idea is that locations with a very low idle time indicate a very high demand in comparison to the supply

of available vehicles. For a profit-maximizing provider, high prices would be reasonable in this case of high scarcity, and vice versa. The dynamic pricing of DriveNow, for example, was based on this idea (Wu et al., 2021). Here, vehicles that exceeded a certain idle time were priced at a discount. Another very practical pricing approach is based on the comparison between the idle time of the customer's indented destination and possible other destinations in the vicinity (Wagner et al., 2015; Brandt and Dlugosch, 2021). Here, if the idle time at an alternative destination falls short of the idle time at the intended destination by at least a threshold, then the business rule offers an incentive for the alternative destination. It should be noted, however, that, for this pricing approach, the customer must specify the destination, which is not current practice. Yet another idea is to strive for a homogeneous idle time (target idle time) across the entire business area (Neijmeijer et al., 2020). Here, the idle times are compared with this target idle time and prices are set accordingly. All these approaches are easy to implement, practical business rules but they are not based on optimization.

To close this literature gap regarding optimization-based approaches, in this work, we develop a novel idle-time based dynamic pricing (ITDP) approach for SMSs. As typical in dynamic pricing in complex systems, the approach builds on approximating state values which quantify the future expected profit to handle the curse(s) of dimensionality. More specifically, the ITDP's central idea is that these state values are formulated based on (expected) idle times. To this end, the (expected) remaining time a vehicle will be in use and generate profit is quantified. This remaining time depends on the overall considered time and the expected idle time. For example, a shorter idle time is equivalent to a longer profitable remaining time, and vice versa. In comparison to the few existing idle-time based approaches named above, our ITDP is anticipative, meaning that it seeks to optimize the immediate expected profit of a pricing decision *as well as* the expected profit to come. The price optimization is performed under consideration of a disaggregated customer choice model and the general formulation of the state value approximation allows to integrate historic idle-time data for different spatio-temporal granualities, as they occur in practice.

Regarding the specifics of the SMSs that we consider, there are two main characteristics to mention. First, two *types* of SMSs exist: free-floating and station-based SMSs (Laporte et al., 2018). The decisive difference between free-floating SMSs and station-based SMSs is that pick-up and drop-off locations for vehicles are not limited to certain predefined locations. Instead, in a free-floating SMS, vehicles can be dropped-off (and picked-up) at any publicly accessible location. Second, from a provider's perspective, regardless of free-floating or station-based, SMSs differ in the *spatio-temporal demand information*. More specifically, it refers to whether the provider has knowledge of origin, destination, and time of demand. In the context of pricing, this difference results in different pricing mechanism, as described in Soppert et al. (2022). For example, in "origin-based pricing", prices charged for a rental only depend on a rental's spatio-temporal origin, meaning its start location and start time. In "trip-based pricing", in contrast, prices may depend on both origin and destination. In this work, we consider a free-floating SMS and formulate the ITDP in a general way that allows to apply it to all variants of spatio-temporal demand information. In the computational studies, we focus exemplarily on an origin-based dynamic pricing, as typical in modern free-floating SMSs.

The contributions of our work are the following:

- We develop the first optimization-based and anticipative dynamic pricing approach for SMSs which is built on idle times.
- With regard to methodology, we propose a general state value formulation that exclusively relies on expected idle times to quantify a SMS's future expected profit.
- Due to the generality of this formulation, the pricing approach allows wide applicability in practice, especially in the sense that readily available historical idle time data – independent of the data's temporal and spatial granularity – can be seamlessly integrated.
- We conduct several computational studies that demonstrate the dominance of the developed approach compared to existing benchmark approaches in literature. The results show that profit can be increased by up to 11 % compared to current pricing practice.

The remainder of the paper is organized as follows. In Section 3.2, we review the relevant literature. Section 6.3 begins with a problem statement and the introduction of notation. Based on this, Section 6.3.2 describes the new dynamic pricing approach based on idle times. Section 6.3.3 then exemplarily describes the integration of idle time data for three different temporal and spatial granularities. Section 3.4 contains the computational studies. Section 6.5 concludes the paper and gives an outlook on future research.

	methodology		foresight		required *historical* data for anticipation					
paper	business rules	optimization	anticipative	myopic	idle time	vehicle history	vehicle distribution	demand	rentals	only current data
Dynamic Pricing with Idle Time										
Wagner et al. (2015)	x		x		-	-	-	-	-	-
Brandt and Dlugosch (2021)	x		x		-	-	-	-	-	-
Neijmeijer et al. (2020)	x			x	-	-	-	-	-	-
Dynamic Pricing without Idle Time										
Singla et al. (2015)		x	x							
Pfrommer et al. (2014)		x	x						x	
Ruch et al. (2014)		x	x				x		x	
Febbraro et al. (2012), Febbraro et al. (2019)		x	x					x		
Kamatani et al. (2019)		x	x							x
Clemente et al. (2017)		x	x						x	
Müller et al. (2021)		x	x			x				
Brendel et al. (2016)	x		x				x		x	
Dötterl et al. (2017)	x		x							x
Chemla et al. (2013)		x		x	-	-	-	-	-	-
Haider et al. (2018)		x		x	-	-	-	-	-	-
Wang and Ma (2019)		x		x	-	-	-	-	-	-
Bianchessi et al. (2013)	x			x	-	-	-	-	-	-
Zhang et al (2019)	x			x	-	-	-	-	-	-
Barth et al. (2004)	x			x	-	-	-	-	-	-
Mareček et al. (2016)	x			x	-	-	-	-	-	-
Angelopoulos et al. (2016), Angelopoulos et al. (2018)	x			x	-	-	-	-	-	-
This paper										
Müller et al. (2022)		x	x		x					

Table 6.1: Literature on dynamic pricing for SMS ("-" means not applicable)

6.2 Literature Review

The literature on SMS optimization is broad, covering various types of systems, optimization problems, control approaches, and methodologies. General overviews on SMS optimization problems have been presented in survey papers on bike sharing (e.g. DeMaio, 2009; Fishman et al., 2013; Ricci, 2015), car sharing (e.g. Jorge and Correia, 2013; Ferrero et al., 2015a,b; Illgen and Höck, 2019), and SMSs in general (e.g. Laporte et al., 2015, 2018).

In this literature review, we focus on *dynamic* pricing in SMSs in the sense that prices depend on the system's current state. We exclude *differentiated* (or static) pricing approaches (see e.g., Agatz et al., 2013; Soppert et al., 2022, and the references therein).

In the following, we introduce a classification scheme for dynamic pricing approaches (Section 6.2.1). Based on this, Section 6.2.2 considers dynamic pricing approaches using idle time data and Section 6.2.3 reviews papers using other data. At the end of each section, we concisely delineate the existing literature from the paper at hand.

6.2.1 Dimensions of Dynamic Pricing

To structure the dynamic pricing approaches for SMSs, we propose the following three *dimensions* which characterize an approach from the provider's perspective (see also Table 6.1).

1. *Methodology* (first column): Prices are either determined by *business rules* or by *optimization*, meaning based on solving some mathematical optimization model.

2. *Foresight* (second column): *Myopic* approaches determine prices based on the immediate (expected) reward (e.g. profit), given the current state of the SMS. In contrast, *anticipative* approaches additionally consider how current decisions influence the SMS's future states and rewards.

3. *Required historical data for anticipation* (third column): Anticipative pricing approaches require some component to predict the future. Thus, they usually require historical data, either to forecast the system's evolution or to directly predict current decisions' implications on future rewards.

With regard to these three dimensions, this paper develops an *anticipative optimization-based* dynamic pricing approach relying on *idle time* data, which we call ITDP for short.

6.2.2 Dynamic Pricing with Idle Time Data

Three papers perform dynamic pricing with idle time data, all using business rules. Both Wagner et al. (2015) and Brandt and Dlugosch (2021) first ask an arriving customer for her intended destination. The approaches calculates the expected idle time for the customer's intended destination as well as for locations in its vicinity. Their approach offers an incentive to the customer for leaving the vehicle at a nearby destination if its idle time undercuts that of the originally entered destination by at least a threshold. The provider chooses the threshold such that his benefit from the diversion exceeds the cost of the incentive offered to the customer. The authors

recognize that this threshold is tedious to set and examine different threshold values. Both papers apply location-period specific idle times (see Table 6.2 and for further explanations Section 6.3.3) as they divide the free-floating system's business area into so-called tiles and calculate average idle times for each tile and time period (Wagner et al. (2015): 1h, Brandt and Dlugosch (2021): 30min). They are indirectly anticipative because when they decide on prices when a customer arrives, they consider idle times at the destination when the trip ends and, thus indirectly capture the system's future state and reward.

Neijmeijer et al. (2020) use idle times in a real-world experiment to set prices. The core idea of the pricing approach is to achieve a good service level by having homogeneous idle times across the entire business area. To price a vehicle when a customer arrives, the average idle time at its current location for the current time period is considered (location-period specific idle time, see Table 6.2 and for further explanations Section 6.3.3). As only current values are considered, we classify the approach as myopic.

As mentioned above, the pricing approaches in all three papers are hands-on business rules where prices are set based on thresholds or a target idle time for the whole system. Moreover, the pricing approach of Neijmeijer et al. (2020) is myopic and does not consider future profit. In contrast, our pricing approach calculates prices using an optimization procedure and anticipates future rewards.

6.2.3 Dynamic Pricing without Idle Time Data

In this section, we consider papers that propose dynamic pricing approaches and thereby do not use idle time data. We structure them along the first two dimensions from Section 6.2.1, i.e. foresight and methodology. In Section 6.2.3.1, we consider the approaches that are closest to ITDP in *both* dimensions, i.e. which are anticipative and optimization-based. Then, we examine the dynamic pricing approaches that share *only one* of the two dimensions with ITDP, i.e. that use anticipative business rules (Section 6.2.3.2) or myopic optimization (Section 6.2.3.3). Finally, in Section 6.2.3.4, we consider myopic business rules.

6.2.3.1 Anticipative Optimization

Several papers use mathematical optimization with models that anticipate future states or rewards. Singla et al. (2015) define empty and full stations based on their current occupancy and predicted rentals. The pricing approach iteratively learns users' reactions to the incentives offered and seeks to align future demand and supply. Pfrommer et al. (2014) propose a model predictive control approach that uses quadratic programming and recalculates prices each period in a rolling horizon fashion. This pricing approach needs data about the current occupancy of the stations and historical rentals for the anticipation. Ruch et al. (2014) build on Pfrommer et al. (2014) and investigate simplified variants that can be used to benchmark more complex approaches. An anticipative variant element needs historical data about the occupancy of all stations. Febbraro et al. (2012) aim at a supply/demand ratio of 1 at all stations. They suggest alternative drop-off locations with a discount to customers. Febbraro et al. (2019) follow up on their earlier paper and formulate and test corresponding optimization models. These optimization models require future demand, which is calculated based on historical demand. Kamatani

et al. (2019) optimize thresholds by Q-learning based on simulated data, which uses data about the current vehicle distribution and the current rentals. Clemente et al. (2017) use a particle swarm optimization based on simulated data of vehicle distributions and the demand. Müller et al. (2021) develop a customer-centric disaggregate and anticipative pricing approach. Their approach focuses on the vehicles that are within a customer's walking distance and evaluate them using a kernel regression based on historical vehicle-specific data, for which the provider must have tracked individual vehicles in the past.

Although the above papers propose a similar dynamic pricing approach in terms of methodology and foresight, they are not directly applicable to the problem considered here in which the provider (only) possesses idle time data. The decisive novelty compared to e.g. Müller et al. (2021) is the type of *required historical data*: ITDP uses readily available idle time data in the anticipative price optimization. This allows ITDP to approximate state values with non-parametric value function approximations and to incorporate complex customer choice behavior. By contrast, the above approaches need data on rentals, vehicle distribution, or vehicle histories.

6.2.3.2 Anticipative Business Rules

Both Brendel et al. (2016) and Dötterl et al. (2017) use business rules and anticipate the future. Dötterl et al. (2017) analyze the vehicles' current state (driving or idle) and predict the near-future occupancy of every station. They differ in the required data. Brendel et al. (2016) requires historical and current data on rentals and occupancy to calculate station thresholds and compare them to current occupancy. In contrast, Dötterl et al. (2017) requires current station occupancy, current rentals, and customer location during the rental time and no historical data to predict near-future occupancy. Potential incentives are then based on the calculated expected future occupancy, such as when users return a vehicle to a station with a predicted shortage.

Besides data requirements, these papers share the well-known pros and cons of business rules: They are easy to understand, but leave parameter tuning to the provider, which often results in inferior performance compared to optimization.

6.2.3.3 Myopic Optimization

Three papers use myopic optimization models. Chemla et al. (2013) overall focus on user-based relocation, but also determine period-specific myopic prices. The authors aim at a service-maximizing fleet distribution, where customer satisfaction is measured by successful and unsuccessful customer actions (pick-up and drop-off because of available or non available bike, empty or full rack). They use a linear program to determine the number of customers who change their travel plans because of the price incentive offered to reach the given target inventory of vehicles for each station.

Two papers do not directly solve a mathematical model, but use it as a basis to develop a heuristic. Haider et al. (2018) model a bi-level program, where the upper level determines prices and minimizes vehicle imbalance, while the lower level represents the cost-minimizing route choice of customers. The problem is transformed into a single-level problem and a heuristic is proposed that iteratively adjusts prices (and, in contrast to the bi-level program, contains some anticipation). Wang and Ma (2019) consider the objective of keeping inventory within a certain

range for a period. For this purpose, they define lower and upper thresholds for each station. The number of rentals from or to a station can be affected by pick-up and drop-off fees. They formulate a quadratic program to determine optimal dynamic pick-up and drop-off fees and solve it with a genetic algorithm.

While the above approaches use optimization, they are restricted by their myopic horizon. Moreover, they capture customer behaviour in aggregate models and therefore cannot exploit the opportunities of existing disaggregated data.

6.2.3.4 Myopic Business Rules

Several works use myopic business rules. Bianchessi et al. (2013) compare the number of vehicles at a station and the mean value of vehicles per station to determine prices. Zhang et al (2019) capture system and customer behavior in a mathematical model. They define prices by comparing the current number of vehicles with demand and propose a negative price that is linear in the undersupply of a rental's destination station. If there is no undersupply, the regular positive price applies. Barth et al. (2004) propose a system that, once it recognizes an imbalance, provides incentives for joint rides of independent customers in one car or splitting a party of customers into multiple cars. Mareček et al. (2016) derive drop-off charges for vehicles depending on the intended destination location's distance to the nearest vehicle. Angelopoulos et al. (2016) and Angelopoulos et al. (2018) propose two algorithms for promoting trips based on the priorities of vehicle relocates between stations.

6.3 Idle-Time Based Dynamic Pricing

In this section, we first state the problem considered and introduce the notation (Section 6.3.1). Based on this, Section 6.3.2 describes the ITDP, i.e., the new idle-time based dynamic pricing approach. In doing so, we assume that an idle time value for each location is known. Section 6.3.3 then exemplarily describes how to obtain these idle time values from idle time data of three different temporal and spatial granularities. We also show the granularities' implications for the pricing approach. To improve readability, the following deliberations focus on a free-floating SMS provider. Nevertheless, please note that the model covers both, station-based and free-floating SMSs.

6.3.1 Problem Statement

We consider a free-floating SMS provider who operates a homogeneous fleet of vehicles that are spatially distributed over a continuous business area. The objective is to maximize the expected profit by means of dynamic price optimization. More specifically, the business area is rectangular and ranges from west ($x = 0$) to east ($x = x_{max}$) and from south ($y = 0$) to north ($y = y_{max}$). The set $\mathcal{X}$ ($\mathcal{Y}$) contains all possible x-coordinates (y-coordinates) of the area. At each point in time t during the considered time horizon (e.g. one day, $0 \leq t \leq t^{total}, \mathcal{T} = \{0, ..., t^{total}\}$), the provider knows the state of the vehicle fleet, in particular the exact position $(x_{i,t}, y_{i,t})$of a vehicle i and whether it is idle or moving. To keep track of the vehicles' states, $\tau_{i,t}$ denotes whether a vehicle i is idle ($\tau_{i,t} = 0$) or in use ($\tau_{i,t} =$ starting time of rental).

Customers arrive randomly over time. More precisely, at time t at most one customer arrives with probability λ_t and opens the provider's mobile application at a location with coordinates (x_t^O, y_t^O), which follow a given time-dependent origin probability distribution $O(t)$, and seeks to rent a vehicle. Then, for each vehicle in the vicinity of this customer, the provider's optimization problem is to determine prices $\vec{p}_t$, (contains a price $p_{i,t}$ per minute for each vehicle within walking distance)where each price has to be selected from a discrete set of price points $\mathcal{M}$. Also, we assume that a rental incurs variable costs c per minute.

The customer choice behavior is formalized as follows: Customers have a (fixed) maximum willingness to walk $\bar{d}$ and a vehicle's distance to the customer is given by d_i. Thus, a customer only considers idle vehicles from the so-called consideration set $\mathcal{C}_{t,(x_t^O, y_t^O)} = \{i \in \mathcal{C} \,|\, d_i \leq \bar{d} \wedge \tau_{i,t} = 0\}$. The customer either chooses vehicle i with probability $q_{i,t}(\vec{p}_t)$ (then, the vehicle is *in use*) or leaves the system with probability $q_{0,t}(\vec{p}_t)$. Vehicles not chosen remain *idle*. The choice probabilities $q_{i,t}(\vec{p}_t)$ and the no choice probability $q_{0,t}(\vec{p}_t)$ depend on the distance of the vehicle to the customer as well as the prices $\vec{p}_t$ for all reachable vehicles of the consideration set. This means that the customer is price and distance sensitive. Thus, the provider can e.g. incentivize her to take a certain vehicle in walking distance by offering a low price (for detailed information on the used multinomial logit model and its parameter estimation, see Appendix 6.A). Choosing vehicle i with probability $q_{i,t}(\vec{p}_t)$, the rental starts at time t, since we neglect the comparably short time the customer walks to the vehicle.

The rental time $l_{i,t}$ in minutes is a realization of the random variable $L_{i,t}$, which follows the distribution ρ_t. Thus, a rental terminates at time $t' = t + l_{i,t}$ (in expectation at $t' = t +$

$\mathbb{E}_{L_{i,t}\sim\rho_t}(L_{i,t})$) at location $(x^D_{i,t'}, y^D_{i,t'})$. Note in this context that, depending on the characteristics of the SMSs, a customer's intended destination might or might not be known to the provider at rental start time t. More specifically, *spatio-temporal demand information* is either origin -, or trip-based, meaning that either only the spatio-temporal origin or both (origin and destination) is known to the provider before a rental.

Finally, we denote the idle time for vehicle i which is not rented as $\varphi_{i,t,(x_{i,t},y_{i,t})}$ (in expectation: $\tilde{\varphi}_{i,t,(x_{i,t},y_{i,t})}$), and the idle time for vehicle i after a rental which starts at t as $\varphi_{i,t',(x^D_{i,t'},y^D_{i,t'})}$ (in expectation: $\tilde{\varphi}_{i,t',(x^D_{i,t'},y^D_{i,t'})}$). Please note that idle time always refers to the time the vehicle is idle until the *next* rental. Further explanations are given in the next subsection.

6.3.2 Idle-Time Based Dynamic Pricing Approach

In this section, we present the new ITDP. As described above, prices $\vec{p}_t$ are optimized whenever a customer arrives at time t at location (x^O_t, y^O_t) and $\vec{p}_t$ only contains prices $p_{i,t}$ for the vehicles within the customer's reach $i \in \mathcal{C}_{t,(x^O_t,y^O_t)}$. The maximization of total expected profit until the end of the considered horizon includes both a myopic and an anticipative component. With regard to different available spatio-temporal demand information (see previous section), the ITDP is general in the sense that it can be specified for origin- and trip-based demand information.

The myopic component considers the expected profit from the currently arriving customer and her choice. It is given by

$$\sum_{i\in\mathcal{C}_{t,(x^O_t,y^O_t)}} q_{i,t}(\vec{p}_t) \cdot \mathop{\mathbb{E}}_{L_{i,t}\sim\rho_t}(L_{i,t}) \cdot (p_{i,t} - c). \tag{6.1}$$

The anticipative component is more complex. It considers expected profit from future customers and is approximated by the sum of the expected profits of the vehicles. More precisely, we use $\tilde{w}^{idle}_{i,t}$ to denote the expected future profit of vehicle i if it remains *idle* now, and $\tilde{w}^{dep}_{i,t}$ to denote expected future profit *after* the current customer's rental if vehicle i *departs* when chosen by the current customer. Thus, expected future profit for the system is

$$\sum_{i\in\mathcal{C}_{t,(x^O_t,y^O_t)}} q_{i,t}(\vec{p}_t) \cdot \left(\tilde{w}^{dep}_{i,t} + \sum_{j\in\mathcal{C}_{t,(x^O_t,y^O_t)}\setminus\{i\}} \tilde{w}^{idle}_{j,t} \right) + q_{0,t}(\vec{p}_t) \cdot \sum_{j\in\mathcal{C}_{t,(x^O_t,y^O_t)}} \tilde{w}^{idle}_{j,t}. \tag{6.2}$$

Thus, to maximize profit, the provider sets the optimal price vector $\vec{p}^{\,*}_t$ according to

$$\begin{aligned} \vec{p}^{\,*}_t = \arg\max_{\vec{p}_t} \sum_{i\in\mathcal{C}_{t,(x^O_t,y^O_t)}} q_{i,t}(\vec{p}_t) \cdot \Bigg(& (p_{i,t} - c) \cdot \mathop{\mathbb{E}}_{L_{i,t}\sim\rho_t}(L_{i,t}) + \tilde{w}^{dep}_{i,t} \\ & + \sum_{j\in\mathcal{C}_{t,(x^O_t,y^O_t)}\setminus\{i\}} \tilde{w}^{idle}_{j,t} \Bigg) + q_{0,t}(\vec{p}_t) \cdot \sum_{j\in\mathcal{C}_{t,(x^O_t,y^O_t)}} \tilde{w}^{idle}_{j,t}. \end{aligned} \tag{6.3}$$

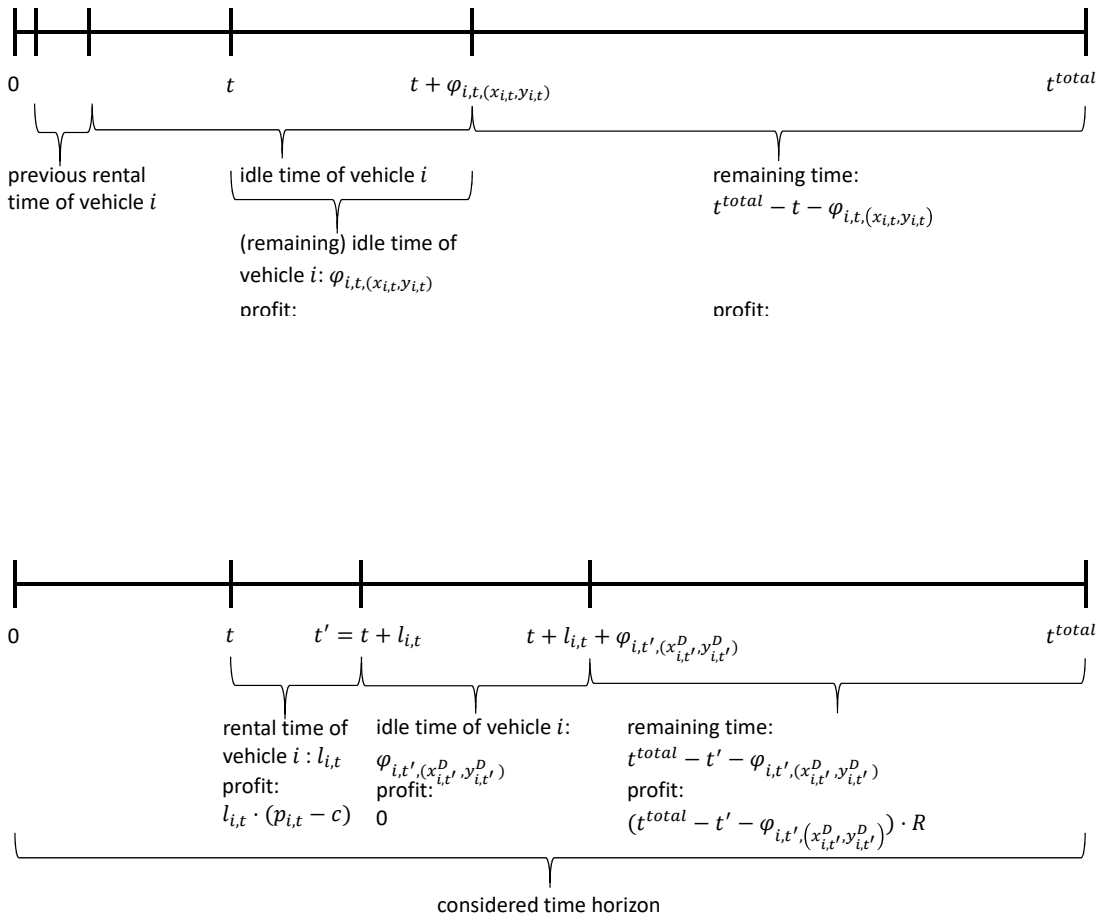

Figure 6.2: Remaining time if vehicle is chosen and rental departs

Obviously, to efficiently solve (6.3), we need an approximation of the expected future profit for each vehicle i for each of the two alternatives (vehicle i is chosen: $\tilde{w}^{dep}_{i,t}$, or not chosen: $\tilde{w}^{idle}_{i,t}$).

As already mentioned, we approximate these values using historical idle time data, which makes use of the fact that idle times are an implicit representation of the expected location- and time-specific demand pattern and that they are location- and time-specific. The dependencies between customer arrival time t, rental time $l_{i,t}$, rental termination time t', and idle times are depicted in Figures 6.1 and 6.2.

We consider two types of idle times. First, we consider a vehicle that is idle since the previous rental ends. This vehicle is not chosen by a customer at time t and remains idle (Figure 6.1). The time from 0 to the current time t has already passed when the customer arrives at time t. Since the customer does not choose vehicle i located at $(x_{i,t}, y_{i,t})$, it remains idle for the idle time $\varphi_{i,t,(x_{i,t},y_{i,t})}$ during which it does not earn any profit. This means, that $\varphi_{i,t,(x_{i,t},y_{i,t})}$ denotes the (remaining) idle time after t and not the idle time after the end of the previous rental. The remaining time after this idle time until the end of the horizon at t^{total} is $t^{total} - t - \varphi_{i,t,(x_{i,t},y_{i,t})}$ and is valued with R per time unit.

Second, consider a vehicle that is chosen by a customer (Figure 6.2). Again, the time from 0 to t has already elapsed. After this time, however, the customer rents vehicle i. The trip has an duration of $l_{i,t}$ time units and yields an profit $l_{i,t} \cdot (p_{i,t} - c)$, already captured in the

myopic component. After the vehicle has been dropped-off, it stands idle again for a certain time $\varphi_{i,t',(x^D_{i,t'},y^D_{i,t'})}$ at its new location $(x^D_{i,t'}, y^D_{i,t'})$ until the next rental starts. During this time, no profit is earned. However, in the remaining time $t^{total} - t' - \varphi_{i,t',(x^D_{t'},y^D_{t'})}$ after the idle time, the vehicle earns again a profit of R per time unit.

The idea is that a shorter idle time is equivalent to a longer profitable remaining time, and vice versa. The benefit of using idle times instead of demand patterns is that idle time data can be easily measured in reality, while (unconstrained) demand is not easy to measure.

The value R is easily determined from historical data by dividing the observed total profit over some time window through the product of the fleet size and the length of the considered time window. The calculation of the remaining time during which a vehicle earns R per time unit is explained in the following.

Since the exact idle time is not known we approximate the values of the idle times (vehicle idle: $\tilde{\varphi}_{i,t,(x_{i,t},y_{i,t})}$, vehicle chosen: $\tilde{\varphi}_{i,t',(x^D_{i,t'},y^D_{i,t'})}$) and consider the stochastic rental time ($\mathbb{E}_{L_{i,t}\sim\rho_t}(L_{i,t})$) because we do not know the exact idle time of the idle vehicle and the exact rental time and subsequent idle time of the departing vehicle. Thus, we have

$$\tilde{w}^{idle}_{i,t} = \left(t^{total} - t - \tilde{\varphi}_{i,t,(x_{i,t},y_{i,t})}\right) \cdot R \qquad \forall i \in \mathcal{C}_{t,(x^O_t,y^O_t)} \tag{6.4}$$

$$\tilde{w}^{dep}_{i,t} = \left(t^{total} - t' - \tilde{\varphi}_{i,t',(x^D_{i,t'},y^D_{i,t'})}\right) \cdot R \qquad \forall i \in \mathcal{C}_{t,(x^O_t,y^O_t)}. \tag{6.5}$$

The expected future profit of a vehicle i at time t ($\tilde{w}^{idle}_{i,t}$, $\tilde{w}^{dep}_{i,t}$) depends on location and time and can be different for each vehicle (depending on the spatial and temporal granularity of idle time). Note that for station-based SMSs, the number of available vehicles considered at a station can be reduced to one if at least one vehicle is available, since these vehicles have the same characteristics in terms of distance and expected future profit. Substituting (6.4) and (6.5) into (6.3) allows the following simplifications

$$\begin{aligned}
\vec{p}^{\,*}_t = &\underset{\vec{p}_{t,(x^O_t,y^O_t)}}{\arg\max} \sum_{i\in\mathcal{C}_{t,(x^O_t,y^O_t)}} q_{i,t}(\vec{p}_t) \cdot \Bigg((p_{i,t} - c) \cdot \underset{L_{i,t}\sim\rho_t}{\mathbb{E}}(L_{i,t}) + \tilde{w}^{dep}_{i,t} \\
&+ \sum_{j\in\mathcal{C}_{t,(x^O_t,y^O_t)}\setminus\{i\}} \tilde{w}^{idle}_{j,t} \Bigg) + \left(1 - \sum_{i\in\mathcal{C}_{t,(x^O_t,y^O_t)}} q_{i,t}(\vec{p}_t)\right) \cdot \sum_{j\in\mathcal{C}_{t,(x^O_t,y^O_t)}} \tilde{w}^{idle}_{j,t} \\
= &\arg\max_{\vec{p}_t} \sum_{i\in\mathcal{C}_{t,(x^O_t,y^O_t)}} q_{i,t}(\vec{p}_t) \cdot \left((p_{i,t} - c) \cdot \underset{L_{i,t}\sim\rho_t}{\mathbb{E}}(L_{i,t}) - \tilde{w}^{idle}_{i,t} + \tilde{w}^{dep}_{i,t} \right) \\
&+ \sum_{j\in\mathcal{C}_{t,(x^O_t,y^O_t)}} \tilde{w}^{idle}_{j,t} \qquad (6.6) \\
= &\underset{\vec{p}_{t,(x^O_t,y^O_t)}}{\arg\max} \sum_{i\in\mathcal{C}_{t,(x^O_t,y^O_t)}} q_{i,t}(\vec{p}_t) \cdot \left((p_{i,t} - c) \cdot \underset{L_{i,t}\sim\rho_t}{\mathbb{E}}(L_{i,t}) - \left(\tilde{w}^{idle}_{i,t} - \tilde{w}^{dep}_{i,t}\right) \right) \\
= &\underset{\vec{p}_{t,(x^O_t,y^O_t)}}{\arg\max} \sum_{i\in\mathcal{C}_{t,(x^O_t,y^O_t)}} q_{i,t}(\vec{p}_t) \cdot \Bigg((p_{i,t} - c) \cdot \underset{L_{i,t}\sim\rho_t}{\mathbb{E}}(L_{i,t}) \\
&- \left(\underset{L_{i,t}\sim\rho_t}{\mathbb{E}}(L_{i,t}) + \tilde{\varphi}_{i,t',(x^D_{i,t'},y^D_{i,t'})} - \tilde{\varphi}_{i,t,(x_{i,t},y_{i,t})} \right) \cdot R \Bigg)
\end{aligned}$$

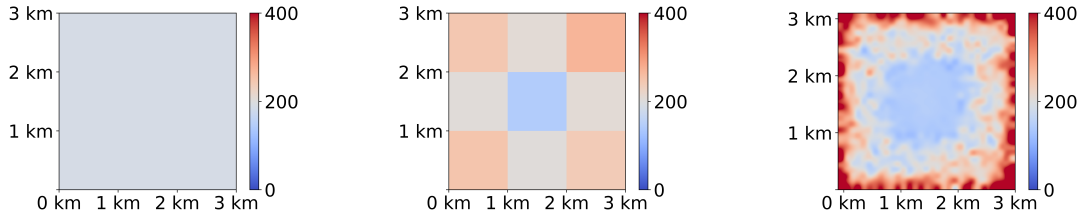

(a) Entire business area: homogeneous idle time across the entire area

(b) Zones: coarse spatial variation possible

(c) Spatial continuous: different expected idle time for each coordinate possible

Figure 6.3: Different granularities of idle time data

In (6.6), the first three equalities are rearrangements of (6.3). The second to last line nicely shows that what matters regarding future profit is the chosen vehicle's difference in future profit ($\tilde{w}^{idle}_{i,t} - \tilde{w}^{dep}_{i,t}$), which mirrors opportunity costs in revenue management (Talluri and Van Ryzin, 2004, Chapter 2.1.2).

As shown by the substitution and the last rearrangement, in addition to the profit from the rental only the difference between the idle time of a departing vehicle and the idle time of a remaining idle vehicle is important. For a departing vehicle, this is the current rental time and the idle time after drop-off ($\mathbb{E}_{L_{i,t}\sim\rho_t}(L_{i,t}) + \tilde{\varphi}_{i,t',(x^D_{i,t'},y^D_{i,t'})}$) and for an idle vehicle, the idle time ($\tilde{\varphi}_{i,t,(x_{i,t},y_{i,t})}$). This eliminates the need for additional calculations to value the vehicles. However, unlike in traditional revenue management applications, this term may become negative. This is the case if the vehicle was at such a "bad" location that we have $\tilde{\varphi}_{i,t,(x_{i,t},y_{i,t})} > \mathbb{E}_{L_{i,t}\sim\rho_t}(L_{i,t}) + \tilde{\varphi}_{i,t',(x^D_{i,t'},y^D_{i,t'})}$.

With regard to the pricing optimization this results in a lower price (compared to a myopic approach) for the vehicle (alternative) i with negative opportunity cost (=positive expected profit) to increase its purchase probability $q_{i,t}(\vec{p}_t)$.

6.3.3 Using Real-World Idle Time Data

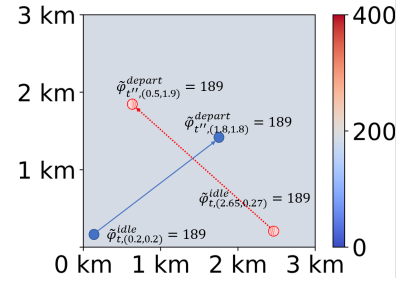

vehicle	value idle: $[t^{total} - t - \tilde{\varphi}^{idle}_{t,(x_{i,t},y_{i,t})}] \cdot R$
$j = 1$	$[1440 - 480 - 189] \cdot 0.0137 = 10.56$
$j = 2$	$[1440 - 480 - 189] \cdot 0.0137 = 10.56$

vehicle	value depart: $[t^{total} - t - \mathbb{E}_{(L_{t''} \sim \rho_t)} L_{t''} - \tilde{\varphi}^{depart}_{t'',(x^D_t,y^D_t)}] \cdot R$
$j = 1$	$[1440 - 480 - 15 - 189] \cdot 0.0137 = 10.36$
$j = 2$	$[1440 - 480 - 15 - 189] \cdot 0.0137 = 10.36$

(a) Business area wide idle time

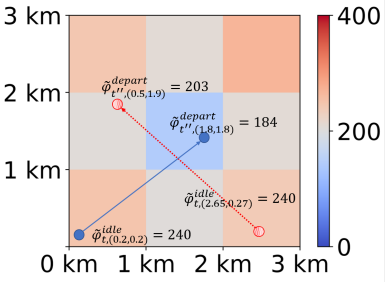

vehicle	value idle: $[t^{total} - t - \tilde{\varphi}^{idle}_{t,(x_{i,t},y_{i,t})}] \cdot R$
$j = 1$	$[1440 - 480 - 240] \cdot 0.0137 = 9.86$
$j = 2$	$[1440 - 480 - 240] \cdot 0.0137 = 9.86$

vehicle	value depart: $[t^{total} - t - \mathbb{E}_{(L_{t''} \sim \rho_t)} L_{t''} - \tilde{\varphi}^{depart}_{t'',(x^D_t,y^D_t)}] \cdot R$
$j = 1$	$[1440 - 480 - 15 - 184] \cdot 0.0137 = 10.43$
$j = 2$	$[1440 - 480 - 15 - 203] \cdot 0.0137 = 10.17$

(b) Location-period specific idle time

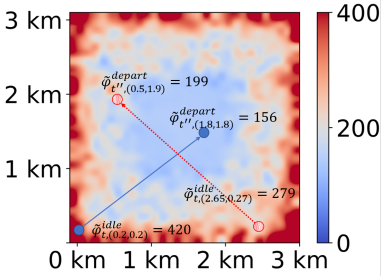

vehicle	value idle: $[t^{total} - t - \tilde{\varphi}^{idle}_{t,(x_{i,t},y_{i,t})}] \cdot R$
$j = 1$	$[1440 - 480 - 400] \cdot 0.0137 = 7.67$
$j = 2$	$[1440 - 480 - 279] \cdot 0.0137 = 9.33$

vehicle	value depart: $[t^{total} - t - \mathbb{E}_{(L_{t''} \sim \rho_t)} L_{t''} - \tilde{\varphi}^{depart}_{t'',(x^D_t,y^D_t)}] \cdot R$
$j = 1$	$[1440 - 480 - 15 - 156] \cdot 0.0137 = 10.81$
$j = 2$	$[1440 - 480 - 15 - 199] \cdot 0.0137 = 10.22$

(c) Continuous idle time

Figure 6.4: Exemplarily calculation of $\tilde{w}^{idle}$ and $\tilde{w}^{dep}$ for different spatial and temporal granularities (Constant rental time: $l = 15$ min)

In this section, we discuss how to obtain the values $\tilde{\varphi}_{i,t,(x_{i,t},y_{i,t})}$ and $\tilde{\varphi}_{i,t',(x^D_{i,t'},y^D_{i,t'})}$ necessary to calculate a price for a vehicle at that specific position from historical data. Moreover, we discuss the implications of different granularities for the pricing approach. Remember that the expected idle time of a vehicle i is a function of the time and its location.

Regarding data granularity, we distinguish two dimensions: spatial and temporal, each with three exemplarily resolutions (see Table 6.2). Regarding spatial granularity, we distinguish between idle time data being available only on the business area level, on a zone level (that is, some partition/discretization of the business area), and spatially continuous idle time data (i.e. possibly different values for all coordinates within the business area).

These three spatial granularities are illustrated in Figure 6.3. At the business area level, $\tilde{\varphi}$ cannot capture spatial differences and indicates the same expected idle time for each location within the business area (Figure 6.3a). By contrast, there are spatial differences for the zone level (Figure 6.3b) and spatially continuous idle time (Figure 6.3c).

Likewise, we also distinguish three temporal granularities. First, we may have only one value for the entire time horizon under consideration (e.g. a day). Second, we consider a discretization into time periods, and, finally, we allow for continuous time. There are nine

	temporal granularity		
spatial granularity	entire time horizon	periods	continuous
entire business area	**business area wide idle time**		
zones		**location-period specific idle time**	
spatial continuous			**continuous idle time**

Table 6.2: Overview of idle time granularities

possible combinations of the aforementioned temporal and spatial granularities.

In this paper, we focus on the three combinations with the same level in each dimension (see Table 6.2), which we denote as

- *business area wide idle time* (Section 6.3.3.1),
- *location-period specific idle time* (Section 6.3.3.2), and
- *continuous idle time* (Section 6.3.3.3).

Regarding customer interaction and experience, two paradigms with variants of spatio-temporal demand information exist. Most major sharing systems (see Soppert et al., 2022) emphasize the customer's freedom to go spontaneously wherever she wants (origin-based). Thus, they refrain from asking for her intended destination and simply wait where the vehicle is dropped-off. By contrast, the majority of the literature considers SMS where the provider asks for the destination before deciding on prices (trip- or destination-based).

In the following sections, we consider both cases (all variants of spatio-temporal demand information, see Section 6.3.2). The rental's origin is always available. However, if the provider knows the destination of the rental, idle times can be calculated much more accurately (but it remains stochastic) and therefore dynamic pricing is more accurate.

6.3.3.1 Business Area Wide Idle Time

The *business area wide idle time* assigns the same expected idle time $\bar{\varphi}^{const}$ to each combination of time t and location $(x_{i,t}, y_{i,t})$ for idle vehicles, respectively t' and $(x^D_{i,t'}, y^D_{i,t'})$ for departing vehicles. The value $\bar{\varphi}^{const}$ is an average idle time for the considered time horizon (e.g. a day) and the whole business area. As expected idle time is location-independent, a rental's destination and knowledge thereof does not matter:

$$\tilde{\varphi}_{i,t,(x_{i,t},y_{i,t})} = \tilde{\varphi}_{i,t',(x^{D\prime}_t,y^{D\prime}_t)} = \bar{\varphi}^{const} \tag{6.7}$$
$$\forall i,\ 0 \le t \le t' \le t^{total},\ 0 \le x \le x_{max},\ 0 \le y \le y_{max}$$

Substituting (6.7) into (6.6) yields

$$\vec{p}^{\,*}_t = \arg\max_{\vec{p}_t} \sum_{i \in \mathcal{C}_{t,(x^O_t, y^O_t)}} q_{i,t}(\vec{p}_t) \cdot (p_{i,t} - c - R) \tag{6.8}$$

as the expected idle time as well as the expected rental length $\mathbb{E}_{L_{i,t}\sim\rho_t}(L_{i,t})$ cancel out. As idle time is the same with and without rental, it obviously does not influence the pricing decision. Thus, the approach is largely myopic (if the homogeneity assumptions were true, no anticipation is necessary), but R still considers that the vehicle will be unavailable for the duration of the rental. It suffices to compare the expected average profit per minute for a chosen vehicle with the expected profit per minute for an idle vehicle. This means that the potential profit of the moving vehicles is compared with their opportunity cost. Thus, ceteris paribus prices from Equation (6.8) are greater or equal myopic prices. This is also reflected by the examples in Figure 6.4a, where we always obtain an opportunity cost of $\tilde{w}_{i,t}^{idle} - \tilde{w}_{i,t}^{dep} = 0.2$.

6.3.3.2 Location-Period Specific Idle Time

The premise for *location-period specific idle time* is that the provider has partitioned his business area into Z zones $z \in \mathcal{Z} = \{1, ..., Z\}$ and the time horizon into θ periods $\vartheta \in \Theta = \{1, ..., \theta\}$. For notational convenience, let us assume that the function $\vartheta(t) : \mathcal{T} \to \Theta$ maps time to time periods and the function $z((x, y)) : \mathcal{X} \times \mathcal{Y} \to \mathcal{Z}$ maps coordinates to zones. For each combination of period ϑ and zone z, the provider disposes of idle time values $\bar{\varphi}_{\vartheta,z}$, for example obtained from averaging corresponding historical data.

Now, for idle vehicles and departing vehicles if their destination is known we have

$$\tilde{\varphi}_{i,t,(x_{i,t},y_{i,t})} = \bar{\varphi}_{\vartheta(t),z((x_{i,t},y_{i,t}))} \quad \forall i, t,\ 0 \leq x \leq x_{max}, 0 \leq y \leq y_{max}, \tag{6.9}$$

$$\tilde{\varphi}_{i,t',(x^D_{i.t'},y^D_{i,t'})} = \bar{\varphi}_{\vartheta(t'),z((x^D_{i.t'},y^D_{i,t'}))} \quad \forall i, t',\ 0 \leq x \leq x_{max}, 0 \leq y \leq y_{max}. \tag{6.10}$$

This is illustrated in Figure 6.4b. Now, we see that the blue vehicle moves from a zone with high idle time to one with medium idle time, which is reflected by an opportunity cost of $\tilde{w}_{blue,t}^{idle} - \tilde{w}_{blue,t}^{dep} = -0.22$. The red one moves to a zone with only slightly less idle time, resulting in $\tilde{w}_{red,t}^{idle} - \tilde{w}_{red,t}^{dep} = -0.05$.

For departing vehicles with unknown destination we average over all zones, determining the expected idle time of the whole business area (all zones) for the period of arrival:

$$\tilde{\varphi}_{i,t',(\cdot)} = \frac{1}{Z} \cdot \sum_{z \in \mathcal{Z}} \bar{\varphi}_{\vartheta(t),z} \quad \forall i, t' \tag{6.11}$$

Here, no simplification of (6.6) is possible. If corresponding information is available, a weighted average regarding the destination is suggested.

6.3.3.3 Continuous Idle Time

The *continuous idle time* described in this section follows the idea to approximate values for departing and idle vehicles directly based on "similar" data points without an artificial discretization of time or space. Obviously, this approach is only applicable in free-floating SMS, since a station-based SMS always has discrete stations (nevertheless, a version that is continuous with regard to time may be considered).

The basic idea beyond this variant is to average similar data points through kernel regression to determine the vehicles' expected idle times. More precisely, the provider follows four steps.

In the first step, beforehand, the provider records vehicle-level data. The data set $\mathcal{K} = \{(\hat{\varphi}_k, (x_k, y_k), t_k)\}$ contains a data point k for each end of a rental (or when a vehicle becomes available after maintenance etc.) with location (x_k, y_k), time t_k of the arrival of a vehicle and the following idle time $\hat{\varphi}_k$.

During the pricing process, when a customer arrives at time t, idle time values for vehicles $i \in \mathcal{C}_{t,(x_t^O, y_t^O)}$ are determined by steps 2 to 4 as follows:

In step 2, the provider determines the sets $\mathcal{K}_{i,t}^{idle} \subseteq \mathcal{K}$ and $\mathcal{K}_{i,t'}^{dep,x} \subseteq \mathcal{K}, x \in \{dk, du\}$ (dk: destination known, du: destination unknown) from the set of all data points $\mathcal{K}$. Since all events in the free-floating SMS are characterized by a certain location and time, it is reasonable to integrate the spatial as well as the temporal dimension in the metric that measures "similarity" and we filter for relevant data points regarding *idle* vehicles as follows:

$$\mathcal{K}_{i,t}^{idle} = \Big\{ (\hat{\varphi}_k, (x_k, y_k), t_k) \in \mathcal{K} \;\Big|\; t_k \leq t < (t_k + \hat{\varphi}_k) \;\wedge\; |(x_k, y_k) - (x_{i,t}, y_{i,t})| \leq h \Big\} \tag{6.12}$$

where $|(x_k, y_k) - (x_{i,t}, y_{i,t})|$ is some *spatial distance* for the vehicle i standing at $(x_{i,t}, y_{i,t})$. For the *departed* vehicles, this step is almost the same. The difference is mainly that the departed vehicle i arrives after the expected rental time at $t + \mathbb{E}_{L_{i,t} \sim \rho_t}(L_{i,t}) (= t')$ and then idles. Moreover, we distinguish whether the provider knows the destination of the rental or not. If the provider knows the destination $(x_{i,t'}^D, y_{i,t'}^D)$ of the vehicle i, we define the following filter:

$$\mathcal{K}_{(x_{t'}^D, y_{t'}^D), t'}^{dep,dk} = \Big\{ (\hat{\varphi}_k, (x_k, y_k), t_k) \in \mathcal{K} \;\Big|\; t_k \leq (t') < (t_k + \hat{\varphi}_k) \;\wedge\; |(x_k, y_k) - (x_{t'}^D, y_{t'}^D)| \leq h \Big\} \tag{6.13}$$

If the provider does not know the destination of the vehicle i, we define the filter as follows:

$$\mathcal{K}_{i,t'}^{dep,du} = \Big\{ (\hat{\varphi}_k, (x_k, y_k), t_k) \in \mathcal{K} \;\Big|\; t_k \leq (t') < (t_k + \hat{\varphi}_k) \Big\} \tag{6.14}$$

In the third step, as the filtered data sets are now available for both idling and departing vehicles, the weights $\kappa_{i,t,k}^{idle}$ for each data point $k \in \mathcal{K}_{i,t}^{idle}$ can now be determined with a *kernel function* (see Powell, 2007, Chapter 8.4.2).

In particular, for idle vehicles, we use

$$\kappa_{i,t,k}^{idle} = \frac{K_{i,t,k}^{idle}}{\sum_{j=1}^{|\mathcal{K}_{i,t}^{idle}|} K_{i,t,j}^{idle}} \quad \forall k \in \mathcal{K}_{i,t}^{idle} \tag{6.15}$$

with the Epanechnikov kernel function

$$K_{i,t,k}^{idle} = \frac{3}{4} \cdot \left(1 - \left(\frac{d_{i,k}}{h}\right)^2\right) \quad \forall k \in \mathcal{K}_{i,t}^{idle} \tag{6.16}$$

with

$$d_{i,k} = \sqrt{(|(x_{i,t}, y_{i,t}) - (x_k, y_k)|)^2} \quad \forall k \in \mathcal{K}_{i,t}^{idle} \tag{6.17}$$

Regarding departing vehicles with unknown destination, the weights $\kappa_{i,t',k}^{dep,du}$ simply average all filtered data points, whereas the calculation of weights $\kappa_{i,t',k}^{dep,dk}$ for departing vehicles with known destination uses again the Kernel function and is similar to idle vehicles:

$$\kappa_{i,t',k}^{dep,du} = \frac{1}{|\mathcal{K}_{i,t',k}^{dep,du}|} \quad \forall k \in \mathcal{K}_{i,t'}^{dep,du} \tag{6.18}$$

$$\kappa_{i,t',k}^{dep,dk} = \frac{K_{i,t',k}^{dep}}{\sum_{j=1}^{|\mathcal{K}_{i,t',j}^{dep,dk}|} K_{i,t',j}^{dep}} \quad \forall k \in \mathcal{K}_{i,t'}^{dep,dk}. \tag{6.19}$$

The calculation of the Epanechnikov kernel is again (6.16), and the distance now is $d_{i,k} = \sqrt{(|(x_{i,t'}^D, y_{i,t'}^D) - (x_k, y_k)|)^2} \quad \forall k \in \mathcal{K}_{i,t'}^{dep,dk}$. Finally, in step 4, we use these weights and sets to calculate the expected idle time for each departing and idle vehicle i:

$$\tilde{\varphi}_{i,t,(x_{i,t},y_{i,t})} = \sum_{k \in \mathcal{K}_{i,t}^{idle}} \kappa_{i,k}^{idle} \cdot \bar{\varphi}_k \quad \forall i \in \mathcal{C}_{t,(x_t^O, y_t^O)} \tag{6.20}$$

$$\tilde{\varphi}_{i,t',(x_{t'}^D, y_{t'}^D)} = \sum_{k \in \mathcal{K}_{i,t}^{dep,x}} \kappa_{i,k}^{dep,x} \cdot \bar{\varphi}_k \quad \forall i \in \mathcal{C}_{t,(x_t^O, y_t^O)}, x \in \{dk, du\} \tag{6.21}$$

where expected idle time for all departing vehicles with unknown destination is identical.

The approach is illustrated by Figure 6.4c. Now, each vehicle has an individual expected idle time that depends on its exact position and, hence, the distance to historical data points. Thus, at a given point in time, the expected idle time for each location can be visualized using a heatmap as in Figure 6.4c.

6.3.4 Comparison

The three aforementioned types of idle times *business area wide*, *location-period specific* and *continuous* differ in three aspects as described in the following and summarized in Table 6.3:

1. By construction, they differ in the level of granularity of the required data, as described in sections 6.3.3.1-6.3.3.3.

2. The second aspect considers the *computational effort*. The effort for calculating the expected idle time with the continuous idle time is the greatest, while the computational cost for the application of the other two idle time functions is very limited.

idle time	granularity	computational effort	pre-calculation possible
business area wide	low	low	yes
location-period specific	middle	low	yes
continuous	high	middle	no

Table 6.3: Properties of the three ITDP variants presented

3. The third aspect considers the *possibility for pre-calculation*. Whereas all values for the business area wide idle time and the location-period specific idle time have the advantage to be pre-calculable due to their small number in order to speed up the pricing process, the continuous idle time has to be calculated online.

6.4 Computational Studies

In this section, we evaluate the developed dynamic pricing approach for all three variants, meaning based on business area wide, location-period specific, and continuous idle times. These three variants are compared in a computational study to four benchmarks. Section 6.4.1 describes the setup of the study, including settings and parameters (Section 6.4.1.1) and considered pricing approaches (Section 6.4.1.2). Based on this, Section 6.4.2 presents and discusses the main results.

6.4.1 Setup

6.4.1.1 Settings and Parameters

We consider a SMS with origin-based pricing, that means the provider does not know the destination of the rental. For the computational study we investigate two *settings* that differ mainly in the size of the business area and the number of vehicles (SMALL and LARGE). The area of the SMALL setting has a size of 9 km² and is equipped with 18 vehicles (LARGE 16 km² and 32 vehicles, all areas are square). Theses settings are realistic settings in terms of vehicle density and distribution. They show that the solution approach is also applicable to larger settings. Remember that the customer's consideration set includes only those vehicles that are within walking distance of the customer, and their number depends on the vehicle density. As we use a realistic density in our examples, they also capture computational complexity of larger systems. Therefore, we can conclude that the solution approach is also applicable to large settings.

The planning horizon is one day and at the beginning, all vehicles are randomly uniformly distributed across the business area. The demand patterns we use replicate what is observed in practice. Demand intensity varies over the course of the day with two peaks (Figure 6.5, see e.g., Reiss and Bogenberger, 2016a). Furthermore, in line with practice, there is also a spatial variation of demand, i.e. between strong demand in the city center and lower demand in peripheral areas. Given a uniform price, this results in different mean idle times (illustrated for the so-called BASE price in Figure 6.6). Demand intensity is modeled by the probability density function (pdf) of the origin probability distribution $O(t)$.

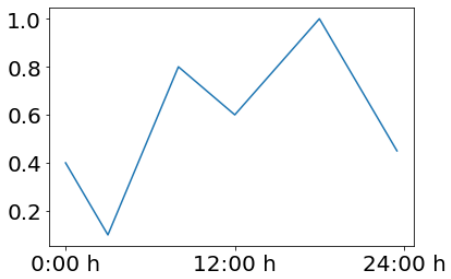

Figure 6.5: Normalized total demand over the course of the day for all settings

Each of the two settings is examined for three different overall demand levels, which differ in the *demand-supply ratio* (DSR). The DSR is the maximum demand (second peak) divided by

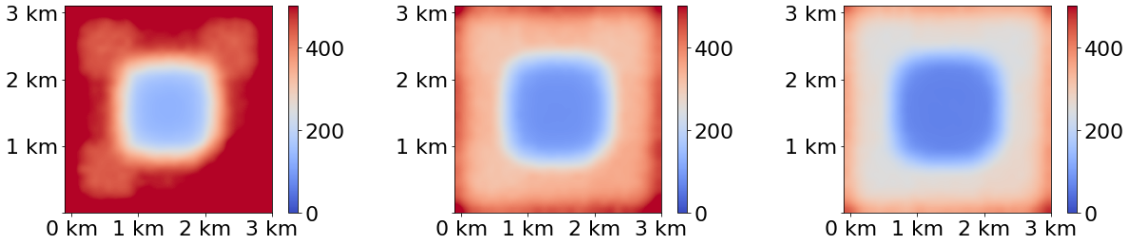

(a) DSR=1/3 (b) DSR=2/3 (c) DSR=1

Figure 6.6: Mean idle time for different DSR for 9 zones with BASE price

the fleet size and we consider the values $\frac{1}{3}, \frac{2}{3}, 1$ by scaling demand appropriately. This can also be seen in Figure 6.6, where as demand increases (increasing DSR), the idle time for all parts of the business area decreases, especially in the peripheral areas.

The other parameters are constant throughout both settings: $M = 3$ price points (prices for short) $p^m \in \mathcal{M}$ are predefined with regard to typical prices in practice: We chose a *base price* per minute of $p^{(2)} = 0.31\,€/\text{min}$ and a price difference of $0.05\,€/\text{min}$ to the so-called *low* and *high* prices, so that $p^{(1)} = 0.26\,€/\text{min}$ and $p^{(3)} = 0.36\,€/\text{min}$. Variable costs are $c = 0.07\,€/\text{min}$.

Further, we assume a maximum willingness to walk of $\bar{d} = 500\,\text{m}$ for all customers (see Herrmann et al., 2014).

The choice behavior follows a multinomial-logit model, where the choice probabilities depend on the utilities for the customer (see Appendix 6.A). A customer's utility $u_{i,t}(\vec{p}_t)$ for alternative (vehicle) i at time t depends on its price $p_{i,t}$ and the vehicle's distance d_i to the customer ($u_{i,t}(\vec{p}_t) = \beta^{price} \cdot p_{i,t} + \beta^{distance} \cdot d_i$). All vehicles are homogeneous, hence their features do not play a role in the choice model. The customer can also decide not to rent a vehicle ($i = 0$) and leave the system. The utility for this alternative is a constant ($u_{0,t}(\vec{p}_t) = ASC_0$). We assume for the computational studies that all customers have the same price sensitivity and choose according to the same choice parameters. The parameters for the one choice model which is fit across all locations can be estimated with a maximum-likelihood estimation based on observations of mobile application openings (for more details see Appendix 6.A). It is possible to generalize this to multi-segment pricing without major changes. The rental time is calculated by drawing the speed from a realistic distribution for urban traffic. We then get the rental/driving time $l_{i,t}$ as the product of the driving speed and the distance between the origin and the destination of the rental.

6.4.1.2 Pricing Approaches

In total, we evaluate seven (variants of) pricing approaches. The three variants of the developed pricing approach ITDP are:

- ITDP-B: A variant of ITDP which uses *business area wide idle time* data (see Section 6.3.3.1).
- ITDP-L: A variant of ITDP which uses *location-period specific idle time* data (see Section 6.3.3.2).
- ITDP-C: A variant of ITDP which uses *continuous idle time* data (see Section 6.3.3.3).

The four benchmarks are:

- B-BASE: Constant uniform pricing, where $p_{i,t}$ is the *base* price for all vehicles $i \in \mathcal{C}$ and every time t. Due to its wide adoption over all SMS types, this pricing can be considered as the de facto standard in practice.
- B-MYOP: *Myopic* version of ITDP without anticipation: $\tilde{\varphi}_{i,t,(x_i,t),y_{i,t}} = \tilde{\varphi}_{i,t,(x^D_{t'},y^D_{t'})} = \tilde{w}^{idle}_{i,t} = \tilde{w}^{dep}_{i,t} = 0$ for all $i \in \mathcal{C}_{t,(x^O_t,y^O_t)}$, resulting in $\tilde{W}_{i,t} = \tilde{W}_{0,t} = 0$ for all $i \in \mathcal{C}_{t,(x^O_t,y^O_t)}$.
- B-TAR: Pricing approach that compares a certain *target idle time* with the current idle time in the vicinity of the vehicle with a radius of the walking distance $\bar{d}$ (similar to the pricing approach of Neijmeijer et al. (2020)). If the current idle time in the vicinity of a vehicle falls below a threshold (i.e. a target idle time minus the parameter γ; we use $\gamma = 30$ min), this vehicle obtains the high price and vice versa. Vehicles with idle times in between both thresholds obtain the base price. The target idle time for this benchmark is the average idle time of period ϑ.
- B-REL: This approach adopts ideas from Wagner et al. (2015) and Brandt and Dlugosch (2021) who consider SMSs where customers reveal their destinations in advance. Their approach then searches for alternative, nearby destinations with lower idle time than the intended one and, if the difference exceeds a threshold, suggests alternative destinations together with incentives. Since we consider a different setting in which the intended destination is unkown, this approach is not directly applicable. However, we adopt the central idea of comparing the difference of idle times for different locations with a given threshold ω. More specifically, we compare the idle time at the rental's origin with the idle time of the whole business area. For this purpose, the business area is divided into 200m×200m tiles. The idle time for a vehicle is calculated in two steps. First, the tile where a vehicle is located and its vicinity is identified (radius of $\bar{d}$ around the center of the tile). The second step begins with calculating the idle time for the current time t, for the time 1 h later as well as 1 h earlier using Kernel regression where the spatial difference to the center of the tile is not bigger than $\bar{d}$. Then, it computes the average of these three idle times. Next, we also need the idle time of the destination. Since the destination is not known, we substitute it with the mean idle time of the whole business area for the three above-mentioned points in time and then compute their average. We compare the difference between these two values with a predefined threshold ω. If this difference is larger than the threshold ($\omega = 30$ min in our study), the vehicles in this tile get high prices and vice versa. All vehicles standing in tiles with smaller deviations get the base price.

Each pricing approach is evaluated in $N = 1000$ simulation runs with common random numbers and we report average values.

6.4.2 Main Results

In this section, we focus on the results for the two different settings (SMALL, LARGE) for the different DSRs. We compare ITDP for different granularities of idle time (ITDP-B, ITDP-L, ITDP-C). In the following subsections, we look at profit, prices and rentals.

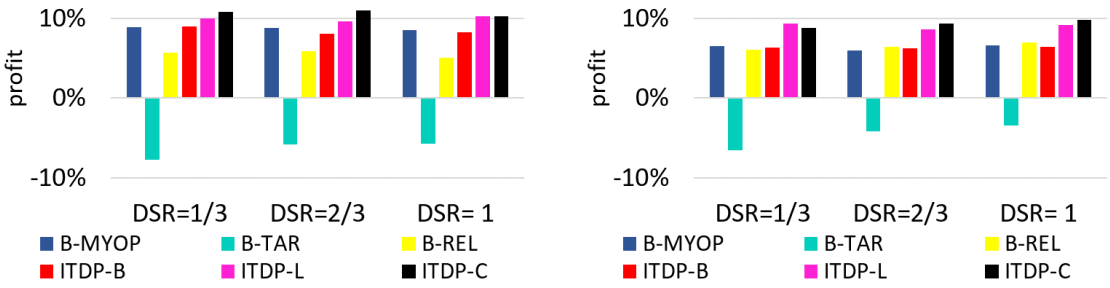

(a) SMALL (b) LARGE

Figure 6.7: Profit improvement over B-BASE

6.4.2.1 Profit

We first discuss profit, whose maximization is the objective of the optimization problem and obviously the most important metric from the provider's perspective. The results for all settings and DSRs are summarized in Figure 6.7. First of all, all results show that for all settings and all DSRs the approach B-TAR is inappropriate, since it consistently generates less profit than B-BASE. At least in this implementation, the goal to have an identical idle time everywhere is not profit maximizing.

The benchmark B-REL performs similarly to the benchmark B-MYOP in the LARGE setting, whereas it performs worse than B-MYOP in the SMALL setting.

Regarding the new idle-time based approaches, the following can be observed: The more detailed the idle time is taken into account, the more profit is generated. While considering the business area idle time leads to a comparable profit to the benchmark B-MYOP, using the continuous idle time leads to the best result in most cases. ITDP-L is in between and better than B-REL and B-MYOP.

Thus, if temporally and spatially differentiated idle time data is available (ITDP-C, ITDP-L) and used for dynamic pricing, a corresponding approach can perform better than myopic pricing.

Finally, the fact that ITDP-B performs similarly to the benchmark B-MYOP can be explained as follows. ITDP-B uses generic idle time data, and thus, the pricing approach is minimally anticipative by incorporating always the same opportunity costs (see Section 6.3.3.1).

In the following subsections (Section 6.4.2.2 - Section 6.4.2.3), we consider the results for SMALL. The corresponding results for LARGE are shown in Appendix 6.B.

6.4.2.2 Prices

Next, we compare the prices set by the different pricing approaches over the course of the day. To that end, we consider results from the SMALL setting with all three DSRs. Figure 6.9 illustrates the average price across all areas during the day (we left out B-BASE that sets constant prices). The demand peak at noon is reflected in the average price of all pricing approaches. As expected, prices are on average higher when demand is high.

A closer look shows that the average price of B-TAR is almost always considerably below all other price curves, which may explain its poor performance. Furthermore, it is remarkable that

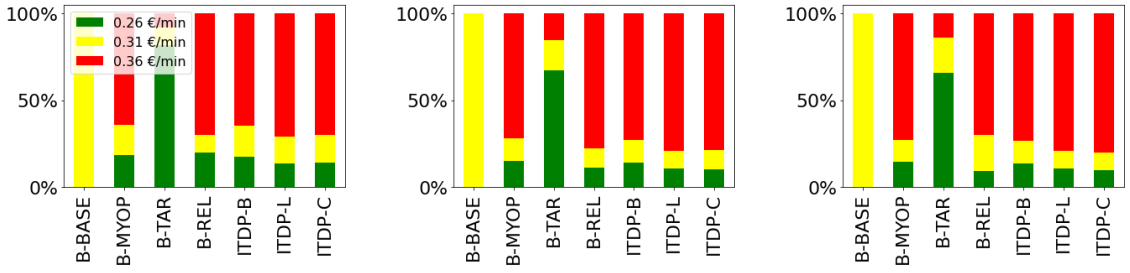

(a) DSR=1/3 (b) DSR=2/3 (c) DSR=1

Figure 6.8: Relative price frequency (SMALL)

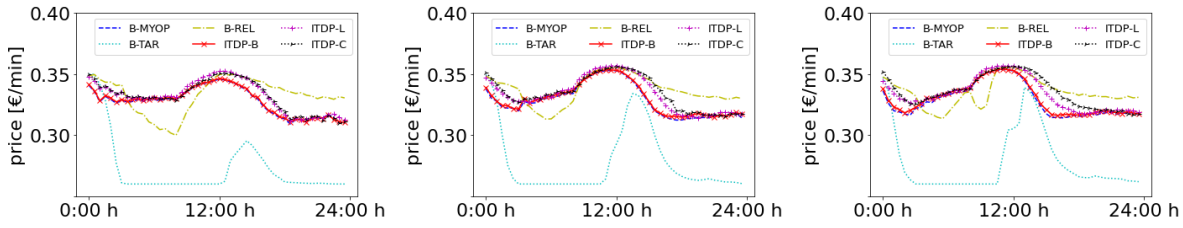

(a) DSR=1/3 (b) DSR=2/3 (c) DSR=1

Figure 6.9: Average prices over the course of the day (SMALL)

the average price of B-REL fluctuates more than the other curves (except B-TAR). Another interesting observation is that the average price of B-MYOP (and in the morning also B-REL) is clearly lower than the average price of ITDP-L and ITDP-C. Obviously, anticipation with spatial and temporal granularity of the idle time data leads to higher prices. The average price of ITDP-B is clearly lower than the average price of ITDP-C and ITDP-L and comparable to the average price of B-MYOP.

The aforementioned average prices are also reflected in the relative price frequency (Figure 6.8). While the frequency of low prices is highest for B-TAR, and then B-MYOP, this price frequency (with increasing spatial and temporal granularity of the idle time data used) decreases successively from ITDP-B via ITDP-L to ITDP-C, while the frequency of high prices for these dynamic pricing approaches increases successively.

6.4.2.3 Rentals

Rentals are another important metric for SMS providers, as higher rentals have a positive impact on service level metrics. For the analysis of the rentals, we consider Figure 6.10, which shows the average hourly rentals for the different pricing approaches over the course of the day for different DSRs in the SMALL setting. The respective results for LARGE are depicted in Appendix 6.B.

The rental curves resemble the demand curve in that there is a minimum of rentals in the morning and a maximum in the afternoon. As expected, the number of rentals increases in the DSR and the number of rentals is lowest (highest) for only high prices (only low prices). The rental curve for B-MYOP is very similar to the rental curve for ITDP-C, although ITDP-C obtains considerably higher profits. Furthermore, the curve of rentals of B-TAR is, together with the curve for the pricing with only low prices, clearly above all other curves.

Please note that the fact that ITDP-L and ITDP-C obtain a higher revenue than B-BASE with a comparable number of rentals proves that their profit increase is not associated with a

worse availability. Finally, the idea behind B-TAR to ensure a good level of service seems to be successful, but at the cost of lower profit. Considerably more trips are made with this pricing approach than with any other pricing approach (except the provider sets only low prices).

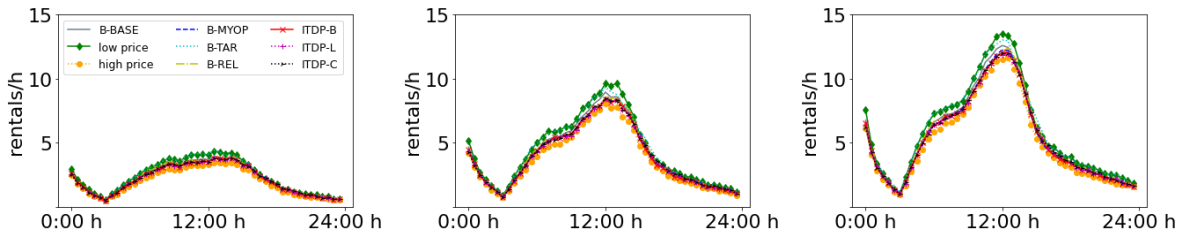

(a) DSR=1/3 (b) DSR=2/3 (c) DSR=1

Figure 6.10: Rentals over the course of the day (SMALL)

6.5 Conclusion

Dynamic pricing has been shown to be an efficient means to manage SMSs and first approaches in which pricing is designed around idle time data have been proposed. In principle, the idea of using idle times within pricing is very promising, because this data is often available to providers in practice. However, so far, only hands-on business rules using idle times have been suggested. In this work, we close this important literature gap by developing an anticipative optimization-based dynamic pricing approach which is based on the integration of idle times. This allows to exploit the full potential of idle time data in dynamic pricing for SMSs.

The specific pricing problem considered is to determine profit-maximizing prices for the vehicles which are located within reach of an arriving customer in an online fashion. Thereby, the developed pricing approach captures a myopic as well as an anticipative part of the expected future profit. While the first considers the potentially upcoming rental, the second approximates the future state values based on idle time data. For both parts, customer choice probabilities are considered through a multinomial-logit model which captures the influence of prices and walking distances. The approach is generic with regard to the state-value approximation because it allows to integrate idle time data independent of the data's granularity in both the spatial and the temporal dimension. More specifically, the approach is capable of integrating business area wide idle times on the one extreme over location-period specific to continuous idle time data on the other extreme. Technically speaking, the latter is enabled by using a non-parametric value function approximation in which a kernel regression calculates the valuation from multiple individual data points.

In an extensive computational study with varying size of business area, fleet size, as well as overall demand levels, we demonstrate the advantages of our dynamic pricing approach compared to various benchmarks. These benchmarks include two idle-time based pricing rules from the literature as well as a myopic price optimization. The results show that the performance of the developed dynamic pricing approach depends on the granularity of the integrated idle time data. It consistently outperforms the reference value of constant uniform base prices and the rule-based approach with target idle times. For the variants of the developed approach with spatio-temporal variation of the idle times, in most cases, substantially higher profits are generated than for the myopic optimization as well as for the rule-based approach from literature that determines prices based on the comparison of idle times.

The idle-time based dynamic pricing approach with continuous idle time outperforms all benchmarks considerably. It improves profits by up to 11 % compared to base pricing, as well as up to 3 percentage points compared to myopic price optimization. From the latter, we conclude that the accurate approximation of state values based on highly granular idle times in our pricing approach is beneficial for its performance. Compared to the rule-based benchmarks from the literature, this variant of our approach obtains up to 3.5 percentage points more profit.

To summarize, our anticipative and optimization-based dynamic pricing approach based on idle time data performs considerably better in comparison to existing approaches in terms of the relevant performance metrics. This shows that the developed approach based on idle times, which are often available for SMSs, is a practice-ready and at the same time successful alternative for dynamic pricing in SMSs.

For future work, multiple directions seem promising to generate additional valuable insights. First, an empirical real-world evaluation of the suggested dynamic pricing approach would be helpful to support the numerical studies. Second, a new rule-based approach based on the insights gained could be developed. Third, the development of a combined dynamic pricing and relocation optimization approach based on idle times would be valuable as this could exploit additional potential. Finally, to investigate the value of additional information (destination known), the use of ITDP could be compared for trip-based and origin-based SMSs.

6.A Customer Choice Model

A customer at position (x_t^O, y_t^O) chooses among the reachable vehicles $i \in \mathcal{C}_{t,(x_t^O,y_t^O)}$ and may also decide not to rent (no choice option). In the Computational Studies (Section 3.4), customer choice behavior follows a multinomial logit model (see e.g. Train , 2009, Chapter 3). Accordingly, the choice probabilities $q_{i,t}(\vec{p}_t)$ depend on the alternatives' deterministic utilities $u_{i,t}(\vec{p}_t)$ for the customer:

$$q_{i,t}(\vec{p}_t) = \frac{e^{u_{i,t}(\vec{p}_t)}}{\sum_{n \in \mathcal{C}_{t,(x_t^O,y_t^O)} \cup \{0\}} e^{u_{n,t}(\vec{p}_t)}}. \tag{6.22}$$

The deterministic utility $u_{i,t}(\vec{p}_t)$ of a vehicle i at time t depends on its price $p_{i,t}$ and its distance to the customer d_i:

$$u_{i,t}(\vec{p}_t) = \beta^{price} \cdot p_{i,t} + \beta^{distance} \cdot d_i. \tag{6.23}$$

The no-choice option has utility $u_{0,t}(\vec{p}_t) = ASC^{NoChoice}$ where $ASC^{NoChoice}$ stands for the alternative-specific constant for the no-choice option. These assumptions imply homogeneous customers and that customers decide solely based on current circumstances (myopic behavior). In particular, they do not act strategically (see, e.g., Gönsch et al., 2013; Gallego and Van Ryzin, 1997; Talluri and Van Ryzin, 2004, Chapter 5.1.4 for discussions of strategic or forward looking customers.).

The choice model is fitted across all locations by using maximum likelihood estimation based on 200,000 observations of mobile application openings. Technically, we used the Python package PandasBiogeme 3.2.10 (Bierlaire, 2020).

6.B Results LARGE

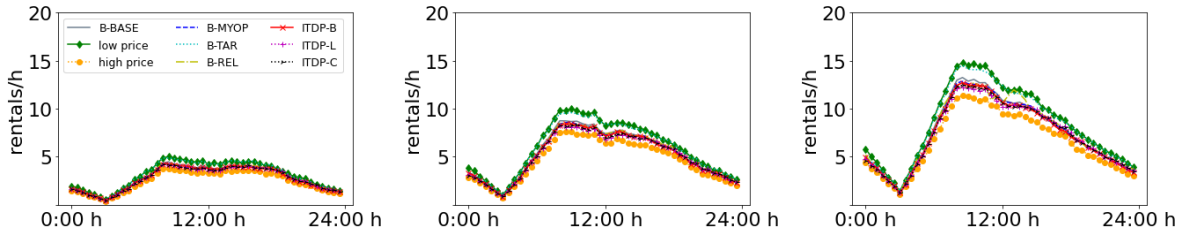

(a) DSR=1/3 (b) DSR=2/3 (c) DSR=1

Figure 6.11: Rentals over the course of the day (LARGE)

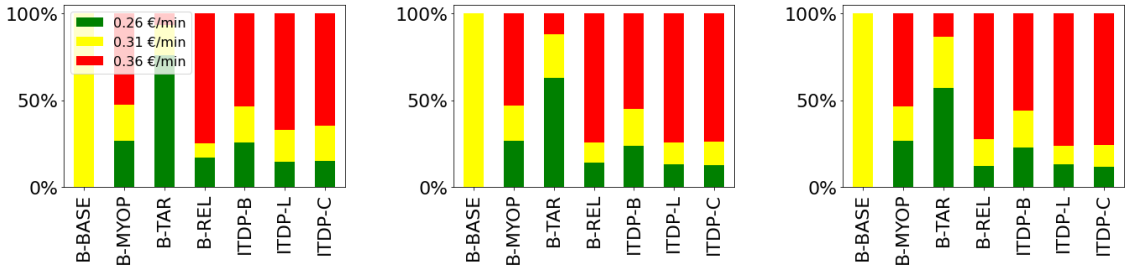

(a) DSR=1/3 (b) DSR=2/3 (c) DSR=1

Figure 6.12: Relative price frequency (LARGE)

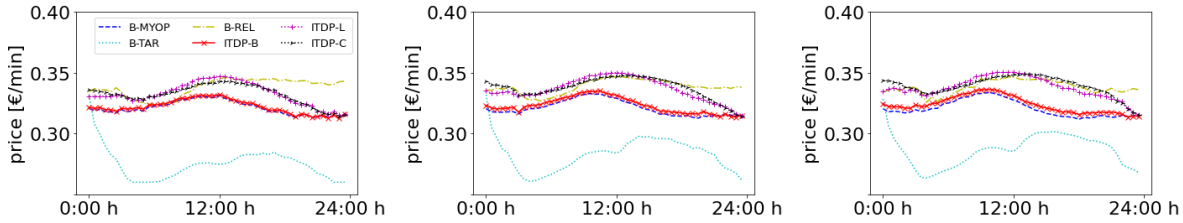

(a) DSR=1/3 (b) DSR=2/3 (c) DSR=1

Figure 6.13: Average prices over the course of the day (LARGE)

6.C List of Notation

sets	
symbol	description
$\mathcal{C}_{t,(x_t^O,y_t^O)}$	consideration set of a customer arriving at time t with the coordinates (x_t^O, y_t^O)
$\mathcal{K}$	historical vehicle data, contains a data point k for each end of a rental
$\mathcal{K}_{i,t}^{idle}$	relevant data points regarding idle vehicles that are similar to vehicle i at time t
$\mathcal{K}_{i,t'}^{dep,x}$	relevant data points regarding departed vehicles that are similar to vehicle i at time t', $x \in \{dk, du\}$ (dk: destination known, du: destination unknown)
$\mathcal{M}$	discrete set of price points
$\mathcal{T}$	time horizon
$\mathcal{X}$	set of all possible x-coordinates
$\mathcal{Y}$	set of all possible y-coordinates
$\mathcal{Z}$	set of locations
Θ	set of periods

Table 6.4: List of notation – part 1

parameters, variables and functions	
symbol	description
c	variable costs
$\bar{d}$	(fixed) maximum willingness to walk
d_i	distance between customer standing at coordinates (x_t^O, y_t^O) and vehicle i
$d_{i,k}$	distance between vehicle i and data point k
$K_{i,t,k}^x$	Epanechnikov kernel function for vehicle i and data point k at time t (or time $t\prime$), $x \in \{idle, dep\}$
$L_{i,t}$	random variable of rental time
$l_{i,t}$	driving/rental time in minutes, realization of $L_{i,t}$
$O(t)$	time-dependent origin probability for the location of the customer
$\vec{p}_t$	price vector
$p_{i,t}$	price for vehicle i at time t
$q_{i,t}(\vec{p}_t)$	choice probability
$q_{0,t}(\vec{p}_t)$	no choice probability
R	average profit after idle time per minute
t	time
t'	point of time after expected idle time $t' = t + \mathbb{E}_{L_t \sim \rho_t}(L_{i,t})$
t^{total}	latest time of considered time horizon
$u_{i,t}(\vec{p}_t)$	utility for choosing vehicle i at time t
$u_{0,t}(\vec{p}_t)$	utility for no-choice at time t
$\tilde{w}_{i,t}^{idle}$	expected future profit of vehicle i at time t if it remains idle
$\tilde{w}_{i,t'}^{dep}$	expected future profit of vehicle i at time t after the current customers's rental
x	coordinate from west to east
x_{max}	easternmost coordinate
$(x_{i,t}, y_{i,t})$	position of a vehicle i at time t
(x_t^O, y_t^O)	customer locations at time t
$(x_{i,t'}^D, y_{i,t'}^D)$	drop-off location of vehicle i at time t'
y	coordinate from south to north
y_{max}	northernmost coordinate
z	location
Z	number of locations
β^{price}	parameter for evaluating price
$\beta^{distance}$	parameter for evaluating distance
ϑ	period
θ	number of periods
$\kappa_{i,t,k}^{idle}, \kappa_{i,t\prime,k}^{dep,du}, \kappa_{i,t',k}^{dep,dk}$	weights of every data point k to value vehicle i at time t (or time $t\prime$)
λ_t	arrival rate of customers at time t
$\tau_{i,t}$	starting time of rental i
$\tilde{\varphi}_{i,t,(xi,t,y_{i,t})}$	idle time of vehicle i at time t at the current location $(x_{i,t}, y_{i,t})$
$\tilde{\varphi}_{i,t',(x_{i,t'}^D, y_{i,t'}^D)}$	idle time of vehicle i at time t' at the destination $(x_{i,t'}^D, y_{i,t'}^D)$
ρ_t	distribution of rental time

Table 6.5: List of notation – part 2

Bibliography

Agatz N, Campbell AM, Fleischmann M, Van Nunen J, Savelsbergh M (2013) Revenue management opportunities for internet retailers. J. Revenue Pricing Manag. 12(2):128–138

Angelopoulos A, Gavalas D, Konstantopoulos C, Kypriadis D, Pantziou G (2016) Incentivization schemes for vehicle allocation in one-way vehicle sharing systems. 2016 IEEE Internat. Smart Cities Conf. (ISC2) 1–7

Angelopoulos A, Gavalas D, Konstantopoulos C, Kypriadis D, Pantziou G (2018) Incentivized vehicle relocation in vehicle sharing systems. Transp. Res. Part C: Emerg. Technol. 97:175–193

Barth M, Todd M, Xue L (2004) User-based vehicle relocation techniques for multiple-station shared-use vehicle systems. Transp. Res. Board 80th Annual Meeting

Bianchessi AG, Formentin S, Savaresi SM (2013) Active fleet balancing in vehicle sharing systems via feedback dynamic pricing. IEEE Internat. Conf. Intell. Transp. Syst. 1619–1624

Bierlaire MA (2020) A short introduction to PandasBiogeme. Technical Report, Transport and Mobility Laboratory, École Polytechnique Fédérale de Lausanne, Lausanne, Switzerland.

Brandt T, Dlugosch O (2021) Exploratory data science for discovery and ex-ante assessment of operational policies: Insights from vehicle sharing. J. Oper. Man. 67(3):307–328

Brendel AB, Brauer B, Hildebrandt B (2016) Toward user-based relocation information systems in station-based one-way car sharing. AMCIS Proc. 1–10

Chemla D, Meunier F, Pradeau T, Calvo RW, Yahiaoui H (2013) Self-service bike sharing systems: Simulation, repositioning, pricing, Working paper, CERMICS - Centre d'Enseignement et de Recherche en Mathématiques et Calcul Scientifique, France.

Clemente M, Fanti MP, Iacobellis G, Nolich M, Ukovich W (2017) A decision support system for user-based vehicle relocation in car sharing systems. IEEE Trans. Syst., Man, and Cybernetics: Syst. 48(8):1283–1296

DeMaio P (2009) Bike-sharing: History, impacts, models of provision, and future. J. Public. Trans. 12(4):3

Dötterl J, Bruns R, Dunkel J, Ossowski S (2017) Towards dynamic rebalancing of bike sharing systems: An event-driven agents approach. EPIA Conf. Artificial Intell. 309–320

Febbraro AD, Sacco N, Saeednia M (2012) One-way carsharing: Solving the relocation problem. Transp. Res. Record 2319(1):113–120

Febbraro AD, Sacco N, Saeednia M (2019) One-way car-sharing profit maximization by means of user-based vehicle relocation. IEEE Trans. Intell. Transp. Syst. 20(2):628–641

Ferrero F, Perboli G, Vesco A, Caiati V, Gobbato L (2015a) Car-sharing services–part a taxonomy and annotated review. Working paper, Istituto Superiore Mario Boella, Turin, Italy.

Ferrero F, Perboli G, Vesco A, Musso S, Pacifici A (2015b) Car-sharing services–part b business and service models. Working paper, Istituto Superiore Mario Boella, Turin, Italy.

Fishman E, Washington S, Haworth N (2013) Bike share: A synthesis of the literature. Transp. Rev. 33(2):148–165

Gallego G, Van Ryzin G (1997) A multiproduct dynamic pricing problem and its applications to network yield management. Oper. Res. 45(1):24–41.

Gönsch J, Klein R, Neugebauer M, Steinhardt C (2013) Dynamic pricing with strategic customers. J. Bus. Econ. 83(5):505–549.

Göppel M, Blumenstock A (2012) Automatisierte Servicedisposition zur Flotteninstandhaltung am Beispiel car2go. Automatisierungstechnik 60(2):102–112

Haider Z, Nikolaev A, Kang JE, Kwon C (2018) Inventory rebalancing through pricing in public bike sharing systems. Eur. J. Oper. Res. 270(1):103 – 117

Herrmann S, Schulte F, Voß S (2014) Increasing acceptance of free-floating car sharing systems using smart relocation strategies: A survey based study of car2go Hamburg. Internat. Conf. Comp. Log. 151–162

Illgen S, Höck M (2019) Literature review of the vehicle relocation problem in one-way car sharing networks. Transp. Res. Part B: Methodol. 120:193–204

Jorge D, Correia G (2013) Carsharing systems demand estimation and defined operations: A literature review. Eur. J. Transp. Infrastruct. Res. 13(3)

Kamatani T, Nakata Y, Arai S (2019) Dynamic pricing method to maximize utilization of one-way car sharing service. IEEE Internat. Conf. Agents (ICA) 65–68

Laporte G, Meunier F, Calvo RW (2015) Shared mobility systems. 4OR 13(4):341–360

Laporte G, Meunier F, Calvo RW (2018) Shared mobility systems: An updated survey. Ann. Oper. Res. 271(1):105–126

Lippoldt K, Niels T, Bogenberger K (2018) Effectiveness of different incentive models in free-floating carsharing systems: A case study in milan. IEEE Intell. Transp. Syst. Conf. (ITSC) 1179–1185

Mareček J, Shorten R, Yu JY (2016) Pricing vehicle sharing with proximity information. 2016 3rd MEC Internat. Conf. Big Data and Smart City (ICBDSC) 1–7

Mooney SJ, Hosford K, Howe B, Yan A, Winters M, Bassok A, Hirsch J A (2019) Freedom from the station: Spatial equity in access to dockless bike share. J. Transp. Geog. 74:91–96

Müller C, Gönsch J, Soppert M, Steinhardt C (2021) Customer-centric dynamic pricing for free-floating shared mobility systems. Working paper, Mercator School of Management, University of Duisburg-Essen, Duisburg, Germany.

Neijmeijer N, Schulte F, Tierney K, Polinder H, Negenborn, R (2020) Dynamic pricing for user-based rebalancing in free-floating vehicle sharing: A real-world case. Internat. Conf. Comput. Logist. 443–456

Pfrommer J, Warrington J, Schildbach G, Morari M (2014) Dynamic vehicle redistribution and online price incentives in shared mobility systems. IEEE Trans. Intell. Transp. Syst. 15(4):1567–1578

Powell WB (2007) Approximate Dynamic Programming: Solving the curses of dimensionality, 2. ed. John Wiley & Sons

Reiss S, Bogenberger K (2015) GPS-data analysis of Munich's free-floating bike sharing system and application of an operator-based relocation strategy. IEEE Intell. Transp. Syst. Conf. (ITSC) 584–589

Reiss S, Bogenberger K (2016a) Optimal bike fleet management by smart relocation methods: Combining an operator-based with an user-based relocation strategy. IEEE Intell. Transp. Syst. Conf. (ITSC) 2613–2618

Reiss S, Bogenberger K (2016b) Validation of a relocation strategy for Munich's bike sharing system. Transp. Res. Proc. 9:341–349

Ricci M (2015) Bike sharing: A review of evidence on impacts and processes of implementation and operation. Res. Transp. Bus. Manag. 15:28–38

Ruch C, Warrington J, Morari M (2014) Rule-based price control for bike sharing systems. 2014 Eur. Control Conf. (ECC) 708–713

Singla A, Santoni M, Bartók G, Mukerji P, Meenen M, Krause A (2015) Incentivizing users for balancing bike sharing systems. Proc. Twenty-Ninth AAAI Conf. Artificial Intell. Pattern 23–729

Soppert M, Steinhardt C, Müller C, Gönsch J (2022) Differentiated pricing of shared mobility systems considering network effects. Transp. Sc. 45(5):1279-1303.

Statista (2021) Number of registered car sharing users in Germany from 2011 to 2021 (in million). https://de.statista.com/statistik/daten/studie/324692/umfrage/carsharing-nutzer-in-deutschland/

Talluri KT, Van Ryzin G (2004) The theory and practice of revenue management, 1st ed. Springer, Boston, MA

Train K (2009) Discrete choice methods with simulation, 2nd ed. Cambridge University Press, Cambridge, UK

Wagner S, Willing C, Brandt T, Neumann, D (2015) Data analytics for location-based services: Enabling user-based relocation of carsharing vehicles. Proc. Internat. Conf. Inf. Syst. (ICIS) 3:279–287

Wang L, Ma W (2019) Pricing approach to balance demands for one-way car-sharing systems. 2019 IEEE Intell. Transp. Syst. Conf. (ITSC) 1697–1702

Weikl S, Bogenberger K (2015) Integrated relocation model for free-floating carsharing systems: Field trial results. Transp. Res. Rec. 2563(1):19–27

Wu C, Le Vine S, Sivakumar A, Polak J (2021) Dynamic pricing of free-floating carsharing networks with sensitivity to travellers' attitudes towards risk. Transp. 49(2): 1–24

Xie XF, Wang ZJ (2018) Examining travel patterns and characteristics in a bikesharing network and implications for data-driven decision supports: Case study in the Washington DC area. J. Transp. Geog. 71:84–102

Zhang J, Meng M, David Z (2019) A dynamic pricing scheme with negative prices in dockless bike sharing systems. Transp. Res. Part B: Methodol. 127:201–224

Chapter 7

Conclusion

This chapter provides an overview of the proposed pricing approaches and results of each chapter and shows the similarities as well as the differences between them. More detailed conclusions can be found in Chapters 2.8, 3.6, 4.6, 5.7 and 6.5.

In Chapter 1 we introduced different forms and planning levels of decision problems of shared mobility systems (SMSs), as well as different modeling techniques for developing solution approaches for differentiated and dynamic pricing. Differentiated pricing in SMSs describes pricing approaches where the demand is assumed to be deterministic, and the prices are set in advance for the considered time horizon. In contrast, dynamic pricing in SMSs describe pricing approaches where the demand is assumed to be stochastic. Thus, the prices are set dependent on the current state of the system. In this thesis, Chapters 2 to 4 deal with differentiated pricing, whereas Chapters 5 and 6 deal with dynamic pricing.

In Chapter 2, we defined and analyzed the problem of origin-based differentiated pricing for SMSs. The paper has addressed the problem of determining spatially and temporally differentiated origin-based minute prices to maximize profit. For this, we proposed a mixed-integer linear program based on a fluid formulation. This linear program incorporates supply-side network effects and was proven to be NP-hard. Thus, we proposed a solution approach that combines the benefits of decomposition on the one hand, and value function approximation from the realm of approximate dynamic programming on the other hand. This solution approach scales to real-life scenarios and integrates the supply-side network effects successfully.

Compared to the de facto standard of constant uniform prices and myopic pricing (no consideration of network effects), this solution approach shows considerable improvements in profit. Furthermore, we have shown that our solution approach can take into account the decreasing marginal value of vehicles, considering both short- and long-term supply side network effects. Thus, this solution approach provides a scalable means to successfully integrate these effects.

However, the solution approach using value function approximation requires parameter estimations in advance, which estimates the parameters for the piece-wise linear function of profit in dependency of the number of available vehicles. This estimation has two general components:

- Generating samples of vehicles' distribution and calculating a corresponding profit-to-come for every sample.
- Determining the value function parameters by solving the least square problem.

This process should not be underestimated in terms of computational time, e.g. the preprocessing of parameter estimation for the Florence case study in Chapter 2 takes about 19 hours. Therefore, we have developed two practicable solution methods that do not require pre-processing for estimating parameters in the next chapter. This saves the additional computational time required for preliminary parameter estimation.

More precisely, in Chapter 3, we proposed two different solution approaches for the problem of origin-based differentiated pricing for SMSs, which maximize the profit by setting spatially and

temporarily differentiated origin-based minute prices. The first solution approach is a simplified mathematical model and formulated as a fluid approximation (simplified model). The second solution approach is a backwards algorithm which can be divided into two steps. In the first step, we computed the vehicle distribution for every period with an appropriate straightforward solution approach. For this, we tested two different approaches: a myopic solution approach and a relaxed solution approach. In the second step, we calculated the prices backwards based on the previously calculated vehicle distributions.

These different proposed pricing approaches can be used for profit maximization in SMSs by considering supply-side network effects with clearly shorter computational times than the given benchmarks (e.g. approximate dynamic programming decomposition approach in Chapter 2). Furthermore, they do not require a pre-processing for estimating parameters in advance, are straightforward to apply and equal in profit than more complex benchmarks (e.g. approximate dynamic programming decomposition approach in Chapter 2). In other words, the practicable solution approaches provide the same results in the computational study as the value-function approximation solution approach described in the previous chapter, but without having to estimate the parameters in pre-processing.

Chapters 2 and 3 do not make a clear methodological distinction between free-floating and station-based SMSs. However, the type of SMS (station-based vs. free-floating) has clear consequences for the matching of supply and demand. For station-based SMSs, rentals correspond to almost the minimum of supply and demand, i.e. they match almost exactly the minimum of both. In contrast, for free-floating SMSs, the rentals, and thus, the matching of supply and demand also depends on other factors, such as zone size or maximum walking distance. In the next chapter, we therefore focused on how the rentals relate to the matching of supply and demand in station-based and free-floating SMSs.

In Chapter 4 we examined the modeling of rentals as the matching of supply and demand in free-floating and station-based SMSs. So far, matching functions for SMSs in optimization models for station-based and free-floating SMSs have been identical. However, we proposed matching functions considering central influencing factors specifically relevant for free-floating SMSs. Thus, this chapter built a bridge between the optimization models for station-based and those for free-floating SMSs, which allows to adapt optimization models designed for station-based to free-floating SMSs. We derived three matching functions: degressive, constant, and infinite coverage rate matching functions, where the latter is state-of-the-art and the degressive and constant coverage rate matching functions are novel.

While infinite coverage rate matching functions consider only available vehicles and demand, degressive and constant coverage rate matching functions consider additional relevant parameters, such as zone size, customers' maximum willingness to walk, successively arriving customers, and decreasing marginal zone coverage due to additional vehicles. Therefore, only the degressive and constant coverage rate matching functions are suitable for modeling free-floating SMSs in general, because they do consider all of these important parameters explicitly or implicitly. In contrast, the infinite coverage rate matching function neglects these additional parameters.

The numerical results show that the infinite coverage rate matching function, in general, overestimates rentals in free-floating SMSs. With the constant and degressive coverage rate matching functions, the rentals prediction is a lot more accurate. Thus, generally, the infinite coverage rate matching function cannot accurately describe matching in a free-floating SMS. Since other free-floating SMS optimization problems, such as relocation or fleet sizing, also rely on accurate rental predictions, they would be affected by an overestimation of rentals as well.

The constant coverage rate matching function, in contrast to the degressive coverage rate matching function, can easily be losslessly linearized. This allows the adaptation of many existing optimization approaches to free-floating SMSs.

In the case study we used this linearization of the constant coverage rate matching function. The numerical results show that the better pricing decisions with the (linearized) constant coverage rate matching function cause significant contribution margin gains in contrast to the pricing decisions with the infinite coverage rate matching function, which determines too high prices due to the overestimation of rentals. Thus, the more accurate matching modeling of the constant coverage rate also effects the decision making in a way that benefits the overall objective.

In Chapters 2 to 4, we assumed that demand is deterministic, so that we could calculate prices in advance. In the following chapters, we assumed that demand is stochastic and not deterministic, so that the future states of SMSs cannot be accurately predicted. For this situation, dynamic pricing is useful. Furthermore, we again considered a free-floating SMS. This means that the vehicles are distributed over the business area, not grouped at stations, and the customer has to walk different distances to reach the vehicles. Therefore, we also considered the disaggregated demand, taking into account individual walking distances and vehicle prices.

In modern free-floating vehicle sharing systems[1], providers have access to disaggregate real-time data regarding the locations of vehicles as well as of customers who open the mobile application to look for available vehicles. In Chapter 5, we demonstrated that this information can be leveraged in dynamic pricing to increase profitability. The *anticipative customer-centric* dynamic pricing approach in vehicle sharing systems takes customers' location as well as their behavior regarding walking distances and prices explicitly into consideration. Thus, vehicles can have different prices for customers who are requesting the price information at the same time but from different locations.

We formally defined the provider's online pricing problem as a Markov decision process and formulated the corresponding dynamic program by stating the corresponding Bellman equation. However, the dynamic program cannot be solved to optimality by classical backwards recursion due to the curse of dimensionality. To solve the online pricing problem, we developed a solution method based on approximate dynamic programming. We approximated state values representing expected future profits that occur *after* the current customer's decision, so that the current customer's choice behavior can still be considered explicitly with a disaggregated choice model in the optimization – in our case by a multinomial logit model. We take the assumption that state values are additive in the vehicle values which represent the profits that individual vehicles

[1] synonymous with SMS

are expected to realize until the end of the considered time horizon. To approximate the vehicle values, we proposed a non-parametric value function approximation, which uses historical vehicle values.

In a computational study we demonstrated the advantages of our dynamic pricing approach compared to various benchmarks. The new pricing approach outperforms all benchmarks significantly. Further, the numerical study demonstrated the advantage of integrating the concept of customer-centricity in dynamic pricing. That is, considering situation-specific customer information, like the position of the customer and distance to the vehicles within walking distance, yields up to clearly more profit. In a sensitivity analysis, we also showed that our results are robust regarding the decisive parameters of the customer choice behavior. An analysis of spatial and temporal variations in demand showed that spatial variation, in contrast to temporal variation, has a stronger effect on the importance of anticipation. For a vehicle sharing system provider this means that if there are already small spatial differences in demand, it is worthwhile to anticipate the future state.

The method of anticipative dynamic pricing as it was used in Chapter 5 requires an approximation of future states. More precisely, they were calculated using historical vehicle values. For this, the provider must have detailed data of each vehicle's departure and arrival times. Conversely, other options require less detailed data to approximate future states, e.g. using idle time data.

Against this background, we developed an anticipative optimization-based dynamic pricing approach which is based on the integration of idle times in Chapter 6. This allows to exploit the full potential of idle time data in dynamic pricing for SMSs.

The developed dynamic pricing approach captures a myopic as well as an anticipative part of the expected future profit. While the myopic part considers the potentially upcoming rental, the anticipative part approximates the future state values based on idle time data. For both parts, customer choice probabilities were considered through a multinomial logit model which captures the influence of prices and walking distances.

The approach is generic with regard to the state-value approximation because it allows to integrate idle time data independent of the data's granularity in both the spatial and the temporal dimension.

In a computational study we demonstrated the advantages of our dynamic pricing approach compared to various benchmarks (two idle time based pricing rules from the literature and a myopic price optimization). The results showed that the performance of the developed dynamic pricing approach depends on the granularity of the integrated idle time data. It consistently outperforms the reference value of constant uniform base prices. For the variants of the developed approach with spatio-temporal variation of the idle times, in most cases, substantially higher profits were generated than for the myopic optimization as well as for the rule-based approach from the literature that determines prices based on the comparison of idle times. Furthermore, we conclude that the accurate approximation of state values based on highly granular idle times in our pricing approach is beneficial for its performance.

To summarize, we developed different pricing approaches for differentiated and dynamic pricing for SMSs. We made the following main observations regarding differentiated pricing.

- For any differentiated pricing approach, it is beneficial to consider supply-side network effects.
- Different types of SMSs (station-based vs. free-floating) require different matching functions to calculate rentals realistically. More precisely, besides available vehicles and demand, matching functions for free-floating SMSs should additionally consider relevant parameters, such as zone size, customers' maximum willingness to walk, successively arriving customers, and decreasing marginal zone coverage due to additional vehicles.

Our main observations for dynamic pricing are the following.

- Explicitly taking into account disaggregated information about each customer's location and behavior in terms of walking distances and vehicle prices increases profits.
- It is useful to approximate the future state of the SMS with vehicle values for the customer's considered vehicles. Vehicle values are calculated based on historical data.
- Vehicle values can also be calculated on the basis of idle times, independent of the data's granularity in both the spatial and the temporal dimension.

For future research, different types of vehicles in SMSs could be considered, e.g. electric vs. conventional vehicles. Namely, in SMSs with electric vehicles, the capacity of the battery and the need for recharging play an important role. In Chapter 5 we focused on dynamic customer-centric pricing, however, dynamic *vehicle-centric* pricing could be interesting as well. This means that customer-specific information is not taken into account, but rather the current distribution of vehicles is used for the pricing for each vehicle. Following from this, the vehicle prices for all customers arriving at the same time are equal. Another possibility is a more holistic view, where SMSs are part of the mobility concept. In this case, the availability of car-sharing systems, bike-sharing systems and public transportation has interactive effects on the demand and thus on the prices of the individual vehicles of the different providers.

DuEPublico

Duisburg-Essen Publications online

UNIVERSITÄT DUISBURG ESSEN

Offen im Denken

ub | universitäts bibliothek

Diese Dissertation wird via DuEPublico, dem Dokumenten- und Publikationsserver der Universität Duisburg-Essen, zur Verfügung gestellt und liegt auch als Print-Version vor.

DOI: 10.17185/duepublico/81570
URN: urn:nbn:de:hbz:465-20240216-102926-6

Dieses Werk kann unter einer Creative Commons Namensnennung - Nicht kommerziell 4.0 Lizenz (CC BY-NC 4.0) genutzt werden.